
# Carbon Dioxide Capture by means of Cyclic Organic Nitrogen Compounds

Alicia García Abuín

USC
UNIVERSIDADE DE SANTIAGO DE COMPOSTELA

*Departamento de Enxeñaría Química*
*Escola Técnica Superior de Enxeñaría*
*Universidade de Santiago de Compostela*

# Carbon dioxide capture by means of cyclic organic nitrogen compounds

Doctoral Dissertation for PhD degree in
Chemical and Environmental Engineering

Santiago de Compostela, January 2012

**Alicia García Abuín**

*Departamento de Enxeñaría Química*
*Escola Técnica Superior de Enxeñaría*
*Universidade de Santiago de Compostela*

O Dr. **José Manuel Navaza Dafonte** profesor do Departamento de Enxeñaría Química da Universidade de Santiago de Compostela,

certifica

que o traballo de investigación titulado "**Carbon dioxide capture by means of cyclic organic nitrogen compounds**", constitúe a memoria, que para optar ó Grao de Doutor pola Universidade de Santiago de Compostela (Programa de Doutoramento de Enxeñaría Química e Ambiental), presenta Dª **Alicia García Abuín**, e que foi realizada, baixo a súa dirección, nos laboratorios do grupo GI-1621 (PFyPT) do Departamento de Enxeñaría Química da Escola Técnica Superior de Enxeñaría.

E para que conste ós efectos oportunos, fírmase o presente informe en Santiago de Compostela, xaneiro de dous mil doce.

**José Manuel Navaza Dafonte**

*"La adquisición de cualquier conocimiento es siempre útil al intelecto, que sabrá descartar lo malo y conservar lo bueno."*

Leonardo da Vinci

# Table of contents

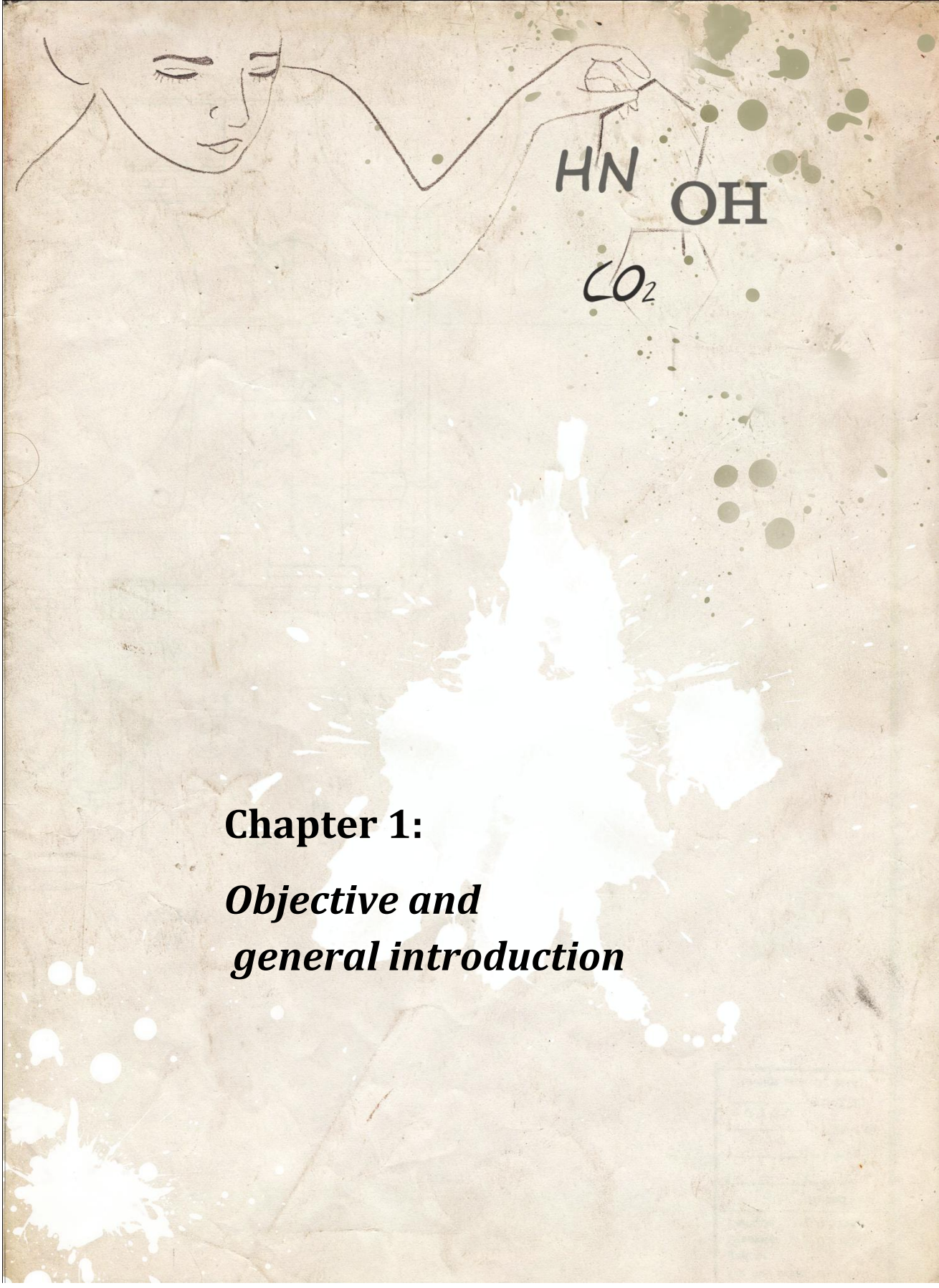


# Chapter 1:

## *Objective and general introduction*

## 1.1. Objective

The objective of this thesis is to evaluate different systems to capture carbon dioxide. Some of them are expected to have a carbon dioxide capture capacity higher than the systems used nowadays and other ones present less risk to health or safety, taking into account that one of the main aims of the REACH European Community Regulation is the progressive change of very hazardous substances applying the substitution principle.

In order to design an industrial absorption equipment, the knowledge of parameters such as mass transfer coefficient of corresponding physical and chemical processes, the gas-liquid interfacial area and the kinetic of the absorption process in case of chemical absorption will be required. In addition, certain physical properties as density, viscosity and surface tension of the liquid phase must be known because they are important for the carbon dioxide removal process.

# 1.2. General introduction

## 1.2.1. Carbon dioxide and climatic change

In 1988 the Intergovernmental Panel on Climate Change (IPCC) was jointly established by the World Meteorological Organization (WMO) and the United Nations Environment Programme (UNEP) in order to assess available scientific and socio-economic information on climate change and its impacts and on the options for mitigating climate change and adapting to it.

Several years after, in 1992, international concern about climate change increase and this lead to the United Nations Framework Convention on Climate Change (UNFCCC)[1]. The ultimate objective of that convention is the "stabilization of greenhouse gas concentrations in the atmosphere at a level that prevents dangerous anthropogenic interference with the climate system".

With regard to the cause of the climatic change, the IPCC identified six anthropogenic gases with climate change potential: $CO_2$ (carbon dioxide), $CH_4$ (methane), $N_2O$ (nitrogen dioxide), $SF_6$ (sulphur hexafluoride), CFC'S (chlorofluorocarbons), and HFC'S (hydrofluorocarbons). Besides, according to Intergovernmental Panel on Climate Change[2]:

- The global average surface temperature has increased during the 20$^{th}$ century by about 0. 6°C.
- About three-quarters of the anthropogenic emissions of carbon dioxide to the atmosphere during the past 20 years are due to fossil fuel burning.
- There is now new and stronger evidence that most of the warming observed over the last 50 years is attributable to human activities.
- Future changes in atmospheric composition and climate are inevitable with increases in temperature and some extreme events, and regional increases and decreases in precipitation, leading to increased risks of floods and droughts.

[1] *IPCC Special report on carbon dioxide capture and storage*. Cambridge University Press. New York, USA 2005.
[2] Paul Hurst. *$CO_2$ capture and storage. An overview of BP's activities*. United Kingdom 2004.

The increase of carbon dioxide concentration in the atmosphere during last millennium is shown in figure 1.1[3].

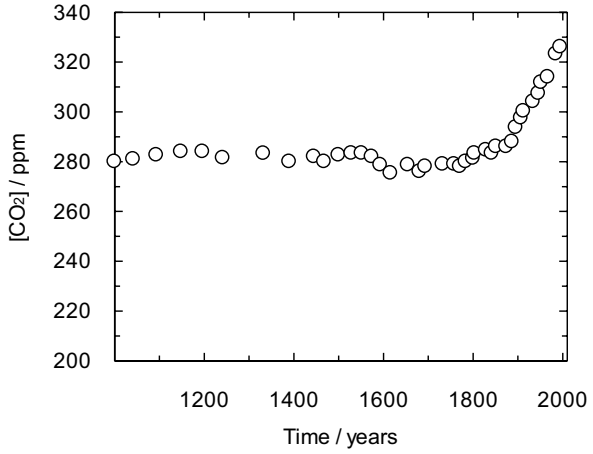


Figure 1.1. Concentration of $CO_2$ in the Earth's atmosphere .

To enforce the reduction of global greenhouse gas emissions, the Kyoto Protocol was established in december 1997 at the United Nations Framework Convention on Climate Change with a global reduction target of at least 5% below 1990 levels by the period of 2008–2012.

## 1.2.2. Sources of carbon dioxide

Carbon dioxide is emitted principally from the burning of fossil fuels (see table 1.1)[4], both in large combustion units such as those used for electric power generation and in smaller, distributed sources such as automobile engines and furnaces used in residential and commercial buildings. Carbon dioxide emissions also result from some industrial processes like cement manufacture or hydrogen production and during the combustion of biomass, as well as from the burning of forests during land clearance.

[3] Paul Hurst. *$CO_2$ capture and storage. An overview of BP's activities*. United Kingdom 2004.
[4] *IPCC Special report on carbon dioxide capture and storage*. Cambridge University Press. New York, USA 2005.

Table 1.1. Profile by process or industrial activity of worldwide large stationary $CO_2$ sources with emissions of more than 0.1 $MtCO_2$ per year in 2005.

| Process | Number of sources | Emissions ($MtCO_2$/year) |
|---|---|---|
| *Fossil fuels* | | |
| Power | 4942 | 10539 |
| Cement production | 1175 | 932 |
| Refineries | 638 | 798 |
| Iron and steel industry | 269 | 646 |
| Petrochemical industry | 470 | 379 |
| Oil and gas processing | | 50 |
| Other sources | 90 | 33 |
| *Biomass* | | |
| Bioethanol and bioenergy | 303 | 91 |
| **Total** | **7887** | **13466** |

Figure 1.2. Global distribution of large stationary sources of $CO_2$ .

According to IPCC, although the sources of carbon dioxide evaluated are distributed throughout the world, the database reveals four particular clusters of emissions: North America

(midwest and eastern USA), Europe (northwest region), East Asia (eastern coast of China) and South Asia (Indian subcontinent). This distribution can be observed in figure 1.2[5].

In table 1.2 the evolution of greenhouse gas emissions in Europe in ninety's is shown[6]:

Table 1.2. Green house gases in Europe

| Country | GHG emissions 1990 | GHG emissions 2000 | Reductions 1990/2000 | Burden sharing | Distance to target |
|---|---|---|---|---|---|
| Denmark | 69.36 | 68.51 | -1.23 | -21 | -19.77 |
| Spain | 286.43 | 385.99 | 34.76 | 15 | -19.76 |
| Austria | 77.39 | 79.75 | 3.06 | -13 | -16.06 |
| Belgium | 142.74 | 152.36 | 6.74 | -7.5 | -14.24 |
| Ireland | 53.70 | 67.00 | 24.76 | 13 | -11.76 |
| Italy | 520.57 | 546.90 | 5.06 | -6.5 | -11.56 |
| Netherlands | 210.34 | 216.92 | 3.13 | -6 | -9.13 |
| Portugal | 64.95 | 84.70 | 30.41 | 27 | -3.41 |
| Germany | 1222.77 | 991.42 | -18.92 | -21 | -2.08 |

[5] *IPCC Special report on carbon dioxide capture and storage*. Cambridge University Press. New York, USA 2005.
[6] Arlt W. *Chemical engineering tasks in climate protection*. EFC working party on distillation, absorption and extraction. Huelva 2004.

Table 1.2. Green house gases in Europe (continuation)

| Country | GHG emissions 1990 | GHG emissions 2000 | Reductions 1990/2000 | Burden sharing | Distance to target |
|---|---|---|---|---|---|
| United Kingdom | 742.49 | 649.11 | -12.58 | -12.5 | 0.08 |
| Greece | 104.90 | 130.05 | 23.98 | 25 | 1.02 |
| France | 559.34 | 550.03 | -1.66 | 0 | 1.66 |
| Finland | 77.09 | 73.96 | -4.07 | 0 | 4.07 |
| Sweden | 70.57 | 69.36 | -1.71 | 4 | 5.71 |
| Hungary | 101.63 | 84.34 | -17.02 | -6 | 11.02 |
| Czech Republic | 192.02 | 147.68 | -23.09 | -8 | 15.09 |
| Slovakia | 72.94 | 49.17 | -32.59 | -8 | 24.59 |
| Poland | 564.42 | 386.19 | -31.58 | -6 | 25.58 |
| Luxembourg | 13.45 | 5.97 | -55.60 | -28 | 27.60 |
| Estonia | 43.49 | 19.75 | -54.60 | -8 | 46.60 |
| Latvia | 31.05 | 11.16 | -64.05 | -8 | 56.05 |
| Lithuania | 51.55 | 0.00 | | -8 | |
| Slovenia | 19.21 | 0.00 | | -8 | |
| **Total** | **5221.63** | **4770.30** | **-8.64** | **-8** | **0.64** |

With regard to future emissions, it is predicted that coal combustion could contribute approximately 41% of the total world carbon dioxide emissions (43,676 million metric tonnes of carbon dioxide) in 2030[7] and it is projected that the number of carbon dioxide emission sources from the electric power and industrial sectors will increase significantly until 2050, mainly in South and East Asia. By contrast, the number of such sources in Europe may decrease slightly[8].

[7] Thitakamol B., Veawab A., Aroonwilas A. *Environmental impacts of absorption-based $CO_2$ capture unit for post-combustion treatment of flue gas from coal-fired power plant*. Elsevier 2007.
[8] *IPCC Special report on carbon dioxide capture and storage*. Cambridge University Press. New York, USA 2005.

### 1.2.3. Technology options for $CO_2$ capture

Depending on the process or power plant application in question, there are three main approaches to capturing the carbon dioxide generated from a primary fossil fuel (coal, natural gas or oil), biomass, or mixtures of these fuels: *pre-combustion, post-combustion and oxyfuel combustion* (figure 1.3)[9].

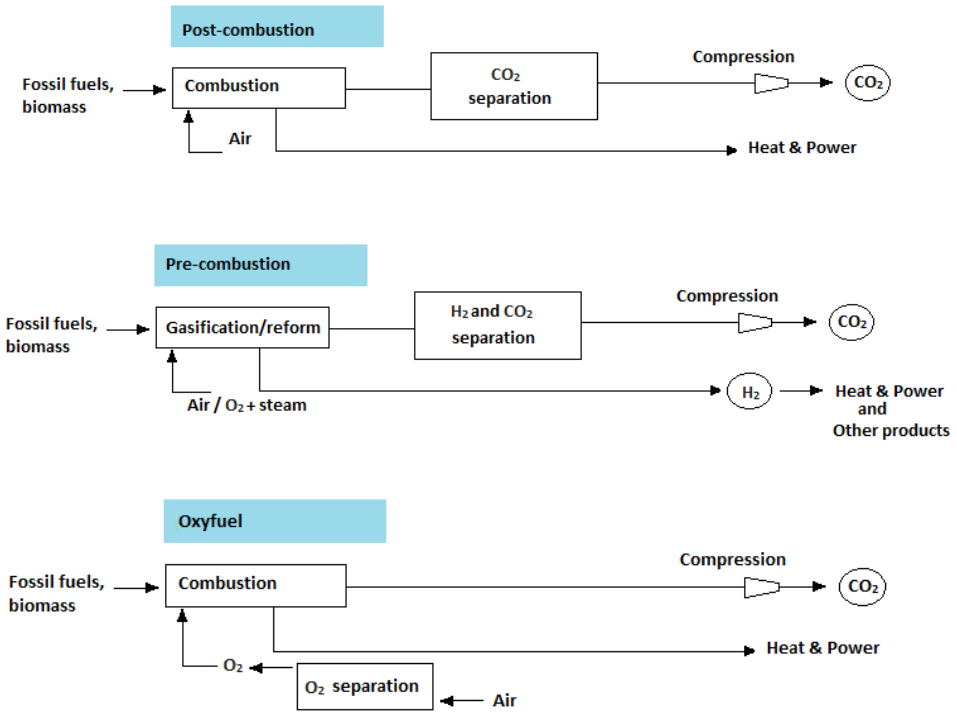


Figure 1.3. Schematic representation of capture systems.

[9] *IPCC Special report on carbon dioxide capture and storage*. Cambridge University Press. New York, USA 2005.

### *1.2.3.1. Post-combustion*

*Post-combustion* capture is a downstream process where carbon dioxide is separated from the flue gases produced by the combustion of fuel or biomass in air. This method requires separating the carbon dioxide from other flue gases because sequestration of combustion gases is not feasible due in part to the cost of gas compression and storage. The low concentration of carbon dioxide in power-plant flue gas (typically 4-14%)[10] means that a large volume of gas has to be handled, which results in large equipment sizes and high capital costs. A further disadvantage of the low carbon dioxide concentration is that powerful chemical solvents have to be used and the regeneration of the solvents to release the carbon dioxide will require a large amount of energy.

The different post-combustion technologies are as follows:

- Absorption processes: amine such as monoethanolamine (MEA) removal of carbon dioxide from flue gas (current Best Available Technology)
- Amine/membrane contactor systems
- Adsorption processes
- Novel adsorbents
- Compact technologies

### *1.2.3.2. Pre-combustion*

*Pre-combustion* systems process the fuel in a reactor with steam and air or oxygen to produce a mixture consisting mainly of carbon monoxide and hydrogen (synthesis gas). Additional hydrogen, together with carbon dioxide, is produced by reacting between carbon monoxide with steam in a second reactor (a shift reactor). The resulting mixture of hydrogen and carbon dioxide can then be separated into a carbon dioxide gas stream, and a stream of hydrogen. If the carbon dioxide is stored, the hydrogen is a carbon-free energy carrier that can be combusted to generate power and/or heat. Although the initial fuel conversion steps are more

[10] Abass A. O. $CO_2$ capture and separation technologies for end-of-pipe applications - A review. *Energy* 2010, 35, 2610-2628.

elaborate and costly than in post-combustion systems, the high concentrations of carbon dioxide produced by the shift reactor (typically 15 to 60% by volume on a dry basis) and the high pressures often encountered in these applications are more favourable for carbon dioxide separation.

#### *1.2.3.3. Oxyfuel combustion*

*Oxyfuel combustion* systems use oxygen instead of air for combustion of the primary fuel to produce a flue gas that is mainly water vapour and carbon dioxide. This results in a flue gas with high carbon dioxide concentrations (greater than 80% by volume). The water vapour is then removed by cooling and compressing the gas stream. Oxyfuel combustion requires the upstream separation of oxygen from air, with a purity of 95–99% oxygen assumed in most current designs. Further treatment of the flue gas may be needed to remove air pollutants and non condensed gases (such as nitrogen) from the flue gas before the carbon dioxide is sent to storage. As a method of carbon dioxide capture in boilers, oxyfuel combustion systems are in the demonstration phase. Oxyfuel systems are also being studied in gas turbine systems.

### 1.2.4. Description of carbon dioxide absorption process

Figure 1.4 illustrates a typical configuration of the carbon dioxide absorption process using regenerable liquid solvent. The process consists of two major sections, an absorption section where carbon dioxide in the flue gas is absorbed into the liquid solvent and a regeneration section where the absorbed carbon dioxide is stripped out by means of heat. In the absorption section, the gas stream containing carbon dioxide is passed upward through the absorber, countercurrent to the solvent entering the absorber at the top. Under proper conditions, carbon dioxide is transferred from the gas stream to the liquid solvent, resulting in a treated gas with low carbon dioxide content passing out of the absorber top and a $CO_2$-rich solvent leaving the absorber at the bottom. The rich solvent is then heated in a rich-lean heat-exchanger, and enters the regenerator at some point near the top. The $CO_2$-rich solvent is heated to boiling in the regeneration section by a hot steam reboiler located at the bottom of the regenerator, and the

captured carbon dioxide is released from the solvent. Finally, the $CO_2$-lean solvent is pumped from the regenerator through the rich-lean heat-exchanger and a cooler before re-introducing to the absorber.

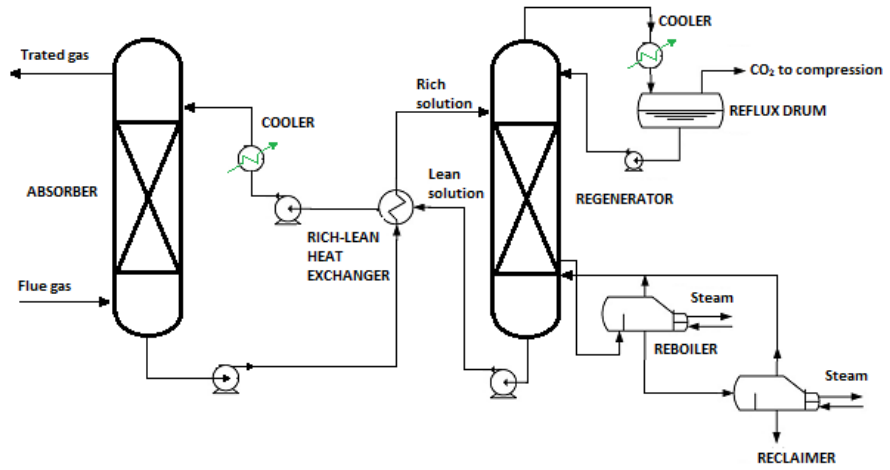


Figure 1.4. Schematic diagram of the typical absorption-based $CO_2$ capture unit[11].

At present, there are a number of absorption solvents commercially available for carbon dioxide capture. They are classified into two categories, chemical and physical solvents.

The physical solvents are commonly used for high pressure gas streams. They require less energy for solvent regeneration than the chemical solvents, but they have a capture capacity lower. Examples of physical solvents are water, propylene carbonate (PC), methanol and N-methyl-2-pyrrolidone (Lurgi's Purisol process). It is commonly known that the use of physical solvent alone is ineffective for low-pressure gas streams.

In order to explain the interfacial mass transfer mechanism which takes place in a physical absorption, three models were proposed. They are the thin film model by Withman, the penetration model by Higbie and the random surface renewal model by Danckwerts. All of them

[11] Thitakamol B., Veawab A., Aroonwilas A. Environmental impacts of absorption-based $CO_2$ capture unit for post-combustion treatment of flue gas from coal-fired power plant. *International Journal of Greenhouse Gas Control* 2007, 1(3), 318-342.

assume that diffusion of gas takes place in a stagnant liquid. From this point of view, all of the models belong to the same class called stagnant liquid models.

As regards to chemical absorption, typical chemical solvents are alkanolamines, which are commonly used in the form of aqueous solutions. These chemical solvents include monoethanolamine (MEA), diethanolamine (DEA), N-methyldiethanolamine (MDEA), diglycolamine (DGA), triethanolamine (TEA), diisopropanolamine (DIPA), and 2-amino-2-methyl-1-propanol (AMP). Mixtures of these single alkanolamines, known as blended amines, are also gaining a great deal of interest from the practitioners due to their process advantages over the single alkanolamines. Most formulations of the blended amines are tertiaryamine-based, which are designed to be used for specific carbon dioxide capture targets and purposes. The tertiary MDEA is gaining recognition as the key component of the blended amines because of its low energy requirements and high carbon dioxide absorption capacity. An addition of primary amine MEA or secondary amine DEA into the MDEA solution helps enhance rate of capturing carbon dioxide, while maintaining the advantages of MDEA[12].

The mass transfer phenomenon with chemical reaction consists of several stages:

1. Diffusion of reactant present in gas phase to the interface.
2. Diffusion from the interface to the liquid phase.
3. Reaction in the liquid phase.
4. Diffusion of the products and reagents in the liquid phase due to the concentration gradients generated by the reaction.

The most studied system about gas-liquid reaction consists of a solution that contains a compound B, which reacts with compound A in gas phase. The overall rate expression for the reaction will take into account the mass transfer resistance and the resistance due to the chemical reaction rate. The relative magnitude of these resistances can vary significantly and each situation requires an analysis. The first step will be to identify these time dependent regimes in each case.

[12] Thitakamol b., Veawab A., Aroonwilas A. Environmental impacts of absorption-based $CO_2$ capture unit for post-combustion treatment of flue gas from coal-fired power plant. *International Journal of Greenhouse Gas Control* 2007, 1(3), 318-342.

Depending on the relative rates of diffusion and reaction between B and A, the absorption systems are classified into different regions. The most common and best studied cases are summarized below.

**a) Very slow reaction**

If the reaction is sufficiently slow, this does not take place significantly in the interface, because it occurs in the bulk of liquid phase and whole liquid becomes and remains saturated with unreacted gas. Under these circumstances, the knowledge of the gas solubility gives its concentration in the liquid.

**b) Slow reaction**

In this case, the concentration of dissolved gas in the bulk of the liquid is substantially less than the saturation, and on the other hand, there is no appreciable reaction of dissolved gas during its transport through the diffusion film.

**c) Moderately fast reaction**

The reaction is fast enough for an appreciable fraction of gas reacts in the film and the concentration of unreacted dissolved gas in the bulk of liquid will be negligible small.

**d) Fast reaction**

The reaction is so fast that it occurs completely in the liquid film, so that the concentration of gas in the bulk of liquid is zero.

**e) Pseudo-first order reaction**

This is a special case of fast reaction and it occurs when the concentration of the reagent B in the bulk of the liquid is higher than the solubility of the gas A.

**f) Instantaneous reaction**

The dissolved gas A reacts instantly with the component B. There is a film in the interface where the concentration of both components is zero. Under these circumstances the rate of reaction is controlled entirely by the diffusion of the reactants.

Reactive absorption is the preferred option used in the gas-processing industry for carbon dioxide removal, and the aqueous solutions of alkanolamines remain an industrial important class of compounds, used in the natural gas, petroleum chemical plants and ammonia industries for the removal of carbon dioxide and hydrogen sulphide from gas streams.

Other option is mixing of the chemical and physical solvents, this could provide some benefits for carbon dioxide capture under low-pressure conditions. For instance, blends of physical and chemical solvents, such as: sulpholane + DIPA and sulpholane + MDEA, are found effective for the removal of carbon dioxide and sulphur compounds (e.g., sulphur dioxide) from gas streams[13]. Sulpholane works as a large storage species for captured carbon dioxide while both DIPA and MDEA (chemical solvents) work as the reactive species for capture activities. These mixed solvents also help reduce the corrosion rate and foaming problems.

## 1.2.5. Carbon dioxide capture: risks and the environment

The table 1.3 collects the hazard statements for the different substances used to capture carbon dioxide at industry, and the table 1.4 collects the hazard statements for the substances used in this thesis. These hazard statements came from the safety data sheets provided by the supplier of the products.

[13] Gupta M., Coyle I., Thambimuthu K. *$CO_2$ capture technologies and opportunities in Canada*. 1st Canadian CC&S Technology Roadmap Workshop 2003.

Table 1.3. Summary of hazard statements and pictograms of chemicals used in $CO_2$ capture.

| CHEMICAL | HAZARD STATEMENTS | PICTOGRAM |
|---|---|---|
| *Ethanolamine (MEA)* | • Causes severe skin burns and eye damage.<br>• Harmful if swallowed and inhaled.<br>• Harmful in contact with skin. |  |
| *Diethanolamine (DEA)* | • May cause damage to organs through prolonged or repeated exposure.<br>• Toxic if swallowed or inhaled.<br>• Toxic in contact with skin.<br>• Toxic to aquatic life with long lasting effects. |  |
| *N-Methildiethanolamine (MDEA)* | • Causes serious eye irritation. |  |
| *Diglycolamine (DGA)* | • Harmful in contact with skin.<br>• Causes severe skin burns and eye damage. |  |
| *Diisopropanolamine (DIPA)* | • Causes serious eye irritation. |  |
| *2-Amino-2-Methyl-1-Propanol (AMP)* | • Causes serious eye irritation.<br>• Causes skin irritation.<br>• Harmful to aquatic life with long lasting effects. |  |
| *Triethanolamine (TEA)* | • Causes serious eye irritation. |  |
| *N-Methyl-2-Pyrrolidone (MP)* | • Causes skin irritation.<br>• Causes serious eye irritation.<br>• May cause respiratory irritation.<br>• May damage the unborn child. |  |
| *Propylene Carbonate (PC)* | • Causes serious eye irritation. |  |
| *Methanol* | • Highly flammable liquid and vapour.<br>• Toxic if swallowed or inhaled.<br>• Toxic in contact with skin.<br>• Causes damage to organs. |  |
| *Sulpholane* | • Harmful if swallowed. |  |

Table 1.4. Summary of hazard statements and pictograms of chemicals used in this work.

| CHEMICAL | HAZARD STATEMENTS | PICTOGRAM |
|---|---|---|
| *Pyrrolidine (PYR)* | • Highly flammable liquid and vapour.<br>• Harmful if swallowed.<br>• Causes severe skin burns and eye damage.<br>• Harmful if inhaled. |  |
| *Piperidine (PIP)* | • Highly flammable liquid and vapour.<br>• Causes severe skin burns and eye damage.<br>• Toxic in contact with skin.<br>• Toxic if inhaled. |  |
| *Ethanolamine (MEA)* | • Causes severe skin burns and eye damage.<br>• Harmful if swallowed.<br>• Harmful in contact with skin.<br>• Harmful if inhaled. |  |
| *2-Pyrrolidone (P)* | Not a dangerous substance according to GHS. | |
| *N-Methyl-2-Pyrrolidone (MP)* | • Causes skin irritation.<br>• Causes serious eye irritation.<br>• May cause respiratory irritation.<br>• May damage the unborn child. |  |
| *N-Ethyl-2-Pyrrolidone (EP)* | • Harmful if swallowed.<br>• Causes serious eye irritation. |  |
| *Glucosamine (GA)* | Not a hazardous substance or mixture according to EC-directives 67/548/EEC or 1999/45/EC. | |

## 1.2.6. Costs of carbon dioxide capture

At the moment, the carbon dioxide capture with amines is the Best Available Technology, however the main disadvantage of amine scrubbing is the cost, which is perceived too high. The high regeneration energy requirements make necessary an optimization process in

large-scale power plants because actual carbon dioxide capture cost remain around 40-70 €/t $CO_2$[14].

One of the main problems is related to the large quantities of heat required to regenerate the amine solvent. This reduces net plant efficiency, because power plants require more fuel to generate each kilowatt-hour of electricity produced.

The increased fuel requirement results in an increase in most other environmental emissions per kWh generated relative to new state-of-the-art plants without carbon dioxide capture and, in the case of coal, proportionally larger amounts of solid wastes. In addition, there is an increase in the consumption of chemicals such as amines.

New or improved technologies for carbon dioxide capture can significantly reduce the cost in the future. There is a considerable uncertainty about the magnitude of future cost reductions, but studies suggest that improvements to current commercial technologies could lower carbon dioxide capture costs by at least 20-30%, while new technologies under development may allow for more substantial cost reductions in the future[15].

### 1.2.7. State of the art

The carbon dioxide absorption process has been, and continues being, widely studied and the proof is the amount of literature on this topic. Numerous studies have been carried out on the kinetics between carbon dioxide and the most usual amines. For MEA, was proposed[16] a second order reaction rate. Other researchers[17] have used the thermolecular-kinetic model instead of the usual zwitterion model to explain the reaction between carbon dioxide and MEA.

[14] IEA. *Annual Energy Outlook 2003*. DOE/IEA-0383.
[15] *IPCC Special report on carbon dioxide capture and storage*. Cambridge University Press. New York, USA 2005.
[16] Versteeg G. F., van Dijck L. A. J., van Swaaij W. P. M. On the kinetics between $CO_2$ and alkanolamines both in aqueous and non-aqueous solutions - An overview. *Chemical Engineering Commuication* 1996, 144, 113-158.
[17] Aboudheir A., Tontiwachwuthikul P., Chakma A., Idem R. Kinetics of the reactive absorption of carbon dioxide in high $CO_2$-loaded, concentrated aqueous monoethanolamine solutions. *Chemical Engineering Science* 2003, 58, 5195-5210.

Carbon dioxide absorption in aqueous solutions of MDEA has been largely studied too[18,19,20,21,22]. Recently, the interest in the use of mixed amine solvents in gas-treating processes is increasing. Blends of primary and tertiary amines (such as mixtures of MEA and MDEA) or secondary and tertiary amines (such as mixtures of DEA and MDEA), which combine the higher equilibrium capacity of the tertiary amine with the higher reaction rate of the primary or secondary amine, have been suggested for industrial gas-treating processes.

Absorption rates of carbon dioxide into aqueous blends of MDEA with MEA (or DEA) have also been studied[23]. The Kinetics of the absorption of carbon dioxide into MEA+MDEA+$H_2O$ was studied[24] and from this work it was concluded that the addition of small amounts of MEA to MDEA results in a significant enhancement of carbon dioxide absorption rates.

However, some problems are associated with the use of alkanolamines in absorption, which including oxidative degradation[25] and high vapour pressure of alkanolamines[26]. These contribute to solvent losses, degradation product handling, and other negative effects in the process. Because of the limitations of these solvents and the wish to reduce the high heat duties needed in the process, new types of amines have been developed: sterically hindered amines, amines with several amino functions, etc.

A recent advance in gas treating technology is the application of sterically hindered amines which offer absorption capacity, absorption rate, selectivity, degradation resistance

---

[18] Littel R. J., van Swaaij W. P. M., Versteeg G. F. Kinetics of carbon dioxide with tertiary amines in aqueous solution. *AIChE Journal* 1990, 36, 1633-1640.
[19] Rinker E. B., Ashour S. S., Sandall O. C. Kinetics and modelling of carbon dioxide absorption into aqueous solutions of N-methyldiethanolamine. *Chemical Engineering Science* 1995, 50, 755-768.
[20] Pani F., Gaunand A., Cadours R., Bouallou C., Richon D. Kinetics of absorption of $CO_2$ in concentrated aqueous methyldiethanolamine solutions in the range 296 K-343 K. *Journal of Chemical & Engineering Data* 1997, 42, 353-359.
[21] Cadours R., Bouallou C. Rigorous simulation of gas absorption into aqueous solutions. *Industrial & Engineering Chemistry Research* 1998, 37, 1063-1070.
[22] Ko J.J., Li M. H. Kinetics of absorption of carbon dioxide into solutions of N-methyldiethanolamine + water. *Chemical Engineering Science* 2000, 55, 4139-4147.
[23] Mandal B. P., Guha M., Biswas A. K., Bandyopadhyay S. S. Removal of carbon dioxide by absorption in mixed amines: Modeling of absorption in aqueous MDEA/MEA and AMP/MEA solutions. *Chemical Engineering Science* 2001, 56, 6217–6224.
[24] Liao C. H., Li M. H. Kinetics of absorption of carbon dioxide into aqueous solutions of monoethanolamine + N-methyldiethanolamine. *Chemical Engineering Science* 2002, 57, 4569 – 4582.
[25] Goff G., Rochelle G. T. Oxidative degradation of aqueous monoethanolamine in $CO_2$ capture controlled by the physical absorption of $O_2$. *Industrial & Engineering Chemistry Research* 2004, 43, 6400–6408.
[26] Kohl A. L., Nielsen R. *Gas Purification*. 5th edition. Gulf Publishing Company. Houston 1997.

advantages over conventional amines for carbon dioxide removal from gases[27]. Besides, sterically hindered amines have been strongly recommended as a potential absorbent because of its lower regeneration energy than for conventional amines. This smaller stripping energy requirement of sterically hindered amine results in greater energy savings and reduces the total operating cost of the acid gas treating unit. A sterically hindered amine is defined as a primary or secondary amine in which the amino group is attached to a secondary or tertiary carbon atom. An example of a well-known sterically hindered amine is the amino-2-methyl-1-propanol (AMP) as a primary alkanolamine and 2-piperidineethanol (PE) as a secondary alkanolamine.

Several research teams have studied the kinetics of the absorption of carbon dioxide into AMP + MEA + $H_2O$[28]. These studies found that the addition of small amounts of MEA to AMP aqueous solutions results in a significant enhancement of carbon dioxide absorption rates.

In the study of absorption of carbon dioxide into aqueous blends of DEA and AMP[29] the researchers have found that the addition of small amounts of DEA to an aqueous solution of AMP significantly enhances the rate of absorption of carbon dioxide and enhancement factor.

Other works[30] have studied the chemical reaction kinetics of carbon dioxide with a sterically hindered amine, 2-amino-2-ethyl-1,3-propanediol (AEPD), in aqueous solutions. Many other studies have been made on developing new sterically hindered amines to reduce the total capital and operating costs in the carbon dioxide absorption process[31].

Other work[32] focused on the development of a new solvent for carbon dioxide capture, using an aqueous solution with a blend of *N*-methyldiethanolamine (MDEA) and triethylene tetramine (TETA), an amine with four amino groups, two primary groups, and two secondary

---

[27] Sartori G., Savage D. W. Sterically hindered amines for $CO_2$ removal from gases. *Industrial and Engineering Chemistry Fundamentals* 1983, 22, 239-249.
[28] Xiao J., Li C. W., Li M. H. Kinetics of absorption of carbon dioxide into aqueous solutions of 2-amino-2-methyl-1 propanol+monoethanolamine. *Chemical Engineering Science* 2000, 55, 161-175.
[29] Mandal B. P., Biswas A. K., Bandyopadhyay S. S. Absorption of carbon dioxide into aqueous blends of 2-amino-2-methyl-1-propanol and diethanolamine. *Chemical Engineering Science* 2003, 58, 4137 – 4144.
[30] Yoon S. J., Lee H., Yoon H.-J., Shim J.-G., Lee J. K., Min B.-Y., Eum H.-M. Kinetics of absorption of carbon dioxide into aqueous 2-amino-2-ethyl-1,3-propanediol solutions. *Industrial & Engineering Chemistry Research* 2002, 41(15), 3651-3656.
[31] Baek J. I., Yoon J. H. Solubility of carbon dioxide in aqueous solutions of 2-amino-2-methyl-1,3-propanediol. *Journal of Chemical and Engineering Data* 1998, 43, 635-637.
[32] Amann J.-M. G., Bouallou C. Kinetics of the absorption of $CO_2$ in aqueous solutions of *N*-methyldiethanolamine + triethylene tetramine. *Industrial & Engineering Chemistry Research* 2009, 48, 3761-3770.

groups, making it very reactive with carbon dioxide. The conclusion of this work was that the addition of small amount of TETA leads to a significant enhancement of the absorption rates compared to an aqueous MDEA solution. Moreover the absorption capacity of the solvent is increased. This type of solvent is a suitable compromise between absorption rate and efficiency of the solvent regeneration.

Other option to capture carbon dioxide is the use of neutralized amino acid salts due to their physical and chemical properties. They have been mentioned as attractive alternatives to alkanolamines as solvents for carbon dioxide absorption[33,34]. Different researchers[35] studied the carbon dioxide absorption potential of the amino acid salts formed from neutralization of the amino acid with organic bases (amines). Assessments of amino acid salts for carbon dioxide absorption have shown that they have a performance similar to MEA.

As it has already been commented, blends of primary or secondary amines with tertiary ones are frequently used for the removal of carbon dioxide from gas mixtures. However, the acceleration of carbon dioxide absorption via the fast formation of carbamates with primary or secondary amines is usually only required locally in certain sections of the absorption column. In other parts of the absorption process homogeneous activating additives like diethanolamine (DEA) can give rise to well-documented undesirable side-effects, such as increased corrosion or higher energy demands for regeneration. To avoid the disadvantages associated, different studies[36,37] proposed using immobilised amine groups (IA) on solid support particles. In this way, one can localise the activating additives to those parts of the absorption process where they are beneficial and exclude them elsewhere. The experiments demonstrate the basic feasibility of using immobilised primary amines in place of homogeneous additives to enhance carbon dioxide absorption in tertiary amine solutions.

---

[33] Kumar P. S., Hogendoorn J. A., Versteeg G. F., Feron P. H. M. Kinetics of the reaction of $CO_2$ with aqueous potassium salt of taurine and glycine. *AIChE Journal* 2003, 49(1), 203–213.
[34] Hamborg E. S., Niederer J. P. M., Versteeg G. F. Dissociation constants and thermodynamic properties of amino acids used in $CO_2$ absorption from (293 to 353) K. *Journal of Chemical & Engineering Data* 2007, 52, 2491–2502.
[35] Aronu U. E., Svendsen H. F., Hoff K. A. Investigation of amine amino acid salts for carbon dioxide absorption. *International Journal of Greenhouse Gas Control* 2010, 4, 771–775.
[36] Schubert S., Grünewald M., Agar D. W. Enhancement of carbon dioxide absorption into aqueous methyldiethanolamine using immobilised activators. *Chemical Engineering Science* 2001, 56, 6211–6216.
[37] Zhang X., Schubert S., Grünewald M., Agar D. W. Studies on the kinetics of carbon dioxide absorption with immobilised amines (IA). *Chemical Engineering Journal* 2005, 107, 97–102.

Other researchers have proposed and thermodynamically analyzed a novel solar thermochemical cycle for the capture of carbon dioxide from air[38]. The cycle encompasses three steps: the carbonation of calcium hydroxide, the decomposition of calcium carbonate, and the hydrolysis of calcium oxide. These carbon dioxide consuming reactions have been proposed for the separation of carbon dioxide from flue gases at concentrations usually exceeding 10%.

### 1.2.8. Gas-liquid contactors

Most of the equipments used to gas-liquid absorption in industrial processes or laboratory scale can be classified into three categories:

1. Contactors in which the liquid flows as a thin film (e.g. a packed column and wetted wall column).

2. Contactors with dispersion of gas in the liquid phase (e.g. bubble column, plate column).

3. Contactors with dispersion of liquid in the gas phase (e.g. spray column, Venturi cleaner).

This classification is not highly specific and there are many contactors that have characteristics of more than one category. In a gas-liquid contactor the mass transfer rate depends on the mass transfer coefficients ($k_L$, $k_G$), the specific interfacial area (*a)* available to the gas-liquid transfer and other factors. In order to absorb the gas physically or chemically in this type of traditional contactors, the main resistance to mass transfer is in the liquid phase (except at very low concentrations of substances absorbed in gas phase). This happens for the absorption of carbon dioxide in physical or chemical solvent. In that way, obtaining the mass transfer characteristics in the liquid side is a critical step in the design of an absorber.

[38] Nikulshina V., Gálvez M. E., Steinfeld A. Kinetic analysis of the carbonation reactions for the capture of $CO_2$ from air via the $Ca(OH)_2$–$CaCO_3$–CaO solar thermochemical cycle*. Chemical Engineering Journal* 2007, 129, 75–83.

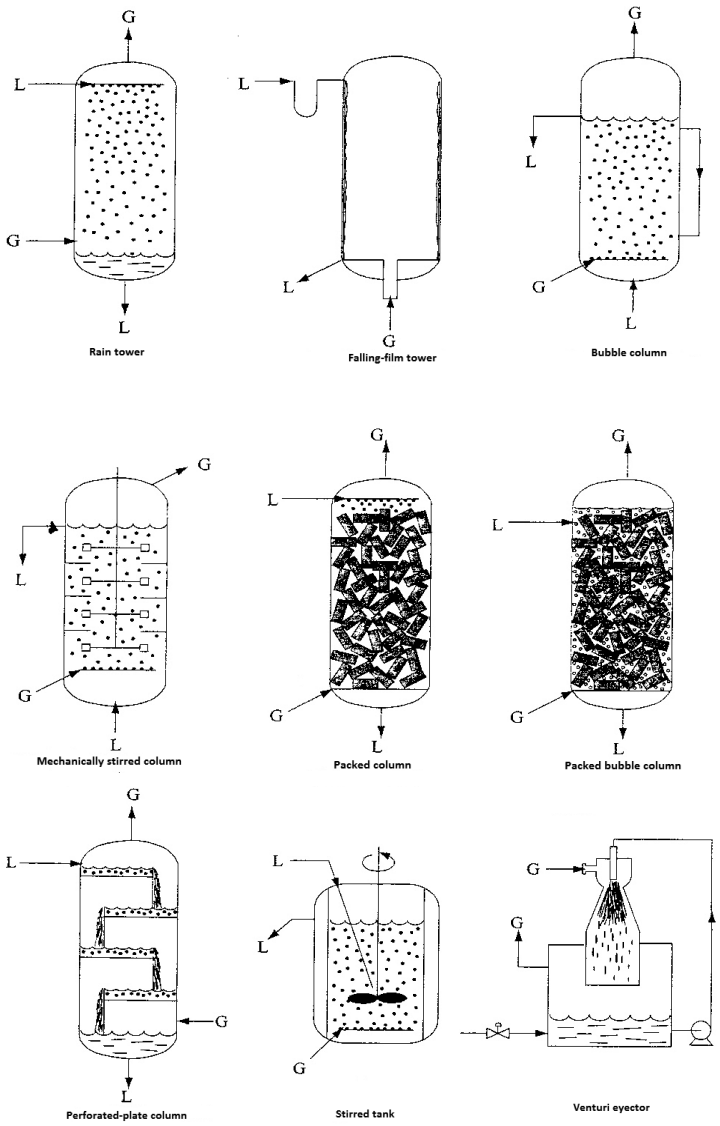


Figure 1.5. Examples of gas-liquid contact equipments

The different gas-liquid contact equipments are detailed below. Besides, in figure 1.5 a diagram of these gas-liquid contactors is shown.

● ***Stirred tank***

This type of gas-liquid contactor is often used in chemical industry to carry out heterogeneous reactions[39,40,41] (gas-liquid, solid-liquid and gas-solid-liquid), because these contactors allow the change in stirring rate in a wide range, as well as achieving high residence times for the liquid phase. This fact makes them optimums to important thermical processes, viscous liquid phases, low gas-liquid rates or autocatalytic processes like aerobic fermentation. However, it presents a higher mechanical complication than the bubble columns and this is a disadvantage when corrosive substances have to be manipulated or when high pressure or temperature are used.

In this type of contactors, there is a version widely used where the gas to be absorbed is fed to the tank by bubbling. With this type of feeding, the interfacial area increases quite a lot. Also, operations in stage can be performed by arranging successive compartments in vertical with dispersers / stirrers mounted on a common axis.

● ***Packed column***

In these kind of columns, the liquid and gas phases flow in co-current, or countercurrent, through the hollows left by the filler. The liquid is distributed on the filler as a film and the gas forming a continue phase. This kind of contactor is often used in order to absorb a component present in a gas phase[42,43]. The pressure drop for the gas phase is relatively low, so the packed towers are appropriated to deal with high gas flow rates. Also, they are used to treat corrosive streams because both the construction and choice of material are easy.

---

[39] Bergeron S., Servio P. $CO_2$ and $CH_4$ mole fraction measurements during hydrate growth in a semi-batch stirred tank reactor and its significance to kinetic modeling. *Fluid Phase Equilibria* 2009, 276(2), 150-155.
[40] Hwang K.-S., Kim D.-W., Park S.-W. Simultaneous absorption of carbon dioxide and sulfur dioxide into aqueous 1,8-diamino-p-menthane. *Separation Science and Technology* 2009, 44(16), 3888-3910.
[41] Di Ciccio M. P., Bottini M., Pepe P. Observer-based nonlinear control law for a continuous stirred tank reactor with recycle. *Chemical Engineering Science* 2011, 66(20), 4780-4797.
[42] Prasad M. H., Hans H. Pilot plant study of post-combustion carbon dioxide capture by reactive absorption: Methodology, comparison of different structured packings, and comprehensive results for monoethanolamine. *Chemical Engineering Research & Design* 2011, 89(8A), 1216-1228.
[43] Kreangkrai M., Raphael O., Paitoon T. Comparative mass transfer performance studies of $CO_2$ absorption into aqueous solutions of DEAB and MEA. *Industrial & Engineering Chemistry Research* 2010, 49(6), 2857-2863.

● ***Rain tower***

In this contactor, liquid is dispersed through spargers from the top of the column, and the gas flows in the opposite direction. Like in packed columns, the amount of fluid retained is small, and the gas phase is continuous. Practically, the tower is empty and it is used in the case of the gas stream containing solid particles. Close to the spargers a high interfacial area is created, but the drops coming down coalesce and the area decreases quickly. For this reason, this contactor is only used in the case of fast absorptions.

● ***Perforated-plate column***

In these columns, the gas and liquid flow separately between stages but they are in contact in each plate. During this contact, the gas is dispersed in liquid phase. This contactor is suitable when an operation in stages is required, when large flow rates of liquid should be treated or in the case of slow reactions which need high contact time[44].

● ***Bubble column***

Those columns are filled with liquid and have a perforated ring (or other type of sparger) at its base to feed and spread the gas phase. The bubbles rise through the liquid, stirring and mixing it[45,46]. Usually, this kind of column has a height of three times the value of its diameter, at least. One of the disadvantages of this type of column is the coalescence between bubbles, and this produce a decrease in the gas-liquid contact efficiency. This problem can be avoided, for instance, filling the column with Raschig rings and working in flooding mode. In this case, the maximum surface velocity of gas stream is much lower than in non-flooded column. Generally, these are contactors used for relatively slow reactions and the key component is in liquid phase. They are cheaper than stirred tanks, because the spread and stirred process are made without mechanical agitation.

---

[44] Dhanasekaran S., Karunanithi T. Mass transfer studies in a novel perforated plate bubble column. *International Journal of Chemical Reactor Engineering* 2010, 8, A116.
[45] Maceiras R., Alvarez E., Cancela A. Effect of temperature on carbon dioxide absorption in monoethanolamine solutions. *Chemical engineering Journal* 2008, 138(1-3), 295-30.
[46] Palmeri N., Cavallaro S., Bart J. C. J. Carbon dioxide absorption by MEA - A preliminary evaluation of a bubbling column reactor. *Journal of Thermal Analysis and Calorimetry* 2008, 91(1), 87-91.

● ***Falling-film column***

Due to this tower has a construction and data processing simple, it has been very used[47,48]. The operating procedure is based on the liquid flows by gravity on the inner surface of a vertical column producing a liquid film that allows work with suitable conditions to obtain valuable data for gas absorption process.

## 1.2.9. Bubble column reactor

Bubble columns are mass transfer and reaction devices in which, one or several gases are brought into contact and react with the liquid phase itself or with a component dissolved or suspended in it. The mass transfer stages, which under certain conditions determine the rate at which the whole process is carried out, may take place both before and after the chemical reaction itself. Hence a good deal of effort is given to engineering measures which ensure a high rate of mass transfer.

The bubble column (BCR) has been proven to be a very effective reactor and is widely used in the chemical industries. Since bubble columns offer several advantages such as high heat and mass transfer rates, compactness and low operating and maintenance costs in comparison to other kinds of multiphase reactors. They are increasingly used in industrial practice (as absorbers, fermenters, strippers, coal liquifiers, and chemical reactors for gas-liquid and gas-liquid-liquid reactions). Because of the high degree of mixing, there is no need of additional internal mixing devices.

[47] Hubert M., Laurent F. Intensification of G/L absorption in microstructured falling film. *Chemical Engineering Science* 2011, 66, 2475-2490.
[48] Chasanis P., Lautenschleger A., Kenig E. Y. Numerical investigation of carbon dioxide absorption in a falling-film micro-contactor. *Chemical Engineering Science* 2010, 65, 1125-1133.

The important position of bubble column reactors is reflected in the loads of research papers appeared in the last decades including a reviews[49,50] and besides there are a lot of books dedicated to their study[51,52,53,54,55].

In its most simple form the bubble column reactor is a vertical cylinder (see figure 1.5). The gas enters at the bottom through a gas distributor which may vary in design. The liquid phase may be supplied in batch form or it may move with or against the flow of the gas phase. In contrast to physical mass transfer operations, counterflow offers no significant advantages, as the reaction itself ensures a sufficient concentration drop during material exchange. The reactor is usually cooled or heated by means of internal heat exchanges to avoid problems with the temperature control.

The top of the bubble column is often widened to facilitate gas separation. The bubble column reactor is characterized by the lack of any mechanical means of agitation; hence gas is distributed more evenly in the liquid phase. The ratio between length and diameter may vary between 3 and 6, and a value of 10 is not infrequent. Indeed this level is often greatly exceeded in laboratory and pilot plant tests. The size of bubble column reactors varies according to intended use and the rate of production. In example, units of 100-200 $m^3$ are regarded as very large in the chemical production industry[56] yet much larger ones are used in biotechnology as process times are generally much longer.

Simple construction and the lack of any mechanically operated parts are two characteristics aspects of bubble column reactors. Hence, no shaft sealing is required which means that even aggressive gases can be converted without any problem even at high temperatures and pressures. It features high heat transfer coefficients, thus ensuring a uniform temperature thorough, even with strong exothermal reactions. This is of special significance

[49] Kantarci N., Borak F., Ulgen K. O. Review bubble column reactors. *Process Biochemistry* 2005, 40, 2263–2283.
[50] Krishna R., van Baten J. M. Mass transfer in bubble columns. *Catalysis Today* 2003, 79–80 67–75.
[51] Haut B., Halloin V., Cartage T., Cockx A. *Chemical Engineering Sci*ence 2004, 59, 5687 – 5694.
[52] Mandal A., Kundu G., Mukherjee D. *Chemical Engineering and Processin*g 2003, 42, 777-787.
[53] Anabtawi M. Z. A., Abu-Eishah S., Hilal N., Nabhan M. B. W. *Chemical Engineering and Proces*sing 2003, 42, 403-408.
[54] Gómez-Díaz D., Navaza J. M., Sanjurjo B. Interfacial area evaluation in a bubble column in the presence of a surface-active substance. Comparison of methods. *Chemical Engineering Journal* 2008, 144, 379-385.
[55] Gómez-Díaz D., Gomes N., Teixeira J. A., Belo I. *Chemical Engineering Journal* 2009, 152, 354–360.
[56] Gerstenberg H. Blasensaulen-reaktoren (bubble column reactors). *Chemie Ingenieur Tech*nik 1979, 51, 208-216.

when reactions in which selectivity is highly dependent on temperature are involved. Bubble columns work equally well when gas throughput is high and even in the case of the simple type indicated before, a high rate of liquid circulation (due to rising gas bubble entrainment) ensures that when any solids such as catalyst, reagent or biomass are involved they are uniformly distributed. On the other hand, liquid circulation does have the adverse effect of increased back-mixing and if conversion expectations are high, the reactor volume will increase accordingly.

### *1.2.9.1. Operating states*

As the liquid phase has a significantly higher density than the gas phase, the liquid flow rate passing through a bubble column is low. The gas flow-rate is the most important parameter and together with the liquid phase coalescence determines the interfacial area for mass transfer. Gas throughput may vary widely according to the methods used and the specified conversion level. The normal range, based on empty reactor cross-sectional area, is in the region of 3-12 $cm \cdot s^{-1}$, although, in practice, very high rates in excess of bubble 1 $m \cdot s^{-1}$ are also used. The gas passing upwards through the reactor in bubble form entrains liquid with it which then proceeds to move downwards again, forming the distinctive flow pattern shown in figure 1.6.

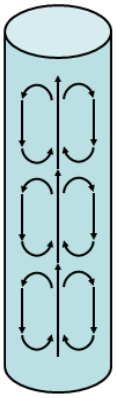

Figure 1.6. Liquid phase circulation patterns

As the bubbles plus entrained liquid tend to rise up through the centre and the larger bubbles in particular also gravitate towards this area, a radial gas hold-up and velocity profile results, despite an initial uniform distribution of gas across the whole cross-section of the reactor. Liquid close to the wall also moves downwards, transporting smaller bubbles with it for a certain distance. A radial cross-exchange of fluid elements is superimposed on the axial circulation pattern, giving rise to a high radial intermixing so that practically no liquid phase concentration gradients can be found in the radial direction.

When gas levels are low, bubbles are uniformly distributed in the liquid. Bubble size distribution is relatively sharply defined and rises uniformly through the column. This is known as homogeneous flow or bubbly flow regime and is represented in figure 1.7. There is practically no bubble coalescence or break-up[57].

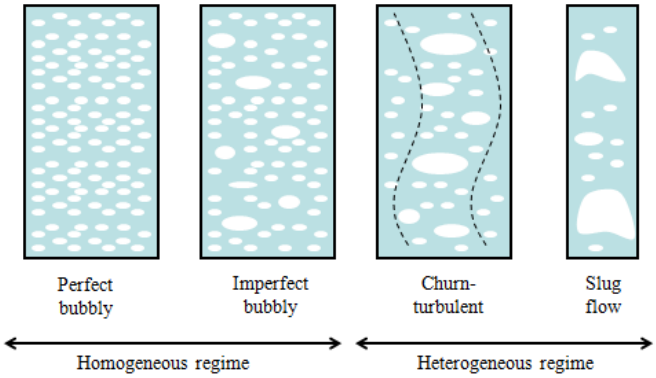


Figure 1.7. Operation states in bubble columns

However, this state is not maintained when gas passes more rapidly through the column. Bubble aggregates and large bubbles are formed and these rise more rapidly than the small bubbles. The churn-turbulent regime, also called the heterogeneous regime is maintained at higher superficial gas velocities (greater than 5 $cm \cdot s^{-1}$ in batch columns). This regime is characterized by the disturbed form of the homogeneous gas–liquid system due to enhanced

[57] Kantarci N., Borak F., Ulgen K. O. Review bubble column reactors. *Process Biochemistry* 2005, 40, 2263–2283.

turbulent motion of gas bubbles and liquid recirculation. As a result unsteady flow patterns and large bubbles with short residence times are formed by coalescence due to high gas throughputs. This flow regime is thus sometimes referred as coalesced bubble flow regime, indicating the much different sizes of the bubbles[58]. Churn-turbulent flow is frequently observed in industrial-size, large diameter columns[59].

A special situation arises in narrow bubble columns as generally used for laboratory work: the large bubbles in the heterogeneous zone are stabilized by the tube wall and move upwards through the column in a piston-like manner. These elongated bubbles (known as slugs) fill practically the whole cross-section and continue to grow by collecting smaller bubbles continuously throughout their upward journey. This is known as slug flow and is most likely to occur in tall appliances with column diameters of around 20 cm or less. Conversion rates and reactor capacity are low and data cannot be transferred to larger-diameter equipment. Slug flow should be strictly avoided in both laboratory and pilot plant, as test results are of little practical value.

[58] Schumpe A, Grund G. The gas disengagement technique for studying gas holdup structure in bubble columns. *Canadian Journal of Chemical Engineering* 1986, 64, 891–896.
[59] Hyndman C. L., Larachi F., Guy C. Understanding gas-phase hydrodynamics in bubble columns: a convective model based on kinetic theory. *Chemical Engineering Science* 1997, 52, 63–77.

### 1.2.10. Outline of this thesis

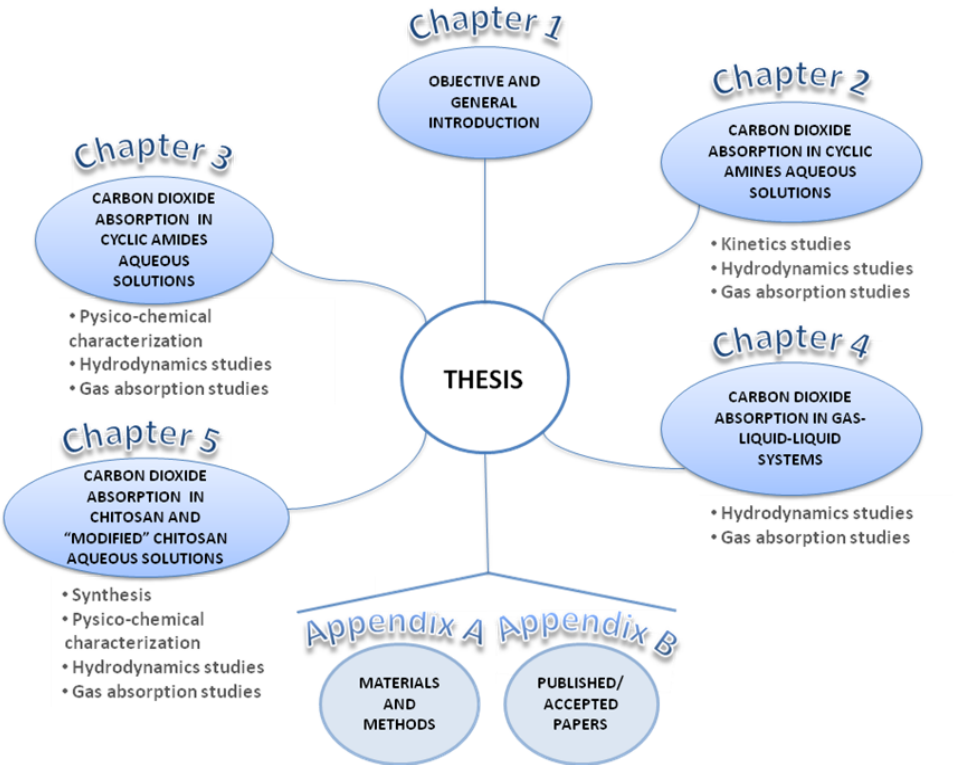

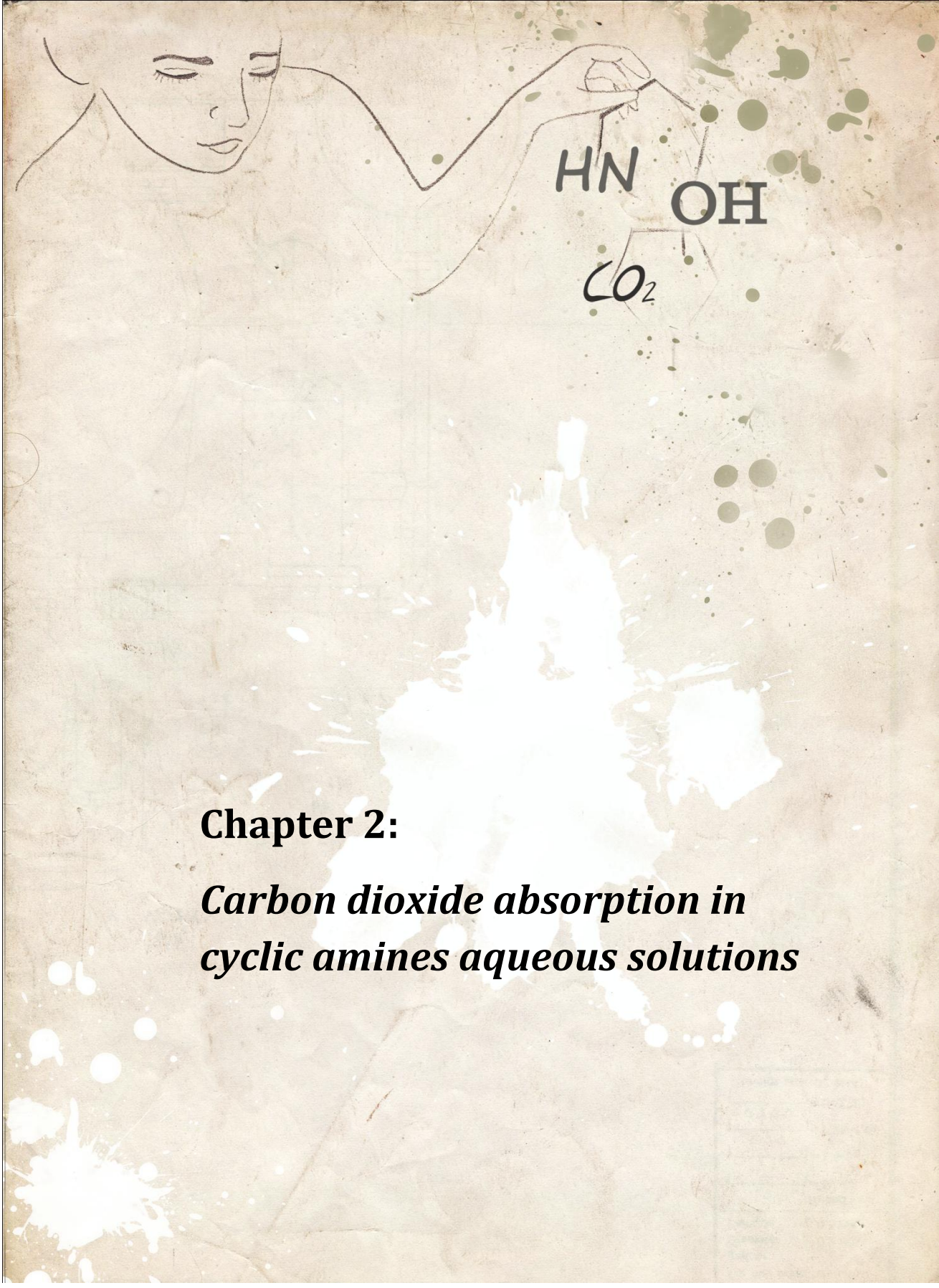


# Chapter 2:

## *Carbon dioxide absorption in cyclic amines aqueous solutions*

# 2.1 Kinetics of $CO_2$ chemical absorption into cyclic amines solutions

*Abstract*

*Chemical reaction kinetics between carbon dioxide with two cyclic amines (pyrrolidine and piperidine) in aqueous solution have been studied using a stirred tank reactor with a planar interfacial area. The operation variables considered in this work have been the amine concentration in the liquid phase and the reaction temperature. Specific absorption rates have been determined under different experimental conditions. Results indicate that the absorption process occurs in a pseudofirst reaction regime exhibited first-order kinetic with respect carbon dioxide and a second order for both cyclic amines. The reaction rate constant was determined under the different experimental conditions and it was fitted depending on the temperature by means of an Arrhenius type equation.*

## 2.1.1. Specific introduction

Globally speaking, about one third of all the anthropogenic carbon dioxide emissions come from fossil fuels, such as coal and oil, used to generate energy. A variety of industrial processes also emit large amounts of carbon dioxide from each plant, for example oil refineries, cement works and iron production[60]. There is a growing political and public concern, supported by consensus among the scientific community, about the global emissions growth, that will soon drive atmospheric carbon dioxide concentrations to levels never seen before, bringing a growing risk of a fast climate change.

The development of more effective processes for acid gases capture (such as carbon dioxide and sulphur dioxide) have produced an important increase in the research studies based on the development of new systems using chemical absorption between the acid gases and selective liquid phases. Absorption processes represent the most important physicochemical operation to remove carbon dioxide from gaseous streams. The absorption can be done either by using physical solvents such as water, methanol (Rectisol process) or N-methyl-2-pyrrolidone (Lurgi's Purisol process), or by using chemical solvents (reactive absorption), for instance, potassium carbonate (Benfield process), monoethanolamine (MEA; Girbotol process), Sulfolan + diisopropanolamine + water (Shell's Sulfinol process)[61] or amines blends[62,63,64]. Reactive absorption is the most preferred option used in the gas-processing industry for carbon dioxide removal, and the aqueous solutions of alkanolamines remain an industrial important class of compounds, used in the natural gas, petroleum chemical plants and ammonia industries for the removal of carbon dioxide and hydrogen sulfide from gas streams. A wide variety of alkanolamines, such as monoethanolamine (MEA), diethanolamine (DEA), di-isopropanolamine

[60] *IPCC Special report on carbon dioxide capture and storage*. Cambridge University Press. New York, USA 2005.
[61] Kohl A., Nielsen R. *Gas purification*. 5th edition. Gulf Publishing Company, Houston 1997.
[62] Bonenfant D., Mimeault M., Hausler R. Estimation of the $CO_2$ absorption capacities in aqueous 2-(2-aminoethylamino) ethanol and its blends with MDEA and TEA in the presence of $SO_2$. *Industrial & Engineering Chemistry Research* 2007, 46, 8968–8971.
[63] Bishnoi S., Rochelle G. T. Absorption of carbon dioxide in aqueous piperazine/methyldiethanolamine. *AIChE J*ournal 2002, 48, 2788-2799.
[64] Chakravarty T., Phukan U. K., Weiland R. H. Reaction of acid gases with mixtures of amines. *Chemical Engineering Progress* 1985, 81, 32-36.

(DIPA), N-methyldiethanolamine (MDEA) have been used industrially for an important number of years[65].

The present study pursues two aims: (i) the development of new alternative amine-based solvents, which are attractive for the enhancement of carbon dioxide capture, based on the use of cyclic amines, and (ii) the kinetic characterization of the reaction between carbon dioxide and cyclic primary amines (piperidine and pyrrolidine).

## 2.1.2. Results and discussion

Carbon dioxide flow density was determined by means of experimental data corresponding to the absorbed quantity of carbon dioxide along the operation time. Figures 2.1 and 2.2 show the experimental results obtained in relation to the carbon dioxide absorption rate, determined for the different liquid phases and experimental conditions employed in this study.

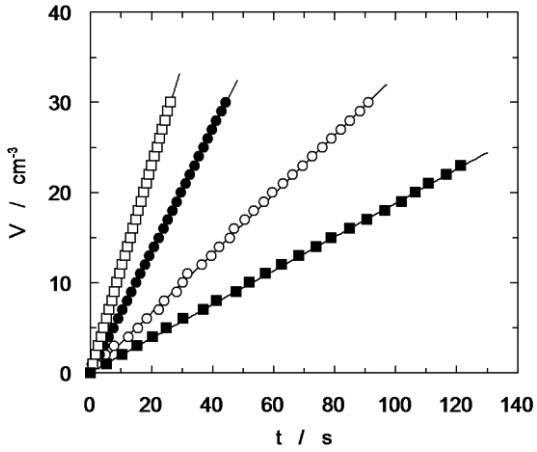


Figure 2.1. Influence of liquid phase composition upon carbon dioxide absorption rate in pyrrolidine aqueous solutions. (■) $C_B$ = 0.1 mol·L$^{-1}$; (○) $C_B$ = 0.3 mol·L$^{-1}$; (●) $C_B$ = 0.4 mol·L$^{-1}$; (□) $C_B$ = 0.5 mol·L$^{-1}$. T = 25 ºC.

[65] Kohl A., Nielsen R. *Gas purification*. 5th edition. Gulf Publishing Company, Houston 1997.

In these figures, the experimental data show a linear trend in all cases, and this behavior allows the use of these experimental data for kinetic determination. The slope of the linear plot, previously noted, allows the calculation of the absorption volumetric flux at different operation conditions. Results from figure 2.1 indicate that there is an influence of the initial pyrrolidine (PYR) concentration in the liquid phase upon the carbon dioxide absorption rate or upon the slope of linear fits. The presence of pyrrolidine in the aqueous solution increases the liquid phase viscosity (see table 2.1) (this effect tend to reduce mass transfer rate in physical absorption), so the obtained behavior confirms the existence of a chemical reaction in the liquid phase between the carbon dioxide and pyrrolidine, since an increase in the volumetric flux (related to the increase in the linear fit slope) is observed when the amine concentration increases in the liquid phase (see table 2.1). The same behavior has been obtained when different concentrations of piperidine were employed.

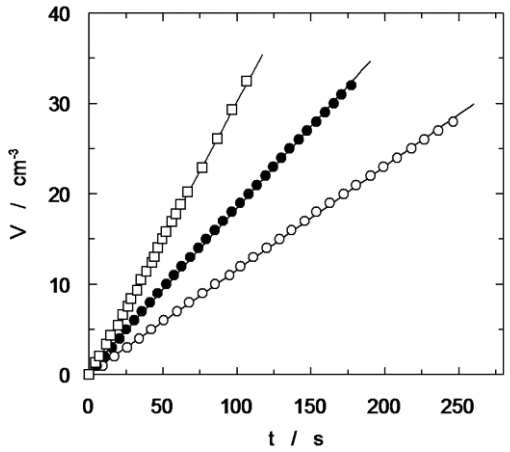


Figure 2.2. Effect of temperature upon carbon dioxide absorption rate in aqueous solutions of pyrrolidine. (○) T = 7 ºC; (●) T = 25 ºC; (□) T = 55 ºC. $C_B$ = 0.1 mol·L$^{-1}$.

Also the analysis of the influence of amines concentration in the liquid phase upon the carbon dioxide absorption rate has been developed, and the results allow to conclude that there is a chemical reaction between amines and carbon dioxide absorbed in the liquid phase. Figure 2.2 shows the effect of temperature upon the rate that the chemical absorption is produced.

Table 2.1. Viscosity of aqueous solutions of pyrrolidine (PYR), piperidine (PIP) at 20 ºC and absorption density for each amine system.

| $C_B$ (mol·L$^{-1}$) | PYR | | PIP | |
|---|---|---|---|---|
| | η (mPa·s) | $N_A \cdot 10^{-4}$ (mol·m$^2$·s$^{-1}$) | η (mPa·s) | $N_A \cdot 10^{-4}$ (mol·m$^2$·s$^{-1}$) |
| 0 | 0.989 | 9.7 | 0.989 | 9.7 |
| 0.1 | 1.023 | 22.4 | 1.016 | 22.4 |
| 0.2 | 1.058 | 35.2 | 1.044 | 34.8 |
| 0.3 | 1.094 | 56.1 | 1.073 | 55.2 |
| 0.4 | 1.131 | 83.0 | 1.105 | 80.9 |
| 0.5 | 1.168 | 117.2 | 1.137 | 113.7 |

Table 2.2. Viscosity of aqueous solutions of glucosamine (GA) and monethanolamine (MEA) at 20 ºC and absorption density for each amine system.

| $C_B$ (mol·L$^{-1}$) | GA | | MEA | |
|---|---|---|---|---|
| | η (mPa·s) | $N_A \cdot 10^{-4}$ (mol·m$^2$·s$^{-1}$) | η (mPa·s) | $N_A \cdot 10^{-4}$ (mol·m$^2$·s$^{-1}$) |
| 0 | 0.989 | 9.7 | 0.989 | 9.7 |
| 0.1 | 1.046 | 16.50 [66] | 1.013 | 12.9 |
| 0.2 | 1.114 | 21.40 [66] | 1.034 | 16.8 |
| 0.3 | 1.168 | 25.10 [66] | 1.055 | 20.0 |
| 0.4 | 1.227 | 27.30 [66] | 1.076 | 23.9 |
| 0.5 | 1.282 | - | 1.096 | 28.8 |

The experimental data show that an increase in temperature to employed in the absorption experiments also produces an increase in the slope of the plot between the carbon dioxide absorbed flow-rate and the operation time. This way, the absorption rate increases as well. Figure 2.2 includes experimental data corresponding to aqueous solutions of pyrrolidine, but a similar behaviour was observed for the same study using piperidine as an amine. The

[66] Gómez-Díaz D., Navaza J. M. Kinetics of carbon dioxide absorption into aqueous glucosamine solutions. *AIChE Journal* 2008, 54, 321-326.

obtained behavior, in relation to the influence of temperature upon the absorption rate, is similar to the corresponding ones using other kind of amines for carbon dioxide chemical absorption[67].

The cyclic amines employed in this work only include an amino group (NH), so the possible influence of the hydroxyl group (common in other amines employed for the carbon dioxide capture)[68] upon the kinetic study must not be taken into account.

Using the experimental data of carbon dioxide absorbed volume along the operation time, the gas flow density has been determined under the different experimental conditions. Figure 2.3 and 2.4 show the results calculated for both experimental systems employed in this work.

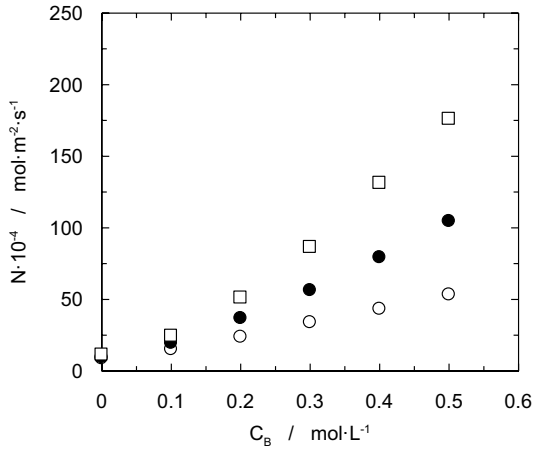


Figure 2.3. Influence of piperidine concentration upon the carbon dioxide absorbed flow. (○) T = 7 ºC; (●) T = 25 ºC; (□) T = 45 ºC.

It is also possible to observe in these figures the influence of each amine concentration in the liquid phase, as well as the effect caused by temperature upon the carbon dioxide absorption rate. The behavior observed for both amines is quite similar to a positive effect upon the absorption rate when the amines concentration increases in the liquid phase. The influence of temperature was also the same, producing an increase in the global gas mass transfer rate.

---

[67] Camacho F., Sanchez S., Pacheco R., Sanchez A., La Rubia M. D. Thermal effects of $CO_2$ absorption in aqueous solutions of 2-amino-2-methyl-1-propanol. *AIChE J*ournal 2005, 51, 2769-2777.
[68] Saha A. K., Biswas A. K., Bandyopadhyay S. S. Absorption of $CO_2$ in a sterically hindered amine: modeling absorption in a mechanically agitated contactor. *Separation and Purification Technology* 1999, 15, 101–112.

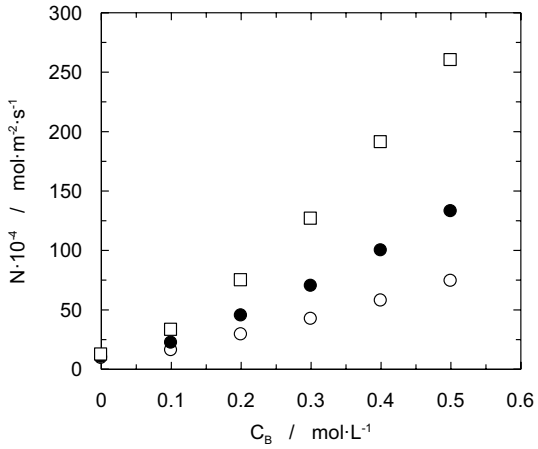


Figure 2.4. Influence of pyrrolidine concentration upon the carbon dioxide absorbed flow. (○) T = 15 ºC; (●) T = 35 ºC; (□) T = 55 ºC

In relation to the use of different amines for carbon dioxide capture, a comparison between the absorption rate data for carbon dioxide using aqueous solutions of ethanolamine (MEA) and glucosamine (GA)[69], have been carried out. MEA is commonly employed for carbon dioxide capture, while the use of aqueous solutions of GA for carbon dioxide removal has been suggested in the last years by our research team, contributing to improvements in operational safety in comparison to more common processes. Figure 2.5 shows this comparison between the behavior of these amines, and the experimental results indicate that cyclic amines (PYR and PIP) allow carbon dioxide capture at a higher absorption rate than aqueous solutions of MEA and GA.

Figure 2.5 also shows that the difference observed regarding absorption rate in the different amine-based systems is important, and it indicates that these cyclic amines improve significantly the carbon dioxide capture process.

The reaction between carbon dioxide and amine involves different parallel chemical reactions, such as the reaction between this gas and hydroxyl ions (bicarbonate formation) and water (carbonic acid formation). However, the influence of these reactions under the conditions employed in the present work could be considered negligible.

[69] Gómez-Díaz D., Navaza J. M. Kinetics of carbon dioxide absorption into aqueous glucosamine solutions. *AIChE J*ournal 2008, 54, 321-326.

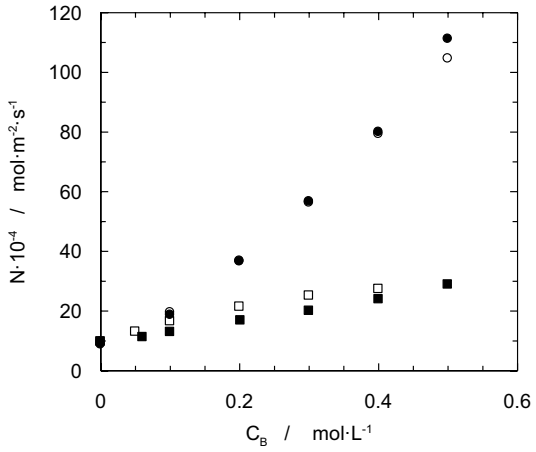


Figure 2.5. Comparison between the absorption flux density corresponding to cyclic amine systems and the corresponding ones for other primary amines. (○) piperidine; (●) pyrrolidine; (□) glucosamine[70]; (■) monoethanolamine. T = 25 ºC.

The carbonic acid formation and reaction is very slow and it must be considered of no influence upon the system studied. Regarding the other parallel reaction, it could be negligible due to the low hydroxyl ions concentration in the system, the way different studies have proved[71,72,73]. The kinetic has been analyzed on the basis of conclusions reached in different studies[74], which indicate that the carbamic reaction is the mechanism of reaction between carbon dioxide and amines when the carbonation relationship (moles of carbon dioxide/moles of amine) is less than 0.5. Under these conditions, three possible regimes could take place: physical absorption, fast-reaction and instantaneous regime. Since the amine concentration is high in the liquid phase and this implies values of $C_{Bo}/C_{Ao} >> 1$, the physical absorption regime must be ruled out.

[70] Gómez-Díaz D., Navaza J. M. Kinetics of carbon dioxide absorption into aqueous glucosamine solutions. *AIChE J*ournal 2008, 54, 321-326.
[71] Lee S., Song H. J., Maken S., Park J. W. Kinetics of $CO_2$ absorption in aqueous sodium glycinate solutions. *Industrial & Engineering Chemistry Research* 2007, 46, 1578-1583.
[72] Pinsent B. R., Pearson L., Roughton F. J. W. The kinetics of combination of carbon dioxide with hydroxide ions. *Transactions of the Faraday Soc*iety 1956, 52, 1512-1520.
[73] Ko J. J., Li M. H. Kinetics of absorption of carbon dioxide into solutions of N-methyldiethanolamine + water. *Chemical Engineering Science* 2000, 55, 4139-4147.
[74] Astarita G., Marrucci G., Gioia F. The influence of carbonation ratio and total amine concentration on carbon dioxide absorption in aqueous monoethanolamine solutions. *Chemical Engineering Science* 1964, 19, 95-103.

An instantaneous regime for the absorption, accompanied by a chemical reaction for order 1 kinetics regards to amine, relates the carbon dioxide flow density with the initial amine concentration, by means of a linear trend. Figure 2.3 and 2.4 involve this relation and the obtained behaviors show a non-linear trend.

The last regime, fast-reaction, allows the calculation of the carbon dioxide flow density ($N_A$) by means of equation 2.1, taking into account that the reaction order for the carbon dioxide, when reacting to aqueous solutions of amines, is commonly one.

$$N_A = C_{Ao}\sqrt{D_A \cdot k_{1,n} \cdot C_B^n} \tag{2.1}$$

where $C_{Ao}$ and $C_{Bo}$ are the initial concentrations of carbon dioxide and amine in the liquid phase, $D_A$ is the gas diffusivity in amine aqueous solutions and $k_{1,n}$ is the overall reaction rate constant. The diffusion coefficient corresponding to carbon dioxide in aqueous solutions of different cyclic amines was calculated employing the expression shown in equation 2.2[75].

$$D_A = D_{A,w} \cdot \left(\frac{\eta_w}{\eta}\right)^{0.8} \tag{2.2}$$

where $D_{A,w}$ is the diffusivity of carbon dioxide in pure water, $\eta_w$ and $\eta$ are the viscosity of pure water and the aqueous solutions of each amine, respectively. The value of carbon dioxide diffusivity in pure water was determined employing the expressions proposed by different studies[76]. On the other hand, the water viscosity and cyclic amines aqueous solutions have been obtained from literature[77]. It has been shown in the literature[78] that the partial order with respect

[75] Ratcliff G. A., Holdcroft J. G. Diffusivities of gases in aqueous electrolyte solutions. *Transactions of the Institution of Chemical Eng*ineers 1963, 41, 315–319.
[76] Versteeg G. F., van Swaaij W. P. M. Solubility and diffusivity of acid gases ($CO_2$, $N_2O$) in aqueous alkanolamine solutions. *Journal of Chemical & Engineering Data* 1988, 33, 29–34.
[77] Gómez-Díaz D., Navaza J. M. Kinetics of carbon dioxide absorption into aqueous glucosamine solutions. *AIChE J*ournal 2008, 54, 321-326.
[78] Charpentier J. C. Measurement of gas–liquid parameters. In: Gianetto A., Silvestone P. L. *Multiphase chemical reactors: theory, design, scale-up*. Hemisphere Publishing Corporation. NewYork USA 1986.

to carbon dioxide is always 1, as we obtained in this work based on the experimental data, but the partial order regarding the amine can vary between 1 and 2, depending on the chosen amine[79].

The initial carbon dioxide concentration in the liquid phase coincides with the concentration in equilibrium in the gas phase, and this parameter could be replaced in equation 2.1 employing Henry's law. These considerations allow us to obtain the linearized expression shown in equation 2.3 to fit experimental data, as well as to calculate the reaction order corresponding to amines:

$$\log\left(\frac{N_A^2 \cdot He^2}{P_A^2 \cdot D_A}\right) = \log\left(k_{1,n}\right) + n \cdot \log\left(C_B\right) \qquad (2.3)$$

where *He* is Henry's constant and $P_A$ is the carbon dioxide partial pressure.

Fitting the experimental values corresponding to the carbon dioxide flow density *versus* the initial amines concentration, the fit agreement is satisfactory and then, kinetic parameters were determined. In relation to the corresponding reaction order for each amine, it was determined for all temperatures and both systems show average values of 2.2 and 2.1 for piperidine and pyrrolidine, respectively. To a large extent of carbon dioxide – aqueous solutions of amines systems the corresponding reaction order is one[80], but in certain systems[81] the same reaction order as in the present work was obtained.

The value of the kinetic constant corresponding to each experimental system has also been determined in present work, using equation 2.3. The calculated values for this parameter and the influence of temperature are shown in figure 2.6.

[79] Bougie D. F., Iliuta M. C. Kinetics of absorption of carbon dioxide into aqueous solutions of 2-amino-2-hydroxymethyl-1,3-propanediol. *Chemical Engineering Sc*ience 2009, 64, 153-162.
[80] Xiao J., Li C. W., Li M. H. Kinetics of absorption of carbon dioxide into aqueous solutions of 2-amino-2-methyl-1-propanol + monoethanolamine. *Chemical Engineering Sci*ence 2000, 55, 161-175.
[81] Camacho F., Sánchez S., Pacheco R., Sánchez A., La Rubia M. D. Absorption of carbon dioxide at high partial pressures in aqueous Solutions of di-isopropanolamine. *Industrial & Engineering Chemistry Res*earch 2005, 44, 7451-7457.

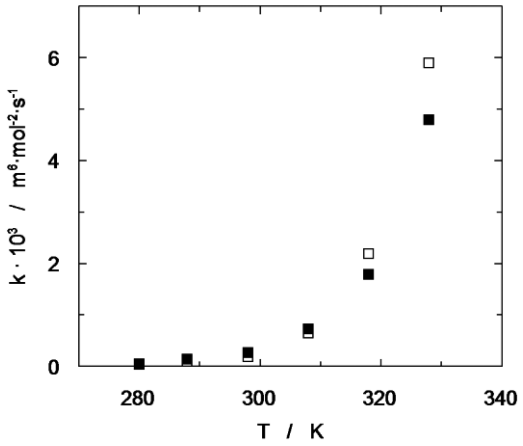


Figure 2.6. Effect of temperature upon the kinetic constant value corresponding to the chemical reaction between carbon dioxide and cyclic amines. (□) carbon dioxide – pyrrolidine system; (■) carbon dioxide – piperidine system.

For low temperature, both systems take similar values for the kinetic constant, but when temperature increases, the carbon dioxide – pyrrolidine system takes high values for this parameter in relation to the other system.

The influence of temperature upon the value of the kinetic constant for the reaction studied in present work has been analyzed. Experimental values have been fitted using an Arrhenius type equation to calculate the pre-exponential factor and the activation energy. Equations 2.4 and 2.5 show the calculated values for both parameters.

Piperidine: $$\ln k = 36.3 - \frac{9144}{T} \quad (2.4)$$

Pyrrolidine: $$\ln k = 37.9 - \frac{9620}{T} \quad (2.5)$$

Table 2.3. Activation energy for the chemicals reaction between carbon dioxide and several amines.

| Amine | Structure | $E_a$ / kJ·mol$^{-1}$ |
|---|---|---|
| Monoethanolamine (MEA) | 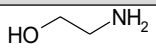 | 41.2[82] |
| Diethanolamine (DEA) | 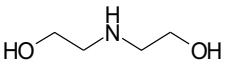 | 32.3[83] |
| Methyldiethanolamine (MDEA) | 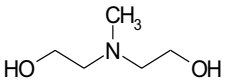 | 19.8[84] |
| 3-amino-1-propanol (AP) | 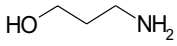 | 43.5[85] |
| 2-amino-2-methyl-1-propanol (AMP) | 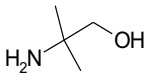 | 68.0[86] |
| 1-amino-2-propanol (MIPA) | 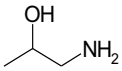 | 41.8[87] |

The values determined for the activation energy were 75.9 and 79.9 kJ·mol$^{-1}$ for piperidine and pyrrolidine, respectively. The calculated values for this parameter are higher than the corresponding ones for the reaction of carbon dioxide and other amines, such as MEA, MIPA, AP[85] and GA[88]. Taking into account the previously commented kinetic parameters, it can be concluded that the value of the pre-exponential parameter for the cyclic amines is higher than the

[82] Hikita H., Asai S., Ishikawa H., Honda M. The kinetics of reactions of carbon dioxide with monoethanolamine, diethanolamine and triethanolamine by a rapid mixing method. *Chemical Engineering Journal* 1977, 13, 7-12.
[83] Ali S. H. Kinetic study of the reaction of diethanolamine with carbon dioxide in aqueous and mixed solvent systems—application to acid gas cleaning. *Separation and Purification Technology* 2004, 38, 281–296.
[84] Ko J. J., Li M. H. Kinetics of absorption of carbon dioxide into solutions of N-methyldiethanolamine + water. *Chemical Engineering Science* 2000, 55, 4139-4147.
[85] Penny D. E., Ritter T. J. Kinetic study of the reaction between carbon dioxide and primary amines. *Journal of the Chemical Society Faraday Transactions*. 1983, 79, 2103-2109.
[86] Camacho F., Sanchez S., Pacheco R., Sanchez A., La Rubia M. D. Thermal effects of $CO_2$ absorption in aqueous solutions of 2-amino-2-methyl-1-propanol. *AIChE Journal* 2005, 51, 2769-2777.
[87] Hikita H., Asai S., Ishikawa H., Honda M. The kinetics of reactions of carbon dioxide with monoisopropanolamine, diglycolamine and ethylendiamine by a rapid mixing method. *Chemical Engineering Journal* 1977, 14, 27-30.
[88] Gómez-Díaz D., Navaza J. M. Kinetics of carbon dioxide absorption into aqueous glucosamine solutions. *AIChE Journal* 2008, 54, 321-326.

corresponding one for other amines previously commented, and these cyclic amine systems also take higher values for the activation energy (see table 2.3).

Table 2.3. Activation energy for the chemicals reaction between carbon dioxide and several amines (continuation).

| Amine | Structure | $E_a$ / kJ·mol$^{-1}$ |
|---|---|---|
| Di-isopropanolamine (DIPA) | 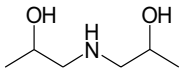 | 59.9[89] |
| N,N-diethylethanolamine (DEEA) | 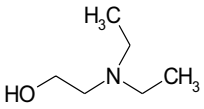 | 95.4[90] |
| Glucosamine (GA) | 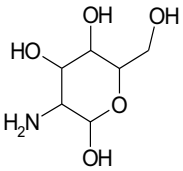 | 47.6[91] |
| Piperidine (PIP) | 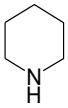 | 75.9 |
| Pyrrolidine (PYR) |  | 79.9 |

The preexponential factor is proportional to the global number of collisions which lead to reaction, while the other part of the equation, that involves the activation energy, is the fraction of collisions that results in reaction (effective collisions).

Bearing these comments in mind, we can conclude that the reaction between carbon dioxide absorbed and the cyclic amines (PYR and PIP) present in the liquid phase, requires a

[89] Camacho F., Sánchez S., Pacheco R., Sánchez A., La Rubia M. D. Absorption of carbon dioxide at high partial pressures in aqueous Solutions of di-isopropanolamine. *Industrial & Engineering Chemistry Research* 2005, 44, 7451-7457.
[90] Vaidya P. D., Kenig E. Y. A study on $CO_2$ absorption kinetics by aqueous solutions of N,N-diethylethanolamine and N-ethylethanolamine. *Chemical Engineerin & Technology* 2009, 32, 556–563.
[91] Gómez-Díaz D., Navaza J. M. Kinetics of carbon dioxide absorption into aqueous glucosamine solutions. *AIChE Journal* 2008, 54, 321-326.

higher activation energy (higher energy barrier) than the corresponding reaction of this gas with other common amines. This behavior is due to the reaction with cyclic amines, which suffer a high steric hindrance that difficult the effective collisions between both molecules. But on the other hand, these cyclic amines provide a higher electronic density regarding other amines (i.e. MEA and GA), that favor the chemical reaction and then increase the reaction rate (shown in figure 2.7).

The Hatta number (*Ha*) and enhancement factor (*E*) have been calculated with the aim of confirming the reaction regime supposed at the beginning of the results and discussion section. Equation 2.6 has been employed to determine the Hatta number,

$$Ha = \sqrt{\frac{k \cdot C_{Bo} \cdot D_A}{k_L^2}} \tag{2.6}$$

where $k_L$ is the liquid phase mass transfer coefficient.

Equation 2.7 has been employed to calculate the value of this enhancement factor, based on the value of carbon dioxide flux density.

$$E = \frac{N_A}{k_L \cdot C_A^*} \tag{2.7}$$

Equations 2.6 and 2.7 include in their expressions the value of mass transfer coefficient corresponding to the liquid phase, $k_L$. This parameter has been determined employing the same aqueous solutions of cyclic amines, but the pH was modified adding hydrochloride to produce an acidic medium and then inhibit the chemical reaction between carbon dioxide and the amines.

In addition, the instantaneous enhancement factor has been calculated employing equation 2.8.

$$E_i = 1 + \frac{D_B}{D_A} \cdot \frac{C_{Bo}}{C_A^*} \tag{2.8}$$

The diffusion coefficient for each cyclic amine ($D_B$) in aqueous solution has been calculated by means of the Wilke-Chang equation modified by Hayduk and Laudie[92,93] (equation 2.9).

$$D_B = \frac{7.4 \cdot 10^{-8} \cdot \sqrt{\varphi_w \cdot M_w} \cdot T}{\eta_w \cdot V_B^{0.6}} \qquad (2.9)$$

where $M_w$ is molecular weight of water, $T$ is temperature, $\eta_w$ is the viscosity of water, $V_B$ is the molar volume of each amine, and $\varphi_w$ is the solvent (water) association factor with a value of 2.26.

Using the previously commented equations we can observe that the values of Hatta number take values in all the cases into the interval established by equation 2.10, which match the characteristics of an instantaneous and pseudofirst reaction order.

$$3 < Ha < \frac{10 \cdot \mathrm{E_i}}{2} \qquad (2.10)$$

Figure 2.7 shows the relation between the enhancement factor and Hatta number in logarithmic coordinates. This plot shows that the enhancement factor experimental data takes values lower than the bisector. Therefore, the instantaneous reaction regime for the absorption accompanied by a chemical reaction between carbon dioxide and pyrrolidine is confirmed. The reactive system formed by carbon dioxide and piperidine aqueous solutions shows the same behavior previously described for aqueous solutions of pyrrolidine.

[92] Wilke C. R., Chang P. Correlation of diffusion coefficients in dilute solutions. *AIChE Journal* 1955, 1, 264-270.
[93] Hayduk W., Laudie H. Prediction of diffusion coefficients for nonelectrolytes in dilute aqueous solutions. *AIChE Journal* 1974, 20, 611-615.

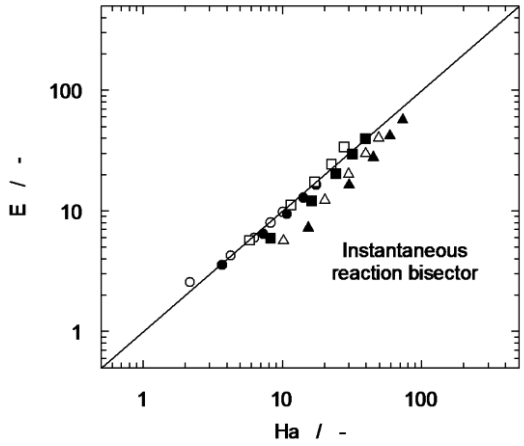


Figure 2.7. Relation between enhancement factor and Hatta number for carbon dioxide – aqueous solutions of pyrrolidine. (○) T = 7 ºC; (●) T = 15 ºC; (□) T = 25 ºC; (■) T = 35 ºC; (△) T = 45 ºC; (▲) T = 55 ºC.

In the case of chemical reaction between carbon dioxide and glucosamine is possible to observe that the values of Hatta number take values in all cases into the interval established by equation 2.11, which match the characteristics of a moderately-fast reaction. This behavior is in agreement with the experimental results showed in figure 2.5.

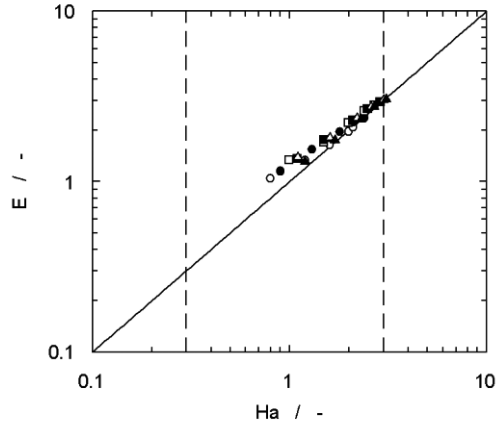


Figure 2.8. Relation between enhancement factor and Hatta number for carbon dioxide – aqueous solutions of glucosamine. (○) T = 7 ºC; (●) T = 15 ºC; (□) T = 25 ºC; (■) T = 35 ºC; (△) T = 45 ºC; (▲) T = 55 ºC.

$$0.3 < Ha < 3 \tag{2.11}$$

Figure 2.8 shows the relation between the enhancement factor and Hatta number in logarithmic coordinates for that system. This plot shows that the enhancement factor experimental data are higher than the bisector. Therefore, there is a relation corresponding to a moderately-fast reaction regime.

### 2.1.3. Conclusions

Two new amines (pyrrolidine and piperidine) have been employed to capture carbon dioxide by chemical absorption, and the reaction kinetic for both systems has been determined. The absorption rate experimental data and the chemical absorption theory have determined the existence of an instantaneous and pseudo-first reaction regime between the carbon dioxide and both cyclic amines. The reaction order corresponding to carbon dioxide was one and two for the amines. The influence of the temperature upon the rate constant has been analyzed, and the activation energy was calculated and compared with the value obtained for other carbon dioxide–amine systems. The conclusion is that the amines employed in the present study show a higher steric hindrance, but also have high electron density, involved in the high reaction rate shown in these experimental systems.

# 2.2 Hydrodynamics in $CO_2$ - cyclic amines systems

*Abstract*

*The present work analyses the influence of different operation conditions upon hydrodynamic parameters, such as the bubble size distribution, the gas hold-up produced in the liquid phase and the gas-liquid interfacial area. The influence upon the hydrodynamic parameters of commonly analysed variables in gas-liquid contactors, such as gas flow-rate and reagent (glucosamine and pyrrolidine) concentration in the liquid phase, has been studied. However, the influence of the operation time must also be taken into account due to the operation regime (semicontinuos). Under these considerations, the chemical absorption intensity varies throughout time and it could produce some changes upon the global absorption process, due to modifications in the mass transfer interfacial area.*

## 2.2.1. Specific introduction

Industrial processes where certain components, present in a gas phase, must be absorbed into a liquid one are common in chemical process industries and, in several cases, this contact is useful to produce reactions among certain substances from both two phases. Bubble contactors (columns, stirred vessels or air-lift contactors) have a wide range of uses in chemical, biochemical and pharmaceutical industries[94], since these equipments provide an effective contact between the gas and liquid phases, allowing to carry out chemical or biochemical reactions under suitable conditions. Besides, the simple construction, low operating cost and high-energy efficiency are interesting characteristics of this kind of equipments. In bubble contactors, the mass transfer rate is influenced by the available gas-liquid interfacial area, which could play a very important role in the global absorption process[95].

When dealing with studies related to the gases absorption in liquid phases using bubbling equipment, the volumetric mass transfer coefficient (defined as the product of the mass transfer coefficient and the gas-liquid specific interfacial area) is commonly used to evaluate the mass transfer process behaviour[96,97,98]. However, the fact is that this parameter is the product of others, so it implies additional difficulties to extract valuable conclusions. It is also important to take into account that one operation variable could produce a different influence upon the mass transfer coefficient and upon the specific interfacial area[99], and then, the sum of these behaviours has influence on the volumetric mass transfer coefficient. When only the volumetric mass transfer coefficient data are available, it is difficult to take decisions to improve the absorption global process by means of modifications upon the operation variables. For these reasons, it is necessary to analyse the influence of each operation variable upon the gas-liquid interfacial area in this kind

[94] Lee S. Y., Tsui Y. P. Succeed at gas/liquid contacting. *Chemical Engineering Progress* 1999, 95, 23-49.
[95] Camarasa E., Vial C., Poncin S., Wild G., Midoux N., Bouillard J. Influence of coalescence behaviour of the liquid and of gas sparging on hydrodynamics and bubble characteristics in a bubble column. *Chemical Engineering and Processing* 1999, 38, 329–344.
[96] Mineta R., Salehi Z., Yoshikawa H., Kawase Y. Oxygen transfer during aerobic biodegradation of pollutants in a dense activated sludge slurry bubble column: Actual volumetric oxygen transfer coefficient and oxygen uptake rate in p-nitrophenol degradation by acclimated waste activated sludge. *Biochemical Engineering Journal* 2011, 53, 266–274.
[97] Cerri, M.O., Badino, A.C. Oxygen transfer in three scales of concentric tube airlift bioreactors. *Biochemical Engineering Journal* 2010, 51, 40–47.
[98] Kilonzo P. M., Margaritis A., Bergougnou M. A. Hydrodynamics and mass transfer characteristics in an inverse internal loop airlift-driven fibrous-bed bioreactor. *Chemical Engineering Journal* 2010, 157, 146–160.
[99] Gómez-Díaz D., Navaza J. M., Quintáns-Riveiro L. C., Sanjurjo B. Gas absorption in bubble column using a non-Newtonian liquid phase. *Chemical Engineering Journal* 2009, 146, 16–21.

of equipments (bubbling contactors), since this parameter could have an important influence upon the mass transfer rate[100,101,102].

A similar situation is observed in absorption processes with a chemical reaction in the liquid phase, because in an important number of studies, the gas-liquid interfacial area is not analysed separately from the global mass transfer process. In physical absorption operations, the mass transfer rate could be considered low (comparing it to the chemical absorption), and then, we can suppose that the interfacial area remains constant along the operation time until the gas saturation is reached. This simplification cannot be used when the absorption process is accompanied by a chemical reaction in the liquid phase that implies a rapid or instantaneous absorption regime. When this situation is produced, the bubbles' size is reduced due to the important mass transfer caused by the fast chemical reaction. Under these conditions, the analysis of the absorption process must take into account the influence of the time upon the gas-liquid interfacial area, both analysing the effect upon the bubble size distribution and upon the gas hold-up in the liquid phase.

## 2.2.2. Results and discussion

### *2.2.2.1. Pyrrolidine*

In relation to the bubble's size, a geometric characteristic (Sauter mean diameter) that allows the behaviour analysis, as well as perform comparisons, has been determined by means of the experimental procedure described in the materials and experimental section. To perform these measurements, different photographs have been obtained under the experimental conditions used in this work and along the bubble column's height. An example of these photographs is shown in figure 2.9. These images have been obtained using a fix amine concentration and gas flow-rate, taking photographs at different operation times. The images let

[100] Tsai R. E., Schultheiss P., Kettner A., Lewis J. C., Seibert A. F., Eldridge R. B., Rochelle G. T. Influence of surface tension on effective packing area. *Industrial and Engineering Chemistry Research* 2008, 47, 1253-1260.
[101] Alves S. S., Maia C. I., Vasconcelos J. M. T. Gas-liquid mass transfer coefficient in stirred tanks interpreted through bubble contamination kinetics. *Chemical Engineering and Processing* 2004, 43, 823–830.
[102] Vandu C. O., Krishna R. Volumetric mass transfer coefficients in slurry bubble columns operating in the churn-turbulent flow regime. *Chemical Engineering Science* 2004, 59, 5417 – 5423.

us reach clearly a first conclusion, that is, the great importance of the chemical reaction in the liquid phase upon the bubble's size. This conclusion is reached observing the important differences in the bubble's diameter at different operation times. Firstly, the bubbles size is minor that the bubbles shown in photographs at higher times. This visual observation indicates that the bubble's size increases in the course of time, that is, when the liquid phase reagent concentration decreases.

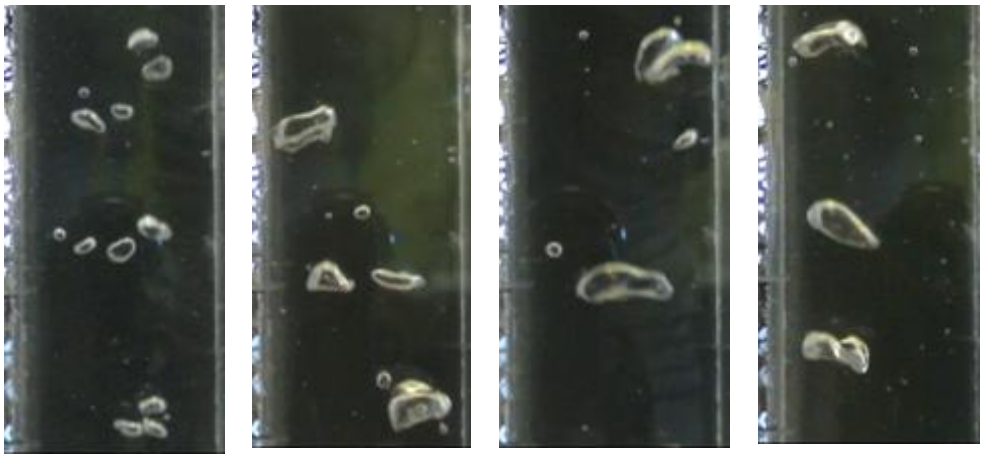

t = 0 s t = 1800 s t = 4200 s t = 9900 s

Figure 2.9. Influence of amine initial concentration upon bubble's size. $C_{PYR}$ = 0.5 mol·L$^{-1}$. $Q_g$ = 40 L·h$^{-1}$.

Different photographs have been analysed (until reaching the number of bubbles indicated in the materials and experimental section) at different bubble column height and under the experimental conditions studied in this work. These measurements allow us to obtain the bubble size distribution that is used to calculate the Sauter mean diameter. An example of this kind of distributions obtained using this methodology is shown in figure 2.10, where the operation time is varied at a fixed amine initial concentration and gas flow-rate.

Firstly, a narrow bubble size distribution is observed and, when time increases, a displacement in the distribution is produced to higher values of bubble diameter. An increase in the distribution width is also observed with similar values for small bubbles at different times. But an important increase in the number of large bubbles is observed when the operation time increases. In relation to the increase in the bubble's size with time, this behaviour is in agreement

with the photographs shown in figure 2.9. This increase could be due to the fact that, when time increases, a decrease in the chemical reaction intensity is observed, and this procedure causes a decrease in the value of the mass transfer rate. This reduction in mass transfer rate produces that the bubbles remain with a higher size because the gas is transferred at a lower rate to the liquid phase.

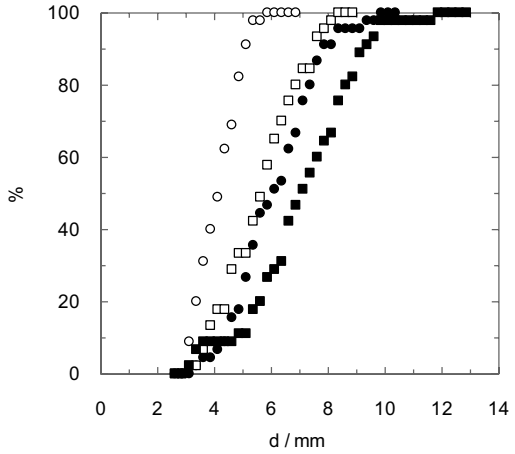


Figure 2.10. Effect of time upon bubble size distribution. $C_{PYR}$ = 0.3 mol·L$^{-1}$. $Q_g$ = 18 L·h$^{-1}$. (○) t = 0 s, (●) t = 1800 s, (□) t = 3600 s, (■) t = 7200 s.

At first, the largest bubbles are found at the bottom of the bubble column because when the gas ascends, the bubbles reduce their size due to gas transfer to react with the pyrrolidine. But when the pyrrolidine reduces the concentration at the liquid phase, bubbles with high diameters are found at the column top, caused by the existence of a coalescence process among the bubbles.

The experimental data corresponding to the bubble size distribution (see figure 2.10), by means of photographs as the examples shown in figure 2.9, are used to calculate the Sauter mean diameter, using the equations showed in the materials and experimental section. This methodology let us uses a unique diameter value to analyse the influence of different variables upon the bubble's size and, then, upon the gas-liquid interfacial area generated into the bubbling contactor. Figure 2.11 shows an example of the evolution of Sauter mean diameter, as well as the

influence of the gas flow-rate upon this parameter when a chemical absorption takes place in the liquid phase.

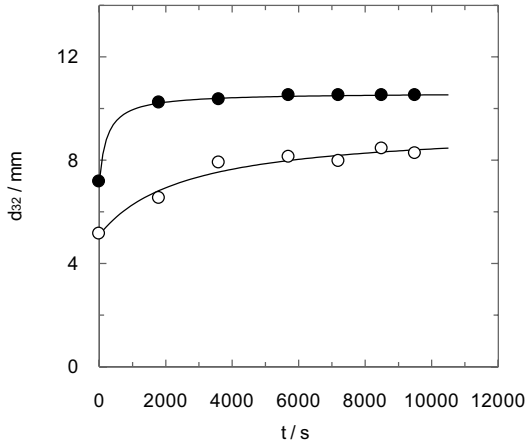


Figure 2.11. Influence of gas flow-rate upon Sauter mean diameter along the operation time. $C_{PYR}$ = 0.1 mol·L$^{-1}$. (○) $Q_g$ = 18 L·h$^{-1}$, (●) $Q_g$ = 40 L·h$^{-1}$.

As the first observation in figures 2.9 and 2.10, figure 2.11 shows an increase in Sauter mean diameter with time until a constant value is reached. Figure 2.11 also shows that, at high values of gas flow-rate, the bubble's size increases quickly and then, it reaches a constant value in a minor operation time. This behaviour is due to the fast reagent consumption in the liquid phase, since the mass transfer increases with the gas flow-rate[103,104,105].

Figure 2.12 shows the influence of the pyrrolidine initial concentration upon the evolution of bubble's size along the experiment time. A similar behaviour is observed for the different amine concentrations; however, the time necessary to reach a constant value for Sauter mean diameter is higher when the pyrrolidine concentration increases. This fact is produced (in

[103] Farines V., Baig S., Albet J., Molinier J., Legay C. Ozone transfer from gas to water in a co-current upflow packed bed reactor containing silica gel. *Chemical Engineering Journal* 2003, 91, 67–73.
[104] Mehrnia M. R., Towfighi J., Bonakdarpour B., Akbarnegad M. M. Influence of top-section design and draft-tube height on the performance of airlift bioreactors containing water-in-oil microemulsion. *Journal of Chemical Technology and Biotechnology* 2004, 79, 260–267.
[105] Yazdiana F., Shojaosadati S. A., Nosrati M., Mehrnia M. R. Vasheghani-Farahani E. Study of geometry and operational conditions on mixing time, gas holdup, mass transfer, flow regime and biomass production from natural gas in a horizontal tubular loop bioreactor. *Chemical Engineering Science* 2009, 64, 540-547.

agreement with previous comments) because a higher amine concentration maintains the chemical reaction for a longer time, and this process does not allow to reach a higher bubble's size.

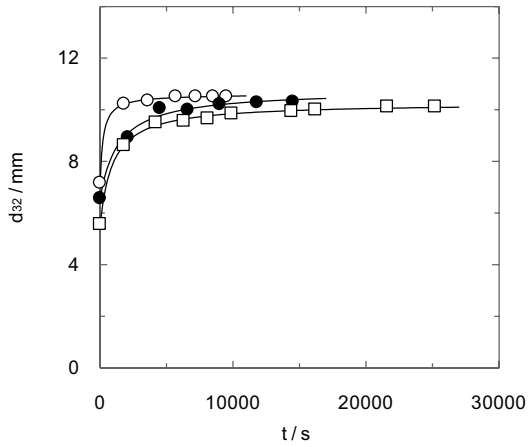


Figure 2.12. Evolution of Sauter mean diameter along the operation time. Influence of pyrrolidine inicial concentration. $Q_g$ = 40 L·h$^{-1}$. (○) $C_{PYR}$ = 0.1 mol·L$^{-1}$, (●) $C_{PYR}$ = 0.3 mol·L$^{-1}$, (□) $C_{PYR}$ = 0.5 mol·L$^{-1}$.

It is commented in the materials and methods section the requirement of knowing the bubble diameter under the different experimental conditions, but the gas hold-up is also needed to use equation A.7 to determine the gas-liquid specific interfacial area. A similar behaviour than the previously one commented for Sauter mean diameter was observed for the gas hold-up in relation to the influence of time: an increase in the gas hold-up with time until reaching a constant value. A difference we have found in relation to these two parameters is that the increase in the gas hold-up is slighter than the intense increase observed for the Sauter mean diameter. In relation to the influence of the gas flow-rate, an increase in this variable produces an increase in the gas hold-up. Also, a low amine concentration causes the constant value in the hold-up to be reached in a minor time.

Using the Sauter mean diameter and the gas hold-up data at each experimental condition, the gas-liquid interfacial area has been calculated. Figure 2.13 shows an example of the obtained behaviour that seems similar to the previously one commented for the bubble diameter.

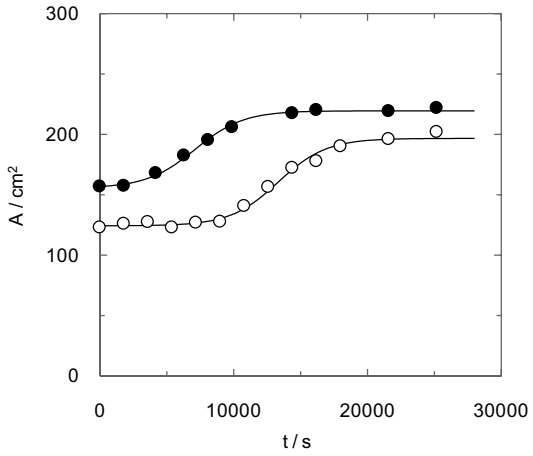


Figure 2.13. Effect of gas flow-rate upon gas-liquid interfacial area. $C_{PYR}$ = 0.5 mol·L$^{-1}$. (○) $Q_g$ = 18 L·h$^{-1}$, (●) $Q_g$ = 40 L·h$^{-1}$.

The interfacial area increases until reaching a constant value, but this behaviour has a different shape that in the case of bubble size. At low operation time, the interfacial area increases slowly, and a larger increase is produced at a higher time, until the final value is achieved.

This behaviour is in agreement with previous studies that have observed a higher importance of the gas hold-up upon the interfacial area value than the effect caused by the Sauter mean diameter[106,107]. The gas hold-up increases slighter than the Sauter mean diameter behaviour, previously commented, and it explains the behaviour shown in figure 2.13. In the analysis of the gas flow-rate influence upon the gas-liquid interfacial area, higher values corresponding to the large gas flow-rate are observed, and this behaviour is in agreement with the most common behaviour found in literature[108,109]. This behaviour is due to the fact that an increase in gas flow-rate produces large bubbles (see figure 2.11), but also high gas hold-up values. The increase in the Sauter mean diameter has a negative influence upon the interfacial

[106] Gómez-Díaz D., Gomes N., Teixeira J. A., Belo I. Oxygen mass transfer to emulsions in a bubble column contactor. *Chemical Engineering Journal* 2009, 152, 354–360.
[107] Cerri M. O., Baldacin J. C., Cruz A. J. G., Hokka C. O., Badino A. C. Prediction of mean bubble size in pneumatic reactors. *Biochemical Engineering Journal* 2010, 53, 12–17.
[108] Cents A. H. G., Jansen D. J. W., Brilman D. W. F., Versteeg G. F. Influence of small amounts of additives on gas hold-up, bubble size, and interfacial area. *Industrial and Engineering Chemistry Research* 2005, 44, 4863-4870.
[109] Painmanakul P., Loubière K., Hébrard G., Mietton-Peuchot M., Roustan M. Effect of surfactants on liquid-side mass transfer coefficients. *Chemical Engineering Science* 2005, 60, 6480–6491.

area, but the opposite influence is caused by the increase in the gas hold-up. We can observe in figure 2.13 that the interfacial area values increase with the gas flow-rate, and this behaviour confirms the higher influence of the gas hold-up upon interfacial area than the Sauter mean diameter.

Also, when gas flow-rate is varied, the enhancement of the gas-liquid interfacial area is produced at different times. The increase in the interfacial area value is produced at a higher time for the lowest gas flow-rate, and this behaviour is due to the fact that the reaction in the liquid phase takes place for a wider time (producing bubbles with low size for a higher time range).

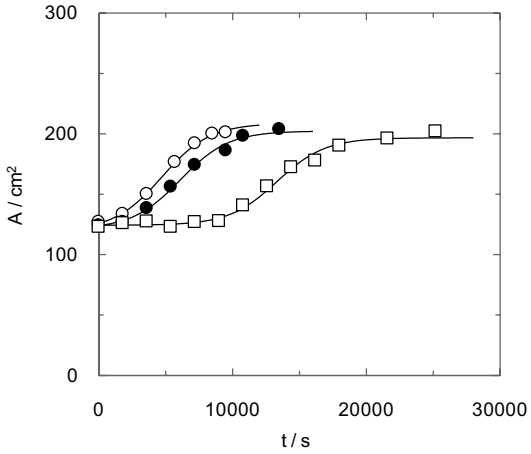


Figure 2.14. In fluence of pyrrolodine initial concentration upon interfacial area. $Q_g$ = 18 L·h$^{-1}$. (○) $C_{PYR}$ = 0.1 mol·L$^{-1}$, (●) $C_{PYR}$ = 0.3 mol·L$^{-1}$, (□) $C_{PYR}$ = 0.5 mol·L$^{-1}$.

The influence of the pyrrolidine initial concentration upon the value of gas-liquid interfacial area has been analysed, and figure 2.14 shows an example of the experimental data. A similar behaviour in relation to its shape has been observed for the different amine concentrations. The gas-liquid interfacial area value reached at the end of the experiments takes similar values, but an increase in the amine initial concentration increases the time necessary to obtain a constant value for the gas-liquid interfacial area. The rate of reagent consumption in the liquid phase produces this behaviour, as it was previously commented.

The interfacial area data has been fitted using a correlation based on important variables corresponding to the system used in this work, and to avoid the presence of time in the correlation. For this reason, different dimensionless numbers have been used taken into account variables, like the gas flow-rate fed to bubble column and the bubble's size. The expression obtained by fitting the experimental data with this correlation is shown in equation 2.12:

$$A = 0.05 \cdot Fr^{-0.04} \cdot Ha^{-0.004} \cdot \left( \frac{d_{32}}{L_C} \right)^{0.76} \qquad (2.12)$$

where *Fr* is the Froud number, *Ha* is the Hatta number, $d_{32}$ is the Sauter mean diameter and $L_c$ is the bubble column side.

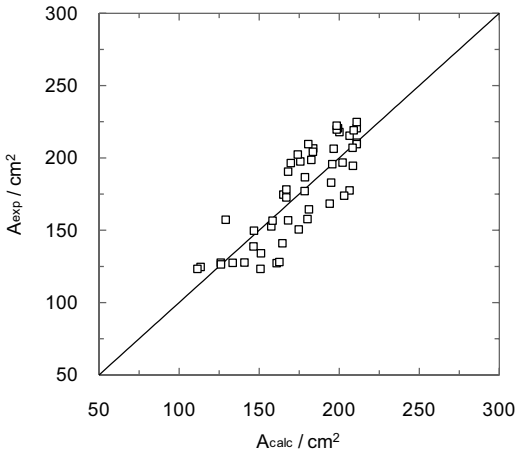


Figure 2.15. Comparison between experimental and calculated interfacial area using equation 2.12.

Figure 2.15 shows the comparison of experimental and calculated data by means of equation 2.12, where we can observe certain dispersion of results with a standard deviation of ± 15 $cm^2$. We can also observe in equation 2.12 the low influence of Hatta number upon the value of gas-liquid interfacial area, and the high importance of bubble's diameter.

### *2.2.2.2. Glucosamine*

The glucosamine is not a hazardous substance, which is an advantage over the amines used to capture carbon dioxide at present (see table 1.4 introduction section).

As in the case of pyrrolidine, a photographic method has been employed (material and methods section) because it has been recommended in different studies to determine this hydrodynamic parameter[110]. In relation to the influence caused by the gas flow-rate upon the interfacial area, an increase in the bubble diameter and the gas hold-up in the bubble column are observed when gas flow-rate is increased. These two parameters have an opposite influence upon the interfacial area, but in figure 2.16 it can be observed that the gas hold-up has a more important weight upon the gas-liquid interfacial area and then, an increase in this value is observed when gas flow-rate is increased.

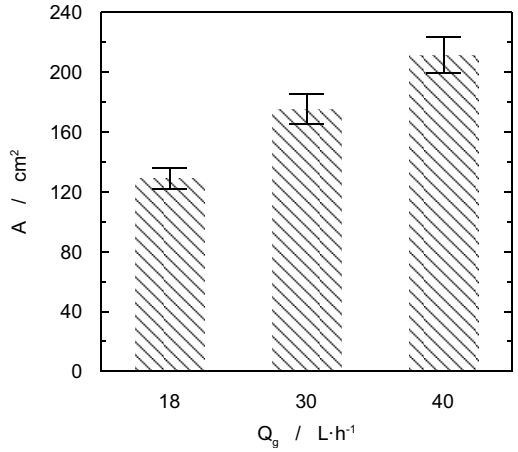


Figure 2.16. Influence of $CO_2$ gas flow-rate upon gas-liquid interfacial area produced in the bubble column reactor.

[110] Gómez-Díaz D., Navaza J. M., Quintáns-Riveiro L. C., Sanjurjo B. Gas absorption in bubble column using a non-Newtonian liquid phase. *Chemical Engineering Journal* 2009, 146, 16–21.

About the influence of the glucosamine and sodium hydroxide concentration upon the interfacial area, previous studies indicate that an increase in the liquid phase viscosity[111] and the presence of electrolyte[112] could have certain influence upon the interfacial area, causing a decrease or increase in this parameter. In this work, the variation of glucosamine concentration does not have any influence upon the gas-liquid interfacial area, with similar values to the determined ones for pure water. An increase in the glucosamine concentration in the liquid phase increases the viscosity[113], and this change in this physical property produces a negative effect upon the interfacial area (previously commented). In this system, the change in viscosity with a glucosamine concentration is low and then, the influence of the glucosamine presence could be considered negligible. The same behaviour has been obtained in the analysis of the influence of sodium hydroxide concentration upon the gas-liquid interfacial area. Also, the fact that the reaction between carbon dioxide and glucosamine was not an instantaneous regime implies a non influence of time upon bubbles size and gas-liquid interfacial area.

### 2.2.3. Conclusions

This work analyses the effect caused by the existence of a chemical absorption between carbon dioxide and pyrrolidine upon the gas-liquid interfacial area in a bubbling contactor. The bubble diameter increases with time due to the decrease in the reaction rate by the consumption of the liquid phase reagent. The chemical reaction has a fast regime and it enhances the mass transfer rate; then, it causes a decrease in bubble's size. Also, the effect of the amine concentration in the liquid phase produces a decrease in the bubble's size caused by the relation between the reaction rate and the mass transfer rate. The gas-liquid interfacial area behaviour is the sum of the gas hold-up and the bubble size distribution effects, and the interfacial area is more influenced by the gas hold-up because an increase in the interfacial area value along the operation time is observed.

---

[111] Juvekar V. A., Sharma M. M. Absorption of carbon dioxide in suspension of lime. *Chemical Engineering Science* 1973, 28, 825–837.
[112] Stemmet C. P., Bartelds F., van der Schaaf J., Kuster B. F. M., Schouten J. C. Influence of liquid viscosity and surface tension on the gas–liquid mass transfer coefficient for solid foam parkings in co-current two-phase flow. *Chemical Engineering Research and Design* 2008, 86, 1094–1106.
[113] Kilonzo P. M., Margaritis A. The effects of non-Newtonian fermentation broth viscosity and small bubble segregation on oxygen mass transfer in gas-lift bioreactors: a critical review. *Biochemical Engineering Journal* 2004, 17, 27–40.

The results for carbon dioxide absorption with glucosamine aqueous solutions indicate that there is no influence of liquid phase composition (in the studied range) upon the interfacial area. However, the gas flow-rate fed to the bubble reactor has an important influence, causing an increase in this parameter due to an increase in the gas hold-up, as well.

# 2.3 Gas absorption in $CO_2$ – cyclic amines systems

*Abstract*

*The present work analyses the carbon dioxide capture process by means of absorption with chemical reaction with glucosamine and pyrrolidine aqueous solutions, using a bubble column reactor (BCR). Experimental results indicate that this reagents have a similar behaviour to other common amines (i.e. monoethanolamine, widely used in carbon dioxide capture), as regarding the capture rate of this acidic gas. The value of the mass transfer coefficient corresponding to the liquid phase has been determined, and the effect of different operation conditions upon the value of that coefficient has also been analysed (amine concentration, pH and gas flow rate).*

## 2.3.1. Specific introduction

The fossil fuel combustion from power plants or refineries is one of the most important sources of carbon dioxide emission[114]. Several technologies are available to reduce the carbon dioxide emission from industrial gas streams, but the chemical absorption with alkanolamines (i.e. monoethanolamine –MEA–, diethanolamine –DEA–, di-2-propanolamine –DIPA–, triethanolamine –TEA–, and methyldiethanolamine –MDEA) is the most widely used method for low partial pressures of carbon dioxide[115,116]. This method is efficient and it usually permits the removal of a high percentage of the carbon dioxide emitted. Previous studies concluded that primary and secondary alkanolamines react, directly and reversibly, to the carbon dioxide by forming a zwitterion intermediate, which is deprotonated by the bases present in the solution to form a stable carbamate[117,118], even though the formation of the carbamate increases the reaction rate but usually limits the loading to 0.5 mol of carbon dioxide/mol of amine[119]. By contrast, tertiary amines do not react directly to the carbon dioxide in order to form carbamate. Generally, tertiary amines react more slowly to carbon dioxide than primary and secondary amines[120].

Studies using 2-amino-2-deoxy-D-glucose, called glucosamine (GA), in order to analyse the absorption of carbon dioxide in a gas-liquid contactor have been performed. The absorption of carbon dioxide in this system is accompanied by a chemical reaction between the glucosamine and the carbon dioxide previously absorbed in the liquid phase. This is a first-order reaction regarding both compounds (carbon dioxide and glucosamine), as it was concluded in a previous

[114] Bonenfant D., Mimeault M., Hausler R. Estimation of the $CO_2$ absorption capacities in aqueous 2-(2-aminoethylamino)ethanol and its blends with MDEA and TEA in the presence of $SO_2$. *Industrial & Engineering Chemistry Research* 2007, 46, 8968-8971.
[115] Liao C. H., Li M. Kinetics of absorption of carbon dioxide into aqueous solutions of monoethanolamine + N-methyldiethanolamine. *Chemical Engineering Science* 2002, 57, 4569-4582.
[116] Horng S. Y., Li M. Kinetics of absorption of carbon dioxide into aqueous solutions of monoethanolamine + triethanolamine. *Industrial & Engineering Chemistry Research* 2002, 41, 257-266.
[117] Versteeg G. F., van Swaaij W. P. M. On the kinetics between $CO_2$ and alkanolamines both in aqueous and non-aqueous solutions I. Primary and secondary amines. *Chemical Engineering Science* 1988, 43, 573-585.
[118] Glasscock D. A., Critchfield J. A., Rochelle G. T. $CO_2$ absorption/desorption in mixtures of methyldiethanolamine with monoethanolamine or diethanolamine. *Chemical Engineering Science* 1991, 46, 2829-2845.
[119] Rinker E. D., Ashour S. S., Sandall O. C. Absorption of carbon dioxide into aqueous blends of diethanolamine and methyldiethanolamine. *Industrial & Engineering Chemistry Research* 2000, 39, 4346-4356.
[120] Linek V., Sinkule J., Havelka P. Empirical design method of industrial carbon dioxide-mixed solvent absorbers with axial dispersion in gas. *Industrial & Engineering Chemistry Research* 1994, 33, 2731-2737.

research[121]. The mechanism suggested for this reaction is a zwiteronic type, where the global process of absorption with a chemical reaction has a moderately fast regime, since the Hatta number (Ha) takes values between 0.3 < Ha < 3 for the experimental conditions used in the present work[121]. The Hatta number is a dimensionless parameter that compares the absorption rate of a solute in a reactive system to the absorption rate of the same solute, in the case of physical absorption.

This new method of carbon dioxide capture has great advantages if we compare it to more conventional systems, based on the use of the amines abovementioned. These advantages are fundamentally a minor need of safety measures and a minor chemical risk when aqueous solutions of glucosamine are manipulated. Moreover, this system shows a kinetic capture of carbon dioxide with a similar rate to other systems based in amines industrially used, such as MEA or DEA[122].

Previous studies have analysed the kinetics of the chemical reaction but not the mass transfer process, necessary to evaluate the global absorption process, which is one of the aim of present study.

Then, the behaviour of glucosamine aqueous solutions is analysed in order to capture carbon dioxide by means of an absorption process with a chemical reaction in a bubble column reactor (BCR), and this process permits the analysis of the mass transfer process and the interfacial area generated between two phases (gas and liquid). Therefore, in addition to the capacity of carbon dioxide absorption, the influence of the carbon dioxide loading have also analysed, the amine concentration in the liquid phase, as well as the gas flow rate fed to the contactor upon the global process of carbon dioxide absorption and the interfacial area gas-liquid.

On the other hand, previous studies performed with pyrrolidine (see section 2.1) indicate that this cyclic amine allows carbon dioxide to capture at a higher absorption rate than aqueous solutions of GA or MEA and for that, the absorption process of carbon dioxide with pyrrolidine has been analysed too.

---

[121] Gómez-Díaz D., Navaza J.M. Kinetics of carbon dioxide absorption into aqueous glucosamine solutions. *AIChE Journal* 2008, 54, 321-326.
[122] Gómez-Díaz D., Navaza J. M., Sanjurjo B., Vázquez-Orgeira L. New absorbent for $CO_2$ removal. *Afinidad* 2007, 64, 705-708.

## 2.3.2. Results and discussion

### *2.3.2.1. Pyrrolidine*

Aqueous solutions of pyrrolidine have shown very interesting characteristics for their use for carbon dioxide capture by means of chemical absorption (see section 2.1 of this chapter) due to the high reaction rate between loaded carbon dioxide and pyrrolidine in comparison with other amines which are commonly used for this kind of separation process[123,124]. Taking as starting point the previously commented studies about kinetics between carbon dioxide and pyrrolidine, the absorption in a bubble column reactor has been performed under different experimental conditions to analyze the behavior of this kind of aqueous solutions for carbon dioxide capture in bubbling equipment.

An example of the experimental data corresponding to absorption rate obtained in this contactor is shown in figure 2.17. The inlet, outlet and absorbed carbon dioxide molar flow are plotted in this figure against operation time. On the basis of these experimental data is possible calculate the quantity of carbon dioxide transferred to the liquid phase. Taking into account the absorbed flow the behavior of this system is characteristic in comparison with the corresponding ones using other amine aqueous solutions. A decrease in absorption rate is observed when operation time increases until this variable reaches a *plateau*. The zone with a constant absorption rate is observed for an important period. Then a decrease in the value of absorption rate is observed until the liquid phase saturation in carbon dioxide is reached, and the absorbed molar gas flow-rate is zero.

The experimental data shown in figure 2.17 has been obtained under the different operation conditions (gas flow-rate and pyrrolidine concentration) and it allows to analyze carefully the absorption process with chemical reaction between carbon dioxide and pyrrolidine.

[123] Mandal B. P., Guha M., Biswas A. K., Bandyopadhyay S. S. Removal of carbon dioxide by absorption in mixed amines: modelling of absorption in aqueous MDEA/MEA and AMP/MEA solutions. *Chemical Engineering Science* 2001, 56, 6217-6224.
[124] Edali M., Aboudheir A., Idem R. Kinetics of carbon dioxide absorption into mixed aqueous solutions of MDEA and MEA using a laminar jet apparatus and a numerically solved 2D absorption rate/kinetics model. *International Journal of Greenhouse Gas Control* 2009, 3, 550-560.

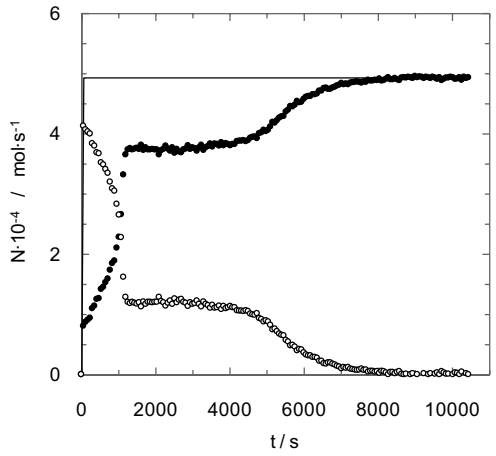


Figure 2.17. Carbon dioxide absorption rate by pyrrolidine aqueous solutions. $C_{PYR}$ = 0.3 mol·L$^{-1}$. $Q_g$ = 40 L·h$^{-1}$. (●) outlet molar flow; (○) absorbed molar flow.

Figure 2.18 shows the experimental data obtained when different pyrrolidine initial concentration is used in the liquid phase. The shape of the curves is similar than the previous one shown in figure 2.17. When pure water is used as liquid phase (in the absence of amine), the behavior is different because a monothonic decrease is observed (without the constant absorption rate zone), due to the kind of absorption (physical). When pyrrolidine concentration increases in liquid phase, the presence of the *plateau* is observed with a higher period when amine concentration increases. This fact is due to a higher amine concentration enhances the reaction between absorbed carbon dioxide and pyrrolidine for a large operation time until reaches the saturation. Also, a higher initial amine concentration produces an increase in the time needed to reach the constant absorption rate period.

In relation with the other variable analyzed in present study (carbon dioxide flow-rate) upon absorption rate, figure 2.19 shows the observed behaviors. An important increase in the absorption rate is observed when a higher gas flow-rate is fed to the bubble column. This behavior is due to an increase in gas flow-rate produces an increase in the value of gas-liquid interfacial area, previously commented in present chapter. This increase in interfacial area increases carbon dioxide mass transfer and this compound, reacts with pyrrolidine in liquid phase. This behavior shows that mass transfer is rate-determining step in this process. The constant absorption rate zone is observed for all the experimental conditions.

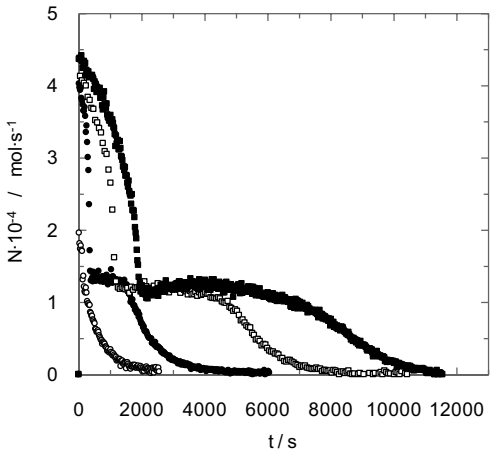


Figure 2.18. Effect of amine concentration upon carbon dioxide absorption rate in pyrroidine aqueous solutions. $Q_g$ = 40 L·h$^{-1}$. (○) $C_{PYR}$ = 0 mol·L$^{-1}$; (●) $C_{PYR}$ = 0.1 mol·L$^{-1}$; (□) $C_{PYR}$ = 0.3 mol·L$^{-1}$; (■) $C_{PYR}$ = 0.4 mol·L$^{-1}$.

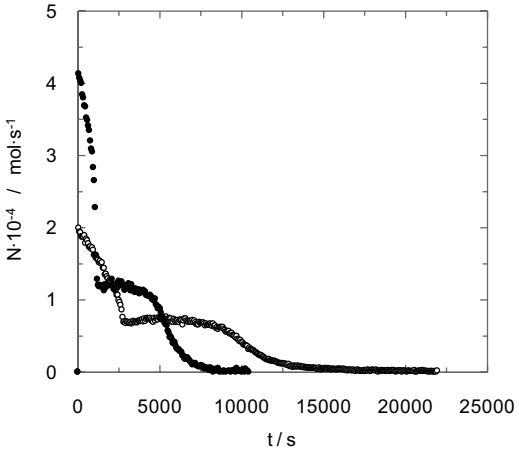


Figure 2.19. Influence of gas flow-rate upon carbon dioxide absorption rate in pyrrolidine aqueous solutions. $C_{PYR}$ = 0.3 mol·L$^{-1}$. (○) $Q_g$ = 18 L·h$^{-1}$; (●) $Q_g$ = 40 L·h$^{-1}$.

Due to the special behavior shown for pyrrolidine aqueous solutions in carbon dioxide capture by chemical absorption, a comparison with the behavior observed for other amines aqueous solutions has been performed, and the experimental data is shown in figures 2.20 and

2.21. Figure 2.20 (using triethanolamine and N-methyldiethanolamine) shows a different behavior than the observed for carbon dioxide – pyrrolidine system because a monothonic decrease in the value of absorption rate is observed until the saturation is reached. On the other hand, figure 2.21 shows the experimental data corresponding to monoethanolamine and 1-amino-2-propanol, and this kind of aqueous solutions produces certain similar behavior than the previously commented for pyrrolidine aqueous solutions. A constant absorption rate period is not obtained but a change in the trend is obtained around 800 s.

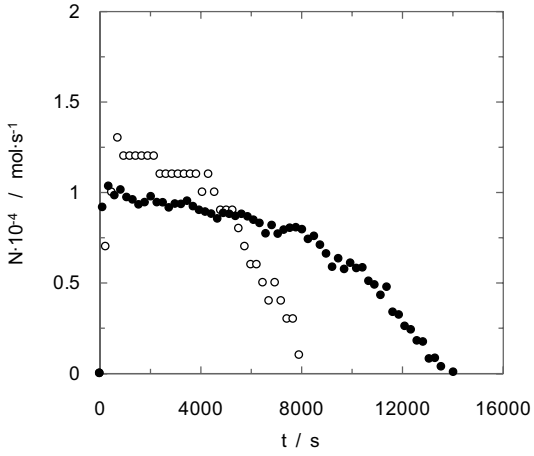


Figure 2.20. Absorption kinetics of carbon dioxide in triethanolamine (TEA) and N-methyldiethanolamine (MDEA). (○) $C_{TEA}$ = 0.5 mol·L$^{-1}$; (●) $C_{MDEA}$ = 0.5 mol·L$^{-1}$. $Q_g$ = 20 L·h$^{-1}$.

On the basis of the experimental data corresponding to absorption rate is possible conclude that the chemical absorption between pyrrolidine aqueous solutions and carbon dioxide takes place by a mechanism with certain differences with well-known systems. Constant absorption rate periods have been observed in chemical absorption processes when a pseudofirst order is present in the experimental system, but this behavior is shown at initial time when the reagent concentration is high and it could be considered “constant” that allows to maintain the absorption rate independent of operation time.

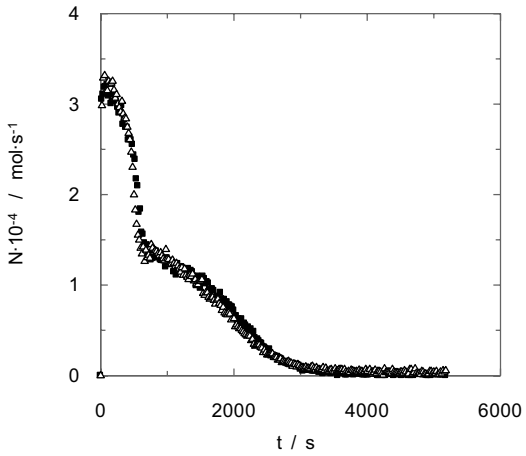


Figure 2.21. Absorption kinetics of carbon dioxide in monoethanolamine (MEA) and 1-amino-2-propanol (MIPA). (○) $C_{MEA}$ = 0.4 mol·L$^{-1}$; (●) $C_{MIPA}$ = 0.4 mol·L$^{-1}$. $Q_g$ = 40 L·h$^{-1}$. $Q_g$ = 40 L·h$^{-1}$.

Attending to the chemical reaction in the liquid phase, different researchers[125] indicates that the following reactions may take place when carbon dioxide is absorbed into amine aqueous solution.

$$CO_2 + R_2NH \leftrightarrows R_2NCOO^- + H^+ \quad (1)$$

$$CO_2 + R_2NH + H_2O \leftrightarrows R_2NH_2^+ + HCO_3^- \quad (2)$$

$$R_2NH + H^+ \leftrightarrows R_2NH_2^+ \quad (3)$$

$$HCO_3^- \leftrightarrows H^+ + CO_3^{2-} \quad (4)$$

$$CO_2 + OH^- \leftrightarrows HCO_3^- \quad (5)$$

Reactions (3) and (4) are considered instantaneous and reversible and at equilibrium, in comparison with the other reactions shown previously[126]. The commonly proposed mechanism for the reaction between carbon dioxide and different amines involves the formation of zwitterion ($R_2NH^+COO^-$) and subsequent deprotonation of zwitterion by a base to produce carbamate ($R_2NCOO^-$) and protonated base ($R_2NH_2^+$), followed by carbamate reversion by

[125] Saha A. K., Biswas A. K., Bandyopadhyay S. S. Absorption of $CO_2$ in a sterically hindered amine: modeling absorption in a mechanically agitated contactor. *Separation and Purification Technology* 1999, 15 101–112.
[126] Mandal B. P., Biswas A. K., Bandyopadhyay S. S. Absorption of carbon dioxide into aqueous blends of 2-amino-2-methyl-1-propanol and diethanolamine. *Chemical Engineering Science* 2003, 58, 4137–4144.

hydrolysis[127]. The zwitterion mechanism was also found to be suitable for modelling the absorption of carbon dioxide into aqueous different amines solutions[128,129].

Though the final product in different experimental systems is bicarbonate, the formation of a zwitterion could be the rate-determining step and the deprotonation step involves only proton transfer and is considered to be very fast[130,131]. Any base present in the solution may contribute to the deprotonation of zwitterion. The contribution of each base would depend on its concentration as well as how strong a base is. Hence, the main contribution to the deprotonation of the zwitterion in this system would come from pyrrolidine and to a lesser extent from $H_2O$ and $OH^-$. Moreover, it has been well recognized that the relative formation of carbamate anion and bicarbonate ion has a crucial effect on the solubility of carbon dioxide in aqueous alkanolamine solutions. The more bicarbonate ions form in equilibrium $CO_2$-alkanolamine-$H_2O$ solutions, the more free amines exist, and these free amines are able to react with carbon dioxide molecules again, which finally leads to a remarkable enhancement in the carbon dioxide loading capacity.

The overall reaction stoichiometry indicates that 2 mol of amine are required per mole of carbon dioxide reacted for the carbamate anion, whereas a one-to-one ratio is required for the bicarbonate ion[132]. The degree of hydrolysis of the carbamate anion is determined by reaction parameters such as the amine concentration, solution pH, and chemical stability of the carbamate anion[133,134,135]. In a rich amine solution the concentration of unreacted amine depends on the carbamate stability constant.

---

[127] Sartori G., Savage D. W. Sterically hindered amines for $CO_2$ removal from gases. *Industrial and Engineering Chemistry Fundamentals* 1983, 22, 239–249.
[128] Saha A. K., Bandyopadhyay S. S., Biswas A. K. Kinetics of absorption of $CO_2$ into aqueous solutions of 2-amino-2-methyl-1-propanol. *Chemical Engineering Science* 1995, 50, 3587–3598.
[129] Xu S., Wang Y. W., Otto F. D., Mather A. E. Kinetics of the reaction of carbon dioxide with 2-amino-2-methyl-1-propanol solutions. *Chemical Engineering Science* 1996, 51, 841–850.
[130] Danckwerts P. V. The reaction of $CO_2$ with ethanolamines. *Chemical Engineering Science* 1979, 34, 443–446.
[131] Versteeg G. F., van Swaaij W. P. M. On the kinetics between $CO_2$ and alkanolamines both in aqueous and nonaqueous solutions—II. Tertiary amines. *Chemical Engineering Science* 1988, 43, 587–591.
[132] Robert J. An investigation of some sterically hindered amines as potential carbon dioxide scrubbing compounds. *Industrial & Engineering Chemistry Research* 1997, 36, 1779-1790.
[133] Caplow M. J. Kinetics of carbonate formation and break-down. *Journal of the American Chemical Society* 1968, 90, 6795-6803.
[134] Chakraborty A. K., Astarita G., Bischoff K. B. $CO_2$ absorption in aqueous solutions of hindered amines. *Chemical Engineering Science* 1986, 41(4), 997-1003.
[135] Ewing S. P., Lockshon D., Jencks W. P. Mechanism of cleavage of carbamate anions. *Journal of the American Chemical Society* 1980, 102, 3072-3084.

$$R_2NCOO^- + H_20 \leftrightarrows R_2NH + HCO_3^- \quad (6)$$

In this work, NMR spectroscopy was employed to follow the speciation in the aqueous solution of pyrrolidine through time in carbon dioxide absorption experiments. The time speciation revision has to imply the study of the different species present in the reaction mechanism between carbon dioxide and pyrrolidine reaction in the liquid phase.

NMR studies have started with the analysis of the original species in each solution. Figure 2.22 shows the $^1H$ and $^{13}C$ NMR spectra of pyrrolidine-$H_2O$ system. Deuterium oxide ($D_2O$) was used as NMR solvent of the different aqueous pryrrolidine solutions. In order to have an internal reference to $^{13}C$ NMR a drop of deuterated methanol has also added.

The $^1H$ NMR aqueous solution of pyrrolidine shows two triplet groups of signals to 2.8 and 1.7 ppm corresponding to the signal of $\alpha$ and $\beta$ protons to nitrogen atom respectively, and the $^{13}C$ NMR spectrum shows also two groups of signals to 46.4 and 25.6 ppm assignated to the equivalent carbons.

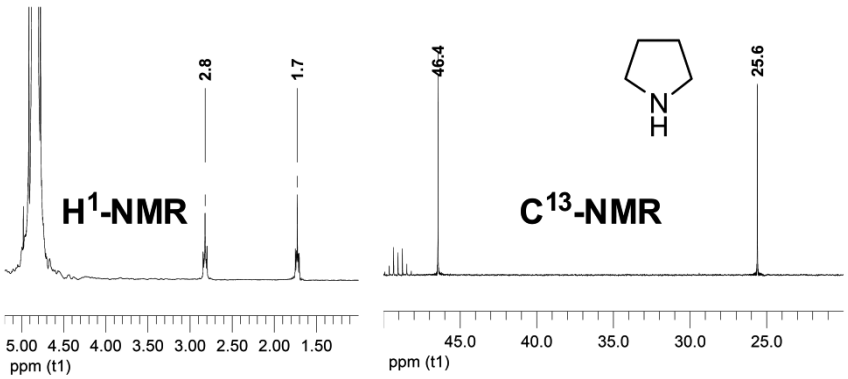


Figure 2.22.$^1H$ and $^{13}C$ NMR spectra of pyrrolidine-$H_2O$ system at 293 K.

Other problem that it must understand in the study of chemical absorption of carbon dioxide in amines is the bicarbonate-carbonate equilibrium. In literature it can be found a substantial discrepancy regards the chemical shift of these ions[136,137]. In literature fast proton exchange in the $HCO_3^-/CO_3^{-2}$ equilibrium has assigned to a $^{13}C$ NMR chemical shift in the range of $165 < \delta < 161$ ppm. To evaluate the signal of $HCO_3^-/CO_3^{-2}$ equilibrium in five samples of mixtures of $HCO_3^-/CO_3^{-2}$ solutions have been analyzed by $^{13}C$ NMR.

Figure 2.23 shows that the chemical shift of 0.1 M aqueous $CO_3^{-2}$ gives a signal to 168.7 ppm. In the other extreme to 161.4 ppm it is found the chemical shift of 0.1 M aqueous $HCO_3^-$ solution. Three new solutions were prepared: a mixture 1:1 of both initial 0.1 M $HCO_3^-$/0.1 M $CO_3^{-2}$ solutions affords a chemical shift of 165.2 ppm, a second mixture 1:2 of both initial 0.1 M $HCO_3^-$/0.1 M $CO_3^{-2}$ solutions that it gave a signal to 166.5 ppm, while a third mixture, 2:1 of both initial 0.1 M $HCO_3^-$/0.1 M $CO_3^{-2}$ solutions, presents the $^{13}C$ NMR signal to 163.9 ppm.

[136] Mani F., Peruzzini M., Stoppioni P. $CO_2$ absorption by aqueous $NH_3$ solutions: speciation of ammonium carbamate, bicarbonate and carbonate by a $^{13}C$ NMR study. *Green Chemistry* 2006, 8, 995–1000.
[137] Jakobsen J. P., da Silva E. F., Krane J., Svendsen H. F. NMR study and quantum mechanical calculations on the 2-[(2-aminoethyl)amino]-ethanol–$H_2O$–$CO_2$ system. *Journal of Magnetic Resonance* 2008, 191, 304–314.

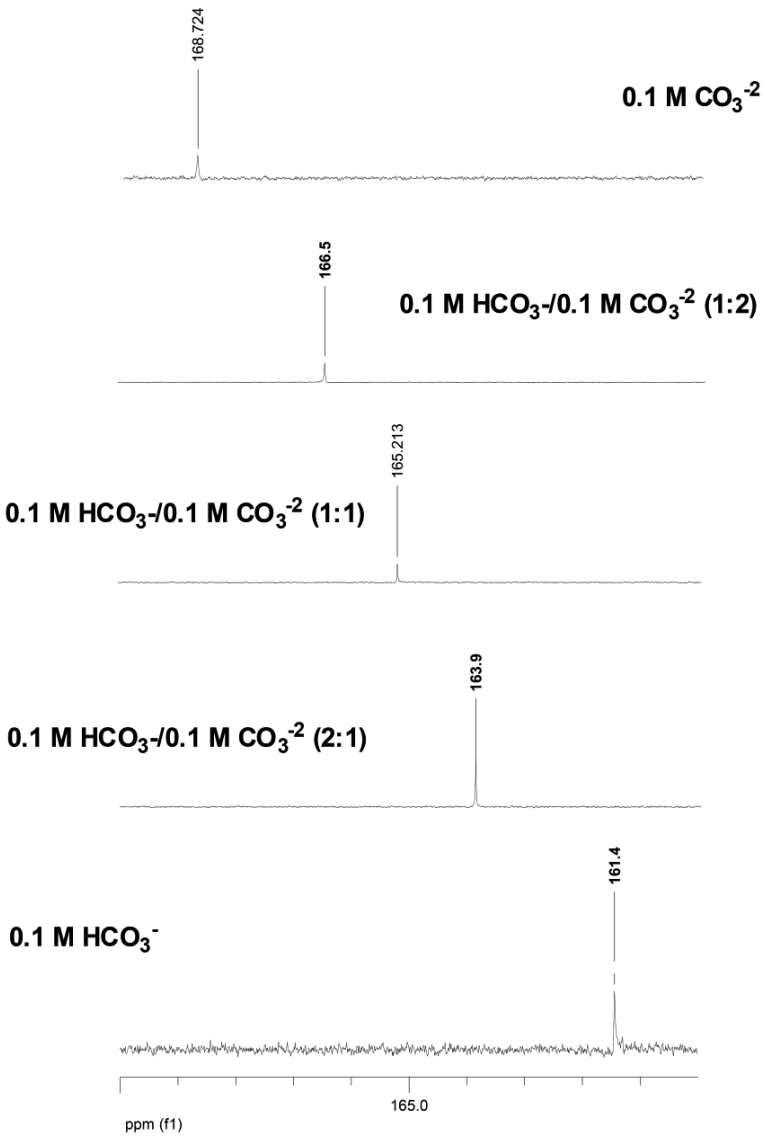


Figure 2.23. $^{13}C$ NMR spectra for $HCO_3^-/CO_3^{-2}$ mixtures.

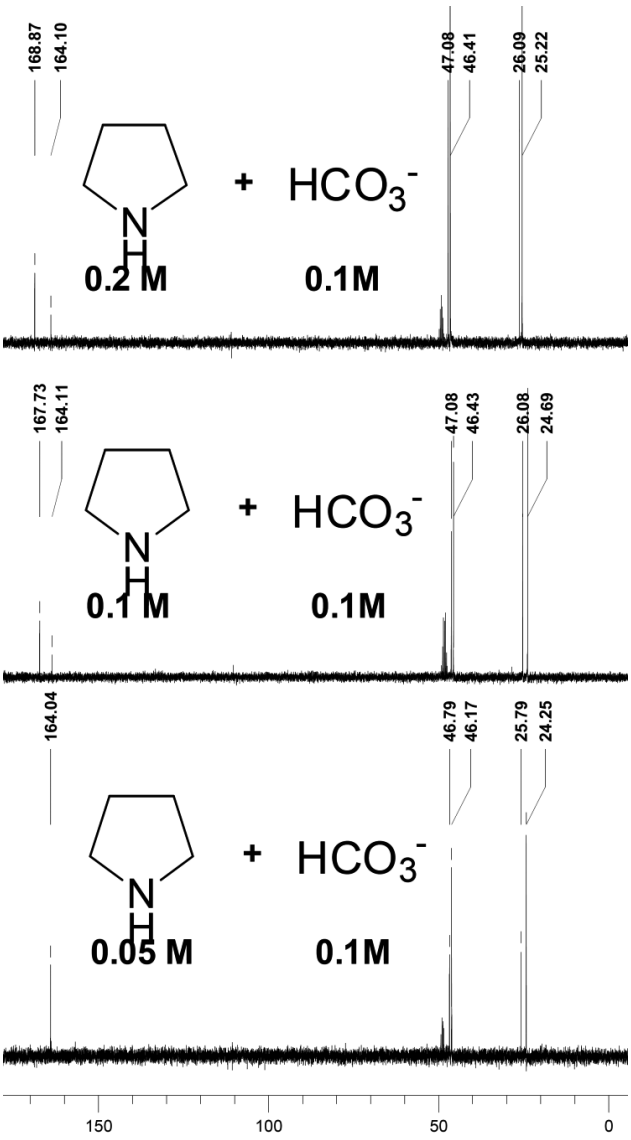


Figure 2.24. $^{13}C$ NMR spectra for pyrrolidine and bicarbonate aqueous solutions.

Also, the interaction between pyrrolidine and bicarbonate ion was analyzed and these experiments consisted in the analysis by $^{13}C$ NMR of different mixtures of bicarbonate aqueous

solutions (0.1 M) and different quantities of pyrrolidine to reach several amine concentrations (0.05 M, 0.1 M and 0.2 M).

Figure 2.24 shows that the spectrum corresponding to the mixture of bicarbonate (0.1 M) and pyrrolidine (0.05 M) shows a signal at low field (164.0 ppm) that is assigned to the equilibrium that produces the carbamate formation but is possible that this signal can be due also to bicarbonate caused by the chemical shift produced by pH, previously commented. On the other hand, the mixtures of bicarbonate aqueous solution with pyrrolidine mixtures of 0.1 M and 0.2 M show the same signal at 164 ppm but also, a second peak was observed at 167.7 and 168.8 ppm respectively. This second peak is assigned to the formation of carbonate ($CO_3^{-2}$) from de bicarbonate with a fast equilibrium. The carbamate ion is produced from the reaction between pyrrolidine and bicarbonate ion as previous studies have concluded[138]. The signal corresponding to this substance (carbamate) remains at 164 ppm.

Other interesting study consisted in the analysis of the chemical shifts corresponding to pyrrrolidine carbons at different values of aqueous solutions's pH. Different measurements were performed at several pH values: 10.4, 5.4, 3.1 y 1.6. The experimental data included in NMR spectra shown in figure 2.25 indicate that proton exchange is very fast and only one peak is observed for both compounds. The spectrum shows at the top of figure 2.25 corresponds to free amine in aqueous solution (pH = 10.4) and the original pH value was modified by the addition of different quantities of hydrogen chloride. At basic medium the signals corresponding to pyrrolidine carbons are present at 46.4 and 25.6 ppm. When the medium is acidified a chemical shift in original peak at high field was observed from 25.6 to 24.5 ppm ($\Delta\delta$ = 1 ppm).

[138] Al-Juaied M., Rochelle G. T. Thermodynamics and equilibrium solubility of carbon dioxide in diglycolamine/morpholine/water. *Journal of Chemical & Engineering Data* 2006, 51, 708-717.

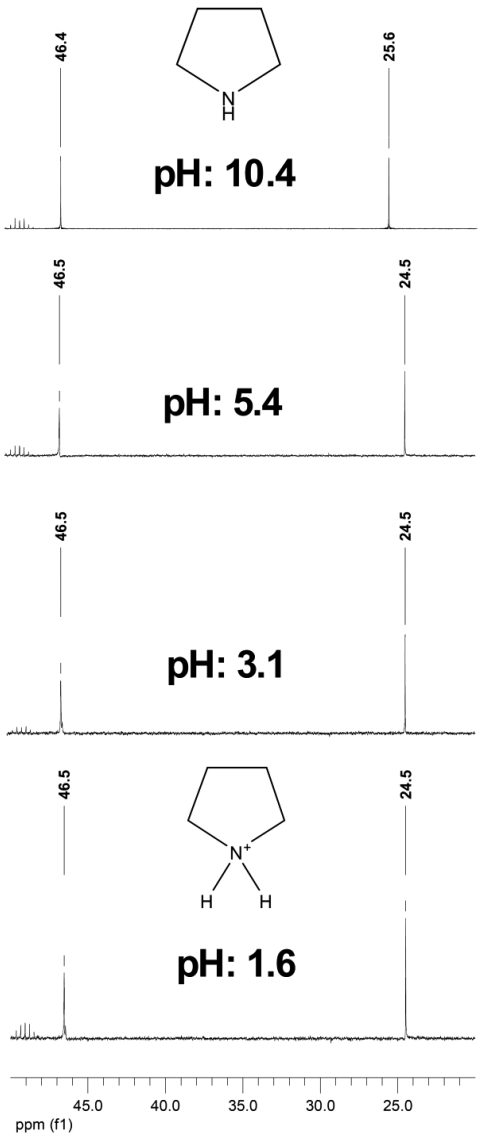


Figure 2.25. $^{13}C$ NMR spectra for pyrrolidine aqueous solution ($C_{PYR}$ = 0.1 mol·L$^{-1}$) at different pH values.

These previous studies with NMR spectroscopy have allowed to obtain the necessary information to obtain conclusions from the analysis, by this experimental technique, of carbon

dioxide – pyrrolidine gas-liquid absorption process. Previous research works[139] have concluded that the nuclear magnetic resonance is a useful technique to analyze this kind of chemical absorption. These previous studies commonly analyze only the initial and final products of absorption process. Present work analyzes the temporal evolution of the species that exist in the liquid phase caused by the chemical reaction between carbon dioxide and pyrrolidine. This information can allow to obtain valuable information about the preferential mechanism of chemical absorption. At initial time (see figure 2.26) two different signals are observed that corresponds to the carbons of pyrrolidine. This spectrum unchanged during the initial period of experiment, although the chemical absorption between carbon dioxide and pyrrolidine is produced and observed on the basis of outlet gas flow-rate and the decrease in bubble's size. This behavior is caused for the non-ideality of bubble reactor.

The chemical absorption between carbon dioxide and pyrrolidine shows a fast regime (previously analyzed) and it produces that bubbles practically disappear in the first zone of column and this fact causes a low liquid turbulence in the contactor. Taking into account that in bubble contactors the gas flow-rate is the stirring agent, at initial experiment time the concentration of substances is not the same in each part of reactor. The situation of sample port (placed in the middle height of bubble column) and the low turbulence at initial time explains the absence of changes in NMR spectra.

At t3 (10 min) time new peaks appears in the $^{13}C$ NMR spectrum. The more interesting signals appear at low field: 168.8 and 164.1 ppm. These signals are assigned to the $HCO_3^-/CO_3^{-2}$ equilibrium (previously commented) and the formation of pyrrolidine's carbamate. The last product is also associated to signal's duplication at high field. Two new peaks appear near to the original pure amine signals (46.4 and 25.6 ppm) caused by the presence of new species. The carbamate signal at 164.1 ppm is associated to the signals present at 47.1 and 26.1 ppm. The peaks at 46.4 and 25.3 ppm correspond to the amine /protonated amine equilibrium existence into the reactor bulk.

[139] Böttinger W., Maiwald M., Hasse H. Online NMR spectroscopic study of species distribution in MEA–$H_2O$–$CO_2$ and DEA–$H_2O$–$CO_2$. *Fluid Phase Equilibria* 2008, 263, 131–143.

During the absorption experiment the signal at 168.8 ppm (in the t3 spectrum) assigned to carbonate/bicarbonate equilibrium shifts to low field: 168.0 ppm (t6), 166.0 ppm (t8), 164.1 ppm (t9), 162.4 ppm (t10), 161.4 ppm (t14) and 161.3 ppm (t18). The observed chemical shift caused by the liquid phase pH, is caused at initial experiment time the carbonate/bicarbonate equilibrium is completely shifted to carbonate ion but at the end of the absorption experiment only exists the bicarbonate ion. In the same way the amine/protonated amine equilibrium shifts to the second one substance from 25.3 ppm (t3) to 24.5 (t18). This signal is in agreement with the previously obtain value of pyrrolidine in acidic medium (see figure 2.26). Since t8 a significance decrease in carbamate signals is observed and these peaks disappear at t18 time.

Speciation studies in the carbon dioxide absorption experiment has been also performed using $^{1}H$ NMR for the same experiment than spectra shown in figure 2.26 ($C_{PYR}$ = 0.3 $mol \cdot L^{-1}$ and $Q_g$ = 18 $L \cdot h^{-1}$). Zero time spectrum shows two signal groups corresponding to protons of $\alpha$ carbon (2.8 ppm) and protons of $\beta$ carbon to nitrogen (1.7 ppm). In the first two samples (t1= 2 min and t2= 5 min) no changes in the spectrum was observed for the same reason than the perviously commented one for $^{13}C$ NMR spectra (non ideal mixing into the bubble contactor at the experiment beginning).

At t3 the spectrum shows the formation of two new signal groups that appears as triplets at 3.2 and 1.85 ppm. These signals are assigned to the formation of carbamate molecule. On the other hand, a chemical shift of initial signals to low field is observed. The triplet at 1.7 ppm moves slightly to 1.8 ppm, and the other one at 2.8 ppm moves to 2.9 ppm. These two signals are produced caused by the equilibrium between the amine and the conjugated acid. This signal group continues changing their chemical shift to low field during the absorption experiment caused by the amine ↔ protonated amine is diplaced to the last one. In the six sample (t6) the spectrum shows these two group signals at 2.0 and 3.2 ppm and also, the presence of carbamate signal at 1.8 ppm (protons of $\beta$ carbon) as a triplet. Along the absorption experiment the carbamate signal (1.85 ppm) decrease its intensity until dissapear. All these experimental results confirm the previous conclusions obtained using the $^{13}C$ NMR spectra.

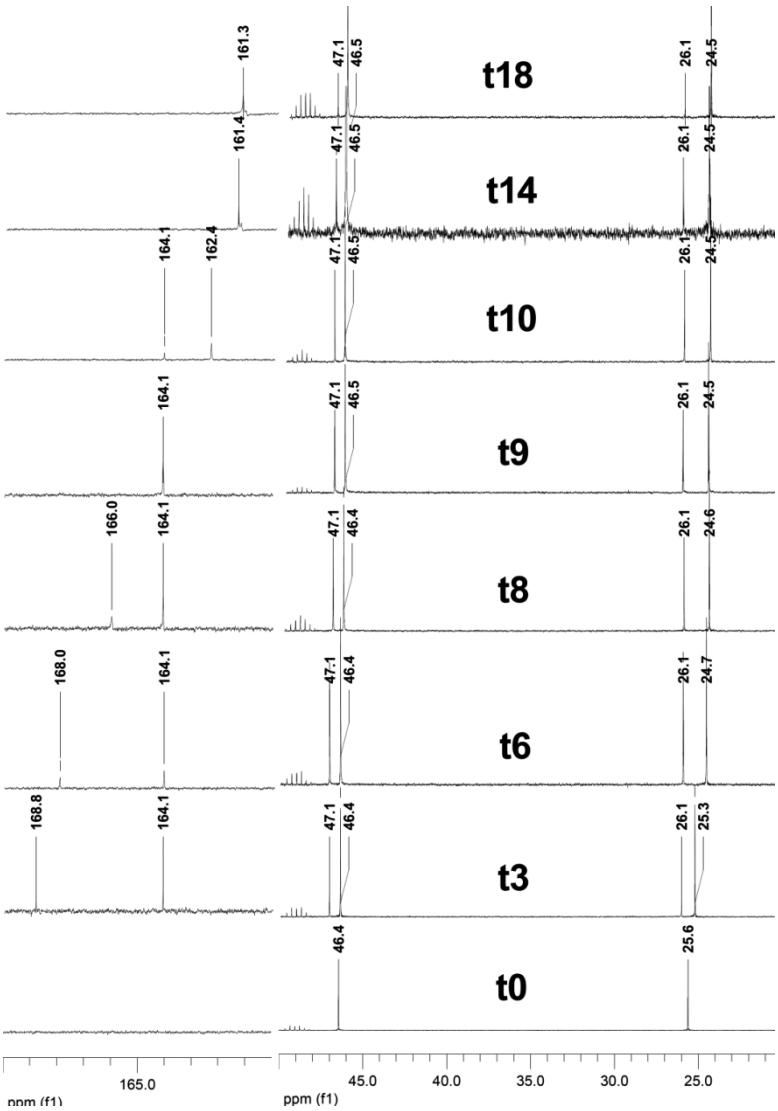


Figure 2.26. $^{13}C$ NMR spectra corresponding to carbon dioxide absorption in pyrrolidine aqueous solutions. $C_{PYR}$ = 0.3 mol·L$^{-1}$. $Q_g$ = 18 L·h$^{-1}$. (t0 = 0 min; t1 = 2 min; t2 = 5 min; t3 = 10 min; t4 = 15 min; t5 = 20 min; t6 = 25 min; t7 = 30 min; t8 = 35 min; t9 = 45 min; t10 = 65 min; t11 = 85 min; t12 = 100 min; t13 = 125 min; t14 = 140 min; t15 = 165 min; t16 = 200 min; t17 = 250 min; t18 = 325 min).

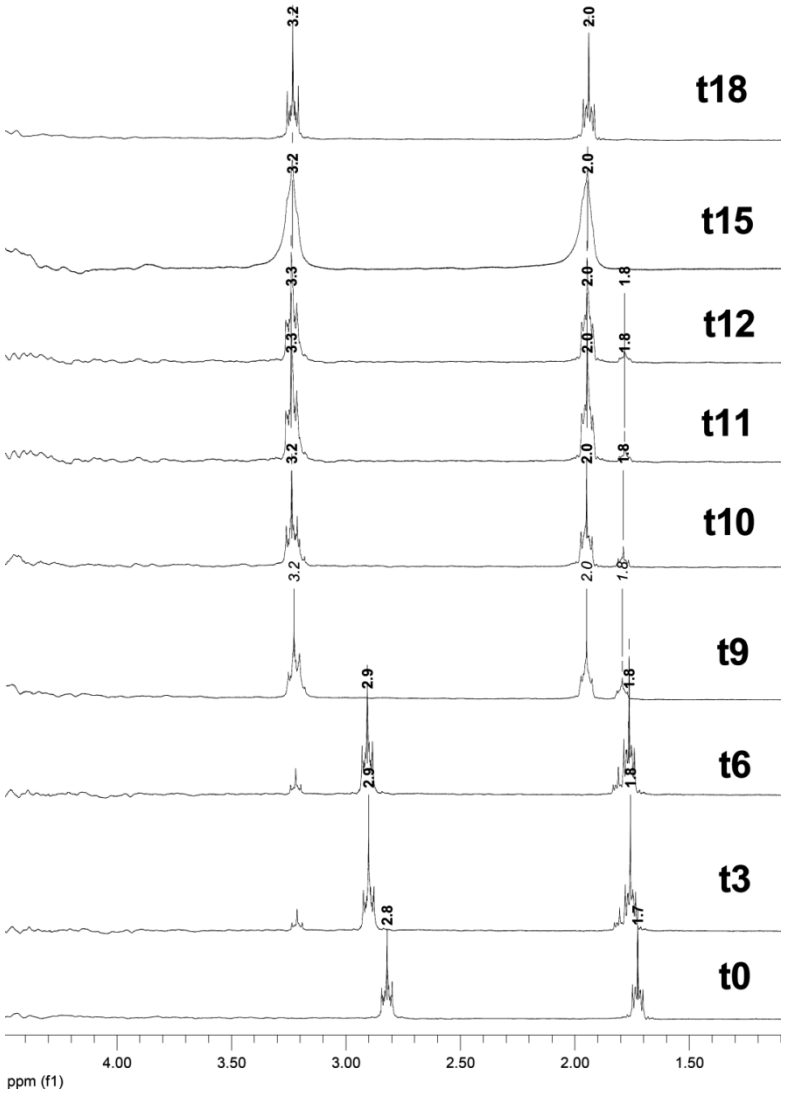


Figure 2.27. $^1$H NMR spectrum corresponding to the chemical absorption of carbon dioxide in aqueous solution of pyrrolidine. $C_{PYR}$ = 0.3 mol·L$^{-1}$. $Q_g$ = 18 L·h$^{-1}$. (t0 = 0 min; t1 = 2 min; t2 = 5 min; t3 = 10 min; t4 = 15 min; t5 = 20 min; t6 = 25 min; t7 = 30 min; t8 = 35 min; t9 = 45 min; t10 = 65 min; t11 = 85 min; t12 = 100 min; t13 = 125 min; t14 = 140 min; t15 = 165 min; t16 = 200 min; t17 = 250 min; t18 = 325 min).

Similar absorption experiments have been carried out under different experimental conditions (amine initial concentration and gas flow-rate) and $^{1}H$ and $^{13}C$ NMR analysis were performed using samples obtained during absorption experiments. Examples of these kinds of spectra are shown in figures 2.28-2.31 for different pyrrolidine concentration in the liquid phase.

The results included in these spectra confirm the previous comments about the NMR information for 0.3 M aqueous solutions of pyrrolidine. Taking into account the lowest concentration solution (0.1 M) the spectra at different experiment times show only the presence of peaks corresponding to bicarbonate (160.2 ppm) and protonated amine (23.5 and 45.5 ppm). The non presence of signals corresponding to other species such as carbamate and carbonate is due to the low amine concentration in the liquid phase. Then the experiment with the lowest amine concentration is similar than the final experimental zone in the previously analyzed system (0.3 M).

On the other hand, experiments for higher amine concentration in the liquid phase shows a similar peaks time evolution than experimental data obtained for 0.3 M pyrrolidine aqueous solutions. At low times the presence of carbamate, carbonate-bicarbonate equilibrium and amine-protonated amina equilibrium is confirmed by the NMR signals.

The same behavior than previous one for 0.3 M aqueous solution is observed: (i) the shift of carbonate-bicarbonate equilibrium peak to 160.2 ppm, corresponding to bicarbonate, and (ii) the initial presence of carbamate signals that disappear when amine concentration decreases. When a high amine concentration is used, the presence of carbamate remains more time in the liquid phase caused by the equilibrium reaction of carbamate hydrolysis.

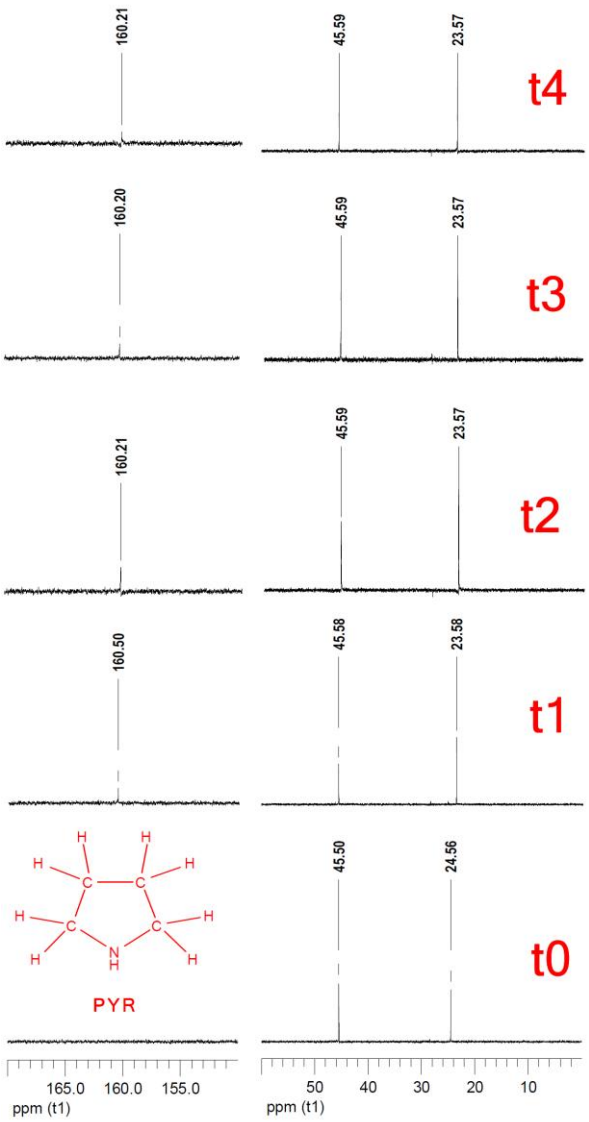


Figure 2.28. $^{13}C$ NMR spectrum corresponding to the chemical absorption of carbon dioxide in aqueous solution of pyrrolidine. $C_{PYR}$ = 0.1 mol·L$^{-1}$. $Q_g$ = 40 L·h$^{-1}$. (t0 = 0 min; t1 = 25 min; t2 = 50 min; t3 = 75 min; t4 = 100 min).

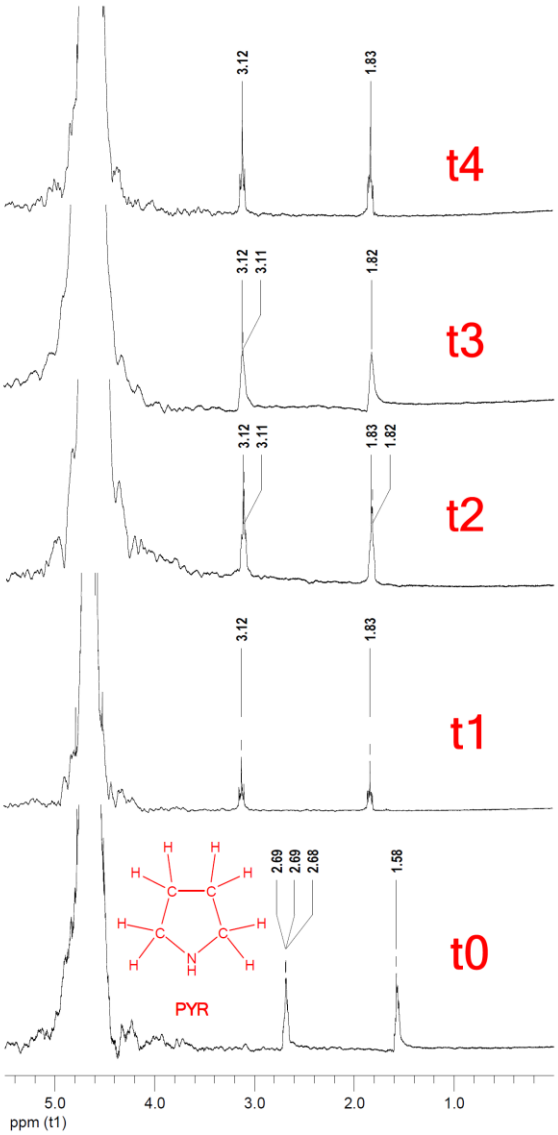


Figure 2.29. $^{1}H$ NMR spectrum corresponding to the chemical absorption of carbon dioxide in aqueous solution of pyrrolidine. $C_{PYR}$ = 0.1 mol·L$^{-1}$. $Q_g$ = 40 L·h$^{-1}$. (t0 = 0 min; t1 = 25 min; t2 = 50 min; t3 = 75 min; t4 = 100 min).

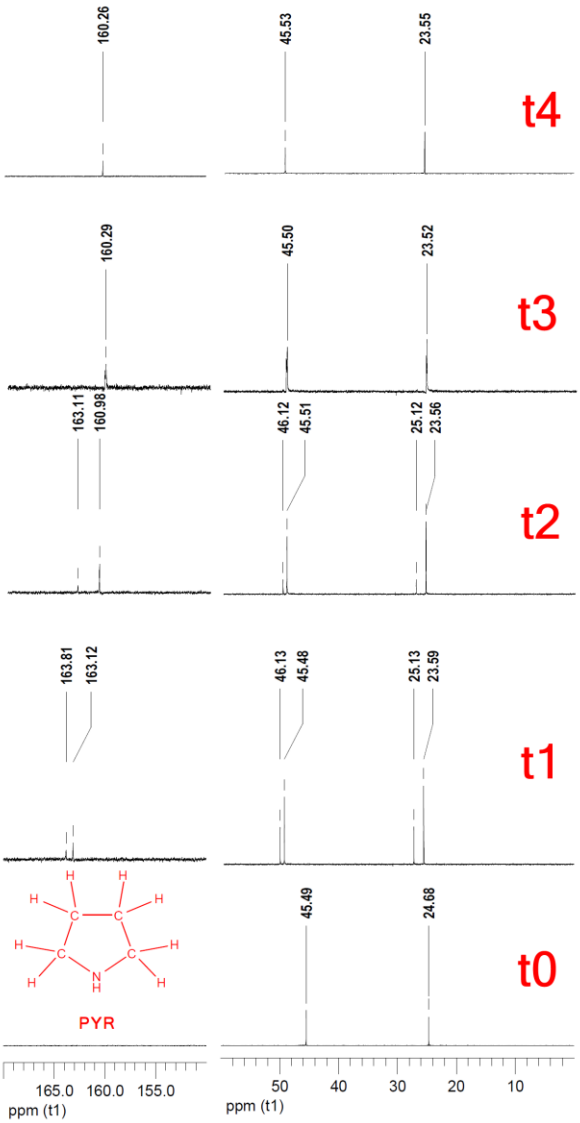


Figure 2.30. $^{13}C$ NMR spectrum corresponding to the chemical absorption of carbon dioxide in aqueous solution of pyrrolidine. $C_{PYR}$ = 0.5 mol·L$^{-1}$. $Q_g$ = 40 L·h$^{-1}$. (t0 = 0 min; t1 = 45 min; t2 = 90 min; t3 = 135 min; t4 = 180 min).

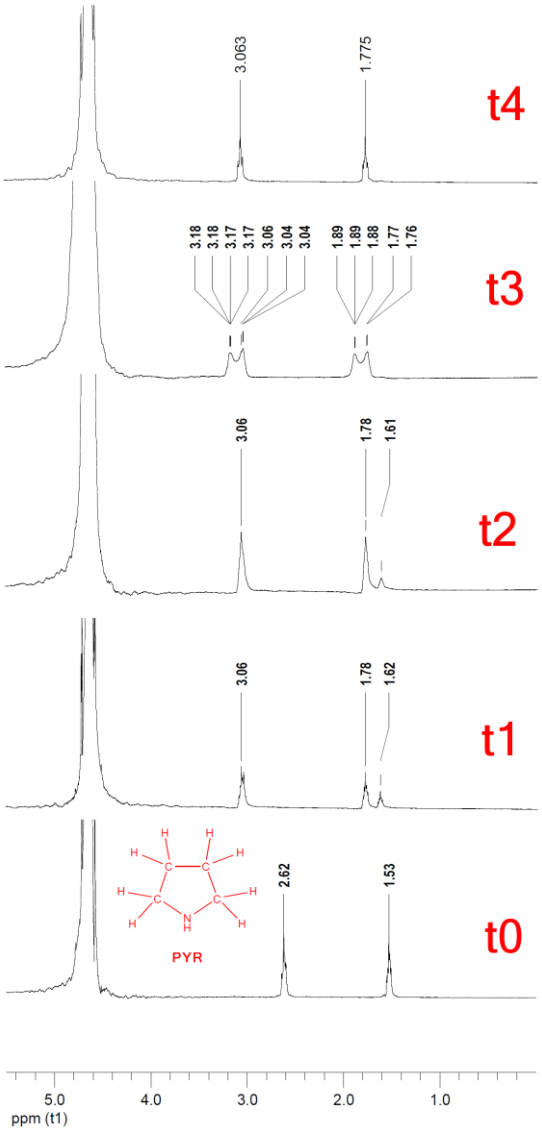


Figure 2.31. $^{1}H$ NMR spectrum corresponding to the chemical absorption of carbon dioxide in aqueous solution of pyrrolidine. $C_{PYR}$ = 0.5 mol·L$^{-1}$. $Q_g$ = 40 L·h$^{-1}$. (t0 = 0 min; t1 = 45 min; t2 = 90 min; t3 = 135 min; t4 = 180 min).

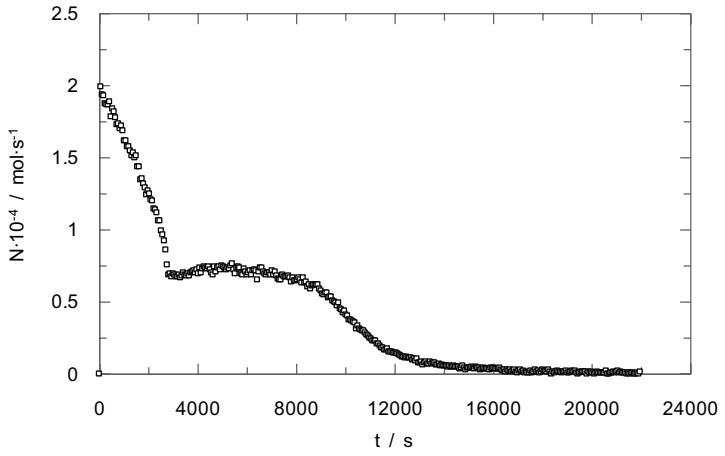


Figure 2.32. Carbon dioxide absorption rate in pyrrolidine aqueous solution. $Q_g$ = 18 L·h$^{-1}$. $C_{PYR}$ = 0.3 mol·L$^{-1}$.

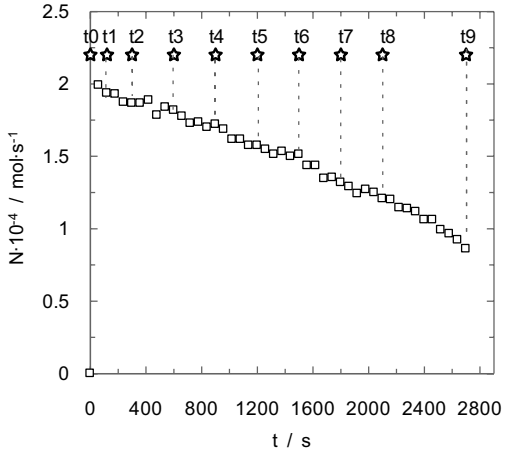


Figure 2.33. Carbon dioxide absorption rate at low operation time (zone 1). $Q_g$ = 18 L·h$^{-1}$. $C_{PYR}$ = 0.3 mol·L$^{-1}$. (□) absorption rate; (✯) samples for NMR. (t0 = 0 min; t1 = 2 min; t2 = 5 min; t3 = 10 min; t4 = 15 min; t5 = 20 min; t6 = 25 min; t7 = 30 min; t8 = 35 min; t9 = 45 min).

Figure 2.32 shows the chemical absorption kinetic under the same experimental conditions than the $^{13}C$ NMR spectra shows in figure 2.26. Also, figures 2.33 and 2.34 show the time situation of samples used to analyze the composition by NMR studies. The aim of this study is relate liquid phase composition and absorption rate.

The chemical absorption of carbon dioxide in pyrrolidine aqueous solutions shows a characteristic behavior (previously commented) and different than other amines aqueous solutions. Figures 2.33 and 2.34 show that this behavior could be divided in three zones: the first and third zones involve a decrease in the value of mass transfer rate, and the second one shows a constant value in the mass transfer rate. On the basis of the conclusions reached analyzing the NMR data, in the first zone, the products species present in the liquid phase are carbonate ion and carbamate and also these products are present in the liquid phase near to zone 2 (mass transfer rate constant period). At this moment, the peak corresponding to the carbonate – bicarbonate ions equilibrium begins to shift from the value of 168 ppm (corresponding to carbonate ion).

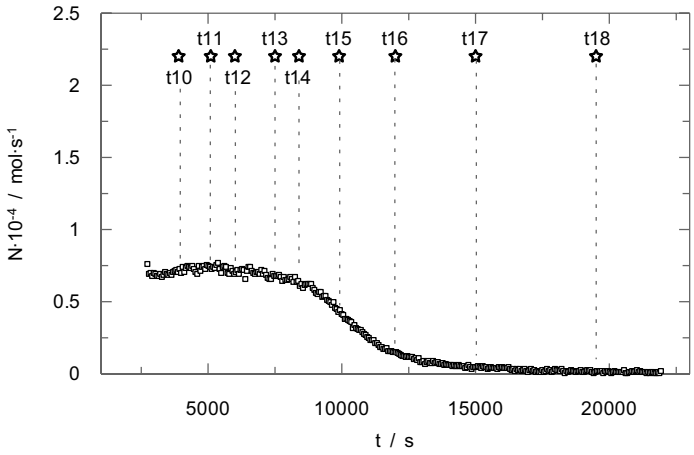


Figure 2.34. Carbon dioxide absorption rate at high operation time (zone 2). $Q_g$ = 18 $L \cdot h^{-1}$. $C_{PYR}$ = 0.3 $mol \cdot L^{-1}$. (□) absorption rate; (✯) samples for NMR. (t10 = 65 min; t11 = 85 min; t12 = 100 min; t13 = 125 min; t14 = 140 min; t15 = 165 min; t16 = 200 min; t17 = 250 min; t18 = 325 min).

This behavior indicates that in the first zone only carbonate ion exists but when amine concentration decreases (due to the chemical reaction with carbon dioxide) the presence of

bicarbonate ion increases. This fact is produced because the liquid phase's pH decreases with the reaction of carbon dioxide and pyrrolidine and then the buffer reaction between bicarbonate and carbonate ions is produced (see figure 2.35). Taking into account the reaction 6, the hydrolysis of carbamate produces bicarbonate ion and pyrrolidine, and this amine will be used to react with carbon dioxide again. Both reactions: carbonate ion and carbamate to produce bicarbonate ion involves the production of pyrrolidine molecules and then these reaction explains the constant mass transfer rate zone with a similar pseudofirst order because in one hand pyrrodine reacts with carbon dioxide and decrease its concentration, but on the other hand amine molecules are been produced by the buffer reaction and the hydrolysis of carbamate. This fact is supported by NMR spectra previously commented because carbamate peak tend to disappear with time by means of the hydrolysis reaction.

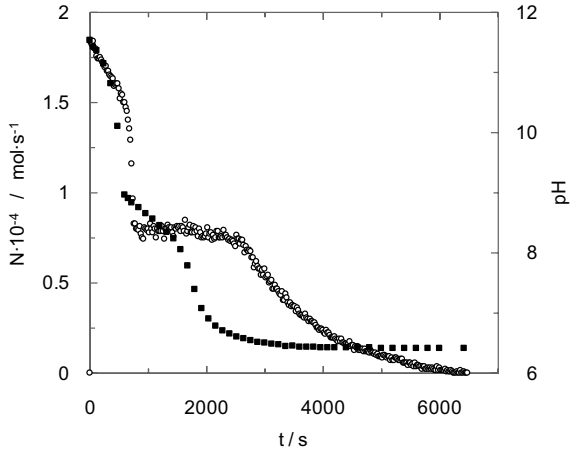


Figure 2.35. Comparison between carbon dioxide absorption rate and liquid phase pH. $Q_g$ = 30 L·h$^{-1}$. $C_{PYR}$ = 0.1 mol·L$^{-1}$. (○) absorption rate; (■) pH.

The zone with the last decrease in mass transfer rate corresponds to physical absorption process when the chemical reaction had concluded caused by the low concentration of reagents. In this zone, only bicarbonate ion peak is observed in the $^{13}C$ NMR. Several researchers[140] have

[140] Park J., Yoon S. J., Lee H. Effect of steric hindrance on carbon dioxide absorption into new amine solutions: thermodynamic and spectroscopic verification through solubility and NMR analysis. *Environmental Science Technology* 2003, 37, 1670-1675.

concluded that the chemical absorption process between carbon dioxide and amines aqueous solutions is produced by the mechanism shows in figure 2.36. Taking into account this mechanism the amine reacts with carbon dioxide to produce bicarbonate ion or carbamate, and then, the first one could produce carbonate ion.

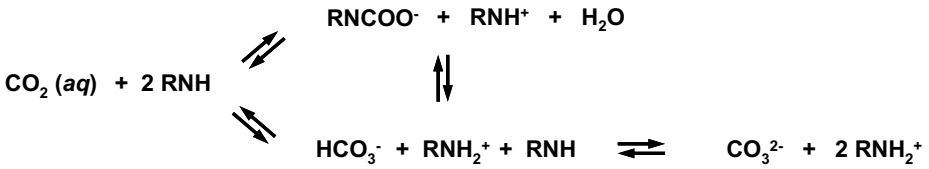


Figure 2.36. Proposed model by Park et al.[141]

On the basis of experimental data obtained in present work is possible to conclude that the mechanism proposed in figure 2.37 is more suitable, because the production of carbamate and carbonate ion is performed via bicarbonate ion, because in absorption experiments, only carbonate ion is observed at initial time due to carbonate – bicarbonate ions equilibrium is instantaneous.

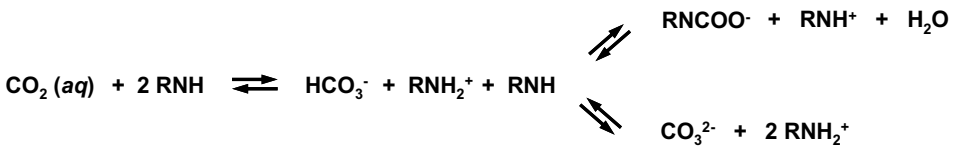


Figure 2.37. Proposed mechanism taking into account figure 2.31.

The observed behavior in present work and the reaction mechanism shown in figure 2.37 are supported by previous studies of other researchers working in carbon dioxide chemical absorption with monoethanolamine aqueous solutions[142]. These studies concluded that the

[141] Park J., Yoon S. J., Lee H. Effect of steric hindrance on carbon dioxide absorption into new amine solutions: thermodynamic and spectroscopic verification through solubility and NMR analysis. *Environmental Science Technology* 2003, 37, 1670-1675.

[142] McCann N., Phan D., Wang X., Conway W., Burns R., Attalla M., Puxty G., Maeder D. M. Kinetics and mechanism of carbamate formation from $CO_2$(aq), carbonate species, and monoethanolamine in aqueous solution. *Journal of Physical Chemistry A.* 2009, 113, 5022-5029.

chemical absorption process is produced by different chemical reactions shown in figure 2.38 as function of amine concentration and pH of the liquid phase. In this figure is possible observes that the reaction between carbon dioxide and amine to produce carbamate takes place only at pH values near to 7 and also, the mechanism proposed by the experimental results obtained in present work are considered as possible ways.

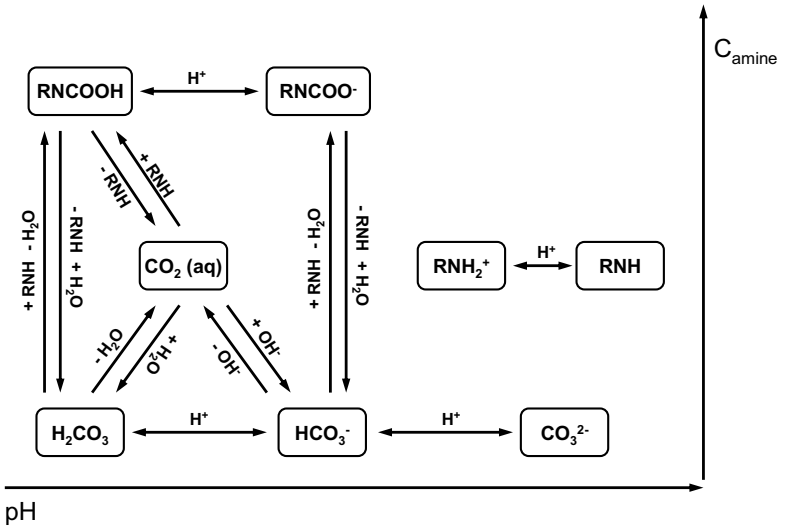


Figure 2.38. General reaction scheme of pyrrolidine + carbon dioxide reaction. ( ↔ ) instanteous protonation equilibria; ( ⇆ ) non-instantaneous equilibria.

The reaction between the carbon dioxide and the pyrrolidine in an aqueous solution is fast, and this characteristic implies that the mass transfer process is the rate limiting reaction stage of the global process. Under certain conditions, the amine concentration at the gas/liquid interface could be the same as in the liquid bulk, and the reaction could be carried out completely at the interface. Equation 2.13 must be used under these conditions.

$$N = C_A^* \cdot a \cdot \sqrt{D_A \cdot k_2 \cdot C_B^{bulk}} \qquad (2.13)$$

where *N*, is the carbon dioxide absorption rate, $C_A^*$ and $D_A$, the solubility and diffusivity of carbon dioxide in the aqueous phase, *a*, is the gas-liquid specific interface area, $k_2$, the rate

constant for the reaction between carbon dioxide and pyrrolidine and $C_B^{bulk}$, the pyrrolidine concentration in the bulk of the aqueous phase.

The use of this expression (equation 2.13) needs the concentration of amine to remain practically constant throughout time[143], but if this condition is not satisfied, then, a part of the chemical reaction between the carbon dioxide and the pyrrolidine is carried out at the interface, and the other part in the liquid bulk. The surface renewal theory developed by Dankwerts contributed to the expression shown in equation 2.14.

$$N = C_A^* \cdot a \cdot \sqrt{D_A \cdot k_2 \cdot C_B^{bulk} + k_L^2} \qquad (2.14)$$

The use of equation 2.14 to fit the experimental data to the mass transfer coefficient calculation implies the knowledge of the specific interfacial area value under the different operation conditions. The specific area determination could be set employing equation 2.13, but the application conditions are not satisfied under the present operation conditions. For this reason, another methodology has been employed for specific area determination (the photographic method used in the previous section).

Equation 2.14 uses the pyrrolidine concentration and this variable has been calculated by means the quantity of carbon dioxide absorbed along the time and then the reaction stoichiometry is basic data to perform the mass transfer coefficient calculation. This calculation will be performed in the first part of the absorption experiments (the first decrease zone in absorption rate), and in this part of the experiments the reaction products present in the liquid phase are the carbonate ion and carbamate. Both products involves that 2 mol of amine are required per mole of carbon dioxide. Taking into account this stoichiometry and using the values of absorption rate and gas-liquid specific interfacial area, the mass transfer coefficient has been performed and figure 2.39 shows an example of use of equation 2.14 for fitting experimental data. A good agreement between the linear fit and the experimental data is observed. Also, figure 2.39 shows the influence of pyrrolidine concentration, and when amine concentration increases, a decrease in the value of intercept (square mass transfer coefficient) is observed.

[143] Juvekar V. A., Sharma M. M. Absorption of carbon dioxide in suspension of lime. *Chemical Engineering Science* 1973, 28, 825–837.

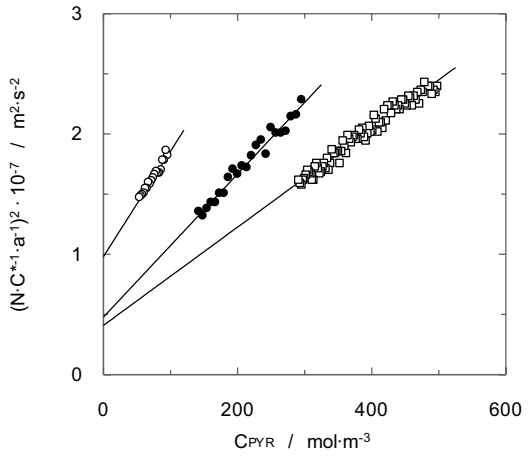


Figure 2.39. Obtaining of mass transfer coefficient for the system carbon dioxide – pyrrolidine. $Q_g$ = 18 L·h$^{-1}$. (○) $C_{PYR}$ = 0.1 mol·L$^{-1}$; (●) $C_{PYR}$ = 0.3 mol·L$^{-1}$. (□) $C_{PYR}$ = 0.5 mol·L$^{-1}$.

The same procedure than in figure 2.39 has been employed to fit the absorption rate experimental data by means of equation 2.14, and then to obtain the value of mass transfer coefficient upon the different experimental conditions. Figure 2.40 shows a comparison of the calculated data for mass transfer coefficient.

With regard to the gas flow-rate effect, when this variable increases, an increase in the mass transfer coefficient is observed too. This fact indicates that this operation variable (gas flow-rate) has an influence on the gas-liquid interfacial area and upon the mass transfer process[144]. This is due to the fact that an increase in the gas flow-rate fed to the bubble column produces a greater energy transmission to the liquid phase and, therefore, the turbulence in the liquid contained in the contactor increases as well. This increase also produces an increase in the mass transfer in the liquid phase, avoiding concentration gradients and diffusional limitations. It is observed that higher differences regarding the gas flow-rate influence are obtained for low concentrations of amine. However, for high concentrations of pyrrolidine in the liquid phase, a slight decrease in the value of the mass transfer coefficients for different analysed flow rates is

[144] La Rubia M. D., García-Abuín A., Gómez-Díaz D., Navaza J. M. Interfacial area and mass transfer in carbon dioxide absorption in TEA aqueous solutions in a bubble column reactor. *Chemical Engineering and Processing: Process Intensification* 2010, 49(8), 852-858.

observed. This behaviour is related to the liquid phase viscosity value, which is a very important physical property in the mass transfer processes. For low pyrrolidine concentrations, viscosity increases slightly[145] and therefore, an increase in the gas flow-rate fed to the bubble column produces a significant increase in the turbulence generated. When, amine concentration increases, the viscosity increases significantly too and then, the effect of the gas flow-rate over the turbulence decreases. For a more viscous liquid, a higher gas flow-rate is necessary to produce the same grade of turbulence.

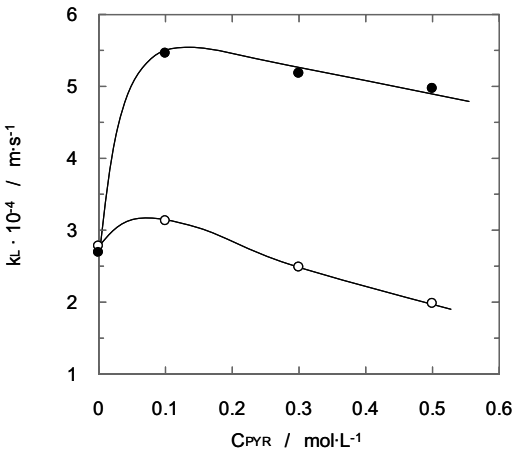


Figure 2.40. Pyrrolidine concentration influence upon mass transfer coefficient. (○) $Q_g$ = 18 L·h$^{-1}$.; (●) $Q_g$ = 40 L·h$^{-1}$.

Regarding the influence of the pyrrolidine concentration in the liquid phase upon the value of mass transfer coefficient, a similar behaviour is observed for previous carbon dioxide – amine systems[146,147]. When the amine concentration increases in the liquid phase, a significant increase in the mass transfer coefficient is observed until it reaches a maximum value, from which the increase of the amine concentration in the liquid phase produces a continuous decrease in the coefficient value. The enhancement of the mass transfer for low concentrations of pyrrolidine is

[145] Álvarez E., Gómez-Díaz D., La Rubia M. D., Navaza J. M. Densities and viscosities of aqueous solutions of pyrrolidine and piperidine from (20 to 50) °C. *Journal of Chemical & Engineering Data* 2005, 50, 1829-1832.
[146] Navaza J. M., Gómez-Díaz D., La Rubia M. D. Removal process of $CO_2$ using MDEA aqueous solutions in a bubble column reactor. *Chemical Engineering Journal* 2009, 146, 184-188.
[147] La Rubia M. D., García-Abuín A., Gómez-Díaz D., Navaza J. M. Interfacial area and mass transfer in carbon dioxide absorption in TEA aqueous solutions in a bubble column reactor. *Chemical Engineering and Processing: Process Intensification* 2010, 49, 852-858.

due to a chemical reaction, which makes the concentration of carbon dioxide in the liquid phase to be nearly zero and, therefore, the driving force is kept high. However, in spite of increasing the concentration of amine, and being therefore able to support the driving force in a high value, is possible observes that the mass transfer rate (based on value of mass transfer coefficient) decreases. This is due to a different effect to the existence of a chemical reaction. The factor which causes this behaviour is, as it was mentioned before, the viscosity of the liquid phase. This physical property plays a very important role in mass transfer processes, having a negative effect[148,149], because it introduces a greater resistance to the mass transfer, probably due to the less renovation of the liquid elements near the interface. In this case, the liquid phase viscosity increases with a pyrrolidine concentration, with a very negative influence upon the mass transfer rate, compensating the positive effect caused by the fast chemical reaction in the liquid phase upon the value of mass transfer coefficient.

#### *2.3.2.2. Glucosamine*

The behaviour of glucosamine aqueous solutions in the absorption process of carbon dioxide has been analysed, at the beginning, in a global way. For that reason, several experimental conditions were used (liquid phase composition and gas flow-rate). Figure 2.41 shows an example of the experimental data obtained of carbon dioxide capture experiments with glucosamine aqueous solutions. In that figure, the absorption kinetics of two liquid phases, consisting of an aqueous solution of glucosamine with the same concentration (0.1 M), are compared. One solution has not been modified. However, a controlled quantity of sodium hydroxide has been added to another one in order to compensate partially the presence of hydrochloric acid, present in the commercial product. When a part of the glucosamine molecules are free (for compensation with sodium hydroxide), the quantity of the carbon dioxide absorbed by the liquid phase increases significantly, which indicates that a process of carbon dioxide absorption is being taken place by means of a chemical reaction. This capture process of transferred gas to the liquid phase is carried out by a chemical reaction between the glucosamine,

[148] Jiao Z., Xueqing Z., Juntag Y. $O_2$ transfer to pseudoplastic fermentation broths in air-lift reactors with different inner designs. *Biotechnology Techniques* 1998, 12, 729-32.
[149] Gómez-Díaz D., Navaza J. M., Sanjurjo B., Vázquez-Orgeira L. Carbon dioxide absorption in glucosamine aqueous solutions. *Chemical Engineering Journal* 2006, 122, 81-6.

present in liquid phase, and the absorbed gas. This behaviour was detected in a previous study since, when the glucosamine from the supplier was used directly, a chemical reaction was not observed, due to the presence of acidic medium.

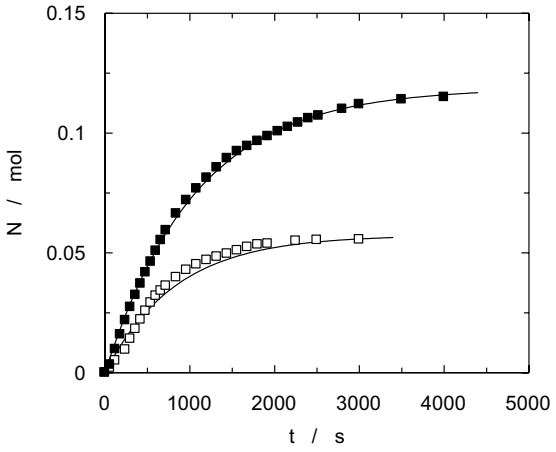


Figure 2.41. Absorption kinetics of $CO_2$-glucosamine aqueous solution system. $C_{GA}$ = 0.1 mol·L$^{-1}$. (□) pH = 4.5 (without NaOH addition); (■) pH = 7.

In relation to the influence of the gas flow-rate fed to the bubble column, figure 2.42 shows the influence of this operation variable upon the carbon dioxide capture kinetic when the other conditions remain constant. On the basis of the experimental data we can observe that, when a high value of gas flow-rate is fed to the gas-liquid contactor, the glucosamine present in the liquid phase is consumed at a high rate and then, the maximum carbon dioxide loading is reached in a shorter operation time. This behaviour is due to two effects produced by the increase of the gas flow-rate: (i) one of them is an increase in the gas-liquid interfacial area, since the increment in the gas volume fed to bubble column reactor implies the formation of a higher number of bubbles. An increase in the number of bubbles commonly produces an increase in the interfacial area and then, upon the gas mass transfer rate. (ii) On the other hand, the increase in the number of bubbles increases the power supplied by the gas to the liquid phase when the bubbles ascend along the BCR (increasing the turbulence). This phenomenon produces an increase of the turbulence near the gas-liquid interface that produces an increase in the mass transfer rate.

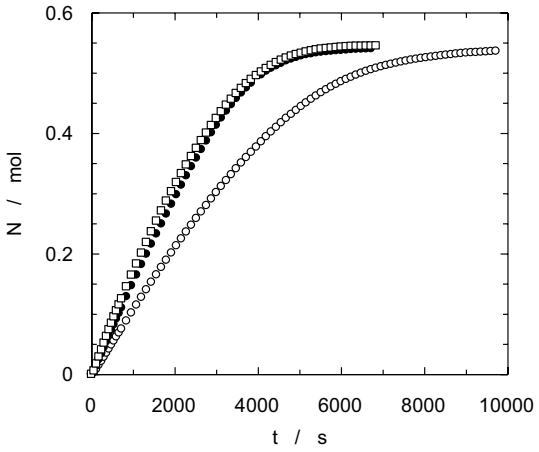


Figure 2.42. Influence of gas flow-rate upon $CO_2$ absorption kinetic. $C_{GA}$ = 0.3 mol·L$^{-1}$. pH = 9. (○) $Q_g$ = 18 L·h$^{-1}$, (●) $Q_g$ = 30 L·h$^{-1}$, (□) $Q_g$ = 40 L·h$^{-1}$.

Using the experimental data shown in figures 2.41 and 2.42 for carbon dioxide absorbed flow-rate along the operation time, under different operation conditions, the carbon dioxide loading has been analysed, taken into account the deprotonated amine concentration (free amine concentration). An example of the data obtained for this parameter (carbon dioxide loading) is shown in figure 2.43, and these data indicate that an increase in the amine concentration produces a decrease in the carbon dioxide loading. This behaviour is in agreement with previous studies using different amines as a reagent to capture acid gases[150,151,152]. This behaviour has been assigned to different causes in previous works: (i) an increase in the liquid phase viscosity due to an increase in the amine concentration, that produces a decrease in the diffusion coefficients, and (ii) aggregation processes between amine molecules when the concentration increases, being an inconvenient to the access of carbon dioxide molecules into the amino group in order to produce the reaction. The first cause abovementioned does not produce the decrease in the carbon dioxide loading, since a reduction in the gas diffusion must influence upon the mass transfer rate, but the

[150] Park J. Y., Yoon S. J., Lee H., Yoon J. H., Shim J. G., J. K. Lee, Min B. Y., Eum H. M., Kang M. C. Solubility of carbon dioxide in aqueous solutions of 2-amino-2-ethyl-1,3-propanediol. *Fluid Phase Equilibria* 2002, 202, 359-366.
[151] Zhang X., Zhang C. F., Xu G. W., Gao W., Wu Y. Q. An experimental apparatus to mimic $CO_2$ removal and optimum concentration of MDEA aqueous solution. *Industrial & Engineering Chemistry Research* 2001, 40, 898-901.
[152] Loubiere K., Hebrard G. Influence of liquid surface tension (surfactants) on bubble formation at rigid and flexible orifices. *Chemical Engineering and Processing* 2004, 43, 1361-1369.

carbon dioxide loading remains constant. Taking into account this hypothesis, the second cause seems to be the behaviour that produces the reduction in the carbon dioxide loading when the amine concentration increases in the liquid phase.

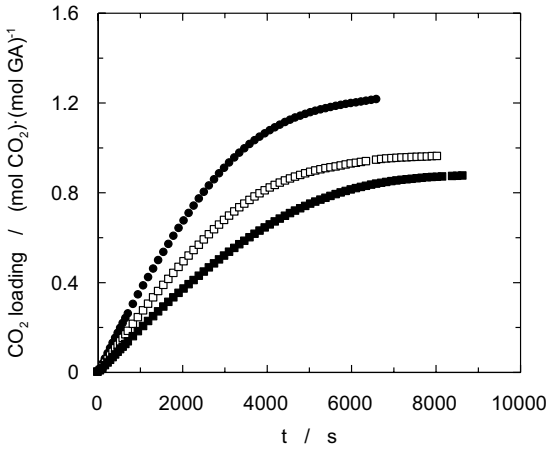


Figure 2.43. $CO_2$ loading obtained for different glucosamine concentration solutions. $Q_g$ = 18 L·h$^{-1}$. pH = 8. (●) $C_{GA}$ = 0.2 mol·L$^{-1}$, (□) $C_{GA}$ = 0.3 mol·L$^{-1}$, (■) $C_{GA}$ = 0.4 mol·L$^{-1}$.

Figure 2.43 also shows that, in certain experiments, the carbon dioxide loading takes higher values than the unity. This behaviour is observed when the free amine concentration in the liquid phase is very low. Then, the carbon dioxide physically absorbed takes an important role in the ratio among the absorbed moles of carbon dioxide and the corresponding ones of free amines in the liquid phase.

As in the case of using pyrrolidine aqueous solutions, NMR studies have been carried out for glucosamine during the absorption process with chemical reaction. Figure 2.44 shows the absorption kinetics for a specific experiment and the sampling times. These samples were subsequently analyzed by NMR.

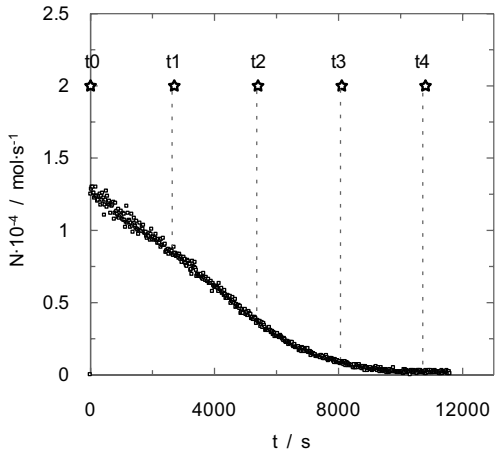


Figure 2.44. Carbon dioxide absorption rate. $Q_g$ = 30 L·h$^{-1}$. $C_{GA}$ = 0.2 mol·L$^{-1}$. pH = 7. (□) absorption rate; (✯) samples for NMR analysis. (t0 = 0 s; t1 = 45 min; t2 = 90 s; t3 =135 s; t4 = 180 s).

In view of the $^{13}C$ NMR spectra (see figure 2.45), a different behavior, with regard to results obtained using pyrrolidine aqueous solutions, can be observed, since from the beginning of the experiment, only the chemical shift of bicarbonate/carbonate equilibrium appears, and it corresponds to pure bicarbonate.

In figure 2.45, it can be observed that carbonate/bicarbonate chemical shift does not change with time in relation with chemical displacement, therefore it can be concluded that bicarbonate is the product of reaction throughout the operating time. For this reason, for the carbon dioxide absorption with chemical reaction by means of glucosamine aqueous solutions, a stoichiometry 1:1 (ratio of carbon dioxide:glucosamine) is chosen.

A similar behavior is observed when different operating conditions are used to perform the gas absorption process with glucosamine aqueous solutions, as shown in figure 2.46.

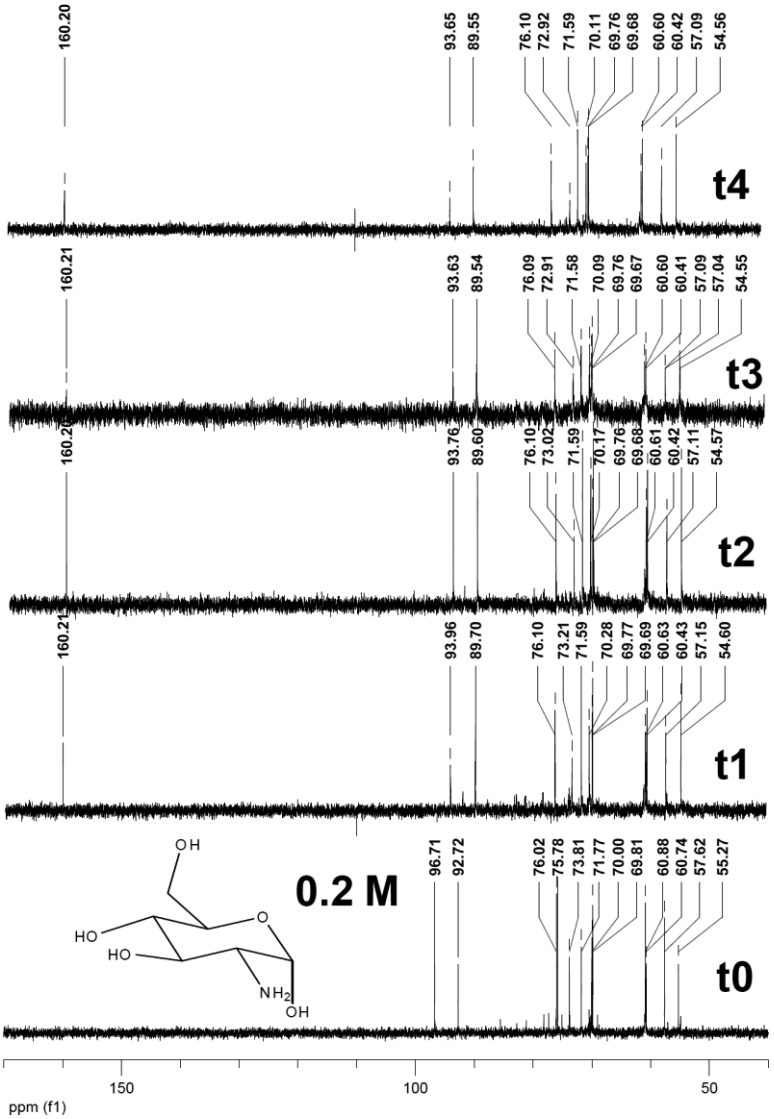


Figure 2.45. $^{13}C$ NMR spectra of samples taken at different operation times (t0 = 0 s; t1 = 45 min; t2 = 90 min; t3 = 135 min; t4 = 180 min s). $Q_g$ = 30 L·h$^{-1}$. $C_{GA}$ = 0.2 mol·L$^{-1}$.

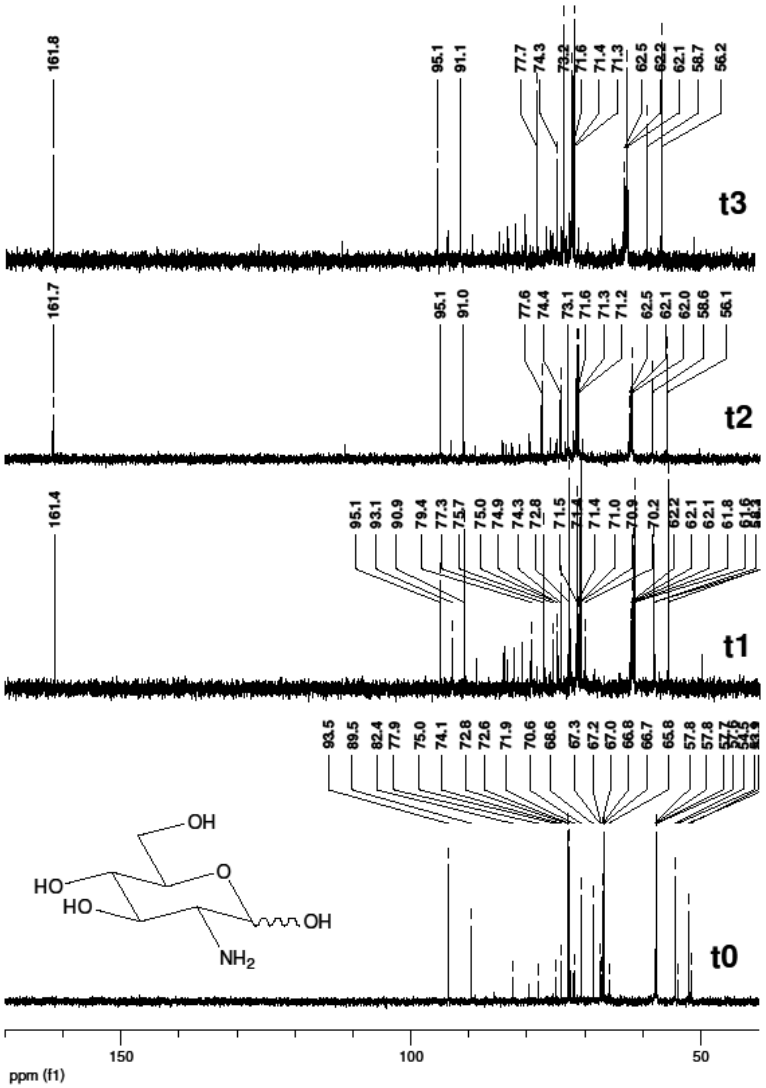


Figure 2.46. $^{13}C$ NMR spectra of samples taken at different operation times (t0 = 0 min; t1 = 50 min; t2 = 100 min; t3 = 150 min). $Q_g$ = 30 L·h$^{-1}$. $C_{GA}$ = 0.4 mol·L$^{-1}$.

Figure 2.47 shows an example of how the experimental data fit employing equation 2.14 for different operation conditions. The linear fits shown in figure 2.47 let us calculate the value of the liquid side mass transfer coefficient by means of the intercept value.

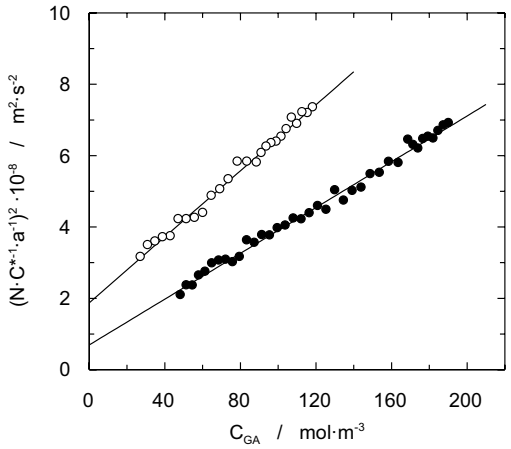


Figure 2.47. Fits corresponding to equation 2.14 to determine the mass transfer coefficient data. $Q_g$ = 18 L·h$^{-1}$. $C_{GA}$ = 0.2 M. (○) pH = 8, (●) pH = 10.

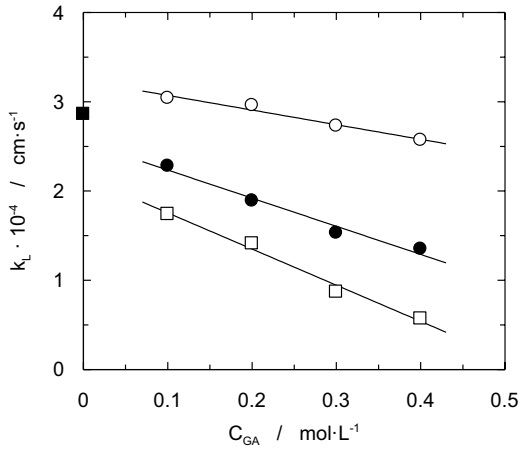


Figure 2.48. Influence of glucosamine concentration and pH upon mass transfer coefficient data. $Q_g$ = 18 L·h$^{-1}$. (○) pH = 7, (●) pH = 8, (□) pH = 9, (■) water.

Figure 2.48 has been built to analyse the influence of the glucosamine initial concentration and for different initial pH, using the values determined for the mass transfer coefficient for systems with different glucosamine concentration in the liquid phase. The obtained behaviour indicates that an increase in glucosamine concentration in the liquid phase produces a decrease in the mass transfer coefficient.

Though the free glucosamine increases, the mass transfer coefficient decreases. This behaviour is assigned to two causes with negative influence upon mass transfer rate: (i) an increase in liquid phase viscosity when the glucosamine concentration increases[153]. This physical property increases too by the addition of different quantities of sodium hydroxide to adjust the pH (see figure 2.49).

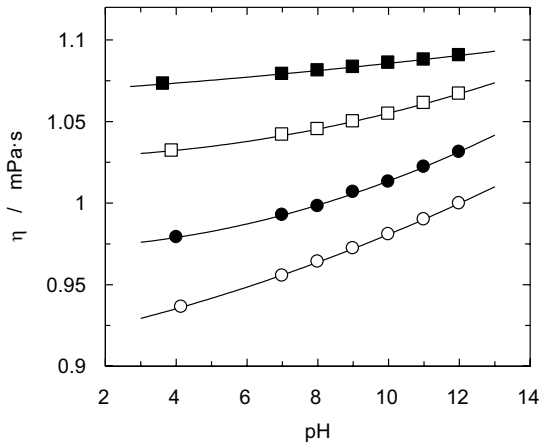


Figure 2.49. Effect of glucosamine concentration and the addition of sodium hydroxide upon the dynamic viscosity value. (○) $C_{GA}$ = 0.1 mol·L$^{-1}$, (●) $C_{GA}$ = 0.2 mol·L$^{-1}$, (□) $C_{GA}$ = 0.3 mol·L$^{-1}$, (■) $C_{GA}$ = 0.4 mol·L$^{-1}$.

The effect of viscosity upon the mass transfer in gas-liquid systems has been deeply studied observing a negative effect in all the cases, producing a clear decrease in the mass

[153] Kilonzo P. M., Margaritis A. The effects of non-Newtonian fermentation broth viscosity and small bubble segregation on oxygen mass transfer in gas-lift bioreactors: a critical review. *Biochemical Engineering Journal* 2004, 17, 27–40.

transfer coefficient value[154,155]. (ii) The presence of electrolytes in the liquid phase, due to the hydrochloride acid (accompanying to glucosamine molecule) and the addition of sodium hydroxide, has a negative effect upon the mass transfer coefficient, as these substances produce an increase in liquid phase viscosity (see figure 2.49).

The influence of the liquid phase pH upon the mass transfer coefficient has also been analysed obtaining two different behaviours (see figure 2.50). When the pH is increased, an increase in the free glucosamine concentration is obtained, but a reduction in the value of mass transfer coefficient is observed (until pH = 10). And then, when the pH increases up to 10, a clear enhancement in the mass transfer coefficient is produced. The mass transfer coefficient reduction observed in figure 2.50, when the pH increases, is due to the previously commented effects. The addition of higher quantities of sodium hydroxide (and electrolytes) produces an increase in viscosity that produces a decrease in the mass transfer coefficient (figure 2.50). When the addition of sodium hydroxide reaches the glucosamine concentration, free hydroxyl ions are present in the liquid phase and then, carbon dioxide molecules could react with both reagents (glucosamine and hydroxyl ions). As different studies have indicated, the reaction between carbon dioxide and hydroxyl ions is fast[156] and then, the mass transfer coefficient increases significantly with regard to the corresponding ones determined for systems with low pH values, without presence of hydroxyl ions in the aqueous solution. The existence of an instantaneous gas-liquid reaction regime (reaction between carbon dioxide and hydroxyl ions) increases the driving force in the system and then, the value of the mass transfer coefficient for high pH values increases too. But the existence of two reactions for carbon dioxide capture for pHs higher than 10 implies that, being the mass transfer coefficient under these operation conditions, it must not be taken into account to be compared to the previous ones, determined for a system where there were only one single reaction between the carbon dioxide and the glucosamine.

In figure 2.50, the influence of the gas flow-rate fed to the bubble column reactor upon the mass transfer coefficient can be observed. For a bubbling equipment, this variable (gas flow-rate) could play an important effect in mixtures and stirring processes upon the liquid phase. The

[154] Gómez-Díaz D., Navaza J. M., Sanjurjo B. Analysis of mass transfer in the precipitation process of calcium carbonate using a gas/liquid reaction. *Chemical Engineering Journal* 2006, 116, 203–209.
[155] Gómez-Díaz D., Navaza J. M., Sanjurjo B., Vázquez-Orgeira L. Carbon dioxide absorption in glucosamine aqueous solutions. *Chemical Engineering Journal* 2006, 122, 81–86.
[156] Danckwerts P. V., Sharma M. M. Absorption of carbon dioxide into solutions of alkalies and amines. Hydrogen sulfide and carbonyl sulphide. *Chemical Engineer (London)* 1966, 202, CE244–CE280.

experimental results obtained from the system employed in the present work show that, under the used experimental conditions, differences between the mass transfer coefficient values for different gas flow-rates are not observed. This behaviour is in agreement with previous studies developed[157,158] in similar experimental systems to the present work.

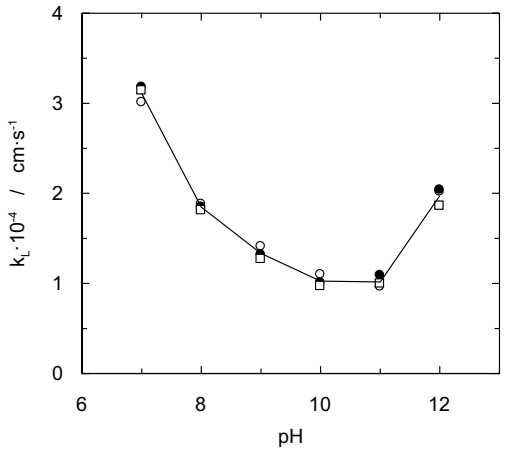


Figure 2.50. Influence of pH and gas flow-rate upon mass transfer coefficient. $C_{GA}$ = 0.2 mol·L$^{-1}$. (○) $Q_g$ = 18 L·h$^{-1}$, (●) $Q_g$ = 30 L·h$^{-1}$, (□) $Q_g$ = 40 L·h$^{-1}$. Solid line corresponds to the mass transfer coefficient medium value for all gas flow-rate.

## 2.3.3. Conclusions

The absorption of carbon dioxide with pyrrolidone aqueous solutions showed a characteristic behaviour in comparison with the corresponding ones using other amine aqueous solutions. A decrease in absorption rate is observed when operation time increases until this variable reaches a *plateau*. This zone (with a constant absorption rate) is observed during an important period. Subsequently, a decrease in the value of absorption rate is observed until the liquid phase saturation in carbon dioxide is reached, and the absorbed molar gas flow-rate is zero.

[157] Gómez-Díaz D., Navaza J. M., Sanjurjo B. Analysis of mass transfer in the precipitation process of calcium carbonate using a gas/liquid reaction. *Chemical Engineering Journal* 2006, 116, 203–209.
[158] Gómez-Díaz D., Navaza J. M., Sanjurjo B., Vázquez-Orgeira L. Carbon dioxide absorption in glucosamine aqueous solutions. *Chemical Engineering Journal* 2006, 122, 81–86.

Studies with NMR spectroscopy have allowed to obtain the necessary information about carbon dioxide – pyrrolidine gas-liquid absorption process. At the first time the products species present in the liquid phase are carbonate ion and carbamate, subsequently the hydrolysis of carbamate produces bicarbonate ion and pyrrolidine, and this amine will be used to react with carbon dioxide again, besides the peak corresponding to the carbonate – bicarbonate ions equilibrium begins to shift from the carbonate to bicarbonate value. These reactions explain the constant mass transfer rate zone.

Regarding the influence of the pyrrolidine concentration in the liquid phase upon the value of mass transfer coefficient, a similar behaviour is observed for previous carbon dioxide – amine systems. When the amine concentration increases in the liquid phase, a significant increase in the mass transfer coefficient is observed until it reaches a maximum value, from which the increase of the amine concentration in the liquid phase produces a continuous decrease in the coefficient value.

The use of glucosamine aqueous solutions to capture carbon dioxide has also been analysed. As in the case of using pyrrolidine aqueous solutions, NMR studies have been carried out and different behavior has been obtained, only the chemical shift of bicarbonate/carbonate equilibrium appears, and it corresponds to pure bicarbonate. For this reason, for the carbon dioxide absorption with chemical reaction by means of glucosamine aqueous solutions, a stoichiometry 1:1 takes place.

The mass transfer coefficient determination has been developed under the different operation conditions, and the results for this parameter show that the gas flow-rate does not show any influence upon the mass transfer coefficient, but the liquid phase composition (glucosamine concentration) produces a decrease in the value of the mass transfer coefficient when the free glucosamine concentration increases in the liquid phase.

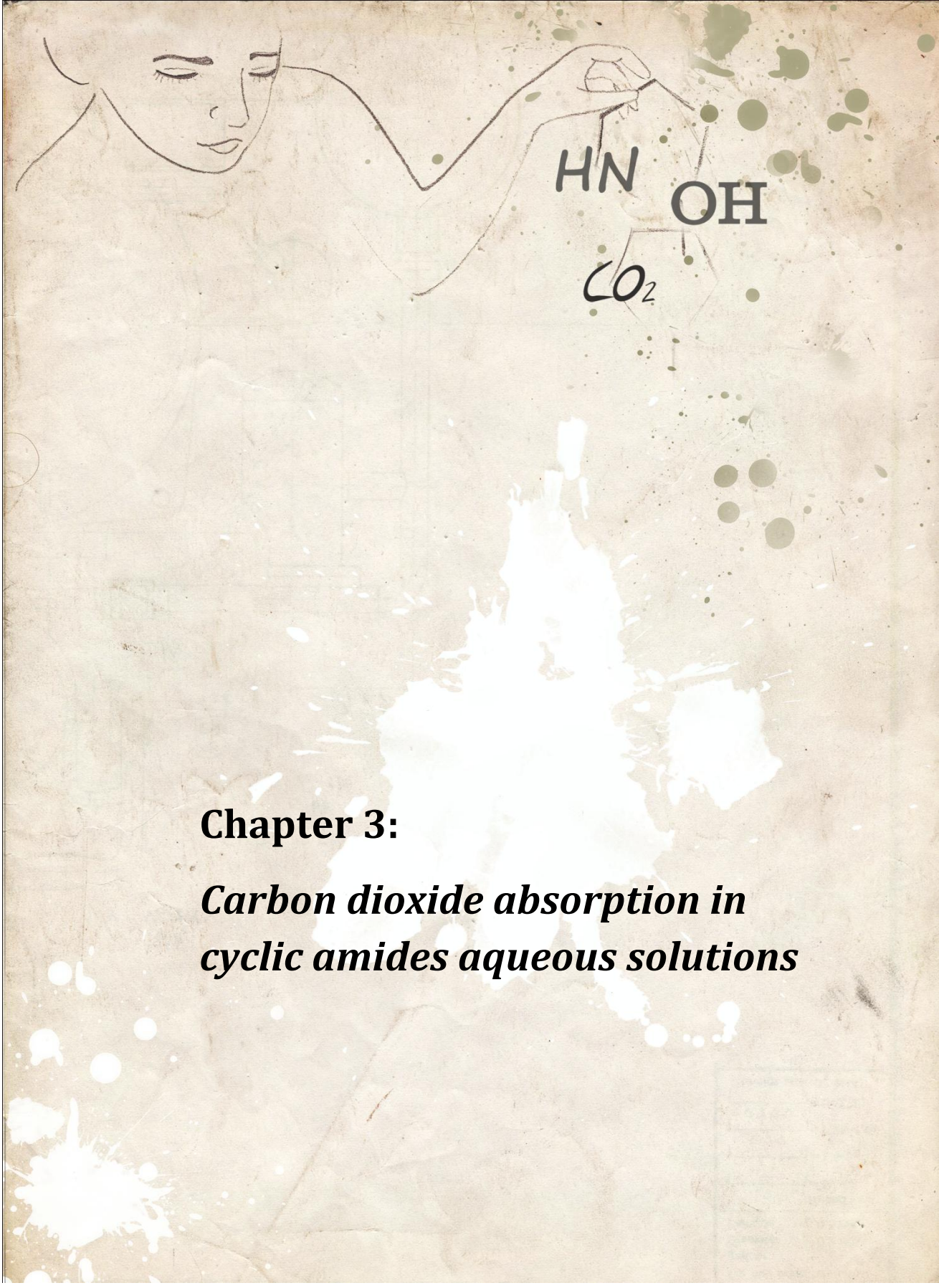


# Chapter 3:

## *Carbon dioxide absorption in cyclic amides aqueous solutions*

# 3.1 Physico-chemical characterization of cyclic amides aqueous solutions

*Abstract*

*Experimental density and viscosity for aqueous solutions of N-ethyl-2-pyrrolidone and N-methyl-2-pyrrolidone were measured over the entire composition range and at different temperatures (20-50) ºC. Excess molar volumes have been calculated and their dependence on composition was mathematically represented by a Redlich-Kister type equation. The hydration of this kind of molecules plays an important role in the thermophysical behaviour of these mixtures.*

*Besides, the surface tension of aqueous solutions of 2-pyrrolidone (P), N-methyl-2-pyrrolidone (MP) and N-ethyl-2-pyrrolidone (EP) has been measured at the same temperatures over the whole range of concentrations. The surface tensions of these aqueous binary mixtures show more concentration dependence on the water-rich side. Addition of a small amount of N-alkyl-2-pyrrolidone reduces the surface tension of water drastically. This effect is related to the presence of hydrophobic groups which tend to accumulate at air-water interface but also the complex interactions between N-alkyl-2-pyrrolidones molecules influence on the surface tension.*

### 3.1.1. Specific introduction

Short chain N-alkyl-2-pyrrolidones are completely miscible over the entire composition range with water. They have been used as cosolvents in the petroleum industry to increase the selectivity and solvent power for extracting aromatic hydrocarbons. These pyrrolidones are also used in pharmaceutical formulations and in the administration of therapeutic agents to the bloodstream painlessly in a controlled manner because they enhance the transdermal transport of drugs. These cyclic amides have excellent thermal and chemical stability and they are used as absorbents of sour gases from crude natural gas or entrainer to alter the separation factor in distillation process[159]. Besides, they have shown important characteristics such as high density, high boiling point and high polarity solvents, which allow their usability at an industrial level. Also, their high solubility in water allows the use of this kind of substance in a wide range of industrial and laboratory operations.

The knowledge of physical properties of systems water + cyclic amides over the entire composition range and at different temperatures is highly useful to understand some interfacial phenomena. For example, viscosity plays an important role regarding the behaviour and hydrodynamics in mass transfer operations[160,161].

Previous studies have analysed cyclic amides, such as 2-pyrrolidone, N-methyl-2-pyrrolidone or 1-vinyl-2-pyrryolidone[162,163,164,165], regards different physico-chemical properties and the influence of the substituent upon the behaviour obtained for different properties and excess parameters. Surface tension of several cyclic amides, such as N-cyclohexyl-2-

[159] Noll O., Fischer K., Gmehling J. Vapor-liquid equilibria and enthalpies of mixing for the binary system water + N-methyl-2-pyrrolidone in the temperature range 80-140 °C. *Journal of Chemical & Engineering Data* 1996, 41, 1434-1438.
[160] Álvarez E., Sanjurjo B., Cancela A., Navaza J. M. Mass transfer and influence of physical properties of solutions in a bubble column. *Chemical Enineering Research and Des*ign 2000, 78, 889-893.
[161] Cents A. H. G., Brilman D. W. F., Versteeg G. F. Gas absorption in an agitated gas-liquid-liquid system. *Chemical Engineering Sci*ence 2001, 56, 1075-1083.
[162] Blumenshine R. L., Sears P. G. Several properties of the 2-pyrrolidone - water system as functions of composition and temperature. *Journal of Chemical & Engineering Data* 1966, 11, 141-143.
[163] García B., Alcalde R., Leal J. M., Matos J. S. Solute-solvent interactions in amide-water mixed solvents. *Journal of Physical Chemistry* 1997, 101, 7991-7997.
[164] Al-Azzwal S. F., Awwad A. M., Al-Dujaili A. H., Al-Noori M. K. Dielectric constants and excess volumes of 2-pyrrolidone + water at several temperatures. *Journal of Chemical & Engineering Data* 1990, 35, 463-466.
[165] George J., Sastry N. V. Densities, viscosities, speeds of sound, and relative permittivity for water + cyclic amides (2-pyrrolidinone, 1-methyl-2-pyrrolidinone, and 1-vinyl-2-pyrrolidinone) at different temperatures. *Journal of Chemical & Engineering Data* 2004, 49, 235-242.

pyrrolidinone[166], N-butyl-2-pyrrolidinone[167] or N-hexyl-2-pyrrolidinone[168], has also been analysed in previous studies and certain kind of pre-aggregation was found before the presence of micelles in aqueous solution.

## 3.1.2. Results and discussion

Present work analyses the influence of mixture composition and temperature upon density, viscosity and surface tension of systems formed by water and different short N-alkyl-2-pyrrolidones at temperatures from 20 ºC to 50 ºC.

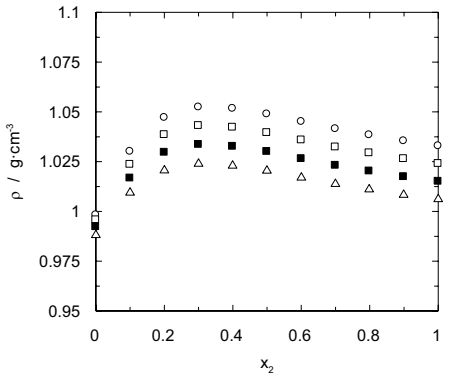


Figure 3.1. Influence of mixture composition and temperature upon density for water (1) + N-methyl-2-pyrrolidone (2) system. ○, t = 20 ºC; □, t = 30 ºC; ■, t = 40 ºC; △, t = 50ºC.

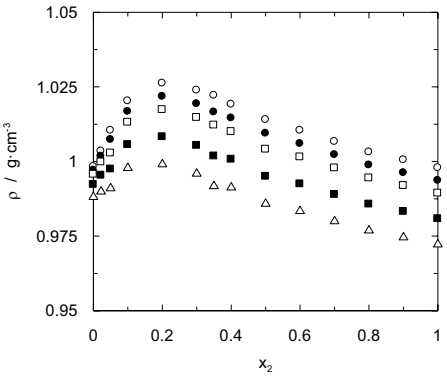


Figure 3.2. Influence of mixture composition and temperature upon density for water (1) + N-ethyl-2-pyrrolidone (2) system. ○, t = 20 ºC; ●, t = 25ºC; □, t = 30 ºC; ■, t = 40 ºC; △, t = 50ºC.

[166] Pethica B. A., Senak L., Zhu Z., Lou A. Surface and colloidal properties of cyclic amides. 5. N-cyclohexyl-2-pyrrolidinone–water mixtures aggregation in solution and adsorption at the air–solution interface. *Colloids and Surfaces A: Physicochemical and Engineering Aspects Science and Technology* 2001, 186, 113–122.
[167] Lou A., Pethica B. A., Somasundaran P., Fan A. Surface and colloid properties of cyclic amides III. Surface activity and micellization of N-butyl-2-pyrrolidinone in water. *Colloids and Surfaces A: Physicochemical and Engineering Aspects Science and Technology* 1999, 20, 569-580.
[168] Lou A., Pethica B. A., Somasundaran P. Surface and colloid properties of cyclic amides II. Phase separation, surface activity and micellization in mixtures of N-hexyl-2-pyrrolidinone and water. *Colloids and Surfaces A: Physicochemical and Engineering Aspects* 1997, 129, 297-303.

The values obtained for the density of the water + N-methyl-2-pyrrolidone system show that a maximum in the value of the density (see figure 3.1) exists. A similar behaviour has been observed for the aqueous solutions of N-ethyl-2-pyrrolidone (see figure 3.2), which has not been observed in the water + 2-pyrrolidone system[169,170]. Extending the alkyl chain, the maximum for the value of the density is located nearer to water-rich region. This implies that, the number of needed molecules of N-ethyl-2-pyrrolidone is lower than in the case of other pyrrolidone, to generate the interactions which produce the presence of these maxima.

Figure 3.3 shows a similar behavior for the densities of N-alkyl-pyrrolidones aqueous solutions but, completely different for the 2-pyrrolidone aqueous solutions, where a maximum is not observed.

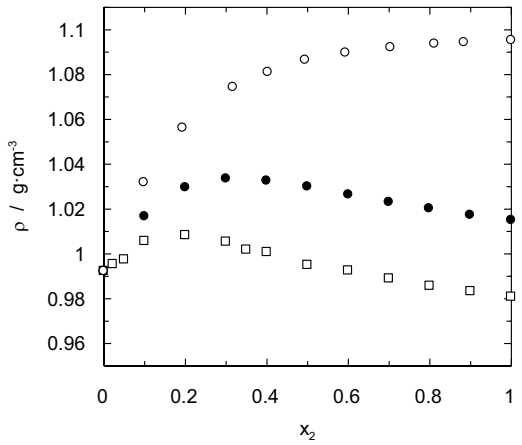


Figure 3.3. Comparison between densities for different systems at 40ºC. ○, water (1) + 2-pyrrolidone (2)[169] system; ●, water (1) + N-methyl-2-pyrrolidone (2) system; □, water (1) + N-ethyl-2-pyrrolidone (2).

About the value of viscosity, a maximum is observed again at low composition of N-methyl-2-pyrrolidone and N-ethyl-2-pyrrolidone (see figure 3.4 and 3.5). Moreover, similar

[169] Blumenshine. R. L., Sears P. G. Several properties of the 2-pyrrolidone- water system as functions of composition and temperature. *Journal of Chemical & Engineering Data* 1966, 11, 141-143.
[170] García B., Alcalde R., Leal J. M., Matos J. S. Solute-solvent interactions in amide-water mixed solvents. *Journal of Physical Chemistry* 1997, 101, 7991-7997.

behaviours have been observed for other aqueous systems in which molecules with the presence of amino groups[171,172] have been used.

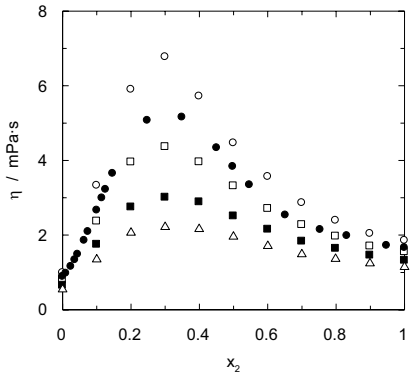


Figure 3.4. Influence of mixture composition and temperature upon viscosity for water (1) + N-methyl-2-pyrrolidone (2) system. ○, t = 20 ºC; ●, t = 25ºC[173]; □, t = 30 ºC; ■, t = 40 ºC; △, t = 50ºC.

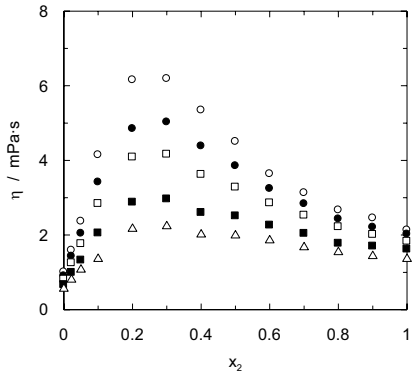


Figure 3.5. Influence of mixture composition and temperature upon viscosity for water (1) + N-ethyl-2-pyrrolidone (2) system. ○, t = 20 ºC; ●, t = 25ºC; □, t = 30 ºC; ■, t = 40 ºC; △, t = 50ºC.

As it happens with the density, the viscosity for both N-alkyl-pyrrolidones aqueous solutions shows a similar behaviour (see figure 3.6), but very different to the 2-pyrrolidinone aqueous solutions ones.

Another interesting aspect is the influence of temperature over the behaviour of these systems and over the different physical properties. For the density and viscosity a constant decrease in the value of these physical properties is observed when temperature increases.

[171] Álvarez E., Gómez-Díaz D., La Rubia D., Navaza J. M. Densities and viscosities of aqueous solutions of pyrrolidine and piperidine from (20 to 50) °C. *Journal of Chemical & Engineering Data* 2005, 50, 1829-1832.
[172] Bernal-Garcia J. M., Galicia-Luna L. A., Hall K. R., Ramos-Estrada M., Iglesias-Silva G. A. Viscosities for aqueous solutions of N-methyldiethanolamine from 313.15 to 363.15 K. *Journal of Chemical & Engineering Data* 2004, 49, 864-866.
[173] George J., Sastry N. V. Densities, viscosities, speeds of sound, and relative permitivities for water + cyclic amides (2-pyrrolidinone, 1-methyl-2-pyrrolidinone, and 1-vinyl-2-pyrrolidinone) at different temperatures. *Journal of Chemical & Engineering Data* 2004, 49, 235-242.

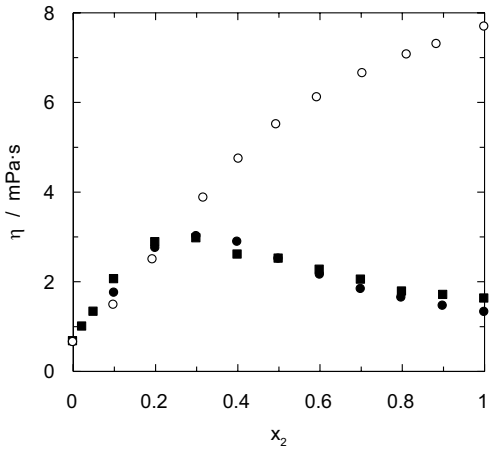


Figure 3.6. Comparison between viscosities for different systems at 40ºC. ○, water (1) + 2-pyrrolidone[174] (2) system; ●, water (1) + N-methyl-2-pyrrolidone (2) system; ■, water (1) + N-ethyl-2-pyrrolidone (2).

In order to estimate the non-ideality of these systems, the excess molar volume was calculated, using equation 3.1.

$$V^E = \sum_{i=1}^{3} x_i \cdot M_i \cdot \left(\rho^{-1} - \rho_i^{-1}\right) \qquad (3.1)$$

where $x_i$ , $M_i$ and $\rho_i$ are the molar fractions, molecular weights and densities of pure components, respectively.

[174] Blumenshine R. L., Sears P. G. Several properties of the 2-pyrrolidone – water system as functions of composition and temperature. *Journal of Chemical & Engineering Data* 1966, 11, 141-143.

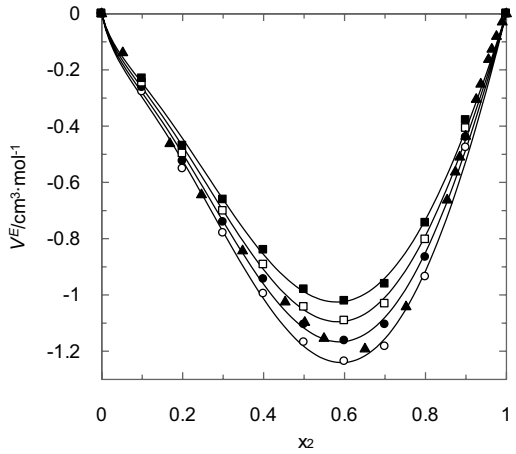


Figure 3.7. Excess volume and Redlich-Kister (solid lines) fit for water (1) + N-methyl-2-pyrrolidone (2) system. ○, T = 20 ºC; ●, T = 30 ºC; □, T = 40 ºC; ■ T = 50 ºC; ▲, T = 25 ºC[175].

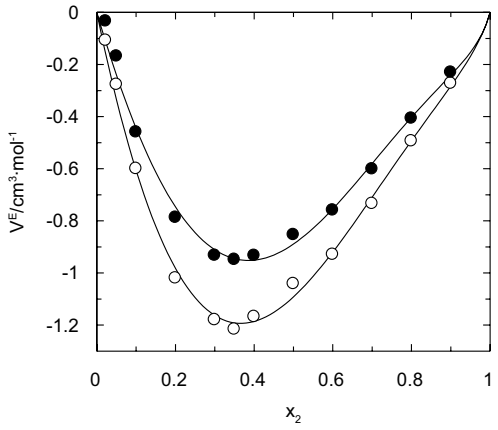


Figure 3.8. Excess molar volumes for water (1) + N-ethyl-2-pyrrolidone (2) system. ○, t = 20 ºC; ●, t = 50 ºC. Solid lines corresponds to Redlich-Kister equation 3.2.

[175] George J., Sastry N. V. Densities, viscosities, speeds of sound, and relative permittivities for water + cyclic amides (2-pyrrolidinone, 1-methyl-2-pyrrolidinone, and 1-vinyl-2-pyrrolidinone) at different temperatures. *Journal of Chemical & Engineering Data* 2004, 49, 235-242.

The behaviour of the excess volume (figure 3.7 and 3.8), is in agreement with previous studies for another N-alkyl-pyrrolidones[176,177]. The magnitude order for the excess volume agrees with these previous works and the presence of the ethyl group (EP) has an effect on the decrease of the excess volume lesser than the presence of a methyl group (MP).

The values calculated for excess molar volumes were fitted using a Redlich-Kister type equation 3.2.

$$\Delta Y = x_1 \cdot x_2 \cdot \sum_{j=1}^{4} q_j \cdot x_2^{(j-1)/2} \qquad (3.2)$$

The Redlich-Kister type equation fits satisfactorily (i. e. figure 3.7) the excess molar volumes calculated from experimental data in present work. The results obtained for fitting parameters are shown in Table 3.1 and 3.2 for the systems studied in this work.

Table 3.1. Fit parameters corresponding to Redlich-Kister equation for excess volume $V^E$ for water (1) + N-methyl-2-pyrrolidone (2) from t = (20 to 50) ºC.

| ***Parameter*** | ***T*/ºC = 20** | ***T*/ºC = 30** | ***T*/ºC = 40** | ***T*/ºC = 50** |
|---|---|---|---|---|
| $A_0$ | -8.334 | -7.793 | -7.185 | -6.575 |
| $A_1$ | 30.840 | 28.899 | 26.566 | 24.203 |
| $A_2$ | -56.050 | -53.196 | -49.536 | -45.692 |
| $A_3$ | 27.773 | 26.827 | 25.325 | 23.626 |
| $\sigma$ | 0.02 | 0.02 | 0.02 | 0.02 |

Table 3.2. Fit parameters corresponding to Redlich-Kister equation for excess volume $V^E$ for water (1) + N-ethyl-2-pyrrolidone (2) from t = (20 to 50) ºC.

| ***Parameter*** | ***T*/ºC = 20** | ***T*/ºC = 30** | ***T*/ºC = 40** | ***T*/ºC = 50** |
|---|---|---|---|---|
| $A_0$ | -1.26 | 3.56 | 3.85 | 5.17 |
| $A_1$ | -34.48 | -54.48 | -52.27 | -55.65 |
| $A_2$ | 67.57 | 97.97 | 93.01 | 96.88 |
| $A_3$ | -35.14 | -50.67 | -48.08 | -49.74 |
| $\sigma$ | 0.02 | 0.04 | 0.04 | 0.04 |

[176] George J., Sastry N. V. Densities, viscosities, speeds of sound, and relative permittivities for water + cyclic amides (2-pyrrolidinone, 1-methyl-2-pyrrolidinone, and 1-vinyl-2-pyrrolidinone) at different temperatures. *Journal of Chemical & Engineering Data* 2004, 49, 235-242.

[177] Al-Azzwal S. F., Awwad A. M., Al-Dujaili A. H., Al-Noori M. K. Dielectric constants and excess volumes of 2-pyrrolidone + water at several temperatures. *Journal of Chemical & Engineering Data* 1990, 35, 463-466.

With regard to surface tension, an example of the experimental data obtained are shown in figure 3.9 that includes the data for the system formed by water + 2-pyrrolidone over the entire range of composition and for different temperatures.

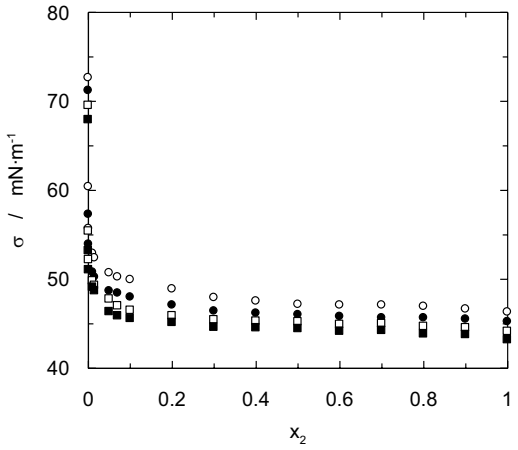


Figure 3.9. Influence of mixture composition and temperature for water (1) + 2-pyrrolidone (2) system. ○, T = 20 ºC; ●, T = 30 ºC; □, T = 40 ºC; ■, T = 50 ºC.

The behaviour shown in this figure proved that the addition of small quantities of P to water produces a drastically decrease in surface tension value. The higher decrease in the surface tension was produced at low concentration of P.

The behaviour shown for this system is similar than the observed for the other mixtures studied in present work and it is in agreement with previous studies in systems with this kind of compounds[178,179]. In relation with the influence of temperature upon the value of surface tension the experimental results show that when temperature increases a continuous decrease in the value of surface tension is observed (see figure 3.9). The observed behaviour in relation with the

[178] Lou A., Pethica B. A., Somasundaran P., Fan A. Surface and colloid properties of cyclic amides III. Surface activity and micellization of N-butyl-2-pyrrolidinone in water. *Journal of Dispersion Science and Technology* 1999, 20, 569-580.
[179] Lou A., Pethica B. A., Somasundaran P. Surface and colloid properties of cyclic amides II. Phase separation, surface activity and micellization in mixtures of N-hexyl-2-pyrrolidinone and water. *Colloids and Surfaces A: Physicochemical and Engineering Aspects* 1997, 129, 297-303.

influence of temperature on the surface tension value is common and it has been detected for different systems[180,181].

The experimental data shown in figure 3.10 for all systems analysed in present work at 25 ºC indicate that when the mixtures enrich in N-alkyl-2-pyrrolidone the value of surface tension tends at a constant value close to the corresponding one for each pure N-alkyl-2-pyrrolidone after the initial decrease in the surface tension with low additions of organic compound. This kind of behaviour indicates that the systems employed in present study produce aggregation processes[182] that have influence on the surface tension observing the previously commented behaviour.

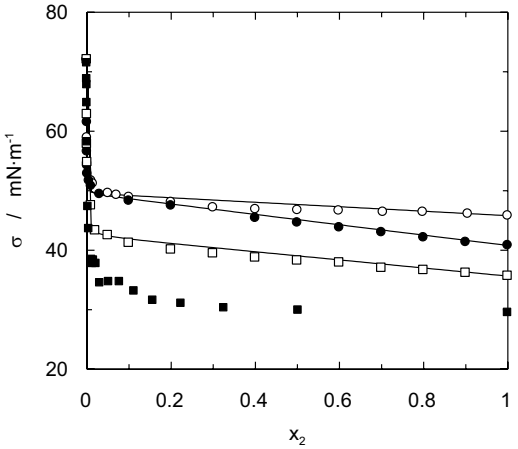


Figure 3.10. Influence of mixture composition and fit results of equation 3.3 for: ○, water (1) + 2-pyrrolidone (2) system; ●, water (1) + N-methyl-2-pyrrolidone (2) system; □, water (1) + N-ethyl-2-pyrrolidone (2) system. T = 25 ºC. ■, water (1) + N-butyl-2-pyrrolidinone (2) system at 23.5 ºC[183]. Solid lines correspond to equation 3.3.

[180] Domanska U., Pobudkowska A., Rogalski M. Surface tension of binary mixtures of imidazolium and ammonium based ionic liquids with alcohols, or water: cation, anion effect. *Journal of Colloide and Interface Science* 2008, 322, 342–350.
[181] Queimada A. J., Marrucho I. M., Coutinho J. A. P. Surface tension of pure heavy N-alkanes: a corresponding states approach. *Fluid Phase Equilibria* 2001, 183–184, 229–238.
[182] Login R. B. Pyrrolidinone-based surfactants. *JAOCS* 1995, 72, 759-770.
[183] Lou A., Pethica B. A., Somasundaran P., Fan A. Surface and colloid properties of cyclic amides III. Surface activity and micellization of N-butyl-2-pyrrolidinone in water. *Journal of Dispersion Science and Technology* 1999, 20, 569-580.

Figure 3.10 shows the behaviour obtained for these experimental systems using N-alkyl-2-pyrrolidone with different hydrophobic chain length. These experimental results indicate that when the chain length increases the decrease in the value of the surface tension from the pure water data is higher. Also, figure 3.10 includes the bibliographic data corresponding to the system formed by water and N-butyl-2-pyrrolidinone[184] that confirms the behaviour and the trends observed analysing the experimental data of present work.

This behaviour is due to the hydrophobic nature of alkyl group that increases with increasing the chain length and then, the trend to accumulate the organic molecules at air-liquid interface increases too, producing a decrease in the value of surface tension.

For a given temperature, an equation developed by Connors and Wright[185] can fit the surface tension *vs* composition data and has been successfully used by different authors[186]. This equation is expressed as a model with two adjustable parameters, *a* and *b* equation 3.3.

$$\frac{\sigma_1 - \sigma}{\sigma_1 - \sigma_2} = \left(1 + \frac{a \cdot x_1}{1 - b \cdot x_1}\right) \cdot x_2 \qquad (3.3)$$

where $\sigma$, $\sigma_1$ and $\sigma_2$ are the surface tension of the mixture, water and N-alkyl-pyrrolidone respectively and $x_1$ and $x_2$ the mole fraction of water and N-alkyl-pyrrolidone.

Figure 3.10 shows the good fit found with equation 3.3 in relation with the surface/composition data for these systems studied at 25 ºC. A low effect of the temperature upon these parameters values has been observed. Using *a* and *b* parameters from equation 3.3, is possible calculate the binding constant, *K*, using equation 3.4.

$$K = \frac{a}{1 - a} \qquad (3.4)$$

[184] Lou A., Pethica B. A., Somasundaran P., Fan A. Surface and colloid properties of cyclic amides III. Surface activity and micellization of N-butyl-2-pyrrolidinone in water. *Journal of Dispersion Science and Technology* 1999, 20, 569-580.
[185] Connors K. A., Wright J. L. dependence of surface tension on composition of binary aqueous-organic solutions. *Analytical Chem*emistry 1989, 61, 194-198.
[186] Vázquez G., Álvarez E., Navaza J. M., Rendo R., Romero E. Surface tension of binary mixtures of water + monoethanolamine and water + 2-amino-2-methyl-1-propanol and tertiary mixtures of these amines with water from 25 ºC to 50 ºC. *Journal of Chemical & Engineering Data* 1997, 42, 57-59.

The values for the fit parameters of equation 3.3 and the binding constant, *K*, are shown are listed in tables 3.3-3.5.

Table 3.3 Fit parameters for equation 3.3 and 3.4 for water (1) + 2-pyrrolidone (2) mixture.

| *T*/ºC | *a* | *b* | *K* |
|---|---|---|---|
| **20** | 0.8385 | 0.99980 | 5.19 |
| **25** | 0.8573 | 0.99985 | 6.01 |
| **30** | 0.8670 | 0.99986 | 6.52 |
| **40** | 0.8620 | 0.99988 | 6.25 |
| **50** | 0.8534 | 0.99989 | 5.82 |

Table 3.4. Fit parameters for equation 3.3 and 3.4 for water (1) + N-methyl-2-pyrrolidone (2) mixture.

| *T*/ºC | *a* | *b* | *K* |
|---|---|---|---|
| **20** | 0.7177 | 0.99976 | 2.54 |
| **25** | 0.7219 | 0.99980 | 2.60 |
| **30** | 0.7278 | 0.99982 | 2.67 |
| **40** | 0.7314 | 0.99984 | 2.72 |
| **50** | 0.7392 | 0.99984 | 2.83 |

Table 3.5. Fit parameters for equation 3.3 and 3.4 for water (1) + N-ethyl-2-pyrrolidone (2) mixture.

| *T*/ºC | *a* | *b* | *K* |
|---|---|---|---|
| **20** | 0.8128 | 0.99928 | 4.34 |
| **25** | 0.8133 | 0.99941 | 4.36 |
| **30** | 0.8150 | 0.99950 | 4.40 |
| **40** | 0.8246 | 0.99960 | 4.70 |
| **50** | 0.8256 | 0.99971 | 4.73 |

### 3.1.3. Conclusions

A similar behaviour for the densities of N-alkyl-pyrrolidones aqueous solutions is observed, however the density of the 2-pyrrolidone aqueous solutions show a different behaviour.

With regard to the viscosity, both N-alkyl-pyrrolidones aqueous solutions shows a similar behaviour but very different to the 2-pyrrolidinone aqueous solutions ones.

The results for the surface tension indicate that when the chain length increases the decrease in the value of the surface tension from the pure water data is higher. This behaviour is due to the hydrophobic nature of alkyl group that increases with increasing the chain length.

# 3.2 Hydrodynamics in $CO_2$ - cyclic amides systems

*Abstract*

*Present work analyses the carbon dioxide absorption process in N-alkyl-pyrrolidones aqueous solutions, taking into account hydrodynamic studies using a bubble column contactor. Then, the analysis of the influence caused by the solute concentration and the gas flow-rate is complemented by the study of the effect caused by the alkyl group upon the previously commented studies.*

*The influence of these variables upon the bubble size distribution as well as the gas hold-up allows the evaluation of gas-liquid interfacial area, and the influence of liquid phase physical properties upon this parameter.*

### 3.2.1. Specific introduction

In the last years, the acid gases separation in industrial streams has been performed by gas-liquid absorption using different contactors. This kind of separation can be done using physical solvents such as water, methanol (Rectisol process) or N-methyl-2-pyrrolidone (Lurgi's Purisol process), or by chemical solvents (reactive absorption), such as potassium carbonate (Benfield process), monoethanolamine (Girbotol process), Sulfolan + diisopropanolamine (Shell's Sulfinol process)[187] or amines blends[188,189].

Being more specific, the Purisol process, that employs N-methyl-2-pyrrolidone, was first applied to natural gas sweetening; however, this procedure has shown higher importance in other processes such as in the hydrogen purification. These procedures are based on cycles of absorption-desorption of pollutant gases, differing from other processes that involve a heterogeneous chemical reaction between the gas and liquid phases. The Purisol process has been carefully analysed for its use in power stations[190], for desulphurization and also for carbon dioxide capture. The regeneration process of the solvent has been performed by means of pressure changes to desorb the pollutant gases. This way, the thermal regeneration necessary in chemical absorption is avoided, which produces the liquid phase degradation[191] and increases the energetic costs.

### 3.2.2. Results and discussion

An important part of this work involves studies about bubble size distribution produced in the bubble column contactor and the gas hold-up observed under the different experimental conditions. In relation to the first parameter (bubble size), a mean bubble diameter (Sauter mean

[187] Kohl A., Nielsen R. *Gas purification*. 5th edition. Gulf Publishing Company. Houston 1997.
[188] Bonenfant D., Mimeault M., Hausler R. Estimation of the $CO_2$ absorption capacities in aqueous 2-(2-aminoethylamino) ethanol and its blends with MDEA and TEA in the presence of $SO_2$. *Industrial & Engineering Chemistry Research* 2007, 46, 8968–8971.
[189] Bishnoi S., Rochelle G. T. Absorption of carbon dioxide in aqueous piperazine/methyldiethanolamine. *AIChE Journal* 2002, 48, 2788-2799.
[190] Schütz M., Daun M., Weinspach P.-M., Krumbeck M., Hein K. R. G. Study on the $CO_2$-recovery from an ICGCC-plant. *Energy Conversion and Management* 1992, 33, 357-363.
[191] Supap T., Idem R., Tontiwachwuthikul P., Saiwan C. Kinetics of sulfur dioxide- and oxygen-induced degradation of aqueous monoethanolamine solution during $CO_2$ absorption from power plant flue gas streams. *International Journal of Greenhouse Gas Control* 2009, 3, 133 – 142.

diameter) has been determined on the basis of bubble size distribution existing into the bubble column for the different experimental conditions (type of amide, gas flow-rate and amide concentration). An example of the photographs used to obtain the abovementioned bubble size distribution is shown in figure 3.11.

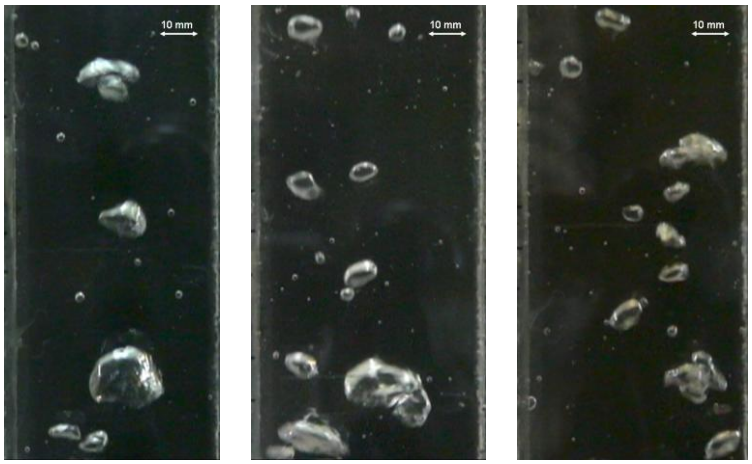


$C_{MP}$ = 0.1 mol.L$^{-1}$ $C_{MP}$ = 0.3 mol.L$^{-1}$ $C_{MP}$ = 0.5 mol.L$^{-1}$

Figure 3.11. Bubble contactor photographs using MP aqueous solutions. $Q_g$ = 30 L·h$^{-1}$.

We can also observe in this figure the influence caused by the presence of one solute (N-methyl-2-pyrrolidone, MP) upon the bubble size. These photographs show that coalescence and rupture processes are observed into the contactor under these experimental conditions. These processes could have an important effect upon the Sauter mean diameter, as well as upon the gas-liquid interfacial area. The photographs also allow us to obtain a first conclusion, only based on the direct observation of these photographs. They indicate that, for aqueous solutions of MP, an increase of solute concentration in the liquid phase produces a decrease in the bubbles size. This behaviour is inconsistent with the fact that an increase in the value of MP concentration produces an increase in the liquid phase viscosity[192] (see previous section), and the increase in this physical

[192] George J., Sastry N.V. Densities, viscosities, speeds of sound, and relative permittivities for water + cyclic amides (2-pyrrolidinone, 1-methyl-2-pyrrolidinone, and 1-vinyl-2-pyrrolidinone) at different temperatures. *Journal of Chemical & Engineering Data* 2004, 49, 235-242.

property usually produces an increase in the bubble size[193]. On the other hand, the presence of this kind of substance also produces important changes in other physical properties that could be an important influence upon the bubbles size produced into the contactor. For this kind of substances, the effect caused by small quantities upon the surface tension value indicates a similar behaviour to the previously one studied for surfactants aqueous solutions[194] and it has been commented in the section about the characterization of aqueous solutions of amides. This behaviour comprises a dramatic decrease in the surface tension value with the addition of very low solute quantities, caused by the accumulation of this kind of molecules at a gas-liquid interface. When surfactants are used, there is a difference with the present experimental systems since, for the first ones, very low concentrations are used in the liquid phase and, then, non-influence upon the liquid viscosity is observed[194]. In relation to the previously analysed effect of surface tension upon the bubble diameter[195], a decrease in this physical property produces also a decrease in the bubbles size, and this influence could be in agreement with the behaviour shown in figure 3.11.

The data treatment of the images taken to the bubbles into the contactor (the photographs shown in figure 3.11, for instance), has allowed us to obtain the bubble size distribution under the different experimental conditions employed in this work (type of N-alkyl-pyrrolidone, concentration of solute and gas flow-rate). An example of the obtained results for the bubble size distribution along the bubble contactor is shown in figure 3.12. This figure shows that, under certain operation conditions of gas flow-rate, the use of aqueous solutions of P produces higher bubbles for all the diameter range than in the case of aqueous solutions of MP and EP.

In relation to the width of the bubble size distribution in figure 3.12, a similar width has been observed (for the gas flow-rate employed in figure 3.12) for all the N-alkyl-pyrrolidones, with a bubble diameter range of 4-5 mm.

---

[193] Gómez-Díaz D., Navaza J. M., Quintáns-Riveiro L. C., Sanjurjo B. Gas absorption in bubble column using a non-Newtonian liquid phase. *Chemical Engineering Journal* 2009, 146, 16–21.
[194] Gómez-Díaz D., Navaza J. M., Sanjurjo B. Density, kinematic viscosity, speed of sound, and surface tension of tetradecyl and octadecyl trimethyl ammonium bromide aqueous solutions. *Journal of Chemical & Engineering Data* 2007, 52, 2091-2093.
[195] Sardeing R., Painmanakul P., Hébrard G. Effect of surfactants on liquid-side mass transfer coefficients in gas–liquid systems: A first step to modelling. *Chemical Engineering Science* 2006, 61, 6249-6260.

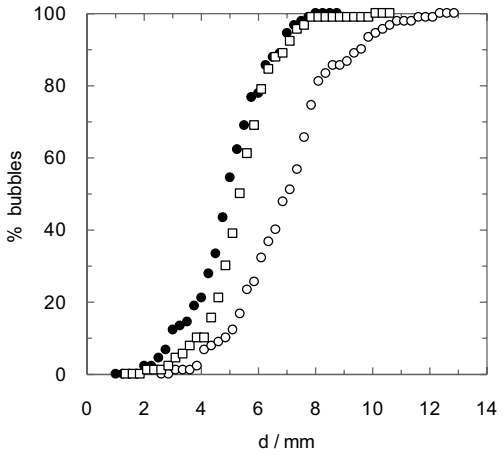


Figure 3.12. Influence of N-alkyl-pyrrolidone type upon bubble size distribution. $Q_g$ = 18 L·h$^{-1}$. $C_P = C_{MP} = C_{EP}$ = 0.5 mol·L$^{-1}$. (○) P; (●) MP; (□) EP.

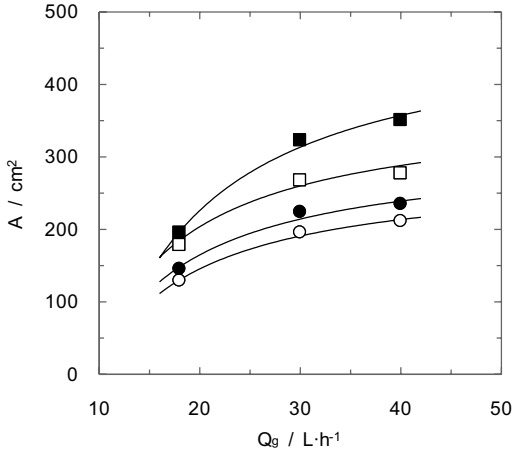


Figure 3.13. Influence of gas flow-rate upon the gas-liquid interfacial area. Aqueous solutions of MP: (○) $C_{MP}$ = 0 mol.L$^{-1}$; (●) $C_{MP}$ = 0.1 mol.L$^{-1}$; (□) $C_{MP}$ = 0.3 mol.L$^{-1}$; (■) $C_{MP}$ = 0.5 mol.L$^{-1}$.

As it is mentioned in the material an methods section, the calculated data of the Sauter mean diameter, obtained from the bubble size diameter distribution data as well as the gas hold-

up under the different experimental conditions, are used to calculate the gas-liquid interfacial area, using equation A.7. Figure 3.13 shows the determined values for the gas-liquid interfacial area determined by this methodology.

It can be observed in this figure the influence of the gas flow-rate fed to the bubble contactor and also, the influence of MP concentration upon interfacial area. In relation to the first operation variable (gas flow-rate), an increase in the value of this variable, produces an increase in the gas-liquid interfacial area, tending to a constant value at a high gas flow-rate. This behaviour has been commonly observed in literature[196,197], since an increase in this variable (gas flow-rate) produces an increase in the gas hold-up (with positive influence upon the interfacial area). At the same time, an increase in gas flow-rate produces an increase in the bubble size, but this fact has a negative influence upon the gas-liquid interfacial area. Taking into account the data shown in figure 3.13, the influence of the gas hold-up is higher for low gas flow-rates, and an increase in the interfacial area is observed; however, when higher values of this variable are fed in the bubble column, the negative influence of the bubble size compensates the positive effect previously commented (caused by gas hold-up), and a low influence of the gas flow-rate upon the interfacial area is observed.

On the other hand, in relation to the influence of the liquid phase composition (concentration of MP in the case of figure 3.13), the behaviour observed has been an increase in the value of the gas-liquid interfacial area when the MP concentration increases in the liquid phase. This behaviour is related to the previous discussion about the photographs shown in figure 3.11, and the influence of physical properties upon the bubbles size. The conclusion reached in figure 3.11 indicates that an increase in the MP concentration produced a decrease in the bubble's diameter. This fact is in agreement with the data calculated for the gas-liquid interfacial area, shown in figure 3.13. The behaviour showed in figure 3.13 is due to the important decrease in the surface tension value when the MP concentration increases in the liquid phase, and this phenomenon produces a decrease in bubbles size that has been confirmed in different studies[198,199]. The effect caused by the surface tension is higher than the possible influence of

[196] Yang W., Wang J., Wang T., Jin Y. Experimental study on gas–liquid interfacial area and mass transfer coefficient in three-phase circulating fluidized beds. *Chemical Engineering Journal* 2001, 84, 485–490.
[197] Krishn R., van Baten J. M. Mass transfer in bubble columns, *Catalysis Today* 2003, 79–80, 67–75.
[198] Gómez-Díaz D., Navaza J. M., Sanjurjo B. Interfacial area evaluation in a bubble column in the presence of a surface-active substance Comparison of methods. *Chemical Engineering Journal* 2008, 144, 379–385.
[199] Painmanakul P., Loubière K., Hébrard g., Mietton-Peuchot M., Roustan M. Effect of surfactants on liquid-side mass transfer coefficients. *Chemical Engineering Science* 2005, 60, 6480–6491.

viscosity (increase in bubbles diameter) due to the concentration ranges, because the composition used in this work has a higher influence upon the surface tension than for the viscosity[200] (see previous section).

Taking into account the calculated values for the gas-liquid interfacial area for the different N-alkyl-pyrrolidones, for the different concentrations and for each gas flow-rate fed to the bubble contactor, the different behaviours have been analysed. In relation to the influence of the gas-flow-rate upon the interfacial area value, the obtained behaviours are similar to the previously commented one in figure 3.13. But the influence of the solute concentration upon the interfacial area indicates significant differences shown in figure 3.14.

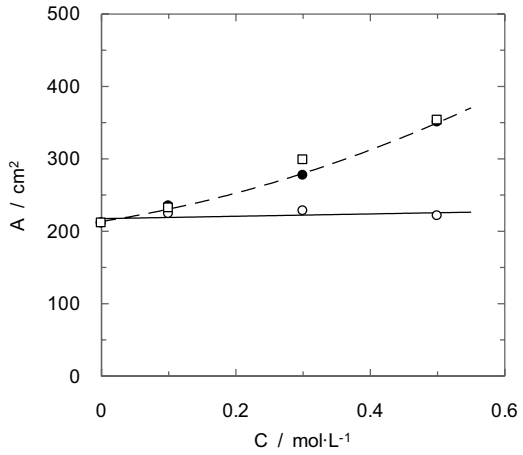


Figure 3.14. Influence of N-alkyl-pyrrolidone type and concentration upon the interfacial area. $Q_g$ = 40 L·h$^{-1}$. (○) P; (●) MP; (□) EP.

That is, for aqueous solutions of MP and EP, an increase in the value of the gas-liquid interfacial area is observed when the MP and EP concentration increases in the liquid phase, due to the high decrease in the bubble diameter caused by the reduction in the surface tension. For aqueous solutions of P, the observed behaviour consists in a non-influence of the solute concentration, obtaining a constant value of gas-liquid interfacial area. This behaviour could be

[200] George J., Sastry N. V. Densities, viscosities, speeds of sound, and relative permittivities for water + cyclic amides (2-pyrrolidinone, 1-methyl-2-pyrrolidinone, and 1-vinyl-2-pyrrolidinone) at different temperatures. *Journal of Chemical & Engineering Data* 2004, 49, 235-242.

due to the presence of P, that develops a lower decrease in the surface tension value than the reduction caused by the other N-alkyl-pyrrolidones and then, the influence of viscosity could inhibit the effect of the surface tension. The experimental data corresponding to the interfacial area indicate that the alkyl-substituted pyrrolidones show a similar behaviour in relation to the hydrodynamic parameters analysed in this study, with clear differences with P aqueous solutions that could affect upon the global mass transfer process.

### 3.2.3. Conclusions

The present work has analysed the influence of the presence of different N-alkyl-pyrrolidones in water solution, upon different hydrodynamic parameters corresponding to a bubble column.

The use of aqueous solutions of P produces higher bubbles than in the case of aqueous solutions of MP and EP for a fixed gas flow-rate. An increase in the MP concentration produced a decrease in the bubble's diameter and an increase in the value of the gas-liquid interfacial area due to the important decrease in the surface tension value when the MP concentration increases.

For aqueous solutions of P, a non-influence of the solute concentration is observed and a constant value of gas-liquid interfacial area is obtained because a lower decrease in the surface tension value is produced and the influence of viscosity could inhibit the effect of the surface tension.

For aqueous solutions of MP and EP, a similar increase in the value of the gas-liquid interfacial area is observed when the MP and EP concentration increases in the liquid phase, due to the high decrease in the bubble diameter caused by the reduction in the surface tension. This fact implies that MP could be substituted by EP in Lurgi's Purisol process taking into account that EP needs minor safety measurements and presents a minor chemical risk (see table 1.4 in general introduction section).

# 3.3 Gas absorption in $CO_2$ - cyclic amides systems

*Abstract*

*This work analyses the carbon dioxide absorption process in N-alkyl-pyrrolidones aqueous solutions, taking into account mass transfer processes, using a bubble column contactor. Then, the analysis of the influence caused by the solute concentration and the gas flow-rate is complemented by the study of the effect caused by the alkyl group upon the previously commented studies mass transfer.*

*The volumetric mass transfer coefficient and the mass transfer coefficient have also been determined, calculated and analysed, on the basis of their obtained behaviour and the influence of each variable.*

### 3.3.1. Specific introduction

As it has been commented in previously section, in the last years the acid gases separation in industrial streams has been performed by gas-liquid absorption using different contactors and this kind of separation can be done using physical solvents such as water, methanol (Rectisol process) or N-methyl-2-pyrrolidone (Lurgi's Purisol process)[201].

Due to the interest of the carbon dioxide absorption process using aqueous solutions of N-methyl-2-pyrrolidone, in this work the absorption of this gas in these aqueous solutions have been analysed. Besides, other cyclic amides, such as 2-pyrrolidone and N-ethyl-2-pyrrolidone have been used, to evaluate the differences between these solvents and N-methyl-2-pyrrolidone, upon the absorption process in bubbling equipment, what implies the analysis of the hydrodynamic and the mass transfer processes. An important fact is that N-ethyl-2-pyrrolidone and 2-pyrrolidone presents less health hazards than N-methyl-2-pyrrolidone[202] (see table 1.4 in general introduction section) and for this reason these substances could be a more suitable absorbent for carbon dioxide than N-methyl-2-pyrrolidone.

### 3.3.2. Results and discussion

The present work includes studies about mass transfer process of carbon dioxide to aqueous solutions of N-alkyl-pyrrolidones, previously studied in relation to the gas-liquid interfacial area produced in the bubble contactor. Both parameters are important to understand the absorption process of carbon dioxide in these aqueous solutions. As a preliminary step, different studies have been carried out in order to determine the kind of absorption (physical or chemical absorption) that takes place in the systems analysed in this work. This previous study is necessary since, in research works developed in present work, the reaction between the carbon dioxide and the pyrrolidine was detected, and due to the similar chemical structure and the presence of an amino group, to confirm the absorption type for each system is necessary. These

[201] Kohl A., Nielsen R. *Gas purification*. 5th edition. Gulf Publishing Company. Houston 1997.
[202] Zolfaghari A., Reza Mortaheb H., Meshkini F. Removal of N-methyl-2-pyrrolidone by photocatalytic degradationin a batch reactor. *Industrial & Engineering Chemistry Research* 2011, 50, 9569-9576.

studies were developed using the experimental procedure previously described in the section dedicated to the reaction kinetics between carbon dioxide and cyclic amines.

Figure 3.15 shows an example of absorption kinetics to analyse the kind of absorption type. A decrease on the slope is observed when amide concentration increases in the liquid phase. This behaviour is opposite to the obtained for pyrrolidine and piperidine aqueous solutions and it indicates the existence of physical absorption for aqueous solutions of 2-Pyrrolidone. The experimental results for different N-alkyl-pyrrolidones showed that physical absorption is produced due to the inhibition of chemical reaction by the presence of ketone group, which reduces the electronic charge near to the amino group. This fact avoids the reaction between the carbon dioxide and the amino group.

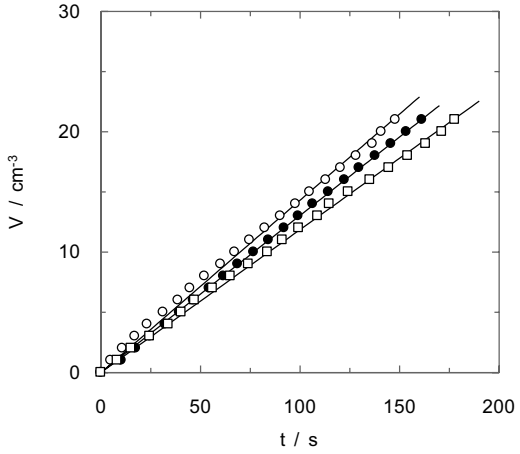


Figure 3.15 Influence of N-alkyl-pyrrolidone type upon carbon dioxide absorption rate. (○) $C_P$ = 0 mol·L$^{-1}$ (water); (●) $C_P$ = 0.1 mol·L$^{-1}$; (□) $C_P$ = 0.5 mol·L$^{-1}$.

Physical absorption experiments have been performed using the same bubbling contactor used in the previous section to put both phases in contact, under the different experimental conditions analysed for the interfacial area (type of solute, concentration of solute and gas flow-rate). In these studies, the carbon dioxide concentration has been recorded along the experiment time, and using the carbon dioxide absorbed concentration, the volumetric mass transfer coefficient ($k_L{\cdot}a$) has been determined (see material and methods section).

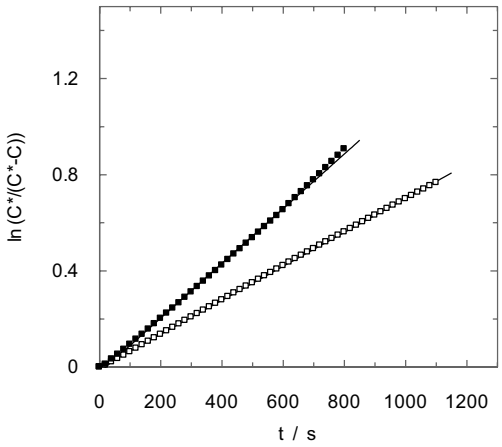


Figure 3.16. Experimental data fitting using equation A.9 (materials and methods section). $Q_g$ = 18 L·h$^{-1}$. (■) $C_P$ = 0 (water), (□) $C_P$ = 0.1 mol.L$^{-1}$.

Figure 3.16 shows that the slope of plotting data is lower for the experiment in the presence of P, in comparison with the pure water experiment. This fact implies that the mass transfer rate is minor for the system in the presence of P for the same experimental conditions.

The corresponding values to the volumetric mass transfer coefficient have been calculated using the procedure described in materials and methods section and are shown in figure 3.16. An example of the calculated data for this parameter is shown in figure 3.17. This figure shows that an increase in the solutes concentration always produces a decrease in the value of volumetric mass transfer coefficient.

However, this decrease is more important for aqueous solutions of P, mainly at a low solute concentration in the liquid phase. This behaviour is in agreement with the previous studies in this work, since a lower value for the specific gas-liquid interfacial area (parameter included in the volumetric mass transfer coefficient) was observed for aqueous solutions of P than the corresponding values for solutions of MP and EP.

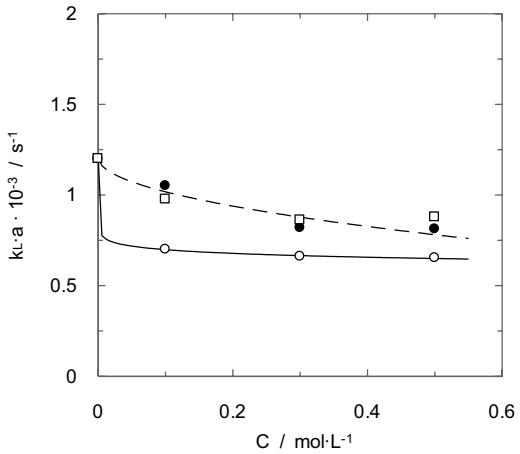


Figure 3.17. Influence of N-alkyl-pyrrolidone type and concentration upon the volumetric mass transfer coefficient. $Q_g$ = 18 L·h$^{-1}$. (○) P; (●) MP; (□) EP.

Taking into account the observed behaviour for the systems with the presence of MP and EP in the previous section, we can observe that an increase in these substances concentration in the liquid phase produces an increase in the interfacial area value, but figure 3.17 shows a decrease in the value of volumetric mass transfer coefficient (the opposite behaviour than for interfacial area). This behaviour implies that the effect caused by the presence of this kind of substances upon the mass transfer coefficient ($k_L$) is more important than the corresponding influence upon the gas-liquid interfacial area; then, the negative effect inhibits the positive one caused by the reduction in the bubbles size previously described.

The decrease in the value of the volumetric mass transfer coefficient previously described (for P aqueous solutions) has been observed for all the experimental systems, as well as for all the gas flow-rates employed in this work in the bubble contactor (see figure 3.18).

The shape of the effect caused by P concentration remains constant, but the gas flow-rate produces an increase in the value of volumetric mass transfer coefficient caused by the increase in the gas-liquid interfacial area, due to the gas flow-rate (see figure 3.13 in hydrodynamic section). The increase in the gas flow-rate could also produces an increase in the

value of mass transfer coefficient[203], but certain studies have shown a non-influence of this variable upon this parameter[204,205].

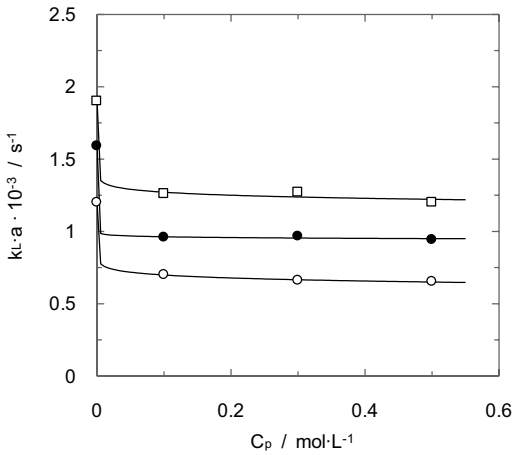


Figure 3.18. Influence of gas flow-rate and P concentration upon the volumetric mass transfer coefficient. (○) $Q_g$ = 18 L·h$^{-1}$; (●) $Q_g$ = 30 L·h$^{-1}$; (□) $Q_g$ = 40 L·h$^{-1}$.

Taking into account that the volumetric mass transfer coefficient and the gas-liquid specific interfacial area have been determined in the present work under different operation conditions, the mass transfer coefficient could be calculated as the quotient between the volumetric mass transfer coefficient and the specific interfacial area. Then, it let us analyse the effect of the variables (type of solute, concentration of solute and gas flow-rate) upon the mass transfer, removing the influence caused upon the interfacial area.

[203] Hashemia S., Macchia A., Servio P. Gas–liquid mass transfer in a slurry bubble column operated at gas hydrate forming conditions. *Chemical Engineering Science* 2009, 64, 3709-3716.
[204] Gómez-Díaz D., Navaza J. M., Sanjurjo B., Vázquez-Orgeira L. Carbon dioxide absorption in glucosamine aqueous solutions. *Chemical Engineering Journal* 2006, 122, 81–86.
[205] Vasconcelos J. M. T., Rodrigues J. M. L., Orvalho S. C. P., Alves S. S., Mendes R. L., Reis A. Effect of contaminants on mass transfer coeffcients in bubble column and airlift contactors. *Chemical Engineering Science* 2003, 58, 1431–1440.

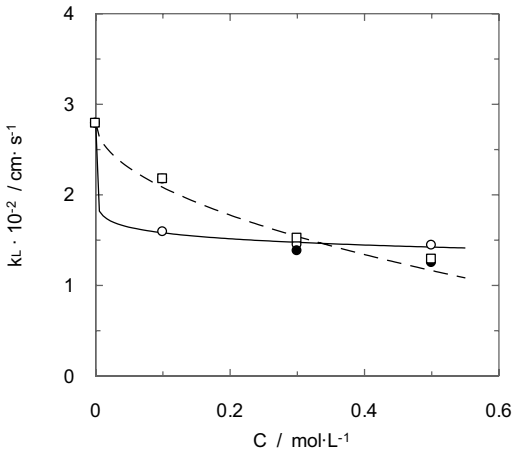


Figure 3.19. Influence of N-alkyl-pyrrolidone type and concentration upon mass transfer coefficient. $Q_g$ = 18 L·h$^{-1}$. (○) P; (●) MP; (□) EP.

Figure 3.19 shows an example of the calculated results for the mass transfer coefficient, and these results indicate once again a difference between the behaviour for aqueous solutions of P in relation to the corresponding one for MP and EP aqueous solutions. In all cases, a similar behaviour, previously commented for the volumetric coefficient, is observed: a decrease in the mass transfer coefficient for all systems when the solutes concentration increases, but with a higher decrease in this coefficient at low P concentration. For this system (aqueous solutions of P), a constant value of mass transfer coefficient is reached; however, for aqueous solutions of MP and EP, a continuous decrease is observed in all the composition range. The same behaviour has been observed for the other gas flow-rates employed in the present work (see figure 3.20).

In relation to the fact that the presence of this kind of substances produces a decrease in the value of mass transfer coefficient, this behaviour is produced due to the trend of this kind of solutes to accumulate molecules at the gas-liquid interface, as it can be observed attending to the surface tension value. The accumulation of one compound at a gas-liquid interface could be analysed on the basis of adsorption isotherms[206]. Previous studies that analysed this kind of systems in gas-liquid absorption have employed the Langmuir isotherm to evaluate the molecules accumulation at the gas-liquid interface[206].

[206] Sardeing R., Painmanakul P., Hébrard G. Effect of surfactants on liquid-side mass transfer coefficients in gas–liquid systems: A first step to modelling. *Chemical Engineering Science* 2006, 61, 6249-6260.

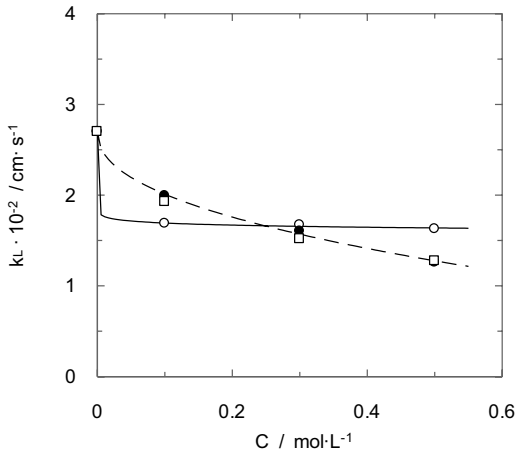


Figure 3.20. Influence of N-alkyl-pyrrolidone type and concentration upon mass transfer coefficient. $Q_g$ = 40 L·h$^{-1}$. (○) P; (●) MP; (□) EP.

The accumulation of P molecules at the interface is shown in figure 3.21, that indicates the degree of accumulation on the basis of $S_e$ parameter (surface coverage ratio), where $S_e$ = 1 indicates the maximum accumulation and $S_e$ = 0 indicates a free surface[207]. The solute concentrations employed in the present work produce accumulation degrees near to saturation (see figure 3.21) and then, an important number of molecules are located at the gas-liquid interface. The procedure of accumulation at the gas-liquid interface commonly produces a reduction in the value of mass transfer coefficient[208,209,210]. Different studies having employed surfactants (compounds that tend to accumulate at the interface), have concluded that the accumulation of molecules at gas-liquid interface also reduce the liquid renewal at the interface, and then produces a decrease in the mass transfer rate. At the same time, and according to the systems employed in this work (aqueous solutions of N-alkyl-pyrrolidones), the increase in the solute concentration near the interface produces an increase in the viscosity value, since these solutes cause this effect upon this physical property. An increase in viscosity produces a decrease

[207] Hebrard G., Zeng J., Loubiere K. Effect of surfactants on liquid side mass transfer coefficients: A new insight. *Chemical Engineering Journal* 2009, 148, 132–138.
[208] Vasconcelos J. M. T., Rodrigues J. M. L., Orvalho S. C. P., Alves S. S., Mendes R. L., Reis A. Effect of contaminants on mass transfer coeffcients in bubble column and airlift contactors. *Chemical Engineering Science* 2003, 58, 1431–1440.
[209] Hebrard G., Zeng J., Loubiere K. Effect of surfactants on liquid side mass transfer coefficients: A new insight. *Chemical Engineering Journal* 2009, 148, 132–138.
[210] Gómez-Díaz D., Gomes N., Teixeira J. A., Belo I. Oxygen mass transfer to emulsions in a bubble column contactor. *Chemical Engineering Journal* 2009, 152, 354–360.

in the gas diffusivity in the liquid phase, and this effect causes a decrease in the mass transfer rate. Then, the accumulation of these substances in the gas-liquid interface is responsible for the reduction in the value of the mass transfer coefficient.

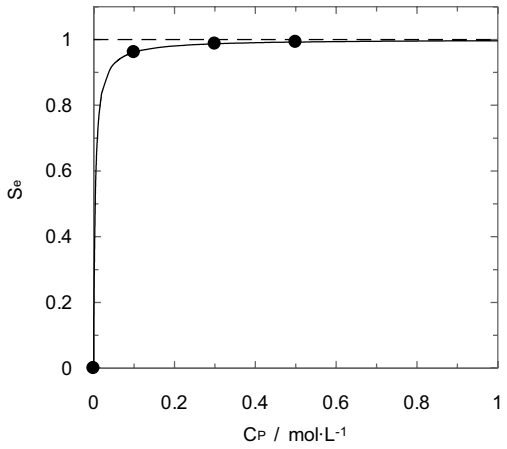


Figure 3.21. Surface coverage ratio for P aqueous solutions. Full circles show the coverage of the gas-liquid surface at the compositions employed in present work.

On the other hand, and related to the difference between the behaviour of aqueous solutions of MP and EP, compared with the trend obtained for aqueous solutions of P, it is necessary to take into account the previous discussion about the bubble's size; more specifically, according to the composition influence upon the bubble's diameter. A different influence of solute concentration upon the bubbles' diameter for aqueous solutions of MP and EP in comparison with solutions of P was observed. This is due to the fact that the first ones produce a decrease in the bubble diameter when the MP (or EP) concentration increases in the liquid phase, while a non-influence of P concentration upon the bubble size was observed. Taking into account this behaviour and the previous studies[211,212,213] that have concluded a clear influence of the bubble size upon the mass transfer (small bubbles -rigid bubbles- show a lower mass transfer rate than

[211] Sardeing R., Painmanakul P., Hébrard G. Effect of surfactants on liquid-side mass transfer coefficients in gas–liquid systems: A first step to modelling. *Chemical Engineering Science* 2006, 61, 6249-6260.
[212] Calderbank P. H., Moo-Young M. B. The continuous phase heat and mass transfer properties of dispersions. *Chemical Engineering Science* 1961, 16, 39–54.
[213] Higbie R. The rate of absorption of a pure gas into a still liquid during a short time exposure. *Transactions of the American Institute of Chemical Engineers* 1935, 31, 365–389.

large bubbles -mobile ones-), we can explain the trends shown in figures 3.19 and 3.20. When MP and EP concentration increases in the liquid phase, a decrease in the bubble size is produced and it causes a decrease in the mass transfer rate and, then, on the mass transfer coefficient. On the other hand, for P aqueous solutions, the bubble diameter remains practically constant and the mass transfer coefficient reaches a constant value after the first decrease (at low concentrations) caused by the accumulation of P molecules at the gas-liquid interface, that produces a decrease in gas diffusivity. An increase in P concentration higher than 0.1 $mol \cdot L^{-1}$ does not produce a decrease in the mass transfer coefficient because the surface coverage does not increase significantly.

### 3.3.3. Conclusions

The experimental results showed that physical absorption is produced between carbon dioxide and aqueous solutions of N-alkyl-pyrrolidones due to the inhibition of chemical reaction by the presence of ketone group.

A decrease in the value of the volumetric mass transfer coefficient has been observed for all the experimental systems analysed, as well as for all the gas flow-rates employed in this work in the bubble contactor. The accumulation of these substances in the gas-liquid interface is responsible for this reduction.

The behaviour observed for MP and EP is very similar (as in the hydrodynamics section). For this reason, EP could be a suitable substitute for the MP in the process of carbon dioxide absorption, since EP presents less risk to the health than MP (see table 1.4 in general introduction section) and, because MP is included in the list of substances of very high concern made by ECHA (European Chemicals Agency)[214].

[214] http://echa.europa.eu/chem_data/authorisation_process/candidate_list_table_en.asp

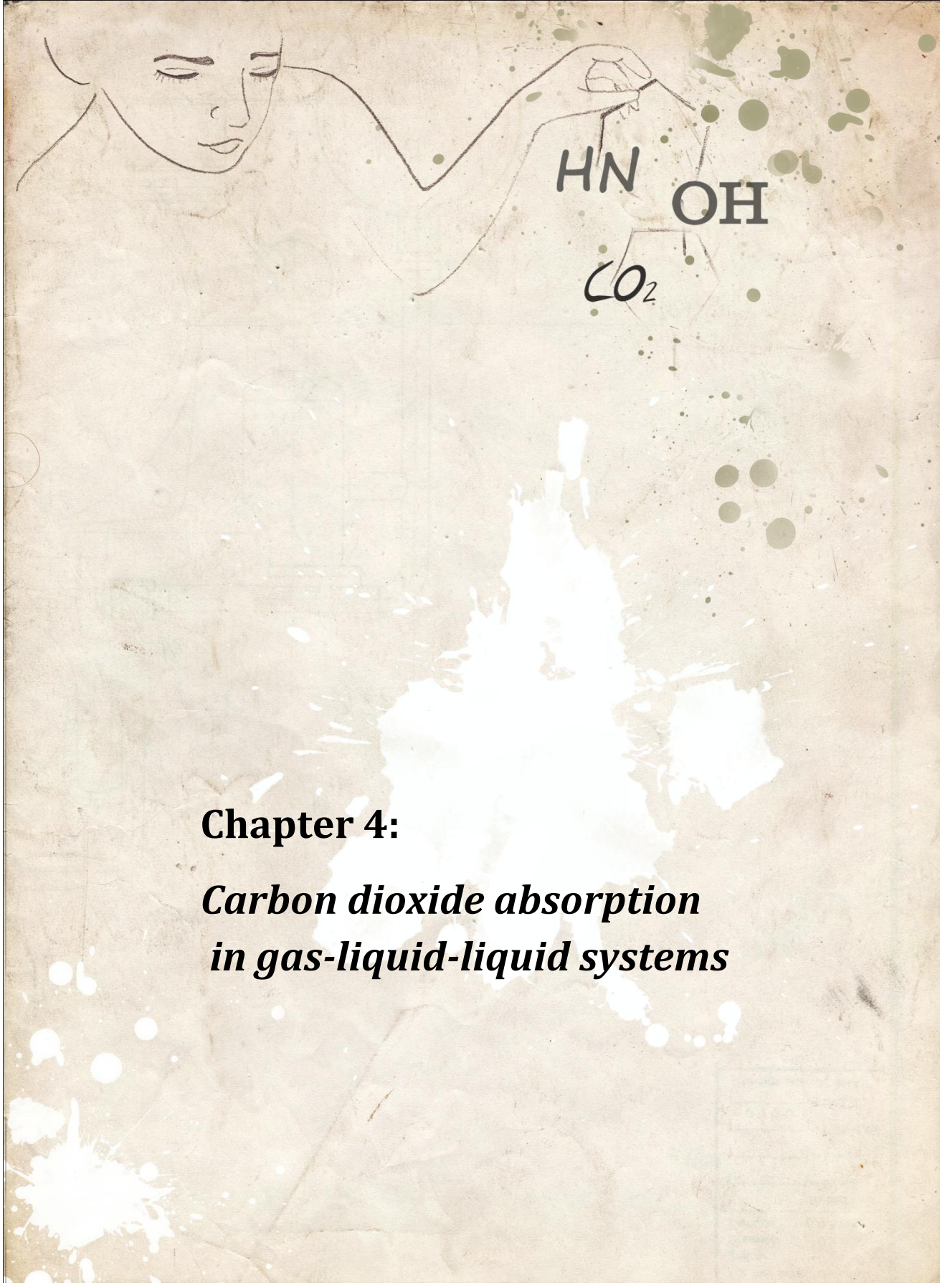


# Chapter 4:

## *Carbon dioxide absorption in gas-liquid-liquid systems*

# 4.1 Hydrodynamics in gas-liquid-liquid systems

*Abstract*

*The present work analyses the hydrodynamic behaviour of a gas phase in a bubble column using different emulsions as liquid phase and Tween80 aqueous solutions. The hydrodynamic behaviour has been analysed on the basis of gas hold-up, bubble diameter and gas-liquid interfacial area; the different variables employed in this study [gas flow-rate, as well as the organic phase nature, the organic phase concentration and surfactant presence and concentration] have been taken into account. The results obtained have been explained on the basis of the liquid phase physical properties, gas-liquid interface contamination and the special characteristics of the gas-liquid-liquid systems and gas-liquid systems.*

### 4.1.1. Specific introduction

Reactors or bioreactors involving two liquid phases (organic and aqueous phases) are used nowadays as an alternative to other systems, since these new reactors may improve the overall process efficiency[215]. Two different application fields have been considered for these reactors: (i) reactors to clean gaseous streams by means of capturing pollutant gases (for instance, the presence of an organic phase could enhance the capture of volatile organic compounds due to the hydrophobic nature of these gases)[216,217]; (ii) bioreactors that enhance the oxygen mass transfer rate by adding an organic phase[218]. This enhancement is very important when the gas absorption is the limiting step in the global process. In these cases, an increase in the oxygen transfer rate could produce an important increase in the process productivity. Several studies[219,220] have analysed the effect of different organic liquids (i. e. toluene, dodecane, heptane, etc) on the oxygen absorption process; however, different experimental results have been obtained showing contradictory conclusions.

On the one hand, several studies have found positive effects upon the global absorption process[221,222] but, on the other hand, the opposite behaviour has also been obtained[223]. This variety of results could be due to the lack of experimental data in these studies: those about the analysis of the interfacial area produced between gas-liquid-liquid systems, as well as the influence of the organic substances upon the gas hold-up, the bubbles size and the interfacial area.

---

[215] Dumont E., Delmas H. Mass transfer enhancement of gas absorption in oil-in-water systems: a review. *Chemical Engineering and Processing* 2003, 42, 419–438.
[216] Dumont E., Andrès Y., Le Cloirec P. Mass transfer coefficients of styrene and oxygen into silicone oil emulsions in a bubble reactor. *Chemical Engineering Science* 2006, 61, 5612 – 5619.
[217] Darracq G., Couvert A., Couriol C., Amrane A., Thomas D., Dumont E., Andres Y., Le Cloirec P. Silicone oil: an effective absorbent for the removal of hydrophobic volatile organic compounds. *Journal of Chemical Technology and Biotechnology* 2010, 85, 309–313.
[218] Dumont E., Andres Y., Le Cloirec P. Effect of organic solvents on oxygen mass transfer in multiphase systems: Application to bioreactors in environmental protection. *Biochemical Engineering Journal* 2006, 30, 245–252.
[219] Da Silva T. L., Calado V., Silva N., Mendes R. L., Alves S. S., Vasconcelos J. M. T., Reis A. Effects of hydrocarbon additions on gas-liquid mass transfer coefficients in biphasic bioreactors. *Biotechnology and Bioprocess Engineering* 2006, 11, 245-250.
[220] Cents A. H. G., Brilman D. W. F., Versteeg G. F. Gas absorption in an agitated gas-liquid-liquid system. *Chemincal Engineering Science* 2001, 56, 1075-1083.
[221] Sharma M. M., Mashelka R. A. Absorption with reaction in bubble columns. *Institution of Chemical Engineering Symposium Series* 1968, 28, 10-21.
[222] Mehta V. D., Sharma M. M. Mass transfer in mechanically agitated gas/liquid contactors. *Chemical Engineering Science* 1971, 26, 461-479.
[223] Linek V., Benes P. A study of the mechanism of gas absorption into oil/water emulsions. *Chemical Engineering Science* 1976, 31, 1037-1046.

Some of these studies have found a behaviour that implies a decrease in the value of the interfacial area with an organic phase presence[224,225]; however, other studies show the opposite behaviour[226,227,228]. Being more precise, certain studies have analysed more deeply in the last few years the influence of alkanes upon the bubble size and the interfacial area[229,230] using a stirred tank contactor, observing a decrease in the bubble diameter when the alkanes concentration increases.

The same behaviour has been found for the interfacial area due to the reduction in the value of the gas hold-up (caused by the increase in viscosity).

The great part of studies that analyses the effect of an organic phase upon gas-liquid hydrodynamics and mass transfer (see previous references) uses mechanical stirred contactors that remain a suitable organic dispersion in the continuous phase. Present work involves the use of a bubble column reactor and for this reason the effect caused for the use of a surfactant for emulsion stabilization upon hydrodynamics has also been studied taking into account the high influence of this kind of substances upon absorption process detected by different studies. These studies have deepened on the influence of different operation variables upon the global mass transfer and, more specifically, upon the gas hold-up[231], the bubbles diameter and gas-liquid interfacial area[232], the interfacial turbulence[233] and, at the same time, upon the mass transfer

---

[224] Yoshida F., Yamane T., Miyamoto Y. Oxygen absorption into oil-in-water emulsions. A study on hydrocarbon fermentors. *Industrial & Engineering Chemistry Process Design and Development* 1970, 9, 570-577.

[225] Ju L. K., Lee J. F., Armiger W. B. Enhancing oxygen transfer in bioreactors by perfluorocarbon emulsions. *Biotechnology Progress* 1991, 7, 323-329.

[226] Hassan I. T. M., Robinson C. W. Oxygen transfer in mechanically agitated systems containing dispersed hydrocarbon. *Biotechnology and Bioengineering* 1977, 19, 661-682.

[227] Rols J. L., Condoret J. S., Fonade C., Goma G. Mechanism of enhanced oxygen transfer in fermentation using emulsified oxygen- vectors. *Biotechnololy and Bioengineering* 1990, 35, 427-435.

[228] Lekhal A., Chaudhari R. V., Wilhelm A. M., Delmas H. Gas/liquid mass transfer in gas/liquid/liquid dispersions. *Chemical Engineering Science* 1997, 52, 4069-4077.

[229] Clarke K. G., Correia L. D. C. Oxygen transfer in hydrocarbon-aqueous dispersions and is applicability to alkane bioprocesses: a review. *Biochemical Engineering Journal* 2008, 39, 405-429.

[230] Correia L. D. C., Aldrich C., Clarke K. G. Interfacial gas-liquid transfer area in alkane-aqueous dispersions and its impact on the overall volumetric oxygen transfer coefficient. *Biochemical Engineering Journal* 2010, 49, 133-137.

[231] Ruzicka M. C., Vecer M. M., Orvalho S., Drahoš J. Effect of surfactant on homogeneous regime stability in bubble column. *Chemical Engineering Science* 2008, 63, 951-967.

[232] Loubière K., Hébrard G. Influence of liquid surface tension (surfactants) on bubble formation at rigid and flexible orifices. *Chemical Engineering and Processing* 2004, 43, 1361-1369.

[233] Kim J. K., Jung J. Y., Kim J. H., Kim M. G., Kashiwagi T., Kang Y. T. The effect of chemical surfactants on the absorption performance during $NH_3/H_2O$ bubble absorption process. *International Journal of Refrigeration* 2006, 29, 170-177.

coefficient[234]. Other researchers have shown some interest in analysing the influence of the surfactants nature, taking into account the molecules size[235] as well as their ionic character[234].

## 4.1.2. Results and discussion

### *4.1.2.1. $CO_2$ - Tween80 - $H_2O$ system*

This part of work has been focused on the effect caused by the presence of different concentrations of a surfactant (T80) in aqueous solution upon the hydrodynamic behaviour, based on the analysis of the gas hold-up and the gas-liquid interfacial area produced in the contactor. In relation to the first parameter (gas hold-up), the behaviour observed for this experimental system is shown in figure 4.1.

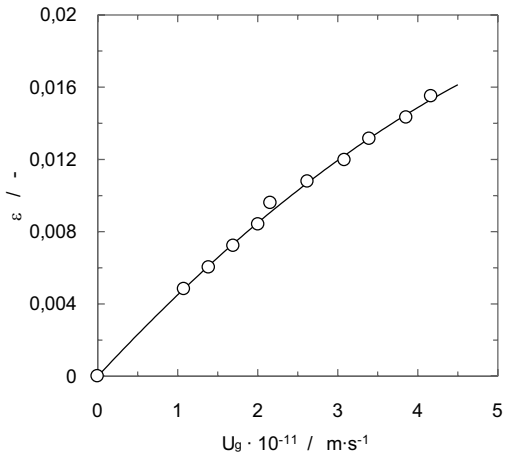


Figure 4.1. Effect of superficial gas velocity upon gas hold-up

[234] Sardeing R., Painmanakul P., Hébrard G. Effect of surfactants on liquid-side mass transfer coefficients in gas-liquid systems: a first step to modelling. *Chemical Engineering Science* 2006, 61, 6249-6260.
[235] Gómez-Díaz D., Navaza J. M., Sanjurjo B. Gas-liquid interfacial area in the presence of different chain length surfactants. *Industrial & Engineering Chemistry Research* 2009, 48, 5894-5900.

The influence of the gas flow-rate (or superficial gas velocity) upon the gas hold-up is shown in this figure, where we can observe that an increase in the gas flow-rate produces an increase in the gas hold-up value. This kind of behaviour shown in figure 4.1 indicates that a change in the bubbling regime is not produced in the studied range. The bubbling regime is pseudo-homogeneous in all cases and, then, the coalescence process is not observed. The experimental data shown in figure 4.1 corresponds to pure water (without Tween80 addition) but the experiments developed with different surfactant concentrations do not show significant changes with regard to the values obtained for carbon dioxide – water system, in agreement with other works using different surfactants[236,237].

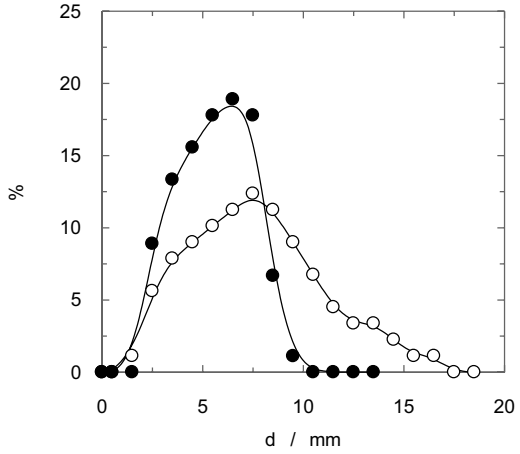


Figure 4.2. Influence of surfactant concentration upon bubble size distribution. $Q_g$ = 30 L·h.$^{-1}$. (○) $C_{T80}$ = 1.46·10$^{-5}$ mol·L$^{-1}$, (●) $C_{T80}$ = 1.22·10$^{-3}$ mol·L$^{-1}$.

Also, the hydrodynamic characterization of the gas-liquid systems employed in present work includes the analysis of the bubbles size distribution produced in the bubble column. The bubble size distribution and gas hold-up could be used to gas-liquid interfacial area determination. An example of bubble size distribution determined in present work is shown in figure 4.2. This figure allows to analyse the influence of surfactant concentration upon bubble size

[236] Gómez-Díaz D., Gomes N., Teixeira J. A., Belo I. Oxygen mass transfer to emulsions in a bubble column contactor. *Chemical Engineering Journal* 2009, 152, 354-360.
[237] Tadakamalla K., Marathe K. V. Hydrodynamic study and optimization strategy for the surfactant recovery from aqueous solutions. *Desalination* 2011, 266, 98-107.

distribution. The experimental results indicate that a higher value in surfactant concentration produces a decrease in the bubble size. This behaviour is in agreement with the results obtained for systems with small chain length surfactant[238,239]. Also, figure 4.2 shows that an increase in surfactant concentration produces a narrower size distribution.

This behaviour is related to the influence caused by the surfactant presence upon the surface tension value. This kind of substances produces an important decrease in the value of the surface tension, and this behaviour has a high influence upon the bubble size produced in the contactor. Figure 4.2 shows the decrease observed in the bubbles size distribution produced by the surfactant. Figure 4.3 shows the influence of surfactant concentration upon the value of surface tension. This isotherm indicates the important influence of low surfactant concentration produces upon the surface tension value. Also figure 4.3 shows the critical micelle concentration calculation with a value of $5 \cdot 10^{-5}$ mol·L$^{-1}$.

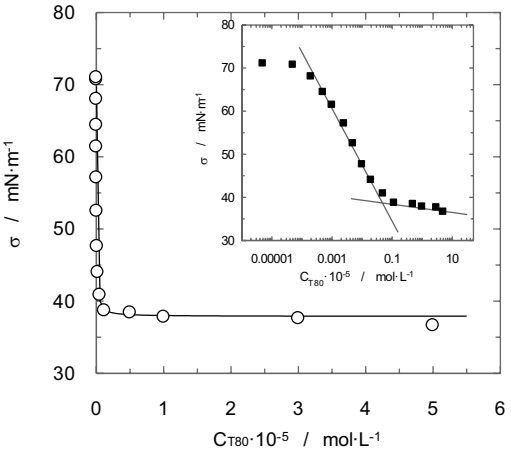


Figure 4.3. Surfactant concentration effect upon surface tension.

[238] Loubière K., Hébrard G. Influence of liquid surface tension (surfactants) on bubble formation at rigid and flexible orifices. *Chemical Engineering and Processing* 2004, 43, 1361-1369.
[239] Gómez-Díaz D., Navaza J. M., Sanjurjo B. Gas-liquid interfacial area in the presence of different chain length surfactants. *Industrial & Engineering Chemistry Research* 2009, 48, 5894-5900.

Using the bubble size distribution for each experimental conditions and the gas hold-up produced in the bubble column, the gas-liquid interfacial area was calculated (see material and methods section). Figure 4.4 summarized the determined data for the interfacial area under the experimental conditions analysed in this work. Regarding the influence of surfactant concentration upon the interfacial area, an increase in this parameter was observed when solute concentration increases in the aqueous solution. This behaviour is due to the presence of this solute, that produces a decrease in the bubble size value (*vide supra*) with non-influence upon the gas hold-up.

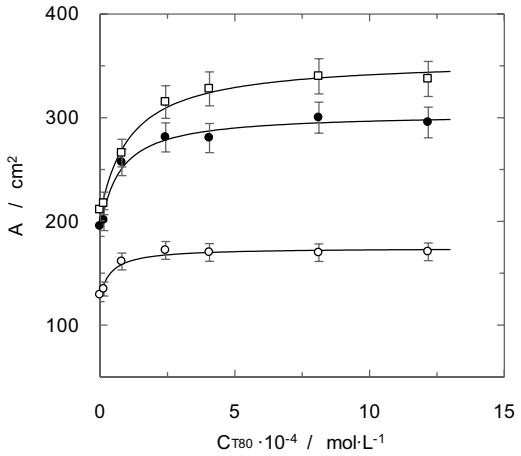


Figure 4.4. Influence of concentration of surfactant and gas flow-rate upon the gas-liquid interfacial area. (○) $Q_g$ = 18 L·h$^{-1}$, (●) $Q_g$ = 30 L·h$^{-1}$, (□) $Q_g$ = 40 L·h$^{-1}$.

On the basis of experimental data, we conclude that the largest change in the value of interfacial area is caused by the addition of small quantities of surfactant. Higher concentrations than 2.5·10$^{-4}$ mol·L$^{-1}$ of surfactant produce practically constant interfacial area values with slight changes, in spite of the fact that important quantities of surfactant were added to the liquid phase. A similar behaviour has been observed for other systems that have employed surfactants in aqueous solution[240,241].

[240] Sardeing R., Painmanakul P., Hébrard G. Effect of surfactants on liquid-side mass transfer coefficients in gas-liquid systems: a first step to modelling. *Chemical Engineering Science* 2006, 61, 6249-6260.
[241] Rosu M., Schumpe A. Influence of surfactants on gas absorption into aqueous suspensions of activated carbon. *Chemical Engineering Sci*ence 2007, 62, 5458-5463.

This behaviour has been observed for all the gas flow-rates employed in this work. In relation to the influence of this operation variable, an increase in this value produces an increase in the interfacial area, although the reason is different to the one previously commented, when the surfactant concentration was varied. Regarding the gas flow rate effect, an increase in this variable does not produce significant changes in the bubble size, but on the other hand, this variable produces an increase in the gas hold-up (see figure 4.1).

Gas-liquid interfacial area data determined under the different operation conditions could be fitted using an equation based on the value of these variables (equation 4.1). Different authors suggest the use of similar equation taken into account the potential trend caused by these operation variables[242,243].

$$A = n_1 \cdot C_s^{n_2} \cdot cmc^{n_3} \cdot Q_g^{n_4} \qquad (4.1)$$

where *Cs* is the surfactant concentration, *cmc* is the critical micelle concentration of Tween80 and *Qg* is the gas flow-rate.

Equation 4.1 includes the surfactant concentration and the gas flow-rate as important operation variables, but this equation also includes the value of the critical micelle concentration. This parameter provides information about the chain length and other properties related to hydrofobicity.

Only one surfactant has been employed in this work and then the value of the critical micelle concentration is constant, but the expression used in equation 4.1 includes this value to preserve the equation general formulation. The use of the same equation allows us to compare the value of the fit parameters with previous and future studies that use other surfactants. Figure 4.5 shows a comparison between experimental and calculated gas-liquid interfacial area under different experimental conditions, observing a good agreement between the experimental values and the corresponding ones calculated using equation 4.1. The proposed equation allows the calculation of the interfacial area with a standard deviation of 18 $cm^2$.

---

[242] Majumder S. K., Kundu G., Mukherjee D. Bubble size distribution and interfacial phenomena in ejector induced downflow bubble column. *Chemical Engineering J*ournal 2006, 122, 1-10.
[243] Molga E. J., Westerterp K. R. Gas-liquid interfacial area and holdup in cocurrent packed bed bubble column reactor at elevated pressures**.** *Industrial & Engineering Chemistry Research* 1997, 36, 622-631.

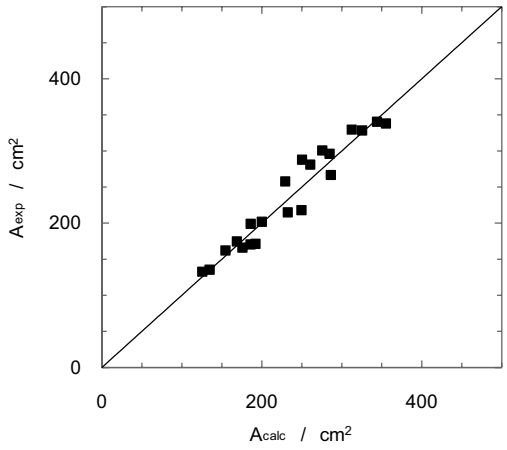


Figure 4.5. Comparison between experimental and calculated gas-liquid interfacial area using equation 4.1.

#### *4.1.2.2. $CO_2$ – Silicone oil – (Tween80) – $H_2O$ system*

Other study developed in the present work has been analysing the experimental data corresponding to the bubble diameter, obtained by means of the methodology mentioned in the material and methods section for the several emulsions. Different photographs of gas-liquid dispersions into the bubble contactor have been analysed according to different experimental conditions (gas flow-rate, surfactant use, and nature and concentration of silicone).

Regarding the influence of the gas flow-rate upon the bubble diameter, different behaviours have been obtained; however, the commonest one indicates that an increase in the gas flow-rate produces an increase in the bubble size. This behaviour is in agreement with previous studies of other experimental systems[244] in bubble contactors.

Taking into account the influence produced by the presence or absence of the surfactant used to stabilize the emulsion, figure 4.6 shows an example of the bubble size distribution, obtained by means of the experiments carried out in this work.

[244] Kulkarni A. A., Joshi J. B. Bubble formation and bubble rise velocity in gas-liquid systems: a review. *Industrial and Engineering Chemistry Research* 2005, 44, 5873-5931.

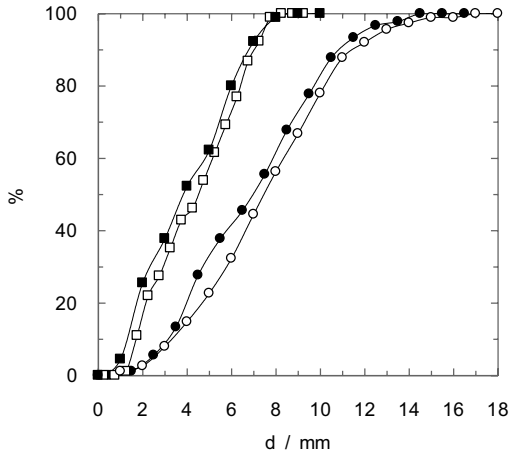


Figure 4.6. Influence of surfactant and silicone oil (S1) presence upon bubble size distribution. (○) water; (□) surfactant aqueous solution ($C_{T80}$ = 0.1 %); (●) emulsion without surfactant ($C_{oil}$ (S1) = 0.5 %); (■) emulsion with surfactant ($C_{oil}$ (S1) = 0.5 % and $C_{T80}$ = 0.1 %). $Q_g$ = 30 $L \cdot h^{-1}$.

These experimental data show that the presence of this surfactant produces: (i) a decrease in the value of the bubble diameter for the entire diameter range and, (ii) a narrower bubble size distribution than the system without a surfactant. In agreement with the conclusions of a previous work[245] about the influence of this kind of substances, producing a decrease in the bubble diameter, this behaviour is assigned to the decrease in the value of the surface tension caused by these substances. This decrease is due to the accumulation of amphiphylic substances in the gas-liquid interface. Regarding the presence of organic substances, this behaviour could be cancelled, since amphiphilic molecules are located at the liquid-liquid interface preferentially[246]. In this system, despite the reduction in the surfactant surface concentration due to the presence of an organic phase, Tween80 keeps on provoking an important influence upon the surface tension, producing a notable decrease with a very low surfactant concentration. This surfactant produces an important decrease in the value of this physical property due to its low critical

[245] Loubière K., Hébrard G. Influence of liquid surface tension (surfactants) on bubble formation at rigid and flexible orifices. *Chemical Engineering and Processing* 2004, 43, 1361-1369.
[246] Gómez-Díaz D., Gomes N., Teixeira J. A., Belo I. Oxygen mass transfer to emulsions in a bubble column contactor. *Chemical Engineering Journal* 2009, 152, 354-360.

micelle concentration (see figure 4.3)[247], in comparison with other surfactants employed in previous studies involving gas absorption[248,249].

The Sauter mean diameter has been calculated using the experimental data representing the bubble size distribution (see material and methods section), and a summary of this data is shown in figure 4.7 to analyse the influence of the silicon type and concentration upon the bubble diameter. Taking into account the data shown in figure 4.7, different conclusions can be reached. On the one hand, an increase in the silicone concentration produces in all cases a decrease in the bubble size value. The obtained trends are different when the surfactant is used in relation to the absence of this substance in the liquid phase. The system without surfactant shows an abrupt decrease in the bubble size with low silicon (S1) concentration until reaching a constant value, and a slighter decrease is observed for systems with surfactant.

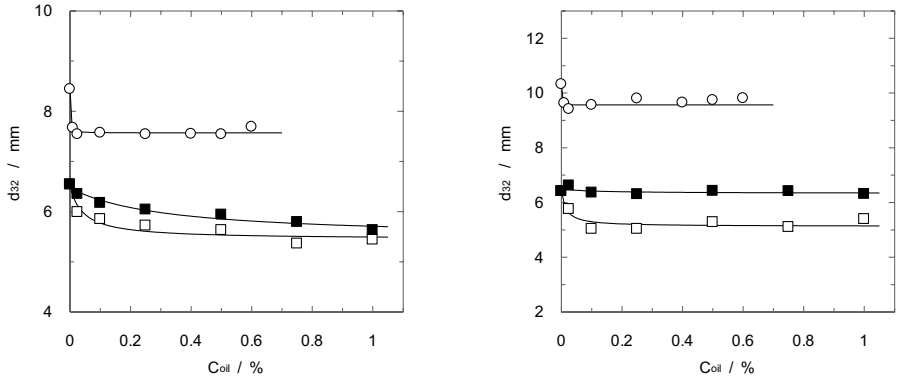


Figure 4.7. Influence of silicone oil type and concentration upon bubbles Sauter diameter. (○) S1 without Tween80, (□) S1 with Tween80, (■) S2 with Tween80.

The systems with surfactant also produce in all cases bubbles of a minor size if we compare them to the systems in absence of Tween80 (see also figure 4.6), being detected important differences. Taking into account the systems with surfactant, the experimental results

[247] Guo H., Zhangb J., Liu Z., Yang S., Sun C. Effect of Tween80 and β-cyclodextrin on the distribution of herbicide mefenacet in soil–water system. *Journal of Hazardous Materials* 2010, 177, 1039–1045.
[248] Gómez-Díaz D., Navaza J. M., Sanjurjo B. Density, kinematic viscosity, speed of sound, and surface tension of hexyl, octyl, and decyl trimethyl ammonium bromide aqueous solutions. *Journal of Chemical and Engineering Data* 2007, 52, 889–891.
[249] Sardeing R., Painmanakul P., Hébrard G. Effect of surfactants on liquid-side mass transfer coefficients in gas-liquid systems: a first step to modelling. *Chemical Engineering Science* 2006, 61, 6249-6260.

show that the low viscosity silicone oil (S1) produces smaller bubbles than the corresponding values for the high viscosity silicone oil (S2). This behaviour is in agreement with previous studies that have analysed the influence of the surface tension and viscosity upon the bubbles size produced in gas-liquid bubbling equipments[250,251,252].

The decrease observed in the bubble diameter, shown in figure 4.7, is assigned to the low surface tension of silicones ($\sigma_{S1}$=19.4 mN·m$^{-1}$, $\sigma_{S2}$=20.7 mN·m$^{-1}$). Previous studies[253,254,255,256,257] have concluded that the presence of substances with a low surface tension produces bubbles of a small size. These studies have employed surface active substances and also different liquid substances with low surface tension (i. e. alcohols or alkanes), but the influence of insoluble substances have not been analysed from the point of view of surface tension. Figure 4.8 shows the experimental data corresponding to this physical property for the experimental systems employed in this work. We can observe in this figure that an increase in silicone S1 oil concentration (in absence of Tween80) produces a decrease in the surface tension value. This behaviour is similar to the corresponding one shown by the presence of surfactants, because an abrupt decrease is observed at a low S1 concentration until a constant value of surface tension is reached. The results corresponding to the influence of S1 concentration upon the surface tension, confirm the abovementioned behaviour corresponding to the influence of S1 concentration upon the bubble diameter (see figure 4.7). A direct relation between bubble diameter and liquid phase surface tension is observed: a decrease in the surface tension also produces a decrease in the

[250] Gómez-Díaz D., Navaza J. M., Quintáns-Riveiro L. C., Sanjurjo B. Gas absorption in bubble column using a non-Newtonian liquid phase. *Chemical Engineering Journal* 2009b, 146, 16–21.
[251] Tecante A., Choplin L. Gas–liquid mass transfer in non-Newtonian fluids in a tank stirred with a helical ribbon screw impeller. *Canadian Journal of Chemical Engineering* 1993, 71, 859–865.
[252] Mouza A. A., Dalakoglou G. K., Paras S. V. Effect of liquid properties on the performance of bubble column reactors with fine pore spargers. *Chemical Engineering Science* 2005, 60, 1465–475.
[253] Clarke K. G., Correia L. D. C. Oxygen transfer in hydrocarbon-aqueous dispersions and is applicability to alkane bioprocesses: a review. *Biochemical Engineering Journal* 2008, 39, 405-429.
[254] Correia L. D. C., Aldrich C., Clarke K. G. Interfacial gas-liquid transfer area in alkane-aqueous dispersions and its impact on the overall volumetric oxygen transfer coefficient. *Biochemical Engineering Journal* 2010, 49, 133-137.
[255] Gómez-Díaz D., Gomes N., Teixeira J. A., Belo I. Oxygen mass transfer to emulsions in a bubble column contactor. *Chemical Engineering Journal* 2009, 152, 354-360.
[256] Sardeing R., Painmanakul P., Hébrard G. Effect of surfactants on liquid-side mass transfer coefficients in gas-liquid systems: a first step to modelling. *Chemical Engineering Science* 2006, 61, 6249-6260.
[257] Mouza A. A., Dalakoglou G. K., Paras S. V. Effect of liquid properties on the performance of bubble column reactors with fine pore spargers. *Chemical Engineering Science* 2005, 60, 1465 – 1475.

bubble size. This behaviour is in agreement with previous studies that have analysed the influence of this physical property upon the bubble size and the interfacial area[258,259,260,261].

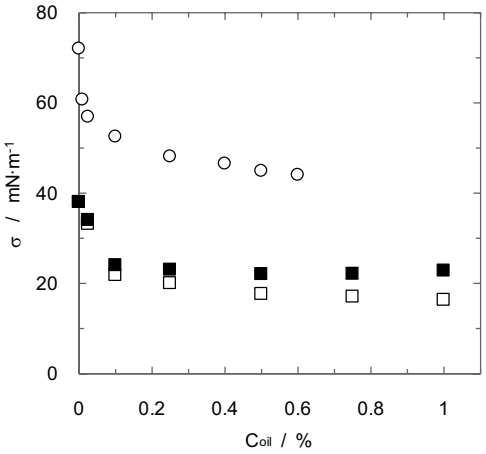


Figure 4.8. Influence of composition upon surface tension. (○) S1 without Tween80, (□) S1 with Tween80, (■) S2 with Tween80.

Regarding the systems that include the presence of Tween80 in the liquid phase, the decrease in the bubble diameter previously commented is observed in comparison to the system with no Tween80 presence. And this behaviour is confirmed with the surface tension experimental data (see figure 4.8), since the addition of Tween80 produces a decrease in the surface tension. For systems with Tween80, the increase in silicone oils (both S1 and S2) concentration also produces a decrease in the surface tension value; however, the observed trend is different, since the abrupt decrease at a low silicone concentration (in the systems without Tween80) is not produced, and a slight decrease is obtained. The characteristic behaviour of these systems in relation to the surface tension is in agreement with the data shown in figure 4.7.

[258] Clarke K. G., Correia L. D. C. Oxygen transfer in hydrocarbon-aqueous dispersions and is applicability to alkane bioprocesses: a review. *Biochemical Engineering Journal* 2008, 39, 405-429.
[259] Correia L. D. C., Aldrich C., Clarke K. G. Interfacial gas-liquid transfer area in alkane-aqueous dispersions and its impact on the overall volumetric oxygen transfer coefficient. *Biochemical Engineering Journal* 2010, 49, 133-137.
[260] Sardeing R., Painmanakul P., Hébrard G. Effect of surfactants on liquid-side mass transfer coefficients in gas-liquid systems: a first step to modelling. *Chemical Engineering Science* 2006, 61, 6249-6260.
[261] Mouza A. A., Dalakoglou G. K., Paras S. V. Effect of liquid properties on the performance of bubble column reactors with fine pore spargers. *Chemical Engineering Science* 2005, 60, 1465 – 1475.

Figure 4.7 also makes possible to evaluate the influence of the gas flow-rate upon the bubble size for the different emulsions analysed in this work. The influence of the organic compound concentration is similar for the different gas flow-rates. However, the fact of increasing the gas flow-rate produces an increase in the difference between the bubble diameter data corresponding to the systems analysed in this work (S1 without Tween80, S1 with Tween80 and S2 with Tween80). For systems with S1, an increase in the gas flow-rate produces slight changes in the bubble diameter with a decrease in the bubble size value; however, when S2 is used in the emulsion, the increase in gas flow-rate produces an increase in the bubble diameter. Then, differences for the systems analysed, in relation to the bubble size, increase when the gas flow-rate increases as well.

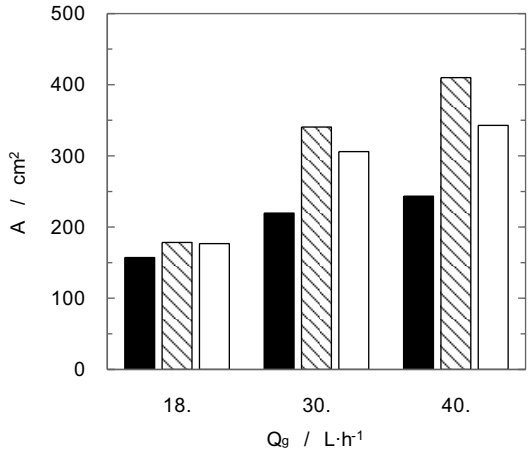


Figure 4.9. Influence of gas flow-rate upon interfacial area produced in the bubble column. $C_{oil}$ = 0.1 %. (Black column) S1 without Tween80, (Striped column) S1 with Tween80, (blank column) S2 with Tween80.

Regarding the value for the gas-liquid interfacial area, it has been obtained using the experimental data concerning the bubble diameter and the gas hold-up. Having analysed the influence of the gas flow-rate fed to the bubble column upon the interfacial area, figure 4.9 shows that an increase in the value of this operation variable produces, in all cases, an increase in the area generated between the gas and liquid phases. This behaviour is similar to the corresponding one in relation to the influence of the gas flow-rate upon the gas hold-up, and also upon the bubble diameter. An increase in the gas hold-up also produces an increase in interfacial area (see

equation A.7 in materials and methods section); however, the effect upon the bubble diameter causes the opposite effect. Then, the effect of the gas hold-up upon the interfacial area is higher than the influence caused by the bubble diameter under these conditions. Being more specific, the increase in the value of the interfacial area when the gas flow-rate increases from 18 $L \cdot h^{-1}$ to 30 $L \cdot h^{-1}$ is higher than the corresponding increase when it is changed from 30 $L \cdot h^{-1}$ to 40 $L \cdot h^{-1}$. This behaviour is due to the change produced on the gas hold-up, which decreases when gas flow-rate increases[262]; then, at high gas flow-rate values, the bubble diameter increases its importance upon the final value of gas-liquid interfacial area.

Figure 4.10 analyses the influence of the gas flow-rate and S1 concentration (with and without surfactant) upon the interfacial area value. The interfacial area increases for all the silicone oil concentration when the gas flow-rate increases, being in agreement with figure 4.9. The highest increase in the interfacial area is also observed when the gas flow-rate is changed from the lowest (18 $L \cdot h^{-1}$) to a medium (30 $L \cdot h^{-1}$) gas flow-rate.

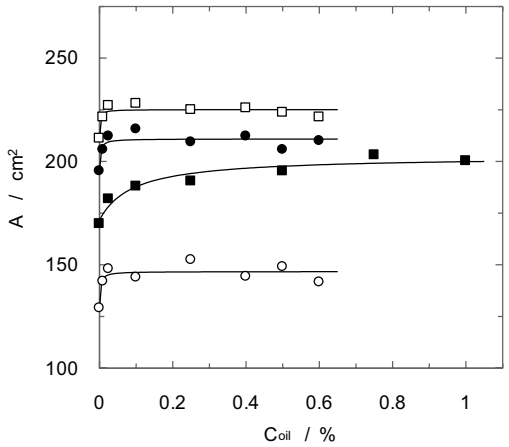


Figure 4.10. Influence of gas flow-rate, silicone oil concentration and surfactant presence upon gas-liquid interfacial area: S1 emulsions without Tween80. (○) $Q_g$ = 18 $L \cdot h^{-1}$, (●) $Q_g$ = 30 $L \cdot h^{-1}$, (□) $Q_g$ = 40 $L \cdot h^{-1}$. S1 emulsion with Tween80: (■) $Q_g$ = 18 $L \cdot h^{-1}$.

[262] Cents A. H. G., Jansen D. J. W., Brilman D. W. F., Versteeg G. F. Influence of small amounts of additives on gas hold-up, bubble size, and interfacial area. *Industrial and Engineering Chemistry Research* 2005, 44, 4863-4870.

In relation to the influence of the organic substance concentration upon the interfacial area, figure 4.10 shows the results corresponding to the system with no surfactant (S1 without Tween80). S2 has not been used without surfactant because the emulsions are unstable. The experimental results shown in figure 4.10 indicate the same behaviour in relation to the influence of S1 concentration at different gas flow-rates. When the silicone oil concentration increases, a fast increase in the interfacial area value is observed, until it reaches a constant value of 0.025 % silicone oil concentration. This behaviour is due to the low silicone S1 concentrations produce a decrease in the bubble diameter value above-named (see figure 4.7). This fact produces an increase in the interfacial area value when the silicone oil concentration increases in the liquid phase, being in agreement with previous studies using low organic compound concentrations[263].

A constant value of the interfacial area is reached when the S1 concentration increases, and this is due to the bubble diameter and gas hold-up, that remain practically constant and independent of the silicone oil concentration. Figure 4.8 showed that the surface tension takes a constant value from a certain silicone oil concentration, what is in agreement with the previously described behaviour for the bubble diameter.

Besides the studies previously commented about the influence of the gas flow-rate and the S1 silicone oil concentration without surfactant upon interfacial area, the same type of studies have been performed for the systems with Tween80, using S1 and S2. Regarding the influence of Tween80 upon the behaviour obtained for the interfacial area, this substance plays an important role, since it causes a decrease in the bubble diameter value, and then an increase in the interfacial area value (see figure 4.10). Previous studies[264,265] indicate that the presence of surface active substances produces the same behaviour (a decrease in the bubble size), caused by the decrease produced upon the surface tension[266,267]. This behaviour is commonly observed in surfactant aqueous solutions, but an organic phase is present in this work and, then, different

[263] Cents A. H. G., Jansen D. J. W., Brilman D. W. F., Versteeg G. F. Influence of small amounts of additives on gas hold-up, bubble size, and interfacial area. *Industrial and Engineering Chemistry Research* 2005, 44, 4863-4870.
[264] Sardeing R., Painmanakul P., Hébrard G. Effect of surfactants on liquid-side mass transfer coefficients in gas-liquid systems: a first step to modelling. *Chemical Engineering Science* 2006, 61, 6249-6260.
[265] Mouza A. A., Dalakoglou G. K., Paras S. V. Effect of liquid properties on the performance of bubble column reactors with fine pore spargers. *Chemical Engineering Science* 2005, 60, 1465 – 1475.
[266] Gómez-Díaz D., Navaza J. M., Sanjurjo B. Density, kinematic viscosity, speed of sound, and surface tension of hexyl, octyl, and decyl trimethyl ammonium bromide aqueous solutions. *Journal of Chemical and Engineering Data* 2007, 52, 889–891.
[267] Cheema M. A., Barbosa S., Taboada P., Castro E., Siddiq M., Mosquera V. A thermodynamic study of the amphiphilic phenothiazine drug thioridazine hydrochloride in water/ethanol solvent. *Chemical Physics* 2006, 328, 243–250.

behaviours could be obtained, due to the different distribution of Tween80 molecules in the interfaces.

Figure 4.10 also shows a comparison between the values of interfacial area for S1 systems with and without Tween80. The behaviour is similar for both systems according to the influence of the silicone oil concentration, producing an increase in the interfacial area when the organic concentration increases, until reaching a constant value.

On the other hand, according to the magnitude of the interfacial area values, the system with Tween80 produces higher values of gas-liquid interfacial area in the bubble column than the system without Tween80. This behaviour is assigned to a better dispersion of the organic phase in the continuous one, caused by the surfactant playing the role of stabilizer. Figure 4.8 evidences that the presence of a surfactant in the liquid-liquid systems produces a decrease in the surface tension value, if we compare it to systems without Tween80. This behaviour is in agreement with the values corresponding to the Sauter mean diameter of the bubbles (see figure 4.7) and the gas-liquid interfacial area (see figure 4.10).

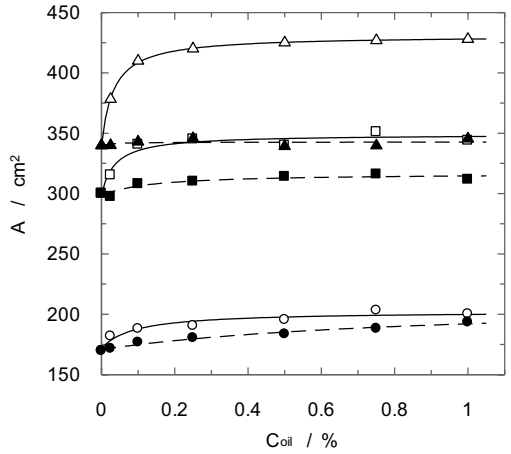


Figure 4.11. Influence of type and concentration of silicone in the presence of surfactant upon gas-liquid interfacial area under different gas flow-rates. $Q_g$ = 18 L·h$^{-1}$: (○) S1, (●) S2. $Q_g$ = 40 L·h$^{-1}$. $Q_g$ = 30 L·h$^{-1}$: (□) S1, (■) S2. $Q_g$ = 40 L·h$^{-1}$: (△) S1, (▲) S2.

In relation to the influence of the silicon nature employed to form the emulsion, figure 4.11 shows the behaviour observed for different experimental conditions: silicone oil type and concentration, and gas flow-rate. The behaviour is similar for all the gas flow-rates, since an increase in the organic concentration produces an increase upon interfacial area. In the case of low viscosity silicon oil (S1), the behaviour is the same as for the previously commented in figure 4.10, a fast increase of the interfacial area at low silicon oil concentrations until reaching a constant value. With regard to the influence of the gas flow-rate, an increase in the interfacial area value is observed when this variable increases, but the increase produced by the organic concentration is more noticeable for high gas flow-rates.

The studies performed using the high viscosity silicon oil (S2) show a slighter increase when the organic concentration is increased, comparing it to the previous data for silicone S1. This behaviour for S2 emulsions indicates that the influence of this substance upon the bubble column interfacial area could be considered negligible. Regarding the influence of the gas flow-rate upon the interfacial area for S2 emulsions, this variable causes an increase in its value, yet the behaviour corresponding to the influence of the silicone oil concentration is the same for low or high gas flow-rates, because the organic concentration effect is practically negligible. Then, when the gas flow-rate is increased, the difference between the interfacial area corresponding to S1 and S2 systems grow continuously. This behaviour is in agreement with the previously shown results for bubble diameter (figure 4.7), that indicates a non-influence of the gas flow-rate upon the bubbles diameter in S1 emulsions; however, the gas flow-rate produces an increase in the bubble size in the case of S2 emulsions. Being more specific, we can observe an important difference between the bubble diameter for S1 and S2 emulsions according to the results corresponding to the highest gas flow-rate (see figure 4.7). Then, taking into account the experimental results, we can conclude that the silicone S2 inhibits the positive effect produced by the surface tension (figure 4.10 shows that both silicones take similar surface tension values), as well as the presence of Tween80 upon bubble diameter (and upon the interfacial area, too). This behaviour could be due to the high viscosity of silicone oil S2, being also in agreement with previous studies that observe the negative influence of viscosity upon the gas-liquid interfacial area[268,269].

[268] Gómez-Díaz D., Navaza J. M., Quintáns-Riveiro L. C., Sanjurjo B. Gas absorption in bubble column using a non-Newtonian liquid phase. *Chemical Engineering Journal* 2009, 146, 16–21.
[269] Jiao Z., Xueqing Z., Juntag Y. $O_2$ transfer to pseudoplastic fermentation broths in air-lift reactors with different inner designs. *Biotechnology Techniques* 1998, 12, 729–732.

The experimental data obtained for the gas-liquid interfacial area has been fitted using an equation based on different operation variables. The correlation used is shown in equation 4.2, and similar equations based on potential effects of the variables have been proposed by other authors[270,271]:

$$A = n_1 \cdot Q_g^{n_2} \cdot \sigma^{n_3} \cdot \eta_{oil}^{n_4} \tag{4.2}$$

where $A$ is the interfacial area, $Q_g$ is the gas flow-rate, $\sigma$ is the surface tension and η is the pure silicones viscosity. The other symbols are fit parameters ($n_1$ = 72.5, $n_2$ = 0.78, $n_3$= -0.40 and $n_4$ = 0.01). Figure 4.12 shows the comparison between the gas-liquid interfacial area experimental data and the corresponding ones obtained using equation 4.2. The proposed equation allows the calculation of the interfacial area with a standard deviation of 28 cm$^2$.

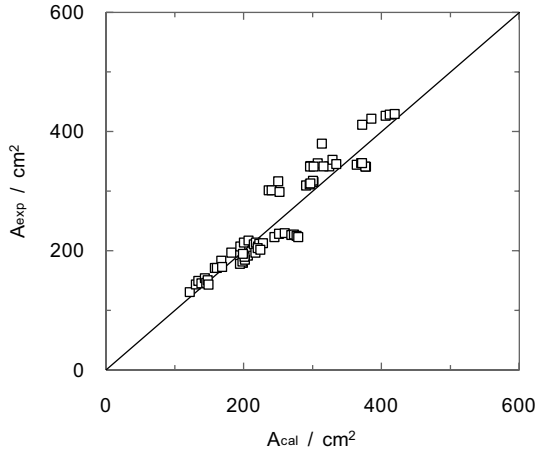


Figure 4.12. Comparison between experimental and calculated (equation 4.2) data for gas-liquid interfacial area in presence of silicones.

[270] Majumder S. K., Kundu G., Mukherjee D. Bubble size distribution and gas-liquid interfacial area in a modified downflow bubble column. *Chemical Engineering Journal* 2006, 122, 1-10.
[271] Molga E. J., Westerterp K. R. Gas-liquid interfacial area and hold-up in a cocurrent upflow packed bed bubble column reactor at elevated pressures. *Industrial and Engineering Chemistry Research* 1997, 36, 622-631.

### 4.1.3. Conclusions

The present work has analysed the influence of the presence of different insoluble substances that could be used to form emulsions in water, upon different hydrodynamic parameters corresponding to a bubble column (gas hold-up, bubble diameter and interfacial area). The influence of the organic phase type and concentration, the presence of a surfactant to stabilize the emulsion and the gas flow-rate fed to the bubble contactor, upon the previously commented hydrodynamic parameters, has been analysed too. The presence of surfactant produces an important increase in gas-liquid interfacial area produced in the bubble column, and caused by an important decrease in the value of bubble diameter, because non-influence of Tween80 upon gas hold-up was detected. On the other hand, an increase in the gas flow-rate produces also an increase in interfacial area due to an increase in gas hold-up.

The system formed by the low viscosity silicone oil (S1) with Tween80 as liquid phase absorbent has shown the highest values of gas-liquid interfacial area in comparison to the other systems. This liquid phase produces bubbles with small diameter due to the reduction in the surface tension value. On the other hand, the systems without Tween80 and using S2 substance show higher bubble diameters than the other one, and producing lower interfacial area values.

The gas flow-rate produces an important enhancement of the gas-liquid interfacial area for the system using S1 with Tween80, since the gas flow-rate produces slight changes in the bubble diameter and important modifications in the gas hold-up. With regard to systems with S2, the high viscosity of this organic compound changes the behaviour of the emulsions, and an increase in gas flow-rate produces an increase in the bubble diameter.

# 4.2 Gas absorption in gas-liquid-liquid systems

*Abstract*

*The present work analyses the mass transfer process of carbon dioxide absorption from a gas phase to a liquid-liquid system based on an aqueous and organic phase. A deep study has been performed analysing different variables, mainly the gas flow-rate fed to the bubble contactor and the silicone oil concentration in the liquid phase. The organic phase has been different kinds of silicone oil with a different viscosity that allows the analysis of the influence of this variable upon mass transfer rate. Present work also analyses gas absorption in Tween80 aqueous solutions and the influence of the presence of this surfactant in the liquid phase, to stabilize the liquid-liquid system, upon the gas-liquid mass transfer process.*

## 4.2.1. Specific introduction

Nowadays, as it has been commented in previous section, the use of reactors or bioreactors involving two liquid phases (organic and aqueous phases) is used as an alternative procedure to other systems, because these new reactors may improve the overall efficiency[272]. In a gas-liquid-liquid (gas-organic-aqueous) system, the gas transfer has been postulated to take place via one or more transfer paths: gas-organic and/or gas-aqueous phase. Due to this, a global volumetric mass transfer coefficient has been proposed. Different studies have suggested that the most likely transfer path will depend on whether the organic adsorbs onto the gas bubble or remains freely dispersed and, if the former, whether it is adsorbed as microdroplets (non-spreading) or as a continuous film (spreading) around the gas-liquid surface. A simplified approach is used in the present work and, supported by different previous studies, neglecting the different paths the carbon dioxide may take to be transferred from the gas bubbles to the aqueous phase. The combined influence of the turbulence properties of the liquid phase upon the volumetric mass transfer coefficient is supported by certain studies about the influence of different hydrocarbons upon this parameter, a behaviour that has been certified in numerous studies using agitated hydrocarbon–aqueous systems[273].

The effect caused by the presence of an organic compound upon the gas-liquid mass transfer coefficient has been studied by different works in the last few years, but the conclusions that have been reached do not let us extract a unique behaviour[274]. On the one hand, certain studies have found positive effects upon the global process[275,276], but other studies have obtained the opposite behaviour[277]. These differences in the experimental results could be due to the non-existence of studies related to the mass transfer interfacial area in this kind of gas-liquid-liquid system. Then, the influence of the nature of this kind of gas-liquid-liquid system upon the gas

[272] Dumont E., Delmas H. Mass transfer enhancement of gas absorption in oil-in-water systems: a Review. *Chemical Engineering and Process*ing 2003, 42, 419-438.
[273] Correia L. D. C., Aldrich C., Clarke K. G. Interfacial gas–liquid transfer area in alkane–aqueous dispersions and its impact on the overall volumetric oxygen transfer coefficient. *Biochemical Engineering Journal* 2010, 49, 133-137.
[274] Clarke K. G., Correia L. D. C. Oxygen transfer in hydrocarbon-aqueous dispersions and is applicability to alkane bioprocesses: a review. *Biochemical Engineering Journal* 2008, 39, 405-429.
[275] Sharma M. M., Mashelkar R. A. Absorption with reaction in bubble columns. *IChemE Symposium Series* 1968, 28, 10-21.
[276] Mehta V. D., Sharma M. M. Mass transfer in mechanically agitated gas/liquid contactors. *Chemical Engineering Sci*ence 1971, 26, 461.
[277] Linek V., Benes P. A study of the mechanism of gas absorption into oil/water emulsions. *Chemical Engineering Sci*ence 1976, 31, 1037-1046.

hold-up, bubbles size and interfacial area are important studies necessary to obtain valuable information about mass transfer.

The studies about gas-liquid interfacial area in this kind of systems developed in previous section let us carry out a deeper analysis about mass transfer removing the influence of different variables (gas and liquid phases physical properties and operation variables) upon the interfacial area, and then, upon the mass transfer process. The great majority of studies involved in this kind of systems (gas-liquid-liquid) use the value of the volumetric mass transfer coefficient to analyse the influence of different organic compounds upon the absorption process. The aim of this work is going deep into the influence of this kind of substance, analysing the volumetric and individual mass transfer coefficient separately in order to reach valuable conclusions about the effect caused by organic compounds upon the gas-liquid mass transfer, as well as the presence or absence of surfactant. Because, as it has been mentioned in previous sections, present work involves the use of a bubble column reactor and for this reason the presence of surfactant to stabilize the emulsion could be necessary.

## 4.2.2. Results and discussion

### *4.2.2.1. $CO_2$ – Tween80 – $H_2O$ system*

This part of work includes gas-liquid mass transfer studies corresponding to the absorption of carbon dioxide in Tween80 aqueous solutions. The operation regime was semicontinuous and then, the liquid phase was placed into the contactor and the gas phase was fed continuously to the bubble column. The absorption kinetics was obtained and this experimental data has been employed to calculate the volumetric mass transfer coefficient ($k_L \cdot a$). The mass transfer coefficient ($k_L$) was determined taking into account the values of the volumetric mass transfer coefficient and the gas-liquid interfacial area. By this way, our aim in this work is analysing the influence of surfactant presence and concentration upon the mass transfer coefficient, as well as analysing the influence upon each parameter individually.

Figure 4.13 shows an example of the behaviour of absorbed carbon dioxide concentration in the Tween80 aqueous solutions. Being more specific, two experiments are compared in figure 4.13 using the same surfactant concentration and different gas flow-rate

values. The experimental data indicate that an increase in the value of the gas flow-rate fed to bubble column produces a higher increase in the carbon dioxide concentration. This behaviour indicates that the mass transfer rate increases with the gas flow-rate and it is complemented with the fact previously commented (previous section): that an increase in the gas flow-rate produces an increase in the interfacial area that, at the same time, produces an increase in the mass transfer rate.

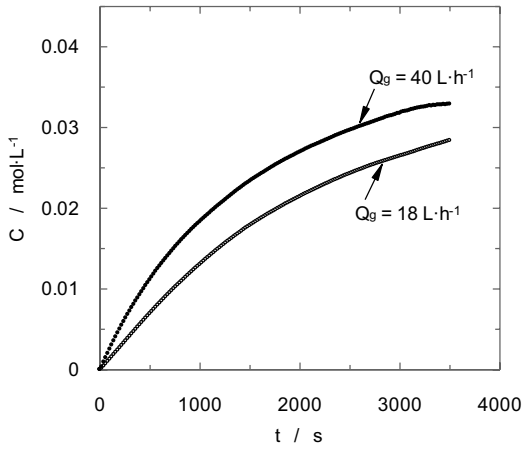


Figure 4.13. Effect of gas flow-rate upon carbon dioxide absorption data. $C_{T80}$ = $4.1 \cdot 10^{-4}$ mol·L$^{-1}$. (○) $Q_g$ = 18 L·h$^{-1}$, (●) $Q_g$ = 40 L·h$^{-1}$.

Using the experimental data corresponding to carbon dioxide absorption rate, the concentration of this substance in the liquid phase along the time has been calculated, and under the experimental regime (semicontinuos) the volumetric mass transfer coefficient could be calculated by means a gas phase mass balance using equation A.9 (section materials and methods).

The solubility of carbon dioxide employed in this work was the same than the corresponding one for water[278] because the presence of low Tween80 concentration has not

[278] Sharma M. M., Danckwerts P. V. Fast reactions of $CO_2$ in alkaline solutions— (a) Carbonate buffers with arsenite, formaldehyde and hypochlorite as catalysts (b) Aqueous monoisopropanolamine (1-amino-2-propanol) solutions. *Chemical Engineering Sci*ence 1963, 18, 729-735.

influence upon this parameter. The use of a pure gas phase implies that the liquid side mass transfer coefficient is the same than the global mass transfer coefficient.

The same experimental procedure has been carried out for the different experiments performed in the present work, and then the volumetric mass transfer coefficient has been calculated for each experimental condition. Figure 4.14 shows the obtained behaviour and the influence of different operation variables, such as gas flow-rate and surfactant concentration. An important decrease in mass transfer coefficient was produced when small quantities of Tween80 were added to the liquid phase, reaching a constant value of mass transfer coefficient and not dependent of surfactant concentration. This behaviour is opposite to the previous one commented about the influence of surfactant concentration upon the value of gas-liquid interfacial area (the increase of surfactant concentration produces an increase in interfacial area until a constant value). The influence of surfactant concentration upon the interfacial area must be an increase in the value of the volumetric mass transfer coefficient; however, the obtained behaviour is the opposite. Taking this fact into account, *a priori* conclusion is that the presence of surfactant in the liquid phase has a very important negative influence upon the mass transfer coefficient, and this important effect is higher than the positive influence caused upon the interfacial area.

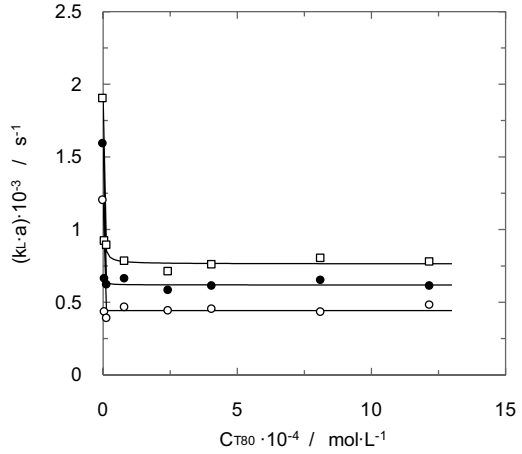


Figure 4.14. Influence of surfactant concentration and gas flow-rate upon volumetric mass transfer coefficient. (○) $Q_g$ = 18 L·h$^{-1}$, (●) $Q_g$ = 30 L·h$^{-1}$, (□) $Q_g$ = 40 L·h$^{-1}$.

On the other hand, in relation to the influence of gas flow-rate fed to the bubble contactor, an increase in the value of the volumetric mass transfer coefficient has been observed when the gas flow-rate increases. Taking into account the previously analysed influence of gas flow-rate upon the interfacial area and the results for volumetric mass transfer coefficient, we can conclude that the gas flow-rate affects positively upon both parameters (mass transfer coefficient and interfacial area).

Using the experimental values of volumetric mass transfer coefficient and the previously determined specific interfacial area, we can calculate the mass transfer coefficient values for each experimental condition by means of equation A.10 (materials and methods section).

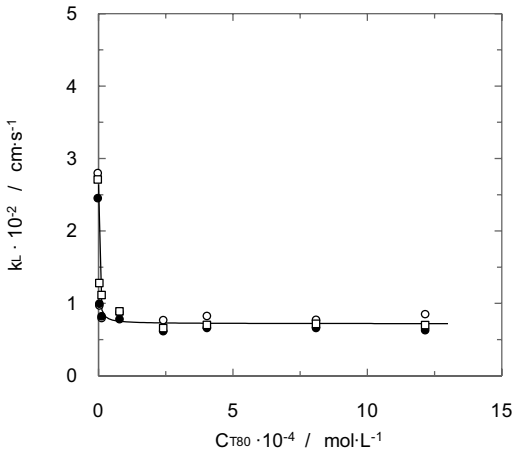


Figure 4.15. Influence of surfactant concentration upon mass transfer coefficient. (○) $Q_g$ = 18 L·h$^{-1}$, (●) $Q_g$ = 30 L·h$^{-1}$, (□) $Q_g$ = 40 L·h$^{-1}$.

The experimental data showed in figure 4.15 shows a similar behaviour than the corresponding to volumetric mass transfer coefficient. A decrease in the mass transfer coefficient value is observed when low additions of surfactant are added to the liquid phase. Therefore, the results support the conclusions proposed *a priori*.

The effect of the gas flow-rate upon the mass transfer coefficient (shown in figure 4.15) indicates that this variable loses importance, and the same values of mass transfer coefficient at different values of gas flow-rate are obtained. Similar results have been observed in previous

studies that show the non- influence of the gas flow-rate upon the mass transfer in this kind of contactors[279].

Previous studies employing similar systems indicate that the presence of surfactant in the liquid phase reduces the mass transfer coefficient until a plateau for higher concentrations than the critical micelle concentration[279]. This reduction has been assigned to different reasons in relation to the increment in the transport resistance caused by the presence of surfactant molecules. This reduction in mass transfer rate is assigned to different effects that act simultaneously (i) reduction in gas diffusivity or (ii) decrease in turbulence near to the interface. Then, it produces a decrease in the driving force that is directly related to the gas mass transfer rate to the liquid phase.

Other studies have concluded that a low surfactant concentration produces an enhancement of mass transfer that produces an increase in the value of the mass transfer coefficient[280,281]. In this work, this increase or enhancement is not observed and this behaviour is assigned to the size of surfactant molecule, compared to the experimental systems that show the enhancement behaviour[282].

The decrease in the mass transfer coefficient by the presence of surfactant molecules in the liquid phase is assigned to different modifications caused by the accumulation of surfactant molecules at the gas-liquid interface. This accumulation causes a reduction in the renewal of the liquid elements and then, a decrease in the value of the driving force. These effects produce a decrease in the mass transfer rate. Different studies[279] have concluded that this reduction in the mass transfer rate is observed until the surfactant concentration reaches the value corresponding to the critical micelle concentration. When this concentration is reached, it is impossible to increase the surfactant concentration at the gas-liquid interface because the micelle formation has already been produced.

---

[279] Vasconcelos J. M. T., Rodrigues J. M. L., Orvalho S. C. P., Alves S. S., Mendes R. L., Reis A. Effect of contaminants on mass transfer coefficients in bubble column and airlift contactors. *Chemical Engineering Science* 2003, 58, 1431-1440.
[280] Gómez-Díaz D., Navaza J. M., Sanjurjo B. Mass-transfer enhancement or reduction by surfactant presence at a gas–liquid interface. *Industrial & Engineering Chemistry Res*earch 2009, 48, 2671.
[281] Kaya A., Schumpe A. Surfactant adsorption rather than "shuttle effect"? *Chemical Engineering Science* 2005, 60, 6504-6510.
[282] García-Abuín A., Gómez-Díaz D., Navaza J. M., Sanjurjo B. Effect of surfactant nature upon absorption in a bubble column. *Chemical Engineering Science* 2010, 65, 4484-4490.

For gas-liquid systems involving the presence of different quantities of surfactants in the liquid phase, a previous work has developed a model that shows a good behaviour for the mass transfer coefficient estimation and, taking into account the special changes produced by this kind of substance, upon the dynamics of gas-liquid systems[283]. This model indicates that in the presence of surfactants the value of mass transfer coefficient could be included between: $k_L^0$: the mass transfer coefficient corresponding to a free surface (Se = 0) and $k_L^1$: the corresponding one value for a saturated surface (Se = 1). These limits are taken into account in equation 4.3.

$$k_L = S_e \cdot k_L^1 + (1 - S_e) \cdot k_L^0 \tag{4.3}$$

On one hand, $k_L^0$ (free surface) is calculated using the model developed by Higbie[284] and in the other hand $k_L^1$ (mass transfer coefficient corresponding to a saturate interface) has different problems for its estimation because the influence of the kind of surface active substance could play an important role. Sardeing et al.[283] suggest one equation that involves the use of Frossling equation[285] for mass transfer calculation and also, taking into account the surfactant nature characteristics (see equation 4.4).

$$\mathrm{k_L^1} = 1.744 \cdot \mathrm{K}^{-0.084} \cdot \mathrm{k_L^{Frössling}} \tag{4.4}$$

where *K* is the surfactant adsorption (at gas-liquid interface) equilibrium constant. High values of this constant imply that the equilibrium is reached in a low time, and then when a clean bubble is produced in the column the accumulation of surfactant at gas-liquid interface is quickly, and this process produces a decrease in mass transfer rate.

[283] Sardeing R., Painmanakul P., Hébrard G. Effect of surfactants on liquid-side mass transfer coefficients in gas-liquid systems: a first step to modelling. *Chemical Engineering Science* 2006, 61, 6249-6260.
[284] Higbie R. The rate of absorption of pure gas into a still liquid during short period of exosure. *Tranactions of American Institute Chemical Engineers* 1935, 31, 365-388.
[285] Frössling N., Über die verdunstung fallender tropfen. *Gerlands Beiträge zur Geophysik* 1938, 52, 170-216.

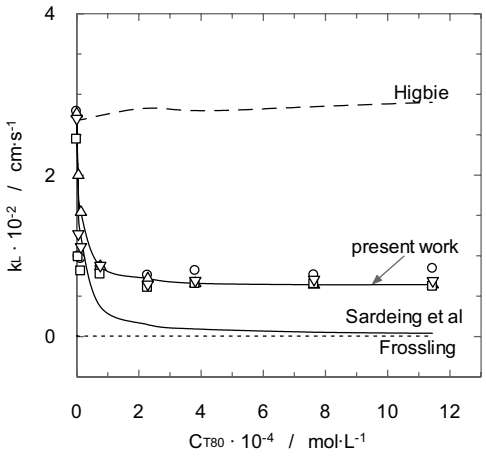


Figure 4.16. Comparison of mass transfer coefficient experimental values with different models. (○) $Q_g$ = 18 L·h$^{-1}$, (□) $Q_g$ = 30 L·h$^{-1}$, (▽) $Q_g$ = 40 L·h$^{-1}$.

Figure 4.16 shows the obtained behaviour for the Higbie, Frössling and Sardeing et al. (using equation 4.4) models. The comparison with the experimental values of mass transfer coefficient (see figure 4.16) indicates that the Higbie's model overestimate the values of mass transfer coefficient except for the system in the absence of surfactant. On the other hand, Frössling's model takes lower values than the experimental ones. At a high surfactant concentration, the experimental values are closer to the corresponding ones to Frössling's model, due to the increase in the surfactant concentration at the gas-liquid interface. The last model, developed by Sardeing et al, allows the calculation of the mass transfer coefficient with better results when it is compared with the experimental data. But the values contributed by this last model when the surfactant concentration increases are very close to Frössling's model, and the experimental data show a *plateau* with a constant value of mass transfer coefficient higher than the value calculated using Frössling equation. Due to the behaviour of Sardeing's model, a modification of this equation has been performed in this work, by means of changing the constant (1.744) of equation 4.4, since this value is related to the surfactant nature[286]. This constant has been determined in the present study using the experimental data of mass transfer coefficient because the surfactant employed is very different (in molecular weight and size) to the

[286] Sardeing R., Painmanakul P., Hébrard G. Effect of surfactants on liquid-side mass transfer coefficients in gas-liquid systems: a first step to modelling. *Chemical Engineering Science* 2006, 61, 6249-6260.

substances used in previous works that have used this model. This fact could indicate that the Sardeing et al model does not take into account some factor related with surfactant nature. Then, equation 4.4 has been modified, obtaining the expression shown in equation 4.5. This modification in the Sardeing et al model allows fitting, with better results, the influence of Tween80 concentration upon the experimental values of mass transfer coefficient, in comparison with the other models analysed (see figure 4.16).

$$k_L^1 = 100 \cdot K^{-0.084} \cdot k_L^{Frössling} \tag{4.5}$$

#### *4.2.2.2. $CO_2$ – Silicone oil – (Tween80) – $H_2O$ system*

The other aim of the present work is analysing the way that an organic liquid phase affects upon the gas-liquid absorption process from a gas phase to an aqueous liquid one. To get this aim, two different silicone oils (S1 and S2) have been employed in the presence and absence of a surfactant, because this last compound in commonly employed to maintain the emulsion stability.

Figure 4.17 shows an example of the experimental data obtained for the absorption rate using the inlet and outlet gas flow-rates in the gas-liquid contactor. The experimental data shown in this figure indicate that the gas absorbed quantity has a fast growth in the initial part of the experiments, but this absorption rate reduces continuously until reaching the solubility value. This behaviour is commonly observed in systems with physical absorption.

Besides, figure 4.17 shows the absorption rate experimental values for a blank experiment (without organic compound and surfactant), as well as an experiment with a liquid phase with certain quantity of silicone oil S1 (low viscosity silicon oil).

The experimental data indicates that under the same operational condition of gas flow rate, the carbon dioxide absorption rate to the liquid phase is higher for the system in the absence of organic compound, since the carbon dioxide concentration in the liquid phase has a fast growth for the system that only uses pure water.

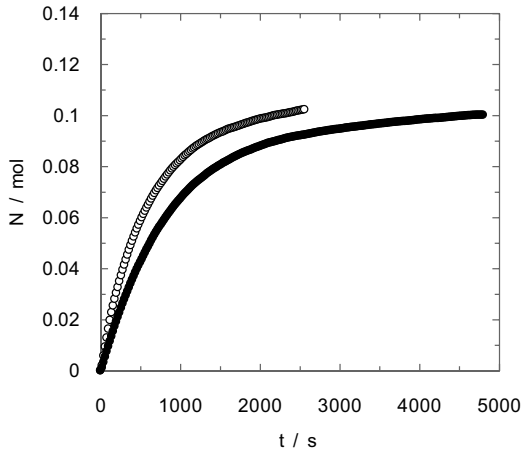


Figure 4.17. Carbon dioxide absorption rate in the bubble column. (○) pure water, (●) water+silicone oil S1 ($C_{oil}$ = 0.5 %). $Q_g$ = 40 L·h$^{-1}$.

As it was previously mentioned in the specific introduction section, there are an important number of discrepancies in relation to the influence of organic insoluble substances upon the gas-liquid mass transfer rate, as certain studies conclude a positive effect[287] but others obtained exactly the opposite results[288].

Figure 4.18 shows the influence of the gas flow-rate upon the absorption rate for one of the systems analysed in this work. The observed behaviour is similar to the previous one shown in figure 4.17. In relation to the influence of the gas flow-rate upon the mass transfer, a clear increase in the absorption rate is observed when the gas flow rate is increased too. This behaviour is commonly obtained in this kind of contactors (bubbling equipment) because the gas flow rate produces changes in gas-liquid interfacial area[289] and also in turbulence in the liquid phase. For the experimental systems employed in the present work, in the previous section it has been concluded that the increase in the gas flow-rate produces an increase in the gas-liquid interfacial area produced in the bubble column. This increase is caused by the increment in the

[287] Dumont E., Delmas H. Mass transfer enhancement of gas absorption in oil-in-water systems: a review. *Chemical Engineering and Processing* 2003, 42, 419–438.
[288] Correia L. D. C., Aldrich C., Clarke K. G. Interfacial gas-liquid transfer area in alkane-aqueous dispersions and its impact on the overall volumetric oxygen transfer coefficient. *Biochemical Engineering Journal* 2010, 49, 133-137.
[289] Cents A. H. G., Jansen D. J. W., Brilman D. W. F., Versteeg G. F. Influence of small amounts of additives on gas hold-up, bubble size, and interfacial area. *Industrial and Engineering Chemistry Research* 2005, 44, 4863-4870.

gas hold-up produced in the bubble column when the gas flow-rate increases, because the effect produced by this variable upon the bubble size is negative for the interfacial area due to the bubble size increases with the gas flow-rate.

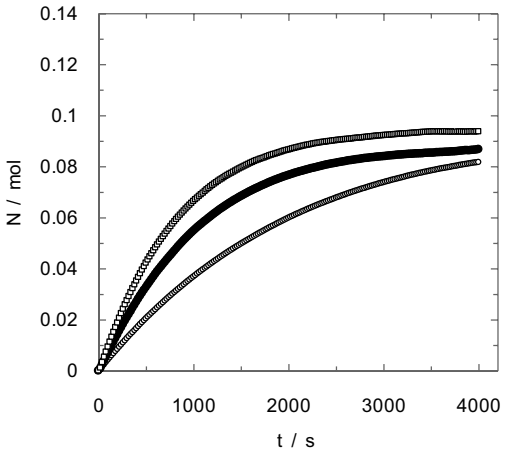


Figure 4.18. Effect of gas flow-rate upon gas-liquid absorption rate, using emulsions with silicone oil S2 ($C_{oil}$ = 0.75 % $_{w/w}$). (○) $Q_g$ = 18 L·h$^{-1}$, (●) $Q_g$ = 30 L·h$^{-1}$, (□) $Q_g$ = 40 L·h$^{-1}$.

Using the experimental data abovementioned in figures 4.17 and 4.18, the volumetric mass transfer coefficient has been determined using the linearised version of equation A.9 (materials and methods section).

Figure 4.19 shows an example of the carbon dioxide absorbed in the liquid phase and the fit of this experimental data using equation A.9 to determine the corresponding volumetric mass transfer coefficient (the slope value of the plot shown in figure 4.19). This data treatment has been performed for all the experiments developed in the present work, to analyze the influence of nature and silicone oil concentration, the use of surfactant and the gas flow-rate upon the absorption process.

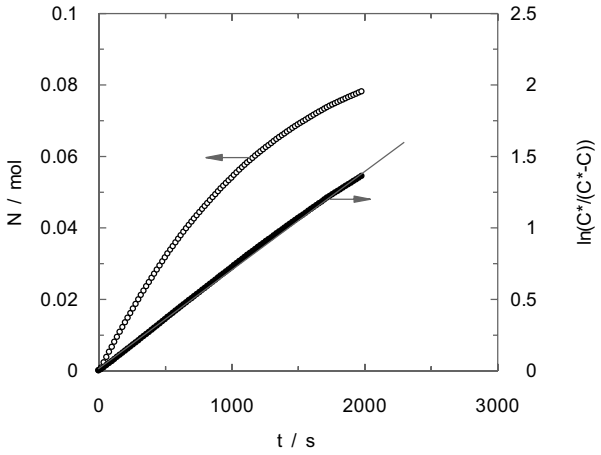


Figure 4.19. Volumetric mass transfer coefficient determination using equation A.9. Emulsions with silicone oil S2 ($C_{oil}$ = 0.1 % $_{v/v}$) and surfactant ($C_{T80}$ = 0.1 % $_{v/v}$). $Q_g$ = 30 L·h$^{-1}$. (○) absorption rate, (●) equation A.9.

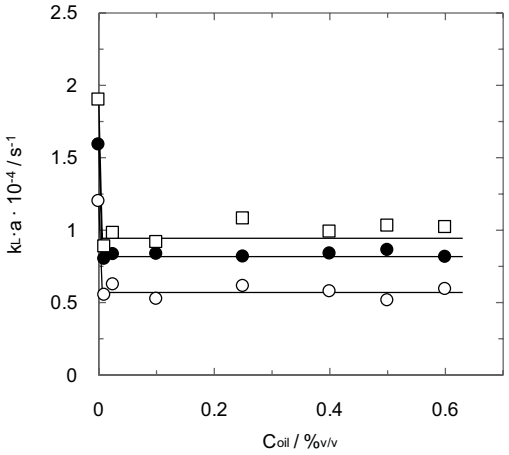


Figure 4.20. Influence of silicone oil concentration upon volumetric mass transfer coefficient for systems with S1 and without surfactant system. (○) $Q_g$ = 18 L·h$^{-1}$, (●) $Q_g$ = 30 L·h$^{-1}$, (□) $Q_g$ = 40 L·h$^{-1}$.

Using the procedure previously described to obtain the volumetric mass transfer coefficient by means of equation A.9, an example of the calculated values for this parameter is shown in figure 4.20. This figure shows the influence of the gas flow-rate upon the volumetric mass transfer coefficient.

An increase in the gas flow-rate produces also an increase in the value of the volumetric mass transfer coefficient in all the gas flow-rate range employed. In relation to the influence of the silicone oil S1 concentration upon the volumetric mass transfer coefficient, the trend observed indicates that there is an important decrease in the value of this parameter when the S1 concentration increases until reaching a constant value. This behaviour is similar to the one previously observed in different studies when surface active substances are present in the liquid phase during an absorption process[290]. Certain studies that have also employed different organic substances[291,292,293] obtained similar and also different conclusions, indicating this way the low knowledge about this kind of systems. This behaviour is included in the type 3 classification suggested by Clarke et al[291] that suggests a decrease in the value of volumetric mass transfer coefficient, that assigns this behaviour to a low agitation in the gas-liquid contactor, but other studies indicate that it isn't the only factor that produces this behaviour. The fact that the experimental systems employed in this study show similar behaviours to the surfactants aqueous solutions is due to the reduction in the surface tension value when the concentration of the silicone oil used is increased in the aqueous solution (see table 4.1). When the silicone oil S1 concentration increases in the liquid phase it is important to take into account that an increase in gas-liquid interfacial area (that is included in the volumetric mass transfer coefficient) is also observed, caused by a reduction in the bubble size. In relation to the influence of the silicone oil S1 concentration upon the value of the volumetric mass transfer coefficient (see figure 4.20), an important decrease in this coefficient is obtained. Then, a first conclusion that could be reached *a priori* is that silicone oil S1 produces a high decrease in the value of the mass transfer coefficient, because this effect cancels the positive influence of the silicone oil concentration upon the interfacial area previously noticed.

---

[290] García-Abuín A., Gómez-Díaz D., Navaza J. M., Sanjurjo B. Effect of surfactant nature upon absorption in a bubble column. *Chemical Engineering Science* 2010, 65, 4484-4490.
[291] Clarke K. G., Correia L. D. C. Oxygen transfer in hydrocarbon-aqueous dispersions and is applicability to alkane bioprocesses: a review. *Biochemical Engineering Journal* 2008, 39, 405-429.
[292] Gómez-Díaz D., Gomes N., Teixeira J. A., Belo I. Oxygen mass transfer to emulsions in a bubble column contactor. *Chemical Engineering Journal* 2009, 152, 354-360.
[293] Cents A. H. G., Brilman D. W. F., Versteeg G. F. Gas absorption in an agitated gas-liquid-liquid system. *Chemincal Engineering Science* 2001, 56, 1075-1083.

Tabla 4.1. Surface tension of liquid phases employed in present work. T=25 ºC

| Without surfactant | | With surfactant | | |
|---|---|---|---|---|
| $C_{oil}$ (%) | $\sigma_{S1}$ (mN·m$^{-1}$) | $C_{oil}$ (%) | $\sigma_{S1}$ (mN·m$^{-1}$) | $\sigma_{S2}$ (mN·m$^{-1}$) |
| 0 | 72.2 | 0 | 38.0 | 38.0 |
| 0.01 | 60.7 | 0.025 | 33.1 | 34.2 |
| 0.025 | 56.9 | 0.1 | 21.8 | 24.8 |
| 0.1 | 52.5 | 0.25 | 20.0 | 23.1 |
| 0.25 | 48.1 | 0.5 | 17.6 | 22.5 |
| 0.4 | 46.5 | 0.75 | 17.0 | 22.1 |
| 0.5 | 44.9 | | | |
| 0.6 | 44.0 | | | |

On the other hand, the influence of the silicone oil type, as well as the presence or absence of a surfactant to stabilize the emulsion, has been studied upon the value of the volumetric mass transfer coefficient (see figure 4.21). Figure 4.21 shows very different behaviours when systems with and without surfactant are compared. For systems without a surfactant, the conclusion that has been reached and previously pointed out indicates that a low silicone oil concentration causes an important decrease in the value of the volumetric mass transfer coefficient. But systems with a surfactant presence in the emulsion (for both silicone oils) show a negligible influence of the silicone oil concentration upon volumetric mass transfer coefficient.

We can observe in figure 4.21 that, at a zero silicone oil concentration, the presence of the surfactant produces a value, for the volumetric mass transfer coefficient, much lower than for the system without surfactant. This behaviour is in agreement with previous works that have analysed the influence of surface active substances upon absorption processes[294]. The reduction in the value of volumetric mass transfer coefficient caused by the surfactant has an important effect, and then, the possible negative effect caused by the silicone oils upon this parameter is not observed.

[294] Vasconcelos J. M. T., Rodrigues J. M. L., Orvalho S. C. P., Alves S. S., Mendes R. L., Reis A. Effect of contaminants on mass transfer coefficients in bubble column and airlift contactors. *Chemical Engineering Science* 2003, 58, 1431-1440.

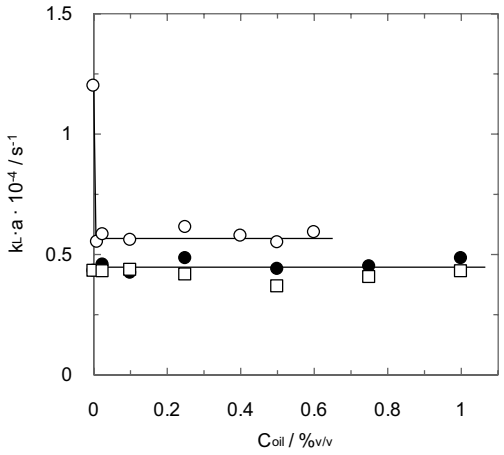


Figure 4.21. Influence of silicone oil concentration and nature upon volumetric mass transfer coefficient. $Q_g$ = 18 L·h$^{-1}$. (○) S1 without surfactant; (●) S1 with surfactant; (□) S2 with surfactant.

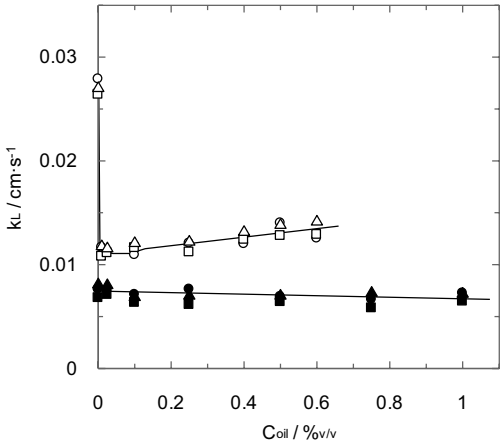


Figure 4.22. Influence of silicone oil concentration, surfactant presence and gas flow-rate upon mass transfer coefficient. S1 without surfactant; system: (○) $Q_g$ = 18 L·h$^{-1}$; (□) $Q_g$ = 30 L·h$^{-1}$; (△) $Q_g$ = 40 L·h$^{-1}$. S1 with surfactant: (●) $Q_g$ = 18 L·h$^{-1}$; (■) $Q_g$ = 30 L·h$^{-1}$; (▲) $Q_g$ = 40 L·h$^{-1}$.

Equation A.10 allows us the calculation of the mass transfer coefficient under the different operation conditions, using the values of the volumetric mass transfer coefficient and the specific gas-liquid interfacial area. The calculated values for this parameter are shown in figure 4.22. This figure shows the influence of the silicone oil S1 concentration and the gas flow-rate, and the effect of the surfactant presence upon the mass transfer coefficient.

In relation to the influence of the silicone oil concentration, an increase in the gas-liquid interfacial area was observed in this study, which is the opposite behaviour to the previous one obtained for the volumetric mass transfer coefficient (see figures 4.20 and 4.21). The increase produced in the interfacial area when the silicon oil concentration increases (with or without surfactant) is due to the reduction in the value of surface tension produced by the presence of these organic substances (see figure 4.23). It is commonly accepted that a decrease in the surface tension value also produces a decrease in the bubble size[295], and this behaviour has a positive influence upon the gas-liquid interfacial area produced into the bubble contactor. The obtained behaviour of the interfacial area in relation to the influence of the silicone oil concentration is a decrease at a low organic substance presence until it reaches a constant value (see previous section).

Figure 4.22 shows the calculated values for the mass transfer coefficient from the experimental ones of volumetric coefficient and specific interfacial area. The data shown in figure 4.22 let us draw different conclusions: in relation to the influence of gas flow-rate, a non-influence of this variable upon the mass transfer coefficient. A similar behaviour has been obtained in previous works[296], and this behaviour indicates that the gas flow-rate has an influence on the absorption process, mainly upon the gas-liquid interfacial area. This operation variable shows a low influence upon the mass transfer coefficient, even though an increase in this variable could produce an increase in turbulence into the bubble contactor causing changes in the liquid elements reneval at the liquid film.

[295] R. Sardeing; P. Painmanakul; G. Hébrard. Effect of surfactants on liquid-side mass transfer coefficients in gas-liquid systems: a first step to modelling. *Chemical Engineering Science* 2006, 61, 6249-6260.
[296] J.M.T.Vasconcelos; J.M.L. Rodrigues; S.C.P. Orvalho; S.S. Alves; R.L. Mendes; A. Reis. Effect of contaminants on mass transfer coefficients in bubble column and airlift contactors. *Chemical Engineering Sci*ence 2003, 58, 1431-1440.

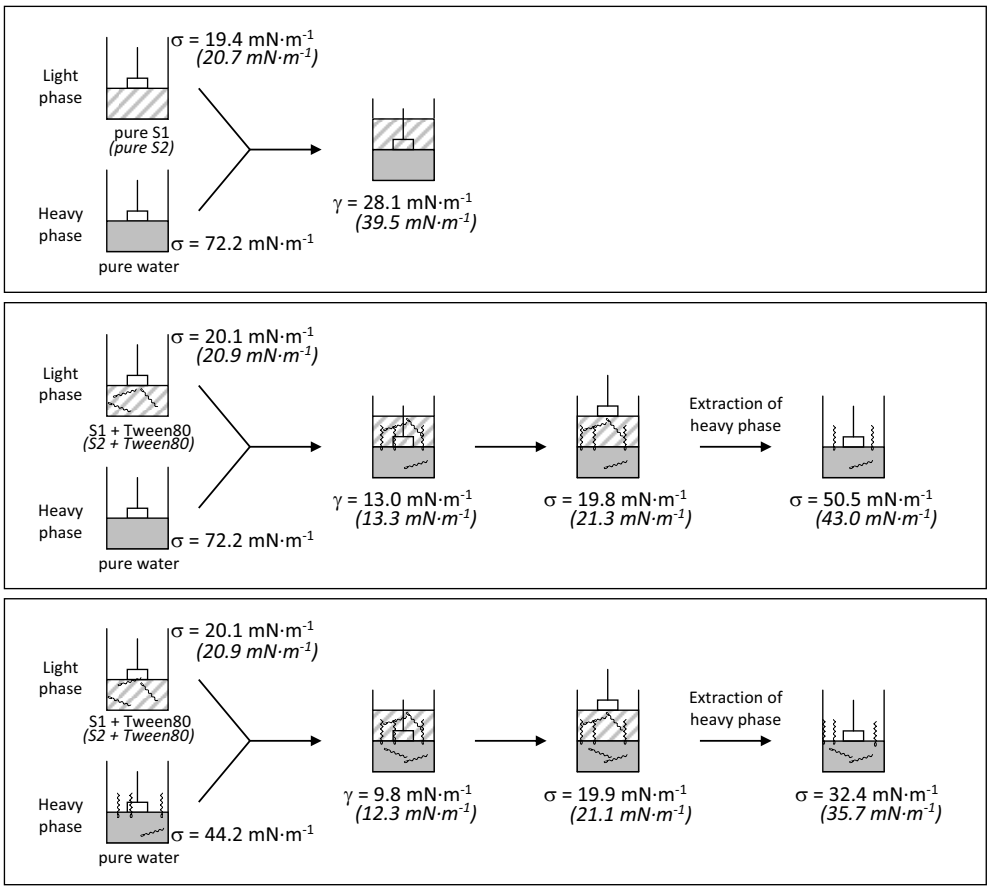


Figure 4.23. Surface and interfacial tension for liquid phases and systems used in this work.

On the other hand, figure 4.22 allows us to compare the behaviour obtained for systems that employ silicone oil S1 with and without surfactant. The comparison is similar to the one previously observed for the volumetric mass transfer coefficient: an important decrease when the silicone oil concentration increases slightly for the systems without a surfactant, but in the case of surfactant use, this decrease in the low silicone oil concentration range is not observed.

In relation to the influence of the surfactant presence upon the mass transfer coefficient, systems without surfactant reach higher values for this parameter than the other systems with surfactant. This compared behaviour is in agreement with the conclusions reached by different

studies[297,298] that have shown the negative influence of this kind of substances upon mass transfer processes caused by the hydrophobic character of part of these molecules, that produces an accumulation of this substance in the gas-liquid interface and this accumulation tend to reduce the mass transfer.

Figure 4.23 indicates that the surfactant molecules are present in all the liquid phases. The presence of Tween80 molecules in water with the presence of silicone oil indicates that this surfactant is present at gas-liquid interface reducing mass transfer rate. In other experimental systems with low surfactant concentrations, the molecules are accumulated at liquid-liquid interface uniquely, and it produces clean gas-liquid interfaces that enhance mass transfer in comparison with pollutant bubbles at interface.

For the system in absence of surfactant, when the decrease in the value of mass transfer coefficient reaches a minimum, a slight increase is observed when the silicone oil concentration increases. This increase at high silicone oil concentrations in the studied range is produced when the gas-liquid interfacial area remains constant (see previous section). Previous studies have shown the same behaviour to the previous one commented for the present system (an increase in mass transfer coefficient before a minimum is obtained)[299,300,301]. The presence of an organic phase produces commonly a negative influence upon the value of mass transfer coefficient[299], and this reduction is assigned to the adsorption of the organic component at the gas-liquid interface producing a decrease in surface tension that produces a reduction in bubble surface mobility (rigid sphere behaviour)[302].

On the other hand, for systems that employ surfactant to stabilize the emulsion, a slight constant decrease in the value of the mass transfer coefficient is observed when the silicone oil concentration increases. The zero concentration silicone oil implies the presence of surfactant in

[297] Rosso D., Huo D. L., Stenstrom M. K. Effects of interfacial surfactant contamination on bubble gas transfer. *Chemical Engineering Science* 2006, 61, 5500.
[298] Painmanakul P., Loubière K., Hébrard G., Mietton-Peuchot M., Roustan M. Effect of surfactants on liquid-side mass transfer coefficients. *Chemical Engineering Sci*ence 2005, 60, 6480-6491.
[299] Clarke K. G., Correia L. D. C. Oxygen transfer in hydrocarbon-aqueous dispersions and is applicability to alkane bioprocesses: a review. *Biochemical Engineering Journal* 2008, 39, 405-429.
[300] Jajuee B., Margaritis A., Karamanev D., Bergougnou M. A. Influence of dissolved hydrocarbons on volumetric oxygen mass transfer coefficient in a novel airlift contactor. *Chemical Engineering Science* 2006, 61, 4111-4119.
[301] Boltes K., Caro A., Leton P., Rodriguez A., Garcia-Calvo E. Gas–liquid mass transfer in oil–water emulsions with an airlift bio-reactor. *Chemical Engineering and Processing* 2008, 47, 2408-2412.
[302] Raymond D. R., Zieminski S. A. Mass transfer and drag coefficients of bubbles rising in dilute aqueous solutions. *AIChE Journal* 1971, 17, 57-65.

aqueous solutions that produces a negative influence upon the mass transfer processes, and this is the reason for the important difference between both systems shown in figure 4.22. When the silicone oil is present in the surfactant aqueous solution, the difference regarding the system without surfactant is due to the amphyphilic nature of this substance, which produces the accumulation of surfactant in the interfaces and, mainly, at the liquid-liquid interface (see figure 4.23). The presence of this kind of substances at interfaces produces a decrease in the mass transfer rate that explains the reduction in the value of the mass transfer coefficient for systems with surfactant.

In relation to the influence of silicone oil nature upon the mass transfer coefficient, examined in the first part of this work, a non-influence of this variable upon the volumetric mass transfer coefficient was observed. Regarding the mass transfer coefficient, figure 4.24 shows the calculated values for these systems, and a similar behaviour is observed, but there are certain differences at the highest gas flow-rate.

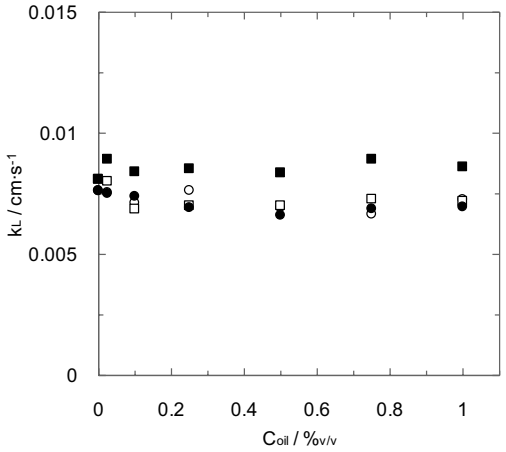


Figure 4.24. Influence of silicone oil concentration and nature, and gas flow-rate upon mass transfer coefficient. S1 with surfactant; system: (○) $Q_g$ = 18 L·h$^{-1}$; (□) $Q_g$ = 40 L·h$^{-1}$. S2 with surfactant: (●) $Q_g$ = 18 L·h$^{-1}$; (■) $Q_g$ = 40 L·h$^{-1}$.

This behaviour could be due to the fact that a high gas flow-rate produces differences in the bubble size distribution for different silicone oils. A minor bubble size is observed for the silicone oil S1 liquid phases in comparison with the systems with S2 (see previous section).

Different studies[303] have concluded that the gas-liquid mass transfer from small bubbles (rigid bubbles) is lower than the mass transfer rate from high size bubbles (mobile ones). This fact explains the behaviour observed in the case of high gas flow-rate, where higher values for the mass transfer coefficient were obtained for systems with S2 in comparison with S1 emulsions.

#### *4.2.2.3. Chemical absorption in $CO_2$ – Silicone oil – (Tween80) – $H_2O$ system*

In present study two substances in aqueous phase (glucosamine and pyrrolidine) have been used, which have previously been analyzed with regard to carbon dioxide absorption with chemical reaction (chapter 2). The aim of this study is to evaluate the influence of an insoluble organic phase upon the global process of gas-liquid mass transfer in a system with chemical reaction. So, different operation variables on carbon dioxide absorption rate have been analyzed.

Figure 4.25 shows the absorption kinetics for the systems with glucosamine in liquid phase. In this figure, the influence of the presence of different compounds: surfactant, silicone oil 1, silicone oil 2 and the combination of these ones with Tween80 is shown. It is observed that the carbon dioxide absorption with chemical reaction with glucosamine in absence of any of the other solutes, practically shows the slowest kinetics, only with higher values of absorption rate than the system composed of GA+S1 in absence of surfactant. More precisely, taking into account the absorption rate shown in figure 4.25, a sequence can be obtained: S1+Tween80+GA > Tween80+GA > S2+Tween80+GA > water+GA > S1+GA. If previous results obtained for the volumetric mass transfer coefficient (in absence of chemical reaction) are taken into account the tendency obtained is as follows: water > S1 > Tween80 ~ S1+Tween80 ~ S2+Tween80. Comparing the results obtained for the volumetric mass transfer coefficient (in absence of glucosamine) and the absorption rate for the system carbon dioxide – glucosamine, an almost opposite behavior is observed, since in the case of physical absorption the highest absorption rate correspond to the system in absence of both silicone oil and surfactant.

[303] Sardeing R., Painmanakul P., Hébrard G. Effect of surfactants on liquid-side mass transfer coefficients in gas-liquid systems: a first step to modelling. *Chemical Engineering Science* 2006, 61, 6249-6260.

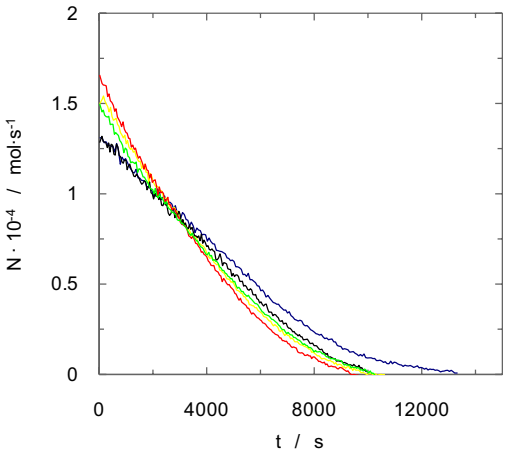


Figure 4.25. Absorption kinetics for systems with glucosamine. (Blue line) GA, (yellow line) GA+T80, (black line) GA+S1, (red line) GA+S1+T80, (green line) GA+S2+T80. $C_{GA}$=0.3 mol·L$^{-1}$. $Q_g$ = 30 L·h$^{-1}$.

The presence of surfactant usually has a negative effect[304], as it has been observed in physical absorption process due to the accumulation of this substance in the interface gas-liquid hindering the mass transfer process. However, in presence of chemical reaction in liquid phase, this substance produces a positive effect, since it is present in different systems where a higher mass transfer rate is observed than in the system composed only of water as solvent.

In view of the experimental data obtained for the absorption rate and compared to the physical absorption process, it may be assumed on the basis of previous studies which have analyzed the influence of micelles upon reaction rate[305], that the improvement observed on the absorption process where surfactant was present may be due to some influence of micelles upon the reaction rate between carbon dioxide and glucosamine. For that, studies of the diffusion of glucosamine molecules in systems in presence or absence of Tween80 have been carried out. The diffusion of these substances has been determined on the basis of DOSY technique (Diffusion Optimized SpectroscopY) by means of proton ($^1$H) nuclear magnetic resonance (NMR). The DOSY

[304] Vasconcelos J. M. T., Rodrigues J. M. L., Orvalho S. C. P., Alves S. S., Mendes R. L., Reis A. Effect of contaminants on mass transfer coefficients in bubble column and airlift contanctors. *Chemical Engineering Science* 2003, 58, 1431-1440.
[305] Kumar B., Ghosh K. K., Rodriquez Dafonte P. Comparative study of the cationic surfactants and their influence on the alkaline hydrolysis of acetylsalicylic acid. *Chemical Kinetics* 2010, 43, 1-8.

spectra were acquired with the standard stimulated echo pulse sequence using LED and bipolar gradient pulses and the experimental data were processed using the MestreC program. An example of the signal variation used to follow the glucosamine molecules is shown in figure 4.26, where it can be observed that the intensity of the signal decreases as the molecules move in the bulk of liquid phase.

The values of intensity of NMR signals can be fitted using the equation 4.6. An example of the obtained results is shown in figure 4.27. The value obtained for the diffusivity from this adjustment is 5.1·10-6 $cm^2 \cdot s^{-1}$.

$$\frac{I}{I_0} = e^{-(\gamma G \delta)^2 \left(\Delta - \frac{\delta}{3}\right) D} \tag{4.6}$$

where $I$ denotes the observed intensity, $I_0$ is the intensity in the absence of gradient pulses, $\gamma$ is the magnetogyric ratio, $\Delta$ is the time between leading edges of the field gradient pulses, $G$ is the gradient strengths, $\delta$ is duration time of the gradient pulse and $D$ is the diffusion coefficient.

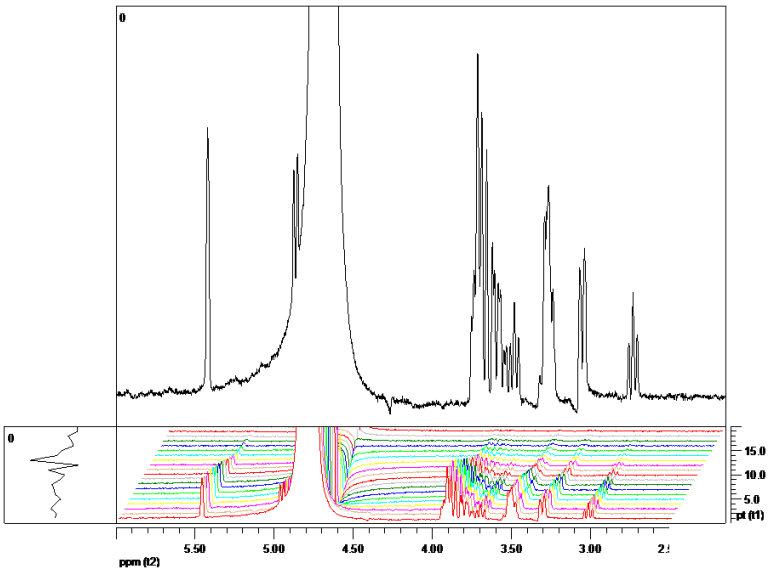


Figure 4.26. $^1H$ NMR spectrum of glucosamine. $C_{GA}$ = 0.1 $mol \cdot L^{-1}$ and T = 25 ºC.

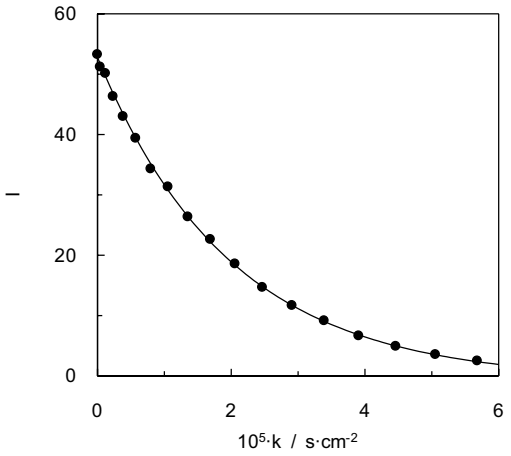


Figure 4.27. Values of intensity of NMR signals ($\delta$ = 3.1ppm) for glucosamine fitted with the equation 4.6.

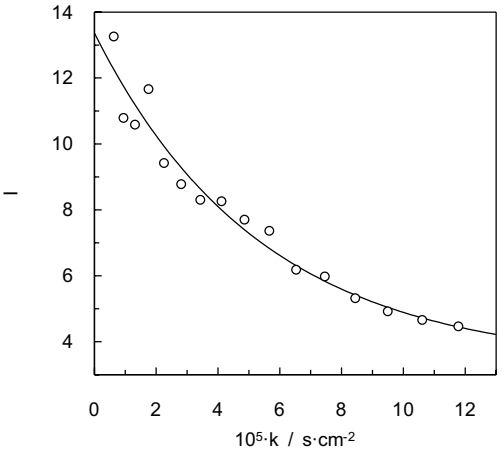


Figure 4.28. Values of intensity of NMR signals ($\delta$ = 3.1ppm) for glucosamine in presence of Tween80 fitted with the equation 4.6. ($C_{T80}$=0.1 % $_{v/v}$)

In the same way, the determination of diffusivity values for the glucosamine in presence of surfactant and the corresponding value for the micelles diffusion (figure 4.28) have been done. The studies carried out with Tween80 aqueous solutions show a worse fit than the shown before

for glucosamine and this fact agrees with the conclusions reached by other authors[306]. These studies indicate that the poor fit of these data to the equation 4.6, for this surfactant, is due to the impurities contained in the Tween80, probably due to the presence of alkyl hydroperoxides.

Table 4.2. Diffusion coefficient values for GA, T80 and GA +T80 at $C_{GA}$ = 0.1 mol·L$^{-1}$ and $C_{T80}$ = 0.1 % $_{v/v.}$

| Substance | D / cm$^2$·s$^{-1}$ |
|---|---|
| GA | $6.37 \cdot 10^{-6}$ |
| Tween80 | $4.90 \cdot 10^{-7}$ [306] |
| GA+T80 | $6.02 \cdot 10^{-6}$ |

Table 4.2 shows the results obtained for each system. In view of the data obtained, a decrease in the value of amine diffusivity in presence of surfactant is observed. Although this decrease is slight this indicates that glucosamine is associating in a low degree with the micelle. This fact is also due to the low surfactant concentration compared with the amine.

Anyway, this amine/surfactant concentration ratio is approximately the used in absorption experiments, therefore the local increase of the glucosamine concentration near the micelles should not be the cause of the behavior previously described for absorption rate.

Therefore, this fact should not be responsible for the enhancement in mass transfer observed for carbon dioxide chemical absorption in glucosamine aqueous solutions in presence of Tween80. So, the surfactant is thought to affect the chemical reaction produced and taking into account its impurities, is believed that these substances produce some type of catalytic effect upon the reaction mechanism. Specifically, the alkyl hydroperoxides can deprotonate the amine and so, a higher concentration of this compound keeps free for reacting with the carbon dioxide previously absorbed. A higher concentration of reagent (glucosamine) would increase the reaction rate, and this would be reflected in the mass transfer rate.

[306] Lafitte G., Thuresson K., Söderman O. Mixtures of mucin and oppositely charged surfactant aggregates with varying charge density. Phase behavior, association, and dynamics. *Langmuir* 2005, 21, 7097-7104.

On the other hand, with regard to the system using pyrrolidine for the reaction with carbon dioxide in liquid phase, the behavior observed has been different to the previously analyzed for the solutions with glucosamine. Figure 4.29 shows the different behaviors for the absorption rate, only for the systems with pyrrolidine and in the presence or absence of surfactant or silicone oil S1.

In this case, the tendency observed in figure 4.29 matches up with the behavior obtained for the system in absence of chemical reaction, it is to say, in absence of pyrrolidine. Therefore, regardless of the affinity that an amine molecule may have to complex with the micelles, in this case, for being an absorption regime very fast, the presence of surface active substance does not produce an effect with capacity for changing the results obtained for the absorption process with chemical reaction. In this case, the presence of silicone oil produces a decrease in the absorption rate and this reduction is higher if the surfactant is present, which agrees with the measures carried out for this type of systems with regard to the surface tension, since they indicate that the surfactant is present in all phases and interphases, hindering in the whole cases the gas mass transfer through the liquid phase.

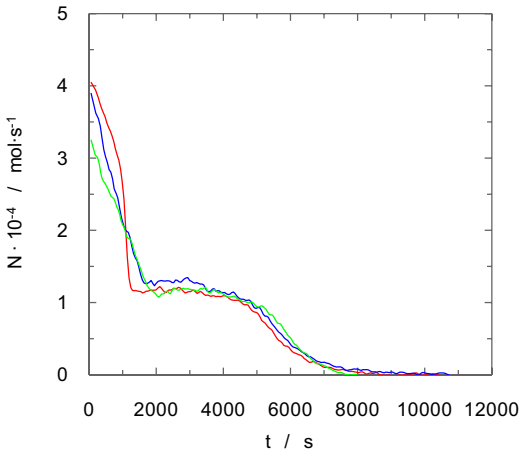


Figure 4.29. Absorption kinetics for systems with pyrrolidine. (Red) PYR, (blue line) PYR+S1, (green line) PYR+S1+T80. $C_{PYR}$ = 0.3 mol·L$^{-1}$. $Q_g$ = 40 L·h$^{-1}$.

Because in previous studies carried out, the presence of surfactant (both in presence and absence of silicone oil) has produced a slight improvement in the mass transfer rate for the system carbon dioxide - glucosamine, additional studies have been done. For this reason, the influence of gas flow fed to the contactor and the glucosamine and silicone oil concentration upon the absorption rate have been analyzed. Figure 4.30 shows the behavior of the absorption rate when two equal systems, with regard to silicone oil concentration, the presence of surfactant and the same gas flow-rate, but with a different concentration of glucosamine are compared. The experimental results show a higher absorption rate for the systems with higher amine concentration, but the decrease in absorption rate is similar, which indicates that the mass transfer rate is similar too.

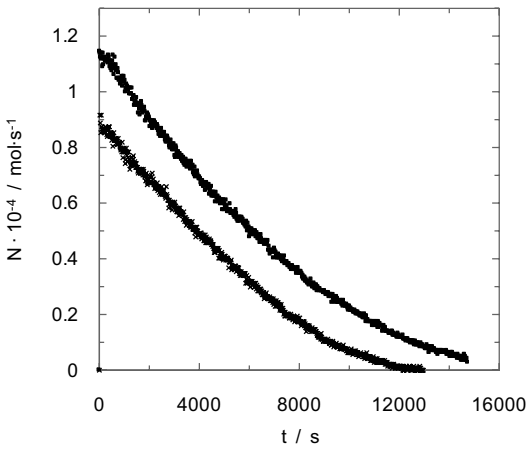


Figure 4.30. Influence of glucosamine concentration ($C_{S1}$ = 0.5% $_{v/v}$, $Q_g$ = 18 L·h$^{-1}$, in presence of Tween80). (×) $C_{GA}$ = 0.2 mol·L$^{-1}$; (■) $C_{GA}$ = 0.4 mol·L$^{-1}$.

In the case of figure 4.31, the influence of gas flow-rate upon mass transfer can be observed. A higher gas flow-rate fed to the contact equipment produces that the absorption process with chemical reaction is completed in less time. This is a common behavior, due to the interfacial area increases when gas flow-rate increase, too.

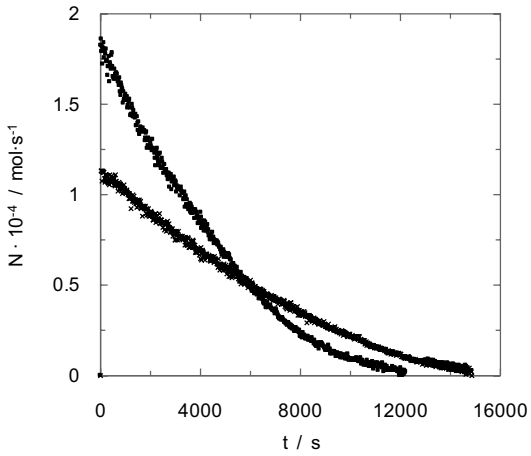


Figure 4.31. Infuence of gas flow-rate fed to the bubble column ($C_{S1}$ = 0.75% $_{v/v}$, $C_{GA}$ = 0.4 mol·L$^{-1}$, in presence of Tween80). (×) $Q_g$ = 18 L·h$^{-1}$; (■) $Q_g$ = 40 L·h$^{-1}$.

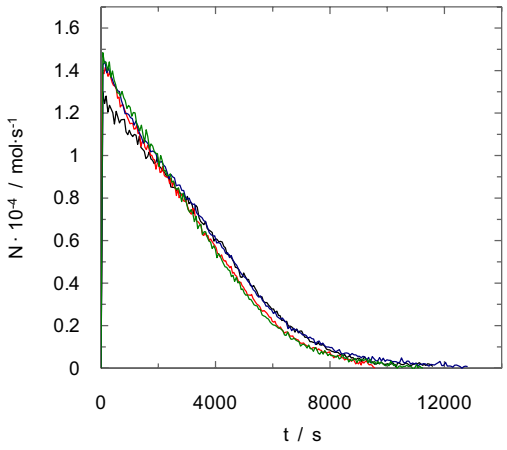


Figure 4.32. Influence of S1 concentration upon absorption rate ($C_{GA}$ 0.2 mol·L$^{-1}$; $Q_g$ = 30 L·h$^{-1}$): (black line) $C_{S1}$ = 0 %; (red line) $C_{S1}$ = 0.25 %; (blue line) $C_{S1}$ = 0.5 %; (green line) $C_{S1}$ = 1 % $_{v/v}$.

The influence of silicone oil concentration upon the absorption rate has also been analyzed, and the experimental results are shown in figure 4.32. As it has been concluded

previously, the presence of silicone oil, with surfactant, produces an enhancement with regard to the system in absence of organic compound and surfactant. Despite the enhancement is observed, there are not differences between the systems with different silicone oil concentration.

In view of the obtained results for this type of systems, in the case of chemical absorption of carbon dioxide with glucosamine, it can be observed that the high influence is due to gas flow-rate, because an increase in this variable produces an increase in the amount of gas fed to bubble column that enhances mass transfer. This fact produces a decrease in operation time. On the other hand, with regard to the influence of silicone oil concentration, this one produces negligible changes on the absorption kinetics.

### 4.2.3. Conclusions

Present work has analysed the influence of insoluble organic substances upon mass transfer coefficient in gas-liquid absorption without chemical reaction, in the presence and absence of surfactant, and using a bubble column contactor. The presence of solutes (Tween80, silicone oil S1 and silicone oil S2) produces a decrease in the volumetric and mass transfer coefficient. In the absence of surfactant to stabilize the emulsion a fast reduction in mass transfer coefficient is obtained at low organic concentration until reach a constant value. On the other hand the presence of surfactant remove the effect of organic phase shown a low and constant mass transfer coefficient. The influence of surfactant distribution at different interfaces (gas-liquid and liquid-liquid) plays an important role in mass transfer process. Also, the fact that silicone oil S1 produces small bubbles has a negative effect upon mass transfer coefficient because small bubbles are considered rigid ones, with a higher resistance to transport.

A modification of Sardeing's model allows fit experimental data for Tween80, taken into account the values corresponding to mobile a rigid bubbles, and the special characteristics (in relation with its surface activity) of Tween80.

Besides, the influence of these substances (Tween80, silicone oil S1 and silicone oil S2) upon the carbon dioxide absorption rate in the presence of glucosamine and pyrrolidine has also been analyzed. With regard to glucosamine, the highest absorption rate corresponds to the system in presence of both silicone oil S1 and surfactant. After several studies, the impurities

present in the surfactant are thought to affect the chemical reaction and produce some type of catalytic effect upon the reaction mechanism.

For the systems with pyrrolidine, because it is an absorption regime very fast, the presence of surface active substance does not produce changes upon the results obtained for the absorption process with chemical reaction. The presence of silicone oil produces a decrease in the absorption rate and this reduction is higher if the surfactant is present, since the surfactant is present in all phases and interphases, hindering in the whole cases the gas mass transfer through the liquid phase.

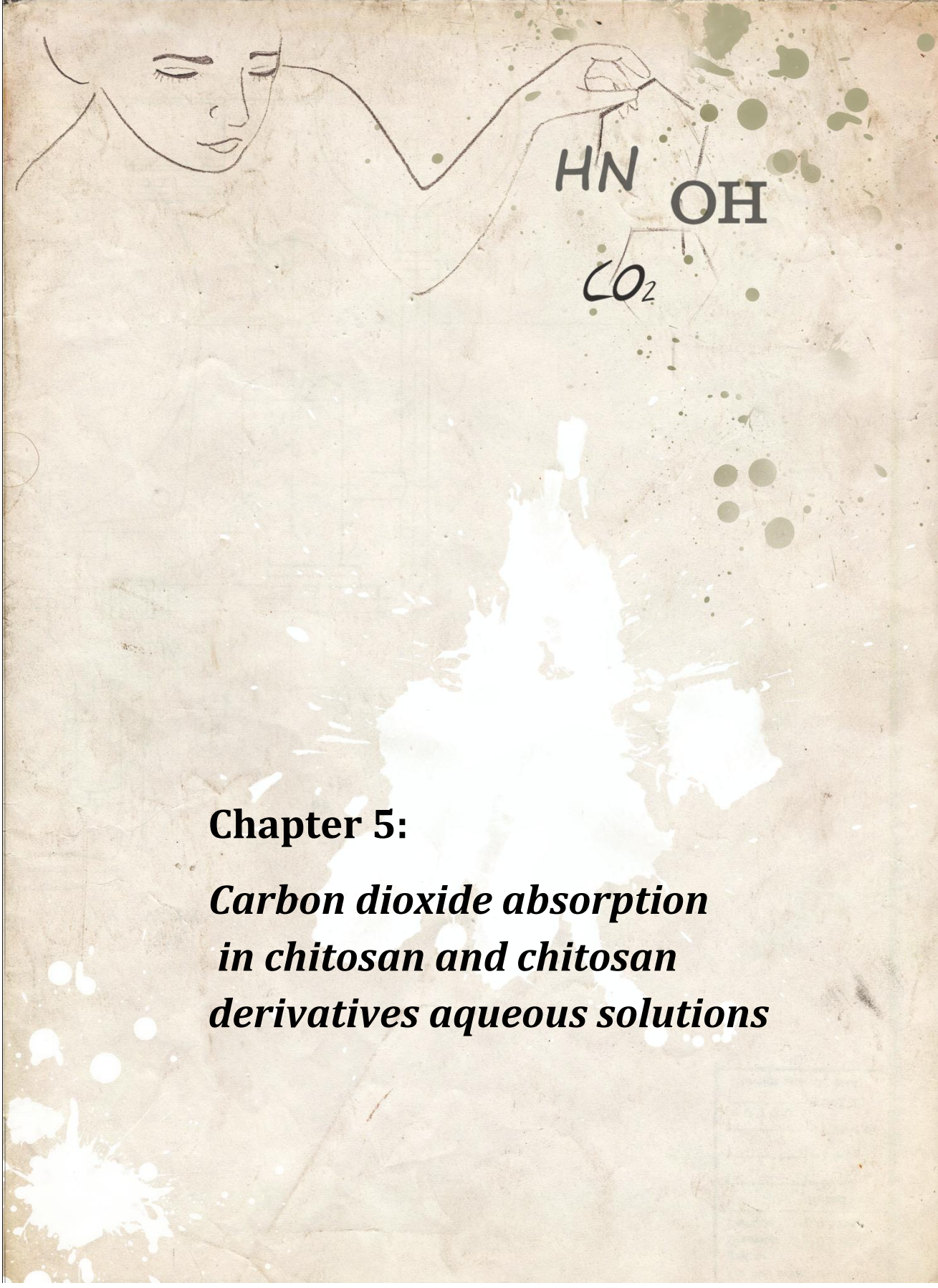


# Chapter 5:

## *Carbon dioxide absorption in chitosan and chitosan derivatives aqueous solutions*

# 5.1 Polymers physico-chemical characterization

*Abstract*

*This work includes in present chapter the analysis and evaluation of chitosan-based polymers in aqueous solution to capture carbon dioxide from a gaseous stream by means of physical or chemical absorption.*

*Then, this research includes the synthesis of soluble polymers from chitosan (materials and methods section) to improve the solubility value and their characterization in relation with important parameters: synthesis optimization and physico-chemical characterization, in absorption processes (Fourier transform infrared spectroscopy, elemental analysis, deacetylation degree, intrinsic viscosity and average molecular weight, rheological behaviour and surface behaviour).*

## 5.1.1. Specific introduction

The development of new systems for carbon dioxide capture has been the aim of numerous studies in the last few years involved in gas absorption processes. Different systems based on the use of amines with different amino groups[307] or the mixture of different amines[308,309] have been the research field of several teams to improve the efficiency of the process and also, to reduce the associate costs of this operation. In relation with the first field (the presence of a higher number of amino groups in the molecule) the aim is to reach a higher carbon dioxide loading and then, a gas-liquid contactor could treat a higher gas flow-rate or could reduce the size of the equipment.

In relation with the use of blends of different amines, the improvement produced upon the absorption process is centred in the reduction in the degradation produced in the regeneration step. This improvement in the global process implies a decrease in the cost of the process by a reduction in amine solution make up flow.

In the last years our research team has developed a system for carbon dioxide absorption by chemical reaction using glucosamine aqueous solutions, and this system has shown suitable results for this aim (carbon dioxide capture) because the chemical absorption rate takes similar or higher values than conventional systems[310].

On the other hand, this system produces important improvements and these advantages are fundamentally a minor need of safety measurements and a minor chemical risk when aqueous solutions of glucosamine are manipulated. Present work tries increase the knowledge about the use of polymers based in glucosamine monomer, chitosan and its derivates.

A difficulty associate to the research aim is the fact that the chitosan shows a very low solubility in water. The solubility of this polymer increases with the presence of acid medium

[307] Cullinane J. T., Rochelle G. T. Kinetics of carbon dioxide absorption into aqueous potassium carbonate and piperazine. *Industrial & Engineering Chemistry Research* 2006, 45, 2531-2545 .
[308] Mandal B. P., Bandyopadhyay S. S. Absorption of carbon dioxide into aqueous blends of 2-amino-2-methyl-1-propanol and monoethanolamine. *Chemical Engineering Science* 2006, 61, 5440-5447.
[309] Subham P., Aloke K. G.; Bishnupada M. Kinetics of absorption of carbon dioxide into aqueous blends of 2-(1-piperazinyl)-ethylamine and N-methyldiethanolamine. *Chemical Engineering Science* 2009, 64, 1618-1622.
[310] Gómez-Díaz D., Navaza J. M. Kinetics of carbon dioxide absorption into aqueous glucosamine solutions. *AIChE Journal* 2008, 54, 321-326.

[311,312]. This fact implies an important limitation for the use of this kind of aqueous solutions for carbon dioxide chemical absorption because the acid medium produces the inhibition of chemical reaction between the amino group and the absorbed carbon dioxide.

## 5.1.2. Results and Discussion

### *5.1.2.1. Fourier transform infrared spectroscopy*

Chitosan (C): The FT-IR spectrum corresponding to chitosan (figure 5.2) shows characteristic bands corresponding to this molecule[313,314]. At 3435 $cm^{-1}$ and 3286 $cm^{-1}$ the O-H stretch and $-NH_2$ group appear, respectively. Also, is possible appreciate the bands corresponding to the C–H group at 2892 $cm^{-1}$. At 1640 $cm^{-1}$ the amide band corresponding to C-O stretch of acetyl group appears and at 1567 $cm^{-1}$ it is possible to observe the amide band corresponding to the N-H stretch.

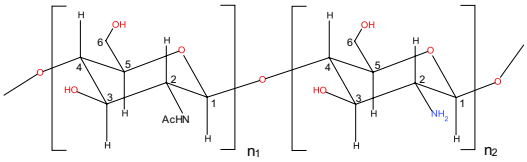


Figure 5.1. Chitosan chemical structure

[311] Miao J., Chen G., Gao C., Lin C., Wang D., Sun M. Preparation and characterization of N,O-carboxymethyl chitosan (NOCC)/polysulfone (PS) composite nanofiltration membranes. *Journal of Membrane Science* 2006, 280, 478–484.
[312] Mansur Y., Laurence D. H. Some chemical and analytical aspects of polysaccharide modification. *Macromolecules* 1984, 17, 272.
[313] Singh J., Dutta P. K., Dutta J., Hunt A. J., Macquarrie D. J., Clark J. H. Preparation and properties of highly soluble chitosan–L-glutamic acid aerogel derivative. *Carbohydrate Polymers* 2009, 76, 188–195.
[314] Balanta D., Grande C. D., Zuluaga F. Extracción, identificación y caracterización de quitosano del micelio de aspergillus niger y sus aplicaciones como material bioadsorbente en el tratamiento de aguas. *Revista Iberoamericana de Polímeros* 2010, 11(5), 297-316.

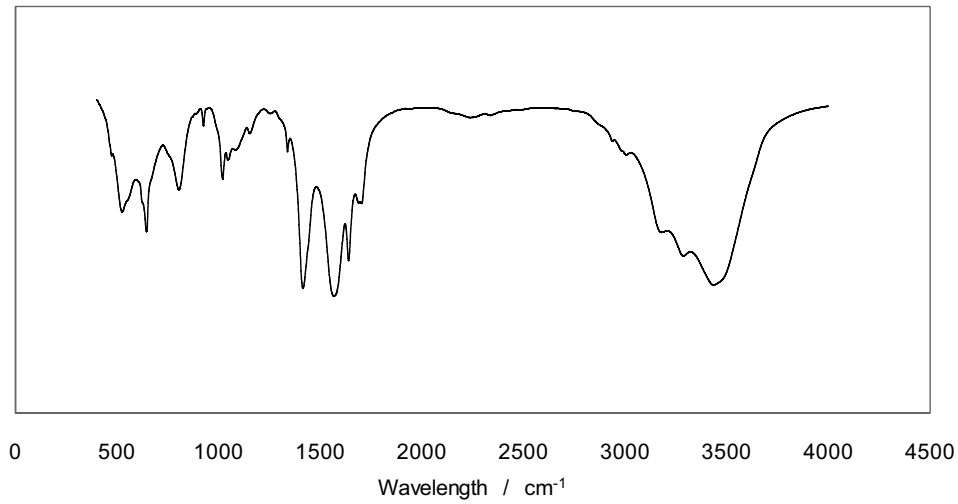


Figure 5.2. FT-IR spectrum corresponding to chitosan.

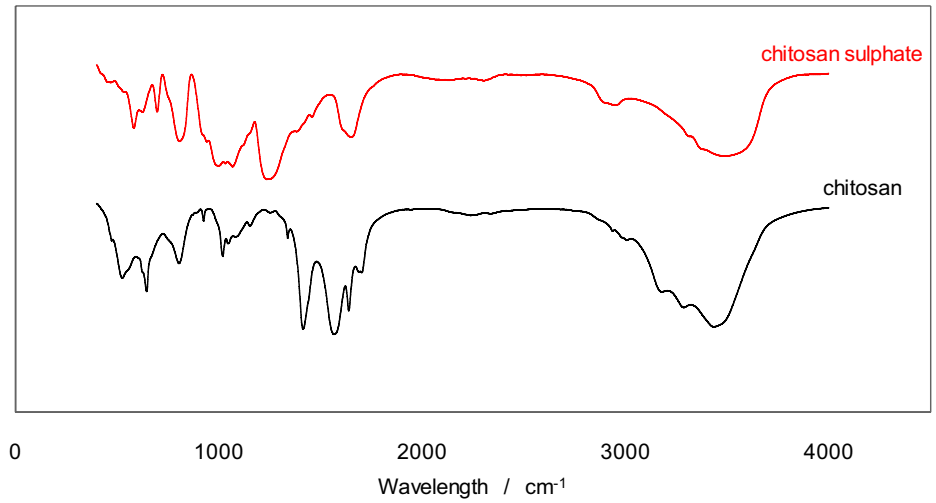


Figure 5.3. FT-IR spectrum corresponding to chitosan and chitosan sulphate.

Chitosan sulphate (CS): FT-IR spectrum corresponding to CS (figure 5.3) showed the appearance of characteristic S=O and S–O bond-stretching absorptions at 1235, 1068, and 807 $cm^{-1}$, respectively, consistent with the sulfonation of chitosan[315].

Carboxymethyl chitosan (CC): The IR spectra of chitosan and carboxymethyl chitosan are shown in figure 5.4. In particular, the spectrum of CC shows the band at 1629 $cm^{-1}$, which can be attributed to the carboxylation. Additionally, the formation of CC is also confirmed by the intensification of the band at 1073 corresponding to C-O-C stretching. The band at 3428 $cm^{-1}$ becomes wider and weaker, which suggests that the carboxylation occurred on some of both the amino and primary hydroxyl sites of the glucosamine units of the chitosan structure[316].

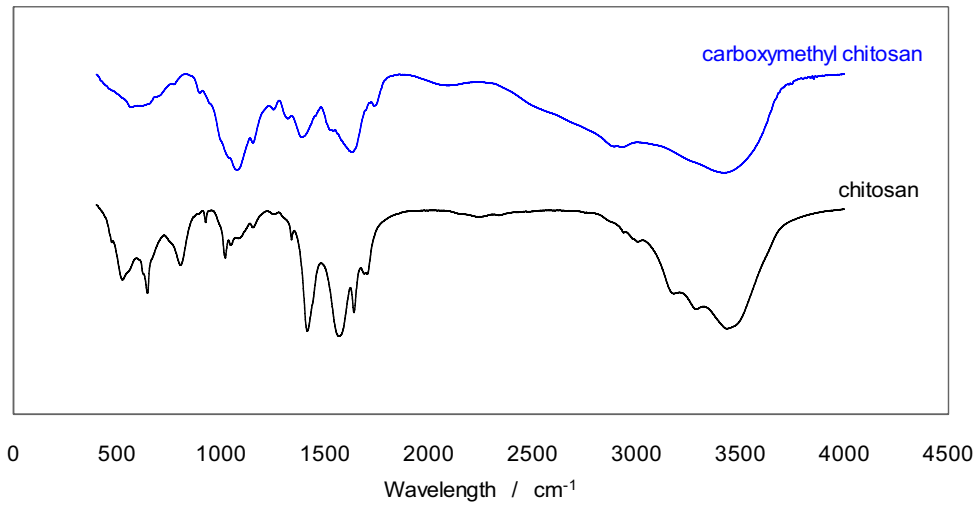


Figure 5.4. FT-IR spectrum corresponding to chitosan and carboxymethyl chitosan.

[315] Suwan J., Zhang Z., Li B., Vongchan P., Meepowpan P., Zhang F., Mousa S. A., Premanode B., Kongtawelert P., Linhardt R. J. Sulfonation of papain-treated chitosan and its mechanism for antiacoagulant activity. *Carbohydrate Research* 2009, 344, 1190-1196.

[316] Miao J., Chen G., Gao C., Lin C., Wang D., Sun M. Preparation and characterization of N,O-carboximethyl chitosan (NOCC)/polysulfone (PS) composite nanofiltration membranes. *Journal of Membrane Science* 2006, 280, 478-484.

### *5.1.2.2. Elemental analysis*

Table 5.1 shows the experimental results for elemental analysis of polymers employed in this work (C, CS and CC). The values obtained for chitosan are similar than the previously published by other authors[317].

Table 5.1. Elemental analysis for different polymers employed in present work.

| Sample | % C | % H | % N | % S |
|---|---|---|---|---|
| C | 39.7 | 6.8 | 7.3 | 0 |
| CS | 25.0 | 4.5 | 4.2 | 6.2 |
| CC | 37.3 | 6.9 | 6.1 | 0 |

In relation with the results obtained for the others polymers, and taking into account that the aim of the inclusion of different functional groups is related with the enhancement of chitosan solubility in water, table 5.1 shows the changes in the elemental analysis for modified polymers in relation with original chitosan.

The values for the chitosan sulphate (CS) show the inclusion of sulphur in the polymer structure, obtaining a similar incorporation than previous works that have used a similar synthesis procedure[317]. On the other hand, for carboxymethyl chitosan (CC) a reduction in the quantity of carbon and nitrogen atoms is observed that could be caused by the inclusion of oxygen. Taken into account these experimental results, it is possible to conclude that the inclusion of the functional groups is produced in both cases.

### *5.1.2.3. Deacetylation degree*

Figure 5.5 shows the different titration curves for each polymer that allow to calculate the deacetylation degree on the basis of inflection points' situation. The values of sodium hydroxide volumes corresponding to these points have been calculated using the first derivate criterion that is shown in figure 5.5. Table 5.2 shows the final value determined for the amino content of each polymer.

[317] Ríos-Donato N., Navarro-Mendoza R., Ávila-Rodríguez M., Mendizábal-Mijares E. Obtención de sulfato de quitosano y su aplicación en el proceso de coagulación-floculación de suspensiones coloidales aniónicas de caolinita. *Revista Iberoamericana de Polímeros* 2006, 7, 145-161.

Table 5.2. Deacetylation degree of polymers used in present work

| Sample | $\%NH_2$ |
|---|---|
| C | 67.5 |
| SC | 0 |
| CC | 67.5 |

Figure 5.5-C corresponds to experimental data for original chitosan and in this plot is possible observes that the first inflection point is reached in a change of pH from values near to initial until near to 6. The second change in this variable is produced until pH=12. This behaviour for the original chitosan is similar than the observed for the carboxymethyl chitosan (figure 5.5-CC) but with important differences in relation with the corresponding behaviour for chitosan sulphate (see figure 5.5-SC).

In the last case, a second inflection point is not observed and the change is produced from the initial pH to a value near to 12. Taken into account this behaviour the non-existence of free amino groups is concluded for CS. This result is in disagreement with previous studies[318] that is using the same synthesis procedure to produce the substitution of sulphate group in hydroxide and amino groups but not with a 100% of substitution.

On the other hand, other studies[319] show also the inclusion of sulphate group in both kind of centres with a 100 % of inclusion (see figure 5.6) that is in agreement with the results obtained in present work.

[318] Gamzazade A., Sklyar A., Nasibov S., Sushkov I., Shashkov A., Knirel Y. Structural features of sulfated chitosans. *Carbohydrate Polymers* 1997, 34, 113-116.
[319] Suwan J., Zhang Z., Li B., Vongchan P., Meepowpan P., Zhang F., Mousa S. A., Premanode B., Kongtawelert P., Linhardt R. J. Sulfonation of papain-treated chitosan and its mechanism for antiacoagulant activity. *Carbohydrate Research* 2009, 344, 1190-1196.

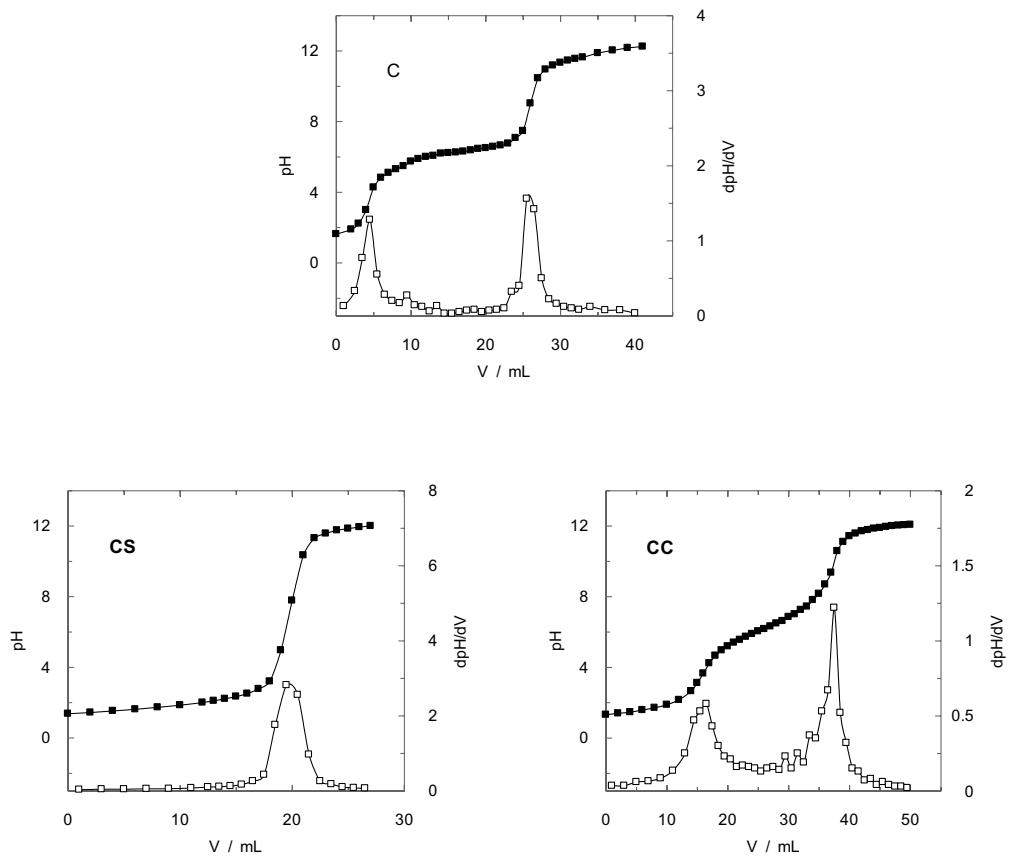


Figure 5.5. Titration curves for deacetylation percentage determination.

The behaviours commented in relation with the titration curves shown in figure 5.5 allow to calculate the polymers deacetilation degree using equation A.3 (see material and methods section), that are shown in table 5.2. For carboxymethyl chitosan (CC) the percentage of free amino groups remains constant regards the original chitosan (C) that indicates that the carboxylic group is included in the hydroxilic centres (3 and 6 carbons) or in the acetylated amino

group, in agreement with previous studies[320]. In relation with the chitosan sulphate, free amino groups do not exist.

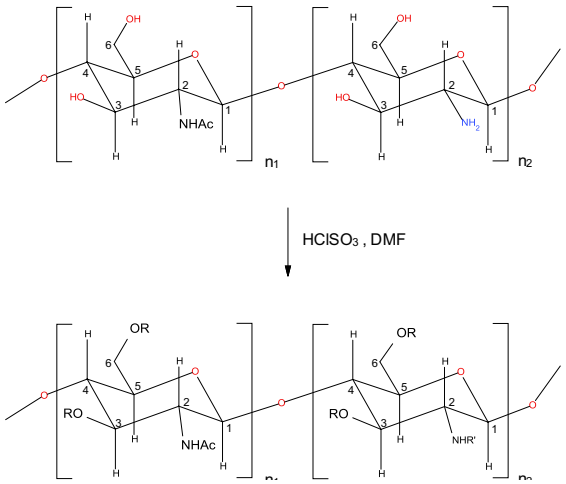


Figure 5.6. Sulfatation reaction of chitosan, where R' = $NaSO_3$ and R = H or $NaSO_3$. $n_1$ = 0.325 y $n_2$ = 0.675.

### *5.1.2.4. Intrinsic viscosity and average molecular weight*

The molecular weight of the polymers employed in this study was unknown so, in order to characterize these polymers, the average molecular weight has been calculated. To do this, it was necessary to determine the intrinsic viscosity obtained by a combined application of Huggins and Kramer equations (equation 5.1 and 5.2). A similar procedure has been employed by different authors[321,322].

[320] Miao J., Chen G., Gao C., Lin C., Wang D., Sun M. Preparation and characterization of N,O-carboxymethyl chitosan (NOCC)/polysulfone (PS) composite nanofiltration membranes. *Journal of Membrane Science* 2006, 280, 478–484.
[321] Chuah H. H., Lin-Vien D., Soni U. Poly(trimethylene terephthalate) molecular weight and Mark–Houwink equation. *Polymer* 2001, 42, 7137–7139.
[322] Ma X., Pawlik M. Intrinsic viscosities and Huggins constants of guar gum in alkali metal chloride solutions. *Carbohydrate Polymers* 2007, 70, 15–24.

$$\frac{\eta_{sp}}{C} = [\eta] + k_1 \cdot [\eta]^2 \cdot C \tag{5.1}$$

$$\frac{\ln \eta_r}{C} = [\eta] + k_2 \cdot [\eta]^2 \cdot C \tag{5.2}$$

where $\eta_{sp} = \frac{(\eta - \eta_s)}{\eta_s}$, $\eta_r = \frac{\eta}{\eta_s}$ are the specific and relative viscosities and, $\eta$ and $\eta_s$ are the viscosities of the solution and the solvent, respectively. To calculate the viscosity it is necessary to know the kinematic viscosity (ν) and density (ρ). The absolute viscosity has been calculated using equation 5.3.

$$\eta = \nu \cdot \rho \tag{5.3}$$

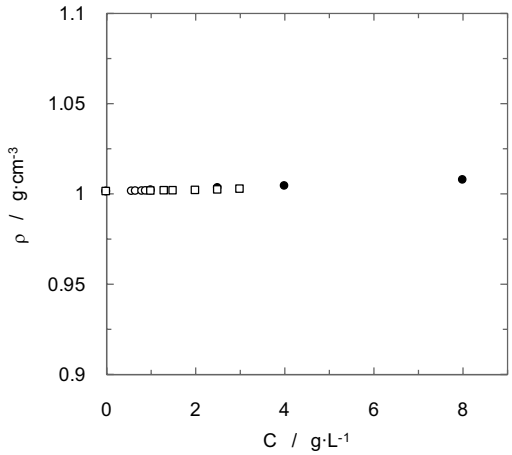


Figure 5.7. Influence of polymer concentration upon density. (○) Chitosan, (●) Chitosan sulphate, (□) Carboxymethyl chitosan.

Different concentrations of chitosan, chitosan sulphate and carboximethyl chitosan in sodium chloride aqueous solution were prepared to obtain relative viscosities in a range of 1.2 to 1.6 to assure a good accuracy and linearity of extrapolation to zero concentration.

The density of polymers aqueous solutions has been settled in order to determine the absolute viscosity from the kinematic viscosity values. The behaviour obtained (see figure 5.7) might indicate slight interactions among the polymer-solvent and polymer-polymer molecules.

Figure 5.8 shows the experimental data obtained for the combined use of Huggins and Kramer equations for all the polymers, on the basis of calculated values of viscosity using kinematic viscosity and density data. For these equations the intercept in these plots correspond with the intrinsic viscosity for each polymer. The good quality of the experimental data is confirmed by the agreement of both linear regressions at zero polymer concentration.

The calculated data for intrinsic viscosity for each polymer are shown in table 5.3. The intrinsic viscosity indicates the effective specific volume of one isolate polymer and for this reason this measurement must be developed by extrapolation at infinite dilution. This value depends to the size and shape of molecule and also the interactions with solvent and work temperature.

The molecular weight was determined using the corresponding Mark-Houwink equation (equation 5.4) and the value of intrinsic viscosity. The Mark-Houwink constants for these polymers were obtained from literature and the value of these parameters and calculated value of average molecular weight are included in table 5.3.

$$[\eta] = K \cdot M_w^a \tag{5.4}$$

Tabla 5.3. Intrinsic viscosity, Mark-Houwink constants and average molecular weight of chitosan (C), chitosan sulphate (CS) and carboxymethyl chitosan (CC).

| Muestra | [η] / mL·g$^{-1}$ | K | a | $M_w$ / g·mol$^{-1}$ |
|---|---|---|---|---|
| C | 607 | $1.81 \cdot 10^{-3}$ [323] | 0.93 [323] | $8.74 \cdot 10^{5}$ |
| SC | 9 | $1.75 \cdot 10^{-5}$ [324] | 0.98 [324] | $6.73 \cdot 10^{5}$ |
| CC | 324 | $7.92 \cdot 10^{-5}$ [325] | 1 [325] | $4.32 \cdot 10^{6}$ |

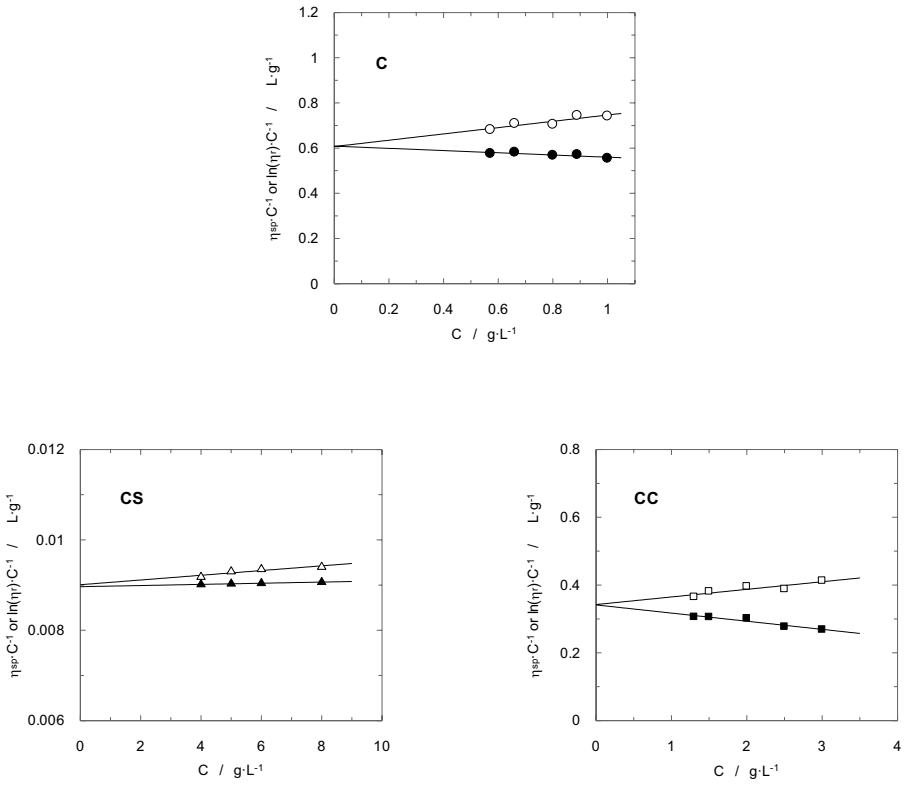


Figure 5.8. Intrinsic viscosity determination for chitosan and chitosan-based polymers.

[323] Maghami G., Roberts G. Evaluation of the viscometric constants for chitosan. *Makromolecular Chem*istry and Physics 1988, 189, 195-200.
[324] Vongchan P., Sajomsang W., Subyen D., Kongtawelert P. Anticoagulant activity of a sulfated chitosan. *Carbohydrate Research* 2002, 337(13), 1239-1242.
[325] Ibrahim M. E., Hugh D. C. S. Poly(ethylene glycol)–carboxymethyl chitosan-based pH-responsive hydrogels: photo-induced synthesis, characterization, swelling, and in vitro evaluation as potential drug carriers. *Carbohydrate Research* 2010, 345, 2004–2012.

In relation to the carboxymethyl chitosan, an increase in the molecular weight is observed regards the value corresponding to the chitosan employed in the synthesis. Different calculus indicates that this phenomenon is due to the contribution in the molecular weight caused by the included group. On the other hand, for chitosan sulphate, the opposite behaviour is observed, a decrease in the molecular weight in comparison with the chitosan. This different behaviour is due to the fact that the reaction between chlorosulphonic acid produces an aggressive chemical reaction with chitosan that causes the rupture of polymer chains, in agreement with previous studies[326] that observes a decrease of molecular weight near to 99% when the chemical reaction between these compounds was performed during 5 hours. In present work the chemical reaction was performed during only 1 hour, and for this reason, the reduction in the molecular weight was low.

#### *5.1.2.5. Rheological behaviour*

In present section the flow behaviour of different aqueous solutions corresponding to the polymers previously analysed under different points of view, has been studies taking into account the special importance of this physical property upon the mass transfer processes and mainly upon gas-liquid absorption[327,328].

Chitosan: The rheological behaviour of aqueous solutions of chitosan (C), chitosan sulphate (CS) and carboxymethyl chitosan (CC) have been analysed on the basis of the influence of shear rate applied to the samples upon the apparent viscosity and shear stress. In relation with chitosan aqueous solutions, due to the low solubility of this polymer in aqueous solution, the solvent employed was an acetic acid aqueous solution (1% $_{v/v}$).

[326] Suwan J., Zhang Z., Li B., Vongchan P., Meepowpan P., Zhang F., Mousa S. A., Premanode B., Kongtawelert P., Linhardt R. J. Sulfonation of papain-treated chitosan and its mechanism for antiacoagulant activity. *Carbohydrate Research* 2009, 344, 1190-1196.
[327] Álvarez E., Sanjurjo B., Cancela A., Navaza J. M. Mass transfer and influence of physical properties of solutions in a bubble column. *Chemical Engineering Research and Design* 2000, 78, 889-893.
[328] Jiao Z., Xueqing Z., Juntag Y. $O_2$ Transfer to pseudoplastic fermentation broths in air-lift reactors with different inner designs. *Biotechnology Techniques* 1998, 12, 729-732.

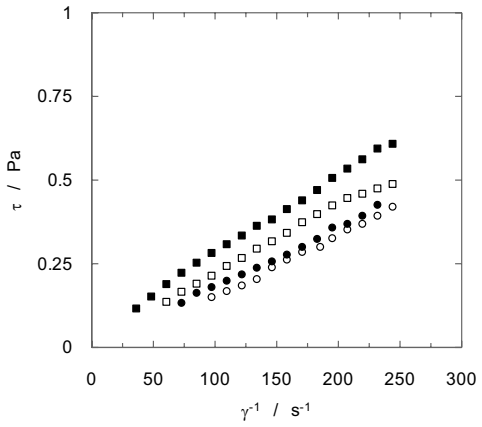


Figure 5.9. Effect of shear rate upon shear stress for chitosan aqueous solutions (○) $C_C$ = 0.4 g·L$^{-1}$; (●) $C_C$ = 1 g·L$^{-1}$; (□) $C_C$ = 2 g·L$^{-1}$; (■) $C_C$ = 4 g·L$^{-1}$.

Figure 5.9 shows the influence of shear rate upon shear stress observing that an increase in shear rate produces an increase to in the value of shear stress, which is a common behaviour in this kind of aqueous solutions.

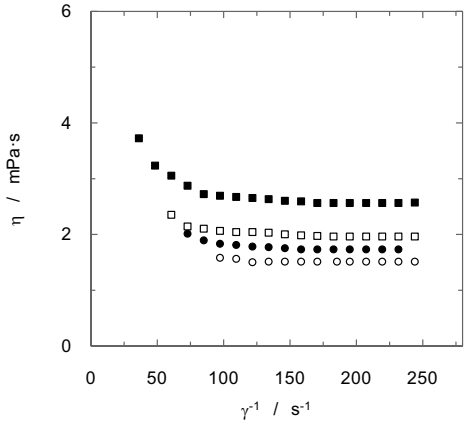


Figure 5.10. Effect of shear rate upon apparent viscosity for chitosan aqueous solutions. (○) $C_C$ = 0.4 g·L$^{-1}$; (●) $C_C$ = 1 g·L$^{-1}$; (□) $C_C$ = 2 g·L$^{-1}$; (■) $C_C$ = 4 g·L$^{-1}$.

The influence of shear rate upon apparent viscosity is shown in figure 5.10 that shows a decrease in this variable when shear rate increases. This behaviour is clearer at low values of shear rate until reach a practically constant value in the viscosity. Taking into account the results show in figure 5.10 the behaviour observed for aqueous solutions of chitosan shows a non-Newtonian flow included in the pseudoplastic fluids because a decrease in the value of viscosity is observed when the shear rate increases. This behaviour is in agreement with previous studies[329,330] that have employed chitosan in aqueous solution. To confirm this behaviour the power law (equation 5.5) has been used to fit the experimental data and more specifically the influence of shear rate upon shear stress.

$$\tau = k \cdot \dot{\gamma}^{n} \tag{5.5}$$

where $\tau$ is the shear stress, $\gamma$ is the shear rate, *k* and *n* are the consistency and behaviour indices.

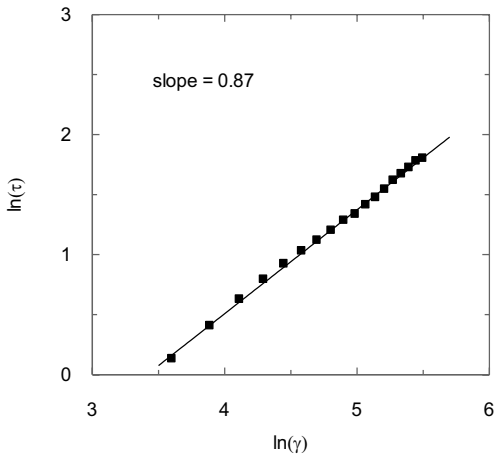


Figure 5.11. Power law fit results for chitosan aqueous solution. $C_C$ = 4 g·L$^{-1}$.

Figure 5.11 shows the power law behaviour in relation with the experimental data at a fix polymer concentration, which is considered suitable, with low deviations. Also figure 5.11 shows

[329] Cho J., Heuzey M.-C., Beégin A., Carreau P. J. Viscoelastic properties of chitosan solutions: Effect of concentration and ionic strength. *Journal of Food Engineering* 2006, 74, 500–515.
[330] Mucha M. Rheological properties of chitosan blends with poly(ethyleneoxide) and poly(vinyl alcohol) in solution. *Reactive & Functional Polymers* 1998, 38, 19–25.

the value of the slope that corresponds with the behaviour index and takes a value minor than 1. For behaviour index values minor than 1 have been obtained for all the chitosan aqueous solutions. This fact confirms the conclusion previously reached: chitosan aqueous solutions have a non-Newtonian and pseudoplastic behaviour.

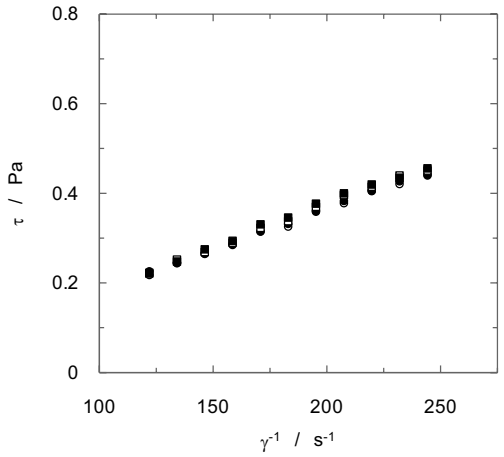


Figure 5.12. Effect of shear rate upon shear stress for chitosan sulphate aqueous solutions (○) $C_{CS}$ = 0.4 g·L$^{-1}$; (●) $C_{CS}$ = 1 g·L$^{-1}$; (□) $C_{CS}$ = 2 g·L$^{-1}$; (■) $C_{CS}$ = 4 g·L$^{-1}$.

Chitosan sulphate: For aqueous solutions of chitosan sulphate, figure 5.12 shows the behaviour corresponding to the influence of shear rate upon shear stress and a similar behaviour is observed for all the concentrations employed in this study. This fact indicates that the effect of chitosan sulphate has non-influence upon the rheological behaviour, in the analysed composition range.

On the other hand and in relation with the influence of shear rate upon apparent viscosity (figure 5.13), the low influence of polymer concentration is observed again but a slight increase in the value of viscosity with polymer concentration is obtained. Non influence of shear rate upon apparent viscosity is observed and this behaviour indicates that these aqueous solutions are included in Newtonian fluids. In comparison with the previously commented behaviour for chitosan aqueous solutions, lower values of viscosity are obtained and this behaviour could be related with a better spatial distribution, confirmed by a minor value in the intrinsic viscosity of this polymer previously commented.

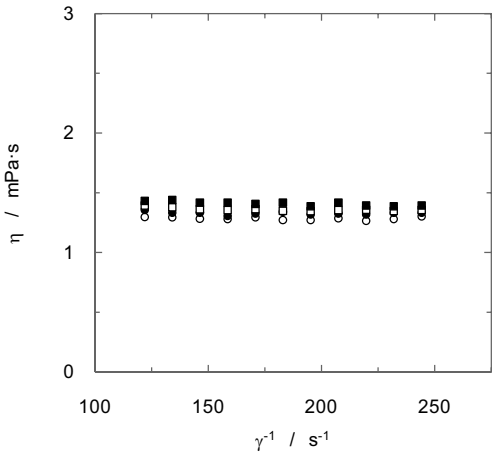


Figure 5.13. Effect of shear rate upon apparent viscosity for chitosan sulphate aqueous solutions (○) $C_{CS}$ = 0.4 g·L$^{-1}$; (●) $C_{CS}$ = 1 g·L$^{-1}$; (□) $C_{CS}$ = 2 g·L$^{-1}$; (■) $C_{CS}$ = 4 g·L$^{-1}$.

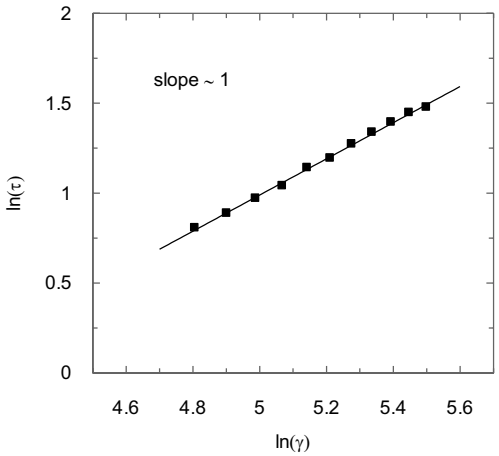


Figure 5.14. Power law fit results for chitosan sulphate aqueous solution. $C_{CS}$ = 1 g·L$^{-1}$.

Using the experimental values of shear stress-shear rate data for the different aqueous solutions, and using the power law to fit this kind of experimental data, figure 5.14 shows a

suitable fit, and also, the slope of this plot shows a value near to 1 that allows to conclude the Newtonian behaviour of these solutions, without influence of shear rate upon the value of viscosity.

Carboxymethyl chitosan: The same procedure that the employed for chitosan and chitosan sulphate has been developed for aqueous solutions of carboxymethyl chitosan. Then in a first moment the influence of shear rate upon shear stress and apparent viscosity have been analysed (see figures 5.15 and 5.16).

Taking into account the observed behaviours, mainly in relation with the influence of shear rate upon apparent viscosity, a different behaviour than the previously one commented for the chitosan sulphate is observed. Then an increase in the shear rate produces an important decrease in the apparent viscosity. For this reason the carboxymethyl chitosan aqueous solutions are included in the non-Newtonian and pseudoplastic fluids.

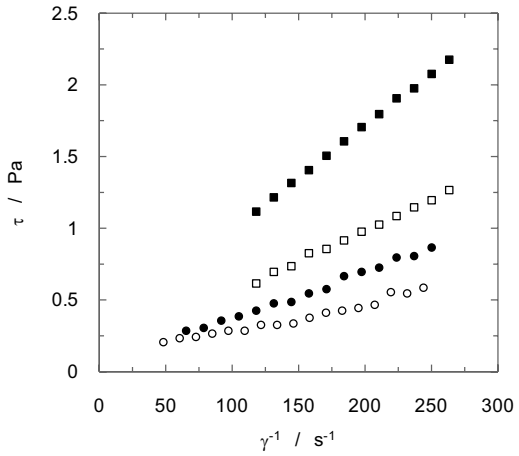


Figure 5.15. Effect of shear rate upon shear stress for carboxymethyl chitosan aqueous solutions (○) $C_{CC}$ = 0.4 g·L$^{-1}$; (●) $C_{CC}$ = 1 g·L$^{-1}$; (□) $C_{CC}$ = 2 g·L$^{-1}$; (■) $C_{CC}$ = 4 g·L$^{-1}$.

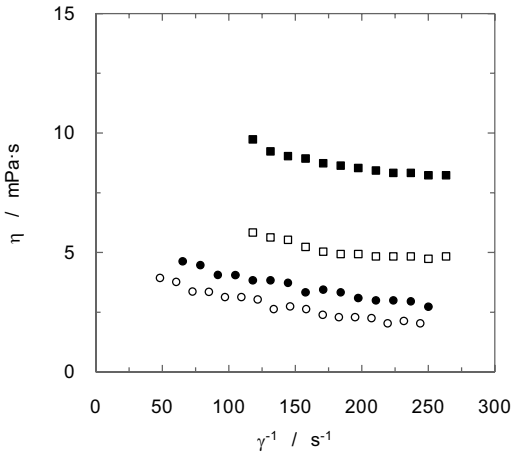


Figure 5.16. Effect of shear rate upon apparent viscosity for carboxymethyl chitosan aqueous solutions (○) $C_{CC}$ = 0.4 g·L$^{-1}$; (●) $C_{CC}$ = 1 g·L$^{-1}$; (□) $C_{CC}$ = 2 g·L$^{-1}$; (■) $C_{CC}$ = 4 g·L$^{-1}$.

The use of power law equation to fit experimental data confirms the behaviour of previously commented: non-Newtonian and pseudoplastic, because the behaviour index takes values minor than 1 (see figure 5.17) for all the experimental conditions.

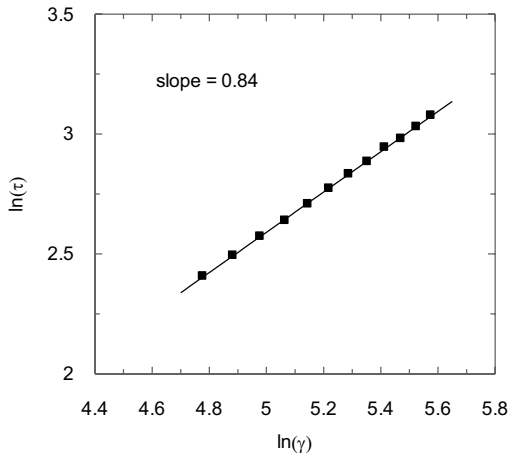


Figure 5.17. Power law fit results for chitosan sulphate aqueous solution. $C_{CC}$ = 2 g·L$^{-1}$.

### *5.1.2.6. Surface behaviour*

Other interesting physical property with high importance in mass transfer processes is the surface tension due to the special influence upon gas-liquid interface, mainly in solutions that involve the presence of amphiphilic solutes (i. e. surfactants)[331,332]. Changes in this property could produce modifications in bubble size distribution and effects upon mass transfer rate due to molecules accumulation at gas-liquid interface.

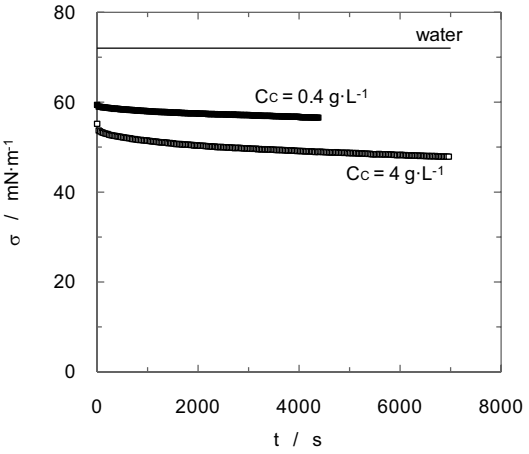


Figure 5.18. Time evolution of surface tension in chitosan aqueous solutions.

Figure 5.18 shows the surface tension of chitosan aqueous solutions and the first conclusion is that the value of this physical property shows a slow dynamic and then this property changes its value along the time until reach a constant value. Different studies have obtained experimental results in agreement with present data for aqueous solutions of different polymers[333,334,335].

[331] Rosu M., Marlina A., Kaya A., Schumpe A. Surfactant adsorption onto activated carbon and its effect on absorption with chemical reaction. *Chemical Engineering Science* 2007, 62, 7336-7343.
[332] RossoD., Huo D. L., Stenstrom M. K. Effects of interfacial surfactant contamination on bubble gas transfer. *Chemical Engineering Science* 2006, 61, 5500–5514.
[333] Nahringbauer I. J. Dynamic surface tension of aqueous polymer solutions, I: Ethyl(hydroxyethyl)cellulose (BERMOCOLL cst-103). *Colloid Interface Science* 1995, 176, 318-328.
[334] Gau C.-S., Yu H., Zografi G. Surface viscoelasticity of hydroxypropyl cellulose and hydroxyethyl cellulose monolayers at the air/water interface. *Macromolecules* 1993, 26, 2524.
[335] Makri E. A., Doxastakis G. I. Surface tension of phaseolus vulgaris and coccineus proteins and effect of polysaccharides on their foaming properties. *Food Chemistry* 2007, 101, 37–48.

This surface tension dynamics is due to the complex behaviour of this kind of substances in aqueous solution and at the gas-liquid interface. An example of the supposed behaviour at gas-liquid interface of this kind of systems is shown in figure 5.19[336]. Taking into account this behaviour, the conformational changes in the polymer chains produce modifications in the surface tension along the time. The same behaviour has been found for the other polymers used in present work (see figure 5.20), but certain differences exist regards the surface tension magnitude for carboxymethyl chitosan aqueous solutions in comparison with aqueous solutions of chitosan and chitosan sulphate. Carboxymethyl chitosan aqueous solutions produce similar values than pure water.

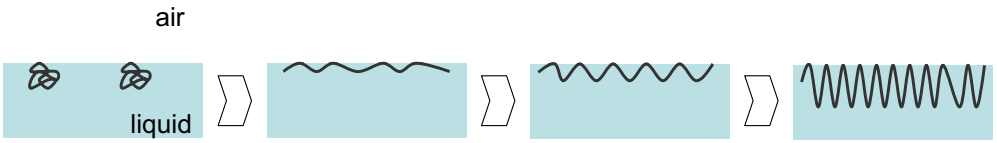


Figure 5.19. Hypothetical polymer conformation at the air-liquid interface[336].

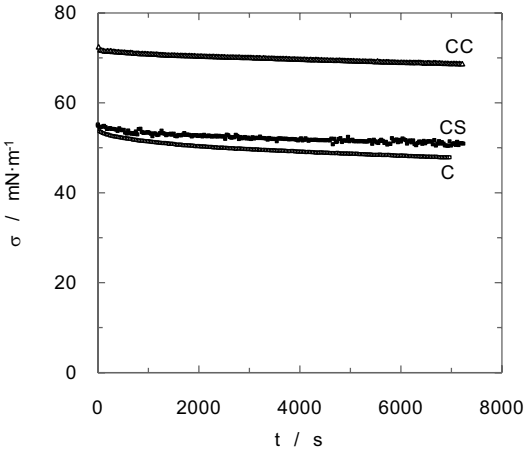


Figure 5.20. Influence of time upon surface tension in aqueous solutions of chitosan (C), chitosan sulphate (CS) and carboxymethyl chitosan (CC). $C_p$ = 4 g·L$^{-1}$.

[336] Nahringbauer I. Polymer-surfactant interaction as revealed by the time dependence of surface tension. The EHEC/SDS/Water system. *Langmuir* 1997, 13, 2242-2249.

On the other hand, figure 5.21 shows the effect caused by the polymers concentration upon the surface tension value obtained at equilibrium. This figure confirms the behaviour previously described at figure 5.20 (for the highest polymer concentration). Aqueous solutions of carboxymethyl chitosan take always higher values for surface tension than the corresponding ones for the other polymers, which show similar behaviour.

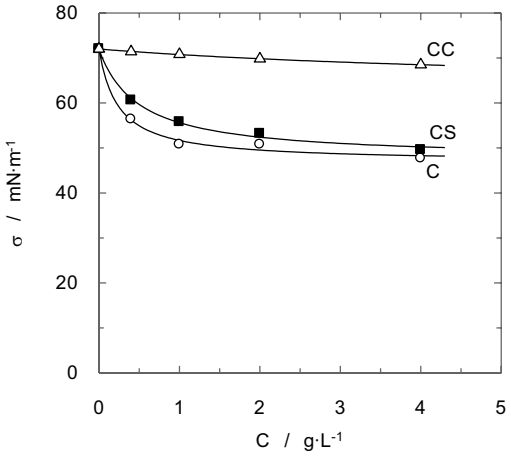


Figures 5.21. Influence of polymers concentration upon surface tension.

In all cases, when polymer concentration increases in the liquid phase, a decrease in the value of surface tension is observed, caused by the increase in the polymer presence at the gas-liquid interface. A similar behaviour in relation with the influence of polymer concentration has been found by different researchers[337,338]. Specifically for aqueous solutions of chitosan and chitosan sulphate a decrease in the value of surface tension is produced when polymer concentration increases until reach a constant value of this property due to the saturation of the interface with polymer molecules that not allow to increase the surface polymer concentration.

[337] Nahringbauer I. Polymer-surfactant interaction as revealed by the time dependence of surface tension. The EHEC/SDS/Water system. *Langmuir* 1997, 13, 2242-2249.
[338] Fainerman V. B., Lylyk S. V., Ferri J. K., Miller R., Watzke H., Leser M. E., Michel M. Adsorption kinetics of proteins at the solution/air interfaces with controlled bulk convection. *Colloids and Surfaces A: Physicochemical and Engineering Aspects* 2006, 282-283, 217-221.

### 5.1.3. Conclusions

In present work, soluble polymers (chitosan sulphate and carboxymethyl chitosan) have been synthesized form chitosan (see material and methods section) and subsequently characterized. Taken into account the experimental results (Fourier transform infrared spectroscopy and elemental analysis) it is possible to conclude that the inclusion of the functional groups is produced in both cases.

The deacetylation degree indicates that the inclusion of sulphate groups reacts with amino groups. On the other hand, carboxymethyl chitosan maintains the same free amino groups than original chitosan.

The analysis of average molecular weight indicates that the synthesis of chitosan sulphate produces a degradation of polymer chains.

Aqueous solutions of chitosan and carboxymethyl chitosan show a non-Newtonian and pseudoplastic behaviour. Chitosan sulphate aqueous solutions show a shear rate non-influence with a Newtonian behaviour.

Also a dynamic surface tension was found for all polymers aqueous solutions with a decrease in the value of this property at equilibrium when polymer concentration increases due to its accumulation at interface.

# 5.2 Hydrodynamics in $CO_2$ - polymers systems

*Abstract*

*The present work analyses the behaviour of the polymer aqueous solutions (C, CS and CC) employed in a bubble column contactor, in relation to the gas-liquid interfacial area produced in the absorber. This study has been developed by means of the analysis about the influence of the operation conditions upon the gas hold-up and the Sauter mean diameter. The last parameter has been determined on the basis of the bubble size distribution obtained from photographs taken in the bubble column.*

*Take into account the rheological behaviour, which has been carried out as a previous step, the results shown in the present work allow to understand the carbon dioxide transfer to a non-Newtonian liquid phase, as well as to evaluate the effect caused by the liquid phase characteristics.*

## 5.2.1. Specific introduction

An important number of processes are based on the use of gas–liquid reactors and biorreactors, and an efficient gas–liquid mass transfer is important to many chemical and biochemical processes. The gas is released in the form of bubbles to yield a large surface area, and also as an efficient mass transfer between the gas and liquid phases. The liquid phases commonly found in the chemical industry are very complex due to the presence of several compounds and to the operating procedures. Consequently, a lot of research has been performed to understand the influence of the liquid phase properties on the bubble formation phenomenon[339,340,341].

The bubble diameter and the gas hold-up distribution are important parameters for a precise control of the gas–liquid mass transfer where physical or chemical absorption processes take place in highly viscous media with a complex rheology. It is known that such processes are most often met in polymerisation reactors and bioreactors. These parameters are also important design factors, since they define the gas–liquid interfacial area available for mass transfer. These parameters (bubble diameter and gas hold-up) depend strongly on the operating conditions, the physico-chemical properties of the two phases, the gas sparger type and the column geometry[342]. The design and scale up of the bubble column reactors could be developed primarily by means of empirical and semi-empirical correlations based on experimental data, and hence the need of general validity correlations, taking into account all the aforementioned parameters affecting the bubble column performance[343].

The important role of physical properties such as viscosity and surface tension has been confirmed, and these properties must be taken into account for experimental data analysis. Certain studies have demonstrated that an increase in viscosity produces a decrease in gas hold-

[339] Liow J.L., Gray N. B. A model of bubble growth in wetting and non-wetting liquids. *Chemical Engineering Science* 1988, 43, 3129–3139.
[340] Terasaka K., Tsuge H. Bubble formation under constant-flow conditions. *Chemical Engineering Science* 1993, 46, 3417–3422.
[341] Anabtawi M. Z. A., Abu-Eishah S. I., Hilal N., Nabhan M. B. W. Hydrodynamic studies in both bi-dimensional and three-dimensional bubble columns with a single sparger. *Chemical Engineering and Processing* 2003, 42, 403-408.
[342] Camarasa E., Vial C., Poncin S., Wild G., Midoux N., Bouillard J. Influence of coalescence behaviour of the liquid and of gas sparging on hydrodynamics and bubble characteristics in a bubble column. *Chemical Engineering and Processing* 1999, 38, 329–344.
[343] Kazakis N. A., Papadopoulos I. D., Mouza A. A. Bubble columns with fine pore sparger operating in the pseudo-homogeneous regime: Gas hold up prediction and a criterion for the transition to the heterogeneous regime. *Chemical Engineering Science* 2007, 62, 3092 – 310.

up. In general, this behaviour has been attributed to the enhanced coalescence and reduced turbulence in viscous fluids, which leads to the formation of larger bubbles[344,345]. The larger bubbles pass more quickly through the fluid with higher bubble rise velocities, resulting in a decreased gas hold-up.

This work analyses the behaviour of a gas-liquid contactor using chitosan, chitosan sulphate and carboxymethyl chitosan aqueous solutions (non-Newtonian and Newtonian media) in a bubble column. These systems have been studied taking into account different parameters such us gas hold-up, bubble diameter and interfacial area.

## 5.2.2. Results and discussion

The medium diameter of bubbles into the column contactor has been determined taking photographs at different heights and analysing the bubble geometrical characteristics obtaining bubble size distributions. Using this kind of distribution, the Sauter mean diameter is calculated. On the basis of the photographs taken under the different experimental conditions used in the present work, the major and minor axis (due to the ellipsoidal shape of the bubbles) are determined, and using the equations shown in the materials and methods section, the Sauter mean diameter and the gas-liquid interfacial area were calculated for the different conditions.

Figure 5.22 shows examples of bubble size distributions obtained for different experimental conditions analysed in present study. These distributions show the size range of the bubbles present in bubble column. The presence of carboxymethyl chitosan produces a clear influence upon the bubble size distribution causing a displacement in the distribution to the right side, and then an increase in the bubble size is produced. This behaviour can be observed directly in the photographs included in the figure 5.23. In this figure the size of the bubbles in the presence of carboxymethyl chitosan is higher than in absence of polymer.

[344] Arjunwadkar S. J., Saravanan K., Kulkarni P. R., Pandit A. B. Gas–liquid mass transfer in dual impeller bioreactor. *Biochemical Engineering Journal* 1998, 1, 99–106.
[345] Nocentini M., Fajner D., Pasquali G., Magelli F. Gas–liquid mass transfer and holdup in vessels stirred with multiple Rushton turbines: water and water–glycerol solutions. *Industrial & Engineering Chemistry Research* 1993, 32, 19–26.

On the other hand, the increase in the bubble diameter previously commented, is produced in the higher bubble's size range. More specifically the corresponding data of bubble size distribution in the absence and presence of polymer show a similar behaviour for bubbles with diameter minor than 6 mm. For higher diameter range, a second group of bubbles is produced in the system with polymer with the presence of higher size bubbles in comparison with the system without polymer. This behaviour is supported by the effect upon viscosity produced by the presence of polymer in the liquid phase. An increase in the presence of this substance produces an increase in liquid phase viscosity (previously commented) and this physical property produces an increase in the gas volume needed to form bubbles and to ascend along the liquid in the bubble column. This behaviour increases the bubble size. A previous section about the rheological behaviour of polymers aqueous solutions conclude the important effect of carboxymethyl chitosan concentration upon viscosity because produces an important increase in this property.

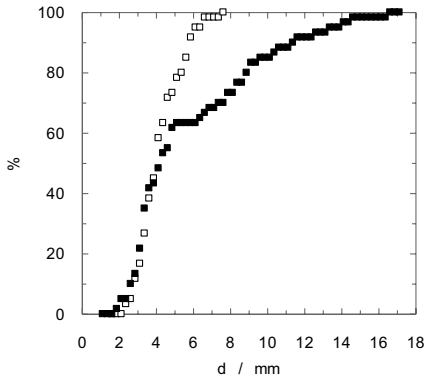


Figure 5.22. Effect of polymer presence upon bubble size distribution. (□) $C_{CC}$ = 0 g·L$^{-1}$; (■) $C_{CC}$ = 4 g·L$^{-1}$. $Q_g$ = 40 L·h$^{-1}$.

(a) (b)

Figure 5.23. Bubbles photographs. Influence of polymer presence. . (a) $C_{CC}$ = 0 g·L$^{-1}$; (b) $C_{CC}$ = 4 g·L$^{-1}$. $Q_g$ = 40 L·h$^{-1}$.

On the other hand, the analysis of surface tension in polymers aqueous solutions studied in previous section shows a decrease in this physical property when polymer concentration increases. A decrease in the value of this parameter produces commonly also a decrease in the

value of bubble diameter[346], but this behaviour has not been observed in this work (see figures 5.22-5.23) due to the important effect produced by the viscosity upon the bubble diameter that removes the reduction in bubbles' size caused by the decrease in surface tension.

Using the bubble size distributions under the different experimental conditions for all the polymers employed in present work, is possible calculate the Sauter mean diameter that allows to obtain the influence of operation conditions upon the bubble size using a medium value of diameter. Figure 5.24 shows an example of the calculated results for this parameter. An increase in the polymer concentration (figure 5.24 corresponds to chitosan sulphate) produces an increase too in the value of Sauter mean diameter that is in agreement with the previously commented behaviour for bubble size distribution. Also, in figure 5.24 is possible analyse the influence of gas flow-rate fed to the bubble column that also produces an increase in the bubble diameter due to a higher quantity of gas must be introduced through the gas sparger, and this fact produces the formation of bubbles with a higher size.

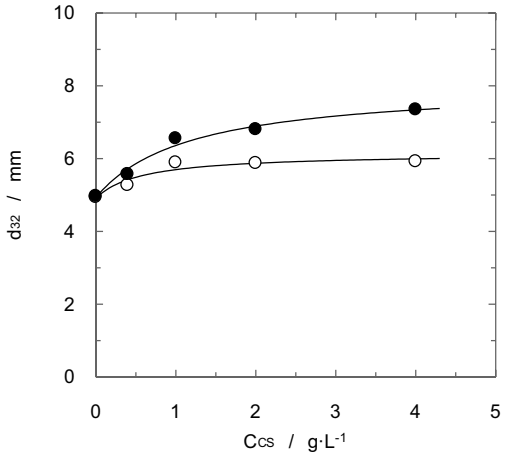


Figure 5.24. Influence of chitosan sulphate concentration upon Sauter mean diameter. (○) $Q_g$ = 18 L·h$^{-1}$; (●) $Q_g$ = 40 L·h$^{-1}$.

The behaviour previously commented has been similar between the different polymers used in this work to generate the liquid phases, in relation with the influence of each polymer concentration and the gas flow-rate.

[346] Chaumat H., Billet A. M., Delmas H. Hydrodynamics and mass transfer in bubble column: Influence of liquid phase surface tension. *Chemical Engineering Science* 2007, 62, 7378 – 7390.

In materials and methods section the methodology to gas-liquid interfacial area calculation on the basis of Sauter mean diameter is described and also using the gas hold-up. In relation with the last variable, figure 5.25 shows the influence of polymer concentration and gas flow-rate upon the value of gas hold-up. The obtained behaviour is different for the chitosan and chitosan sulphate in comparison with the data obtained for carboxymethyl chitosan aqueous solutions. For C and CS, a decrease in the value of gas hold-up is observed at low polymer concentration reaching a constant value without influence of polymer concentration. This fact is due to the low increase in viscosity produced when polymers concentration increases in liquid phase and the important effect caused by surface tension with low polymer concentration (previously commented). This low change in viscosity doesn't produce significant changes in the quantity of gas in contact with the liquid phase. On the other hand, aqueous solutions of carboxymethyl chitosan (CC) are highly influenced in the value of viscosity by the presence of polymer. This behaviour produces important changes on the hydrodynamic behaviour of the bubble column and then upon the gas hold-up[347] because it could increase the residence time significantly or modify the bubble diameter previously commented. For this system, figure 5.25 shows a continuous decrease in the value of gas hold-up reaching minor values at high polymer concentration in comparison with aqueous solutions of chitosan and chitosan sulphate.

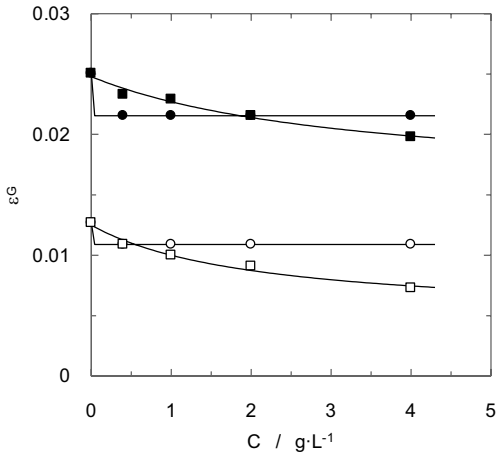


Figure 5.25. Influence of polymers' concentration upon gas hold-up. C and CS: (○) $Q_g$ = 18 L·h$^{-1}$; (●) $Q_g$ = 40 L·h$^{-1}$. CC: (□) $Q_g$ = 18 L·h$^{-1}$; (■) $Q_g$ = 40 L·h$^{-1}$.

[347] Urseanu M. I., Guit R. P. M., Stankiewicz A., van Kranenburg G., Lommen J. H. G. M. Influence of operating pressure on the gas hold-up in bubble columns for high viscous media. *Chemical Engineering Science* 2003, 58, 697–704.

Taking into account the previously determined values for Sauter mean diameter and gas hold-up for all the systems (aqueous solutions of C, CS and CC) and under all the experimental conditions analysed in present work (polymer concentration and gas flow-rate), the gas-liquid interfacial area has been determined, and the experimental results obtained for this variable are shown in the graphs included in the figure 5.26 for all the polymers analysed.

The behaviours show in figure 5.26 indicates a common trend for this kind of systems (polymers aqueous solutions), that consists in a decrease in the value of interfacial area when polymer concentration increases in the liquid phase. This behaviour is in agreement with previous studies[348,349] that have analysed the presence of different polymers in several contactors. The effect produced by the presence of polymer in the liquid phase (a decrease in the value of interfacial area) is due to the increase in viscosity, and the effect produced for this physical property upon the value of bubble size and gas hold-up. An increase in viscosity produces a monotonic increase in bubble size previously commented. This fact produces a priori a decrease in the value interfacial area because this variable is in the divisor in equation A.7 (see materials and methods section). On the other hand an increase in the gas hold-up produces an increase in the value of gas-liquid interfacial area, but in this system (see figure 5.26) was observed a decrease in the value of this parameter when polymer concentration increases in the liquid phase. Taking into account these behaviours, the influence of polymer concentration upon Sauter mean diameter and gas hold-up have negative effect upon the gas-liquid interfacial area produced in the contactor and this fact is reflected in the data included in figure 5.26. On the other hand, an increase in polymers concentration produces a decrease in surface tension value that produces commonly a reduction in bubbles' size that could affect positively upon gas-liquid interfacial area. In present work this effect is not observed due to different aspects: (i) the effect caused by liquid phase viscosity is more important (influence observed upon bubble size in figure 5.24), (ii) the low dynamics of polymers produces that the surface tension decreases slowly because the bubbles' surface is renewed constantly while ascend along column and then the surface tension is the corresponding value for low times (i.e. see figure 5.20) with higher values than at equilibrium.

[348] Kilonzo P. M., Margaritis A. The effects of non-Newtonian fermentation broth viscosity and small bubble segregation on oxygen mass transfer in gas-lift bioreactors: a critical review. *Biochemical Engineering Journal* 2004, 17(1), 27-40.
[349] Gómez-Díaz D., Navaza J. M., Quintáns-Riveiro L. C., Sanjurjo B. Gas absorption in bubble column using a non-Newtonian liquid phase. *Chemical Engineering Journal* 2009, 146, 16–21.

Figure 5.26 also shows that an increase in the gas flow-rate fed to the gas-liquid contactor produces in all cases an increase in the gas-liquid interfacial area. This increase could be due to that a higher gas flow-rate produces an increase in the number of bubbles generated that produces an increase in gas hold-up (see figure 5.25). On the other hand this increase in gas flow-rate also produces an increase in bubble diameter that has a negative influence upon gas-liquid interfacial area (previously commented). But in all cases, figure 5.26 shows an increase in interfacial area with gas flow-rate and this behaviour indicates that gas hold-up has a more important influence upon gas-liquid interfacial area than bubble diameter, and these results and conclusions are in agreement with previous works[350].

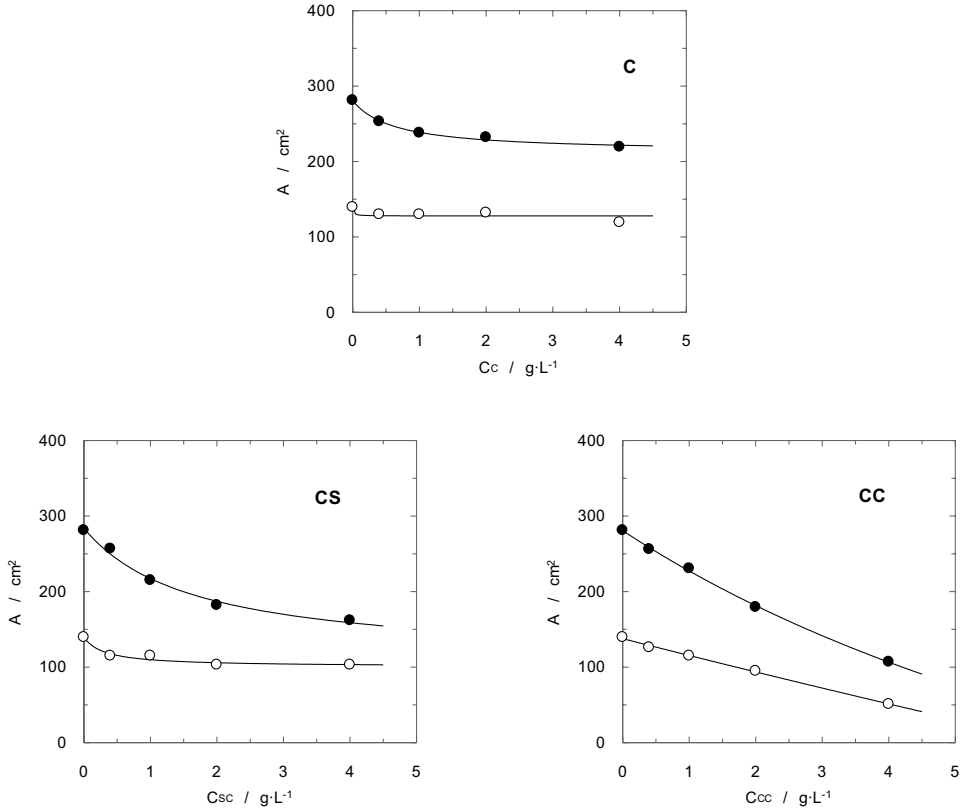


Figure 5.26. Influence of polymer type and concentration upon gas-liquid interfacial area. (○) $Q_g$ = 18 L·h$^{-1}$; (●) $Q_g$ = 40 L·h$^{-1}$.

[350] Maalej S., Benadda B., Otterbein M. Interfacial area and volumetric mass transfer coeffcient in a bubble reactor at elevated pressures. *Chemical Engineering Science* 2003, 58, 2365–2376.

In relation with the polymer nature upon the value of gas-liquid interfacial area, figure 5.27 shows a comparison between the experimental results obtained for the influence of polymer concentration for each solute upon this hydrodynamic parameter. In relation with the influence of polymer concentration analysed in the previous figures observing a decrease in the value of interfacial area due to the increase in bubble size and the decrease in gas hold-up. In relation with the influence of polymer type, the behaviour observed indicates that aqueous solutions of chitosan produce higher values for interfacial area. The obtained trend was: $A_C > A_{SC} > A_{CC}$. This behaviour is in agreement in relation with the values of polymer solution surface tension $\sigma_{CC} > \sigma_{CS} > \sigma_C$. The changes produced in surface tension by the presence of polymers don't achieve an increase in gas-liquid interfacial area, but this property avoids a higher decrease caused by viscosity. On the other hand, the trend observed for interfacial area is not in agreement with the values for viscosity determined in a previous section (taking into account that this physical property has an important influence upon gas-liquid interfacial area): $\eta_{CC} > \eta_C > \eta_{SC}$. On the basis of these results is possible conclude that aqueous solutions of chitosan shows a deviation of the expected trend in relation with the influence of viscosity. Taking into account the modified polymers (CS and CC) the gas-liquid interfacial area produced in CC aqueous solutions is minor than the corresponding one for CS aqueous solutions, that is in agreement with the values of viscosity, because aqueous solutions of CC takes the highest viscosity values (producing an increase in bubble size and a decrease in gas hold-up). The behaviour obtained for C aqueous solutions shows a different trend because the gas-liquid interfacial area must be situated between the other polymers solutions (taking into account the viscosity values). This different behaviour is due to the increase in the electrolyte concentration because acidic medium (acetic acid solution in present work) is used as solvent for chitosan and this fact produces an increase in the presence of electrolytes. This kind of substances has a proved influence upon the gas-liquid hydrodynamic and different studies[351,352] have concluded that the presence of electrolytes reduces the coalescence process (formation of large bubbles due to effective collisions) and then a minor bubble size (minor Sauter mean diameter) is produced, that has a positive effect upon gas-liquid interfacial area. Then the sum of the effects caused by electrolyte presence and surface tension explain the observed behaviour.

[351] Chilekar V. P., van der Schaaf J., Kuster B. F. M., Tinge J. T., Schouten J. C. Influence of elevated pressure and particle lyophobicity on hydrodynamics and gas–liquid mass transfer in slurry bubble columns. *AIChE Journal* 2010, 56, 584-596.

[352] Orvalh S., Ruzicka M. C., Drahos J. Bubble column with electrolytes: Gas holdup and flow regimes. *Industrial & Engineering Chemistry Research* 2009, 48, 8237–8243.

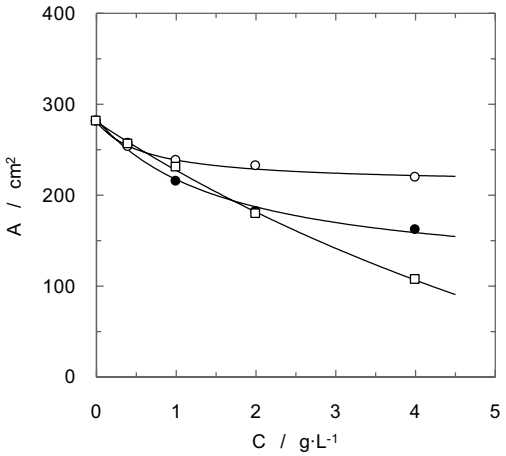


Figure 5.27. Influence of polymer type upon interfacial area. (○) C; (●) SC; (□) CC. $Q_g$ = 40 L·h$^{-1}$.

## 5.2.3. Conclusions

In relation with the hydrodynamic study, the behaviour observed indicate a common trend for the three systems (C-water, SQ-water and CC-water), that consists in a decrease in the value of interfacial area when polymer concentration increases in the liquid phase. This behaviour is due to an increase in the viscosity, and the effect produced for this physical property upon the value of bubble size and gas hold-up. The viscosity shows a higher influence upon interfacial area than surface tension, but the last property reduces the negative influence of viscosity.

The presence of electrolytes in chitosan aqueous solutions produces changes in the expected behaviour due to the "inhibition" of bubbles coalescence.

# 5.3 Gas absorption in $CO_2$ - polymers systems

*Abstract*

*Gas-liquid mass transfer has been investigated in a bubble column using different polymer aqueous solutions and pure carbon dioxide as absorbent and gas phase, respectively. The volumetric mass transfer coefficient and gas/liquid interfacial area has been measured under different operation conditions for the gas/liquid system analysed in this work. The influence of rheological properties, polymer concentration and gas flow-rate upon the mass transfer rate has been studied. The results shown in the present work allow to understand the carbon dioxide transfer to a non-Newtonian and Newtonian liquid phase, as well as to evaluate the effect caused by the liquid phase characteristics.*

### 5.3.1. Specific introduction

Most of the liquid phases used in gas-liquid processes, i.e. in food and pharmaceutical industries, are non-Newtonian fluids. An important number of studies[353,354] have analysed the effect caused by the presence of different polymers on the absorbent phase, with and without chemical reaction: for example, the oxygen transfers in non-Newtonian fermentation broths of different microorganisms. The values of the volumetric transfer coefficient *($k_L$·a)*, obtained at various impeller speeds, air flow-rates and at different initial solutes concentrations, were correlated with operational variables, the geometric parameters of the system and the physical properties of the broths, utilising rigorous techniques in order to obtain a set of reliable and accurate data.

As is well-known, the volumetric mass transfer coefficient, $k_L$·*a*, is one of the most important parameters that govern the performance of gas/liquid (bio)reactors. Therefore, extensive efforts, in the last years, have been directed to estimate this coefficient[355,356]. However, most of them are based on empirical analyses. It is also important to determine the influence of the operational variables (physical properties, stirring rate, gas flow-rate, etc.) on $k_L$·*a* to optimise the absorption process.

The behaviour of these non-Newtonian liquids is commonly studied on the basis of the apparent viscosity variations. Some previous studies proved the important effect that the apparent viscosity of the liquid phase has upon the mass transfer[357,358]. For this reason, it is necessary to include the rheological behaviour in a serious study concerning gas-liquid absorption. The use of a stirred vessel with a non-Newtonian media as liquid phase has important

[353] Park S.-W., Choi B.-S., Lee J.-W. Influence of polyethylene oxide on absorption of carbon dioxide into aqueous diethanolamine solution. *Separation Science and Technolgy* 2007, 42, 979-991.
[354] Nishikawa M., Nakamura M., Yagi H., Hashimoto K. Gas absorption in aerated mixing vessels with non-Newtonian liquid. *Journal of Chemical Engineering of Japan* 1981, 14, 227-232.
[355] Mandal A., Kundu G., Mukherjee D. Interfacial area and liquid-side volumetric mass transfer coefficient in a downflow bubble column. *Canadian Journal of Chemical Engineering* 2003, 81, 212-219.
[356] Jurascik M., Blazej M., Annus J., Markos J. Experimental measurements of volumetric mass transfer coefficient by the dynamic pressure-step method in internal loop airlift reactors of different scale. *Chemical Engineering Journal* 2006, 125, 81-87.
[357] Álvarez E., Sanjurjo B., Cancela A., Navaza J. M. Mass transfer and influence of physical properties of solutions in a bubble column. *Chemical Engineering Research and Design* 2000, 78, 889-893.
[358] Jiao Z., Xueqing Z., Juntag Y. $O_2$ transfer to pseudoplastic fermentation broths in air-lift reactors with different inner designs. *Biotechnology Techniques* 1998, 12, 729-732.

characteristics[359]. A variation on the stirring rate also produces a change in the physical properties of the absorbent phase, since the viscosity of the non-Newtonian liquid is shear-rate dependent.

Previous studies have analysed the non-Newtonian rheological behaviour of different polymers aqueous solutions, as well as the influence of the special characteristics of this kind of liquid phases upon the gas absorption process, using different contactors[360,361]. These studies have shown the great importance of the rheological behaviour upon the gas mass transfer to a liquid phase, due to the important connection between the viscosity and the mass transfer process[362]. In addition, when this kind of liquid phases is employed in certain equipments, the shear rate applied to the non-Newtonian liquid phase has great importance upon the mass transfer because the apparent viscosity value could be highly influenced by the shear rate[363].

Since it is possible to observe, the knowledge of the relation between rheological behaviour and mass transfer has great importance in systems with polymers. For this reason, the aim of this work is characterizing the gas/liquid mass transfer process, analysing the effect caused for different operational variables and the possibility of chemical absorption in chitosan and chitosan derivatives aqueous solutions.

### 5.3.2. Results and discussion

The experimental procedure has been described deeply in the materials and methods section and figure 5.28 shows an example of the experimental data obtained in this kind of studies. The mass transfer rate has been determined on the basis of the differences between the inlet and outlet gas flow-rate along the operation time. Present work tries evaluate the possible

[359] Metzner A. B., Otto R. E. Agitation of non-Newtonian fluids. *AIChE Journal* 1957, 3, 3-10.
[360] Gómez-Díaz D., Navaza J. M. Mass transfer in a flat gas/liquid interface using non-Newtonian media. *Chemical Engineering & Technology* 2003, 26, 1068-1073.
[361] Gómez-Díaz D., Navaza J. M. Analysis of carbon dioxide gas/liquid mass transfer in aerated stirred vessels using non-Newtonian media. *Journal of Chemical Technology & Biotechnology* 2004, 79, 1105-1112.
[362] Mandal A., Kundu G., Mukherjee D. Interfacial area and liquid-side volumetric mass transfer coefficient in a downflow bubble column. *Canadian Journal of Chemical Engineering* 2003, 81, 212-219.
[363] Torrez C., Andre C. Power consumption of a rushton turbine mixing viscous newtonian and shear-thinning fluids. Comparison between experimental numerical results. *Chemical Engineering & Technology* 1998, 21, 599-604.

use of soluble polymers (in aqueous solution) derivates from chitosan for chemical absorption of carbon dioxide. Taking into account this aim, figure 5.28 shows that the use of pure water as absorbent phase produces an enhancement in the outlet gas flow-rate with time until reach the carbon dioxide saturation of liquid phase in comparison with polymer aqueous solution.

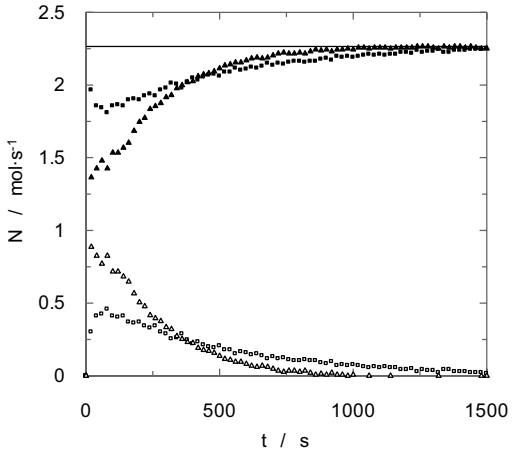


Figure 5.28. Inlet, outlet and absorbed molar gas flow-rate. $C_{CC}$ = 0 g·L$^{-1}$: (▲) outlet; (△) absorbed. $C_{CC}$ = 4 g·L$^{-1}$: (■) outlet; (□) absorbed. Solid line corresponds to fed gas flow-rate. $Q_g$ = 18 L·h$^{-1}$.

Figure 5.28 also compares the behaviour obtained for water with an aqueous solution of carboxymethyl chitosan (CC) and this comparison shows that the mass transfer rate is lower for the polymer aqueous solution. This fact is due to the increase in liquid phase viscosity when a polymer is present, and an increase in this physical property produces a decrease in the mass transfer rate[364,365]. This behaviour doesn't allow conclude that only physical absorption is present for carbon dioxide – CC aqueous solution system but, the calculus developed using the absorption experimental data indicates that the carbon dioxide absorbed reaches a similar value than the solubility of this gas in water. Taking into account both behaviours is possible conclude that doesn't exist chemical reaction between carbon dioxide and carboxymethyl chitosan, and a physical absorption is produced in the contactor. A similar behaviour has been found for chitosan

[364] Gómez-Díaz D., Navaza J. M., Quintáns-Riveiro L. C., Sanjurjo B. Gas absorption in bubble column using a non-Newtonian liquid phase. *Chemical Engineering Journal* 2009, 146, 16–21.
[365] Jiao Z., Xueqing Z., Juntag Y. $O_2$ transfer to pseudoplastic fermentation broths in air-lift reactors with different inner designs. *Biotechnology Techniques* 1998, 12, 729-732.

sulphate (CS) aqueous solutions. In the last case, this behaviour could be expected taking into account that the deacetilation degree showed the complete substitution of amino groups that difficult the chemical reaction between carbon dioxide and amino group.

For chitosan aqueous solution the physical absorption is the regime obtained because acidic medium is necessary to dissolve this polymer, and this medium produces the chemical reaction inhibition between carbon dioxide and the amino group.

Figure 5.29 shows the experimental data obtained for the analysis of gas flow-rate effect produced upon the mass transfer rate. An increase in the gas flow-rate fed to the bubble column produces an increase in the quantity of carbon dioxide transferred in the first part of experiment producing the saturation in a minor time. Is necessary takes into account that the absorption kinetics shown in figures 5.28 and 5.29 indicate the global mass transfer process involving the gas-liquid interfacial area and the mass transfer process. Then, to analyse the influence of each operation variable upon both parameters is necessary.

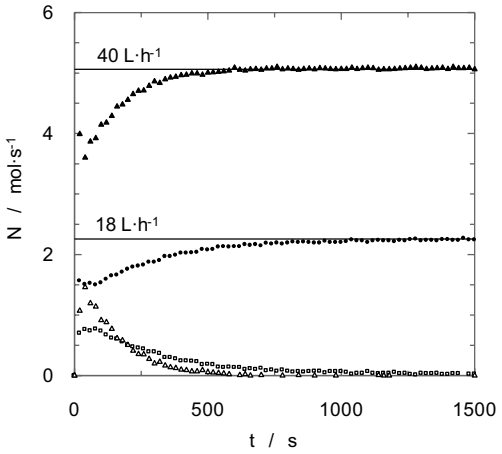


Figure 5.29. Influence of gas flow-rate upon molar gas flow-rates. $C_{SC}$ = 4 g·L$^{-1}$. $Q_g$ = 40 L·h$^{-1}$: (▲) outlet; (△) absorbed. $Q_g$ = 18 L·h$^{-1}$: (■) outlet; (□) absorbed.

The procedure to determine the volumetric mass transfer coefficient is based on the measurement of the amount of gas absorbed per unit time (see materials and methods sections).

Plots of *ln [C*/(C*-C)]* against *time* showed straight lines passing the origin showing that $k_L \cdot a$ was independent of time under the conditions of this work. The carbon dioxide concentration in the bulk of the liquid increases with time until the liquid phase is saturated. The experimental results show that a higher presence of polymer in the liquid phase produces a decrease in the slope of the straight line (corresponding to a lower volumetric mass transfer coefficient) (see figure 5.30).

Similar results have been obtained in previous studies[366,367] employing different systems formed by aqueous solutions of polymers. Two opposite effects or mechanisms (slip and elasticity effects) have been described in literature for different systems when polymer solutions are present and these effects act simultaneously. The slip effects produce an increase of absorption rate, whereas elasticity produces a decrease. According to Mashelkar[368], the overall effect seems to be the reduction on the mass transfer rate.

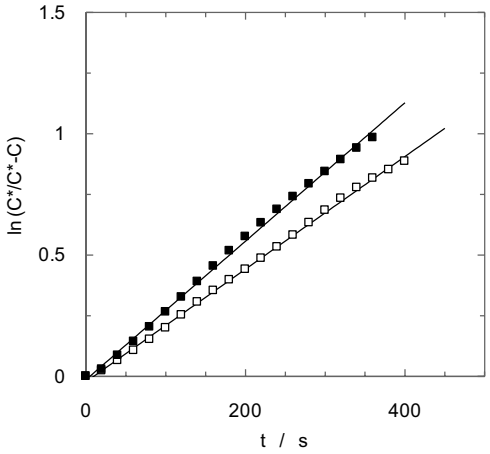


Figure 5.30. Volumetric mass transfer coefficient calculation. $Q_g$ = 18 L·h$^{-1}$. (■) $C_{SC}$ = 0 g·L$^{-1}$; (□) $C_{SC}$ = 0.4 g·L$^{-1}$.

[366] Tecante A., Choplin L. Gas-liquid mass transfer in non-Newtonian fluids in a tank stirred with a helical ribbon screw impeller. *Canadian Journal of Chemical Engineering* 1993, 71, 859-865.
[367] Gómez-Díaz D., Navaza J. M. Analysis of carbon dioxide gas/liquid mass transfer in aerated stirred vessels using non-Newtonian media. *Journal of Chemical Technology & Biotechnology* 2004, 79, 1105-1112.
[368] Mashelkar R. A. Anomalous convective diffusion in films of polymeric solutions. *AIChE Journal* 1984, 30, 353-362.

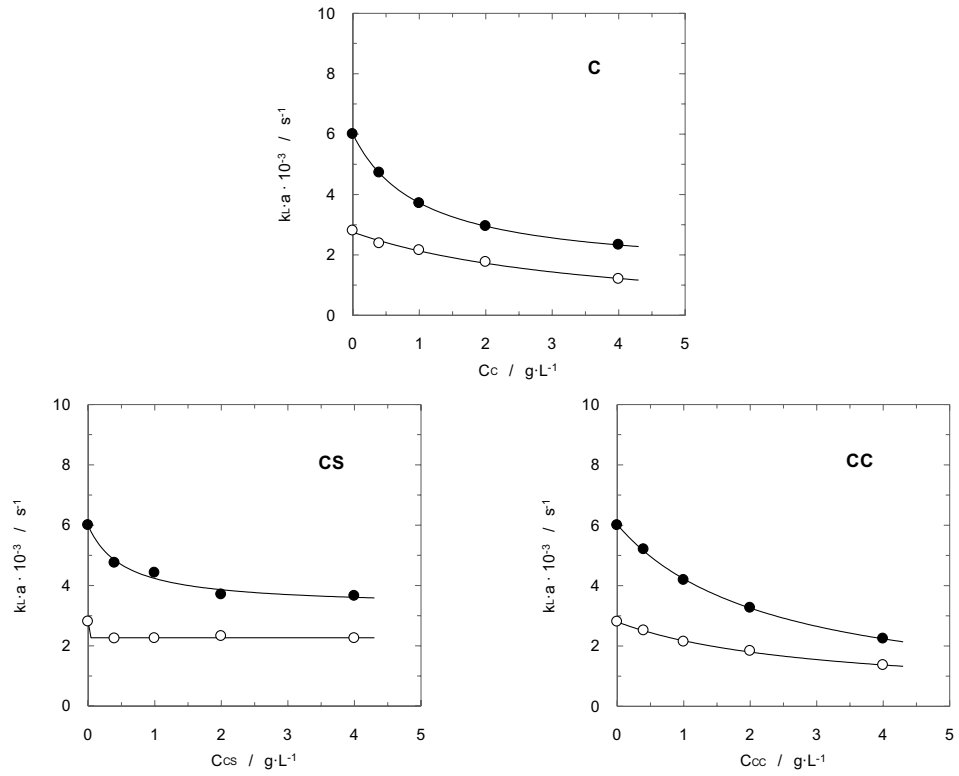


Figure 5.31. Influence of gas flow-rate and polymer concentration upon volumetric mass transfer coefficient. (○) $Q_g$ = 18 L·h$^{-1}$; (●) $Q_g$ = 40 L·h$^{-1}$.

The procedure described in materials and methods section has been used for all absorption rate data under the different experimental conditions employed in present work. Then, from the value of slope determined in the plot shows in figure 5.30 the volumetric mass transfer coefficient has been obtained.

Figure 5.31 shows the values determined for this parameter for all the systems and under several conditions. The first conclusion is reached analysing the values calculated for this coefficient: an increase in the gas flow-rate produces an increase in the volumetric mass transfer coefficient in all cases. All systems show the same behaviour in relation with the influence of gas flow-rate.

On the other hand, figure 5.31 shows a common behaviour observed in literature for the influence of the presence of polymers in aqueous solutions[369,370], and it is in agreement with the comments about figures 5.28 and 5.29. A decrease in the value of volumetric mass transfer coefficient is observed when polymer concentration increases in the liquid phase. This behaviour is related with: (i) a decrease in the value of gas-liquid interfacial area previously commented in other section, caused by an increase in liquid phase viscosity, and (ii) this physical property produces also a decrease in the value of mass transfer rate[371,372] caused by a decrease in diffusion coefficient, that must be confirmed on the basis of mass transfer coefficient value.

The obtained behaviour shows a higher decrease in the value of volumetric mass transfer coefficient at low additions of polymers reaching a relatively constant value. This behaviour is in agreement with previous studies related with the influence of polymer concentration upon gas-liquid interfacial are produced in a bubble contactor[373,374].

With the aim of the individual analysis of mass transfer and avoiding the possible influence of gas-liquid interfacial area upon this one, the equation A.10 (materials and methods section) allows calculate the value of the mass transfer coefficient ($k_L$).

Figure 5.32 shows calculated data for mass transfer coefficient on the basis of the experimental data obtained for gas-liquid specific interfacial area and volumetric mass transfer coefficient.

[369] Kilonzo P. M., Margaritis A. The effects of non-Newtonian fermentation broth viscosity and small bubble segregation on oxygen mass transfer in gas-lift bioreactors: a critical review. *Biochemical Engineering Journal* 2004, 17(1), 27-40.
[370] García-Ochoa F., Gómez E. Bioreactor scale-up and oxygen transfer rate in microbial processes: An overview. *Biotechnology Advances* 2009, 27, 153–176.
[371] Gómez-Díaz D., Navaza J. M., Quintáns-Riveiro L. C., Sanjurjo B. Gas absorption in bubble column using a non-Newtonian liquid phase. *Chemical Engineering Journal* 2009, 146, 16–21.
[372] Jiao Z., Xueqing Z., Juntag Y. $O_2$ transfer to pseudoplastic fermentation broths in air-lift reactors with different inner designs. *Biotechnology Techniques* 1998, 12, 729-732.
[373] Tecante A., Choplin L. Gas-liquid mass transfer in non-Newtonian fluids in a tank stirred with a helical ribbon screw impeller. *Canadian Journal of Chemical Engineering* 1993, 71, 859-865.
[374] Gómez-DíazD., Navaza J. M. Analysis of carbon dioxide gas/liquid mass transfer in aerated stirred vessels using non-Newtonian media. *Journal of Chemical Technology & Biotechnology* 2004, 79, 1105-1112.

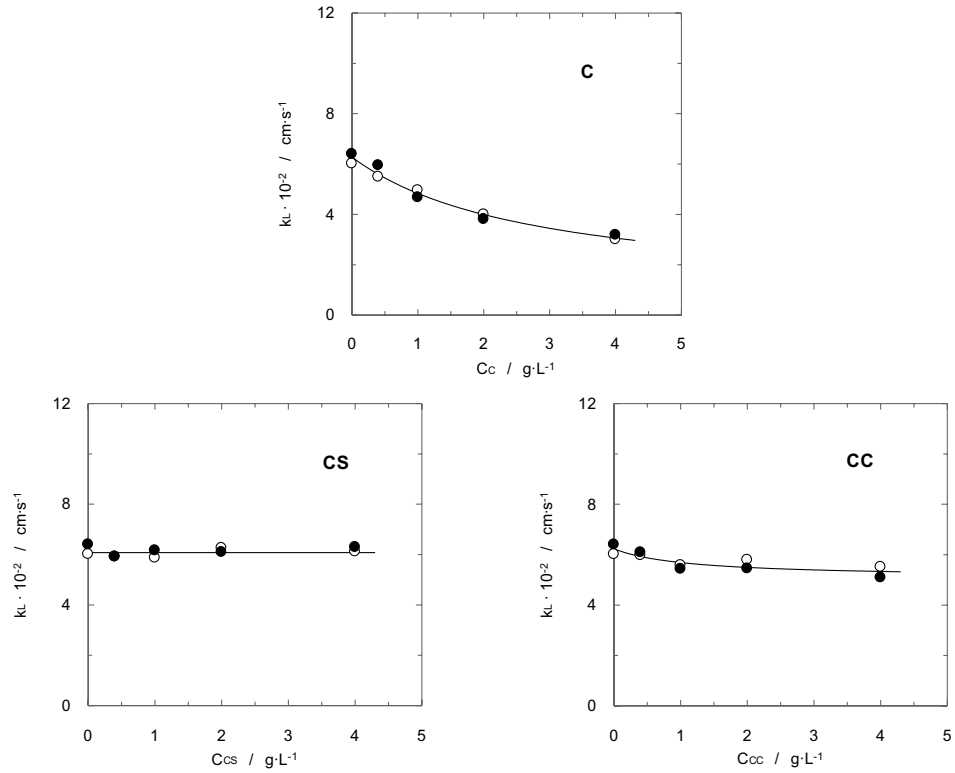


Figure 5.32. Influence of gas flow-rate and polymer concentration upon mass transfer coefficient. (○) $Q_g$ = 18 L·h$^{-1}$; (●) $Q_g$ = 40 L·h$^{-1}$.

A different behaviour is obtained for each system. For chitosan aqueous solutions a monotonic decrease in the value of mass transfer coefficient is observed when polymer concentration increases in the liquid phase. This behaviour is assigned to the increase in viscosity that produces an increase in transport resistance. Also for carboxymethyl chitosan aqueous solutions a decrease in the value of this parameter is observed, but only a low polymer concentration reaching a constant value.

On the other hand, aqueous solutions of chitosan sulphate show a constant value for mass transfer coefficient without influence of polymer concentration. This fact is due to this polymer produces slight changes in liquid phase viscosity (previously analysed in the liquid phase characterization section).

For all systems, the gas flow-rate shows a non-influence upon mass transfer coefficient (see figure 5.32). This kind of behaviour has been observed in previous studies[375] but depends of the type of gas-liquid contactor employed in the absorption process. In this case, this fact indicates that the agitation produced in the bubble contactor caused by the increase in gas flow-rate has a low influence upon mass transfer process.

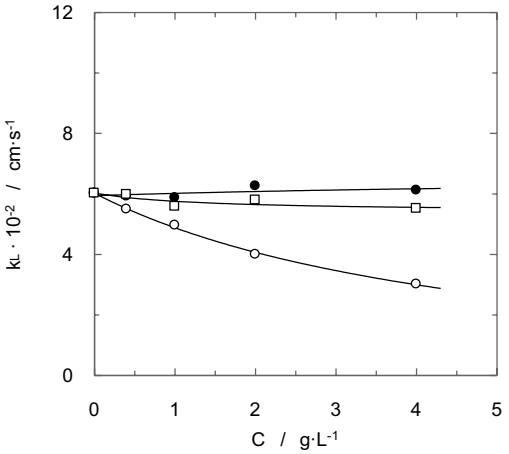


Figure 5.33. Comparison between mass transfer coefficient for all the polymers employed in present work. . (○) C; (●) CS; (□) CC. $Q_g$ = 18 L·h$^{-1}$.

Figure 5.33 shows a comparison between the mass transfer coefficient values for the systems formed by different polymers used in present work. The corresponding values for aqueous solutions of chitosan sulphate (CS) are higher than the mass transfer coefficient for the other systems. This behaviour is in agreement with the previously commented one for volumetric mass transfer coefficient and interfacial area, and related with the low value of liquid phase viscosity for this type of aqueous solutions. On the other hand, the chitosan aqueous solutions take the lowest values for mass transfer coefficient that implies a higher difficulty for mass transfer in this kind of aqueous solutions. The trend observed for mass transfer coefficient indicates a difference in relation with the sequence of viscosity ($\eta_{CC} > \eta_C > \eta_{SC}$), such as in the case of gas-liquid interfacial area (previously discussed), because aqueous solutions of chitosan haven't reach the highest viscosity values. Then the acidic medium plays an important role in the experimental behaviour obtained for these systems. For interfacial area, the presence of acidic

[375] Gómez-Díaz D., Navaza J. M., Sanjurjo B. Analysis of mass transfer in the precipitation process of calcium carbonate using a gas/liquid reaction. *Chemical Engineering Journal* 2006, 116, 203–209.

medium (acetic acid solution) produced an increase in the electrolyte concentration and then, a decrease in bubbles' coalescence was observed, producing a lower decrease in gas-liquid interfacial area. In relation with mass transfer, the presence of acidic medium produces a decrease in mass transfer rate. This fact is produced because this medium inhibits the chemical reaction between carbon dioxide and water (with low extension) and the use of this medium is a commonly used methodology to analyse the physical absorption process or other parallel reactions importance, in systems that involve chemical absorption between carbon dioxide and other compound in liquid phase[376,377]. In present work chemical reaction between carbon dioxide and polymers doesn't exist, but a certain influence of acidic medium upon mass transfer is observed.

### 5.3.3. Conclusions

From the results, it is possible to conclude that chemical reaction between carbon dioxide and chitosan does not exist, and a physical absorption is produced in the contactor. A similar behaviour has been found for chitosan sulphate (CS) and carboxymehtyl chitosan (CC) aqueous solutions.

The influence of polymers concentration upon volumetric mass transfer coefficient consists in a decrease in all cases, caused by the increase of liquid phase viscosity. An increase in gas flow-rate produces an important increase in volumetric coefficient due the influence of this variable upon interfacial area.

The mass transfer coefficient show a decrease when chitosan concentration increases. For chitosan sulphate and carboxymethyl chitosan a low influence was observed. The presence of electrolytes in chitosan aqueous solutions produces an important decrease in mass transfer coefficient.

---

[376] Kumar P. S., Hogendoorn J. A., Timmer S. J., Feron P. H. M., Versteeg G. F. Kinetics of the reaction of $CO_2$ with aqueous potassium salt of taurine and glycine. *AIChE Journal* 2003, 49, 203–213.
[377] Derks P. W. J., Kleingeld T., van Aken C., Hogendoorn J. A., Versteeg G. F. Kinetics of absorption of carbon dioxide in aqueous piperazine solutions. *Chemical Engineering Science* 2006, 61, 6837–6854.

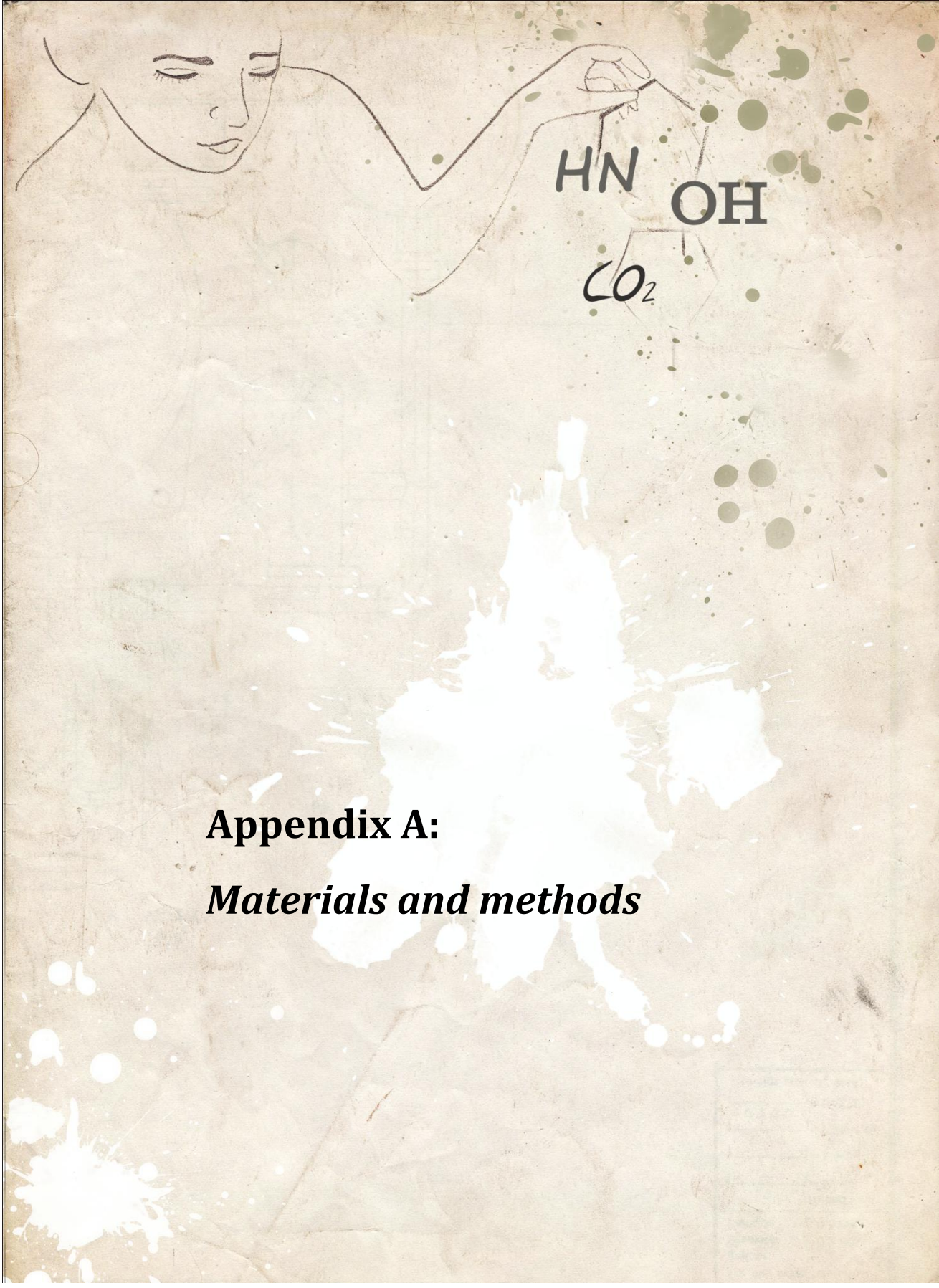


# Appendix A:

## *Materials and methods*

# A.1. Materials

## A.1.1. Chemical substances

Table A.1 shows the different substances used in the studies included in this doctoral thesis.

Table A.1. Chemical substances used in the present work.

| Substance | Purity | CAS Number | Supplier |
|---|---|---|---|
| $CO_2$ gas | 99.998% | 124-38-9 | Carburos Metálicos |
| Pyrrolidine | ≥99% | 123-75-1 | Fluka |
| Piperidine | ≥99% | 110-89-4 | Fluka |
| Ethanolamine | ≥99% | 141-43-5 | Sigma-Aldrich |
| 2-amino-2-deoxy-D-glucose hydrochloride or glucosamine hydrochloride | ≥99% | 66-84-2 | Fluka |
| 2-pyrrolidone | ≥ 99% | 616-45-5 | Fluka |
| N-methyl-2-pyrrolidone | ≥99% | 872-50-4 | Fluka |
| N-ethyl-2-pyrrolidinone | ≥ 98 % | 2687-91-4 | Fluka |
| Silicone oil DC 200 (μ =10 mPa·s) | | 63148-62-9 | Sigma-Aldrich |
| Silicone oil DC 200 (μ =100 mPa·s) | | 63148-62-9 | Sigma-Aldrich |
| Tween80 | | 9005-65-6 | Sigma-Aldrich |
| Chitosan | 99% | 9012-76-4 | Sigma-Aldrich |
| Chlorosulphonic acid | 99% | 7790-94-5 | Sigma-Aldrich |
| Methanol | 99.8% | 67-56-1 | Sigma-Aldrich |
| 2-propanol | 99.5% | 67-63-0 | Sigma-Aldrich |
| Monochloroacetic acid | 99% | 79-11-8 | Sigma-Aldrich |
| Acetic acid | 99.7% | 64-19-7 | Sigma-Aldrich |
| N,N-dimethylformamide | 99.8% | 68-12-2 | Panreac |

Table A.1. Chemical substances used in the present work (continuation)

| Substance | | CAS Number | Supplier |
|---|---|---|---|
| Sodium hydroxide | 98% | 1310-73-2 | |
| Hydrochloric acid | 37% | 7647-01-0 | - |
| Acetone | 99.5% | 67-64-1 | |
| Bi-distilled water | | | |

## A.1.2. Gas – liquid contactors

Three different gas-liquid contactors have been used in present research. The first one has been employed for kinetics studies and in this contactor, the gas transfer occurs through a planar gas-liquid interface. The gas-liquid interfacial area was determined from the geometrical characteristics (internal diameter = 8cm and height = 15 cm) of the stirred cell. Four baffles have been placed in its internal wall to improve mixing and prevent vortex formation during stirring. The liquid phase volume used in these experiments was 250 mL (see figure A.1).

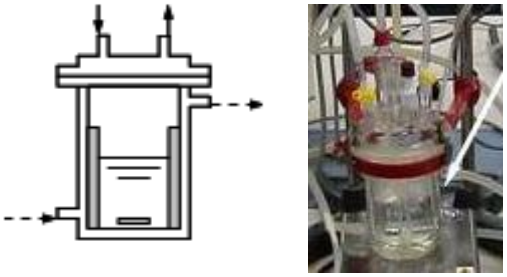

Figure A.1. Gas-liquid contactor for kinetics studies.

The other gas-liquid studies have been performed in two square bubble columns:

a) A bubble column made of methacrylate with 1.03 m high has been used for an important number of studies. This column has a square cross-section with a side length of 6 cm

(figure A.2). The volume of the liquid phase employed in the bubble contactor was 3 L. The gas sparger has been a glass capillary with only one orifice.

Figure A.2. Gas-liquid contactor for absorption and hydrodynamic studies.

b) The other gas-liquid contactor has only been used in the studies with polymers (chitosan and modified ones). This is a square bubble column (side length = 4 cm; height = 65 cm), made in methacrylate and working with liquid volume of 0.9 litres (see figure A.3). Pure carbon dioxide is fed at the bottom of the bubble column using a five holes sparger.

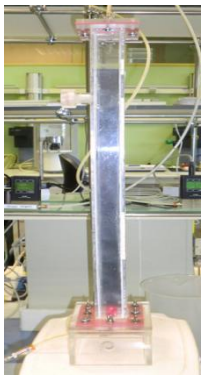

Figure A.3. Gas-liquid contactor for absorption and hydrodynamic studies.

# A.2. Methods

## A.2.1. Synthesis of polymers form chitosan

### *A.2.1.1. Chitosan (C) purification*

The commercial chitosan was treated with a sodium hydroxide aqueous solution (40%) for four hours at a temperature of 95 ºC, and the refined chitosan was obtained after two-times repetition of filtration and neutralization. 5 grams of the refined chitosan was dissolved in 20 g of a 2% aqueous solution of acetic acid and precipitated by neutralization with a 2% sodium hydroxide aqueous solution under stirring. The regenerated chitosan was washed with water and then with methanol, and thereafter immersed in dimethylformamide for 3 hours and pressed. Thus a pretreated chitosan was obtained.

### *A.2.1.2. Chitosan sulphate (CS) synthesis*

Sulfonation of chitosan was performed using the methodology developed in previous studies[378] with several modifications to improve the synthesis of this kind of chitosan[379]. The preparation of sulfating reagent to produce the chitosan modification consists in the addition of chlorosulphonic acid (4.5 mL) dropwise with stirring to 30 mL of N,N-dimethylformamide which had been previously cooled to temperature in the range of 0–4 ºC. The reaction mixture was then stirred without cooling until the solution reached room temperature. One gram of solvent, including the chitosan, was added to the sulfonating reagent, and the reaction mixture was stirred overnight at room temperature. The polymer was neutralized with a sodium hydroxide aqueous solution (20%) and then precipitated in cold methanol**.**

[378] Gamzazade A., Skyyar A., Nasibov S., Suskov A., Knirel Yu A. Structural features of sulfated chitosans. *Carbohydrate Polymers* 1997, 34, 113–116.
[379] Suwan J., Zhang Z., Li B., Vongchan P., Meepowpan P., Zhang F., Mousa S. A., Premanode B., Kongtawelert P., Linhardt R. J. Sulfonation of papain-treated chitosan and its mechanism for antiacoagulant activity. *Carbohydrate Research* 2009, 344, 1190-1196.

#### *A.2.1.3. Carboxymethyl chitosan (CC) synthesis*

Carboxymethyl chitosan was synthesized by means of the procedure described in the literature[380,381]. Purified chitosan (5 g) was suspended in 30 g of a sodium hydroxide aqueous solution (50%) and was swelled for one hour at room temperature and kept at −20 ºC for twelve hours for alkalization, then thawed at room temperature. The alkali chitosan was suspended in isopropanol (150 mL) and the resulted slurry was stirred at a moderate speed. Subsequently, monochloroacetic acid (20 g) was added in five equal portions every five minutes. The mixture was stirred for four hours in a water bath at 50 ºC. Afterward, the resultant solution was adjusted to pH 7 and filtered. Then the resulting solution was concentrated, and precipitated by pouring into acetone. The white precipitate was thoroughly rinsed with methanol, vacuum dried at 50 ºC and stored in a desiccator.

## A.2.2. Physico-chemical characterization

#### *A.2.2.1. Surface and interfacial tension measurements*

Surface tension was determined employing a Krüss K-11 tensiometer and the Wilhelmy plate method. The plate employed was a commercial platinum one supplied by Krüss. This platinum plate was cleaned with water and acetone and flame-dried before each measurement. In general, each surface tension value reported was an average of ten measurements, except in the case of polymers because they present a measure of dynamic surface tension. Before measuring surface tension, the samples were stirred in a thermostated vessel that was closed to prevent evaporation. The measurement vessel was connected to a thermostat-cryostat bath (Selecta Frigiterm) controlled.

[380] Chen L. Y., Tian Z. G., Du Y. M. Synthesis and pH sensitivity of carboxymethyl chitosan-based polyampholyte hydrogels for protein carrier matrices. *Biomaterials* 2004, 25(17), 3725-3732.
[381] Miao J., Chen G., Gao C., Lin C., Wang D., Sun M. Preparation and characterization of N,O-carboxymethyl chitosan (NOCC)/polysulfone (PS) composite nanofiltration membranes. *Journal of Membrane Science* 2006, 280, 478–484.

Figure A.4. Krüss K-11 tensiometer used to determine the surface and interfacial tension.

### *A.2.2.2. Density*

The density of pure components and mixture of different solutes were measured with an Anton Paar DSA 5000 (figure A.5) vibrating tube densimeter and sound analyser.

Figure A.5. Anton Paar DSA 5000 density and sound analyser.

### *A.2.2.3. Kinematic and dynamic viscosity*

The kinematic viscosity ( $\nu$) was determined from the transit time of the liquid meniscus through a capillary viscosimeter supplied by Schott, capillary N° 0c, (0.46 ± 0.01) mm internal diameter and $K$ = 0.003201 $mm^2 \cdot s^{-1}$, using equation A.1.

$$\nu = K \cdot (t - \theta) \tag{A.1}$$

where $t$ is the efflux time, $K$ is the characteristic constant of the capillary viscometer, and $\theta$ is a correction value to correct end effects. Both parameters were obtained from the capillaries supplier (Schott). An electronic stopwatch was used to measure efflux times. In the measurements it was used a Schott-Geräte AVS 350 Ubbelohde viscometer.

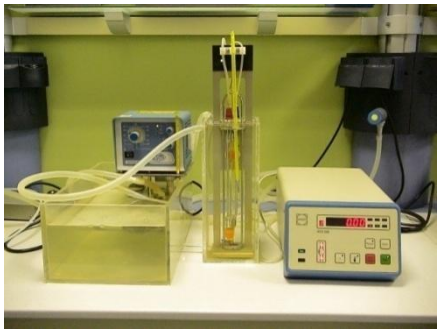

Figure A.6. Schott-Geräte AVS 350 Ubbelohde.

Each measurement was repeated at least 5. The dynamic viscosity (η) was obtained from the product of the kinematic viscosity (ν) and the corresponding density (ρ) of the mixture, in terms of equation A.2 for each mixture composition.

$$\eta = \nu \cdot \rho \tag{A.2}$$

#### *A.2.2.4. Rheological behaviour*

An Anton Paar DV-1P digital thermostated rotational viscosimeter with two coaxial cylinders has been used to carry out the rheological measurements.

Figure A.7. Anton Paar DV-1P rotational viscosimeter

### *A.2.2.5 . Fourier transform infrared spectroscopy*

The chitosan (C), chitosan sulphate (CS) and carboxymethyl chitosan (CC) powders were mixed with KBr in the ratio of 1:100 in mass and pressed into a pellet. The spectra were obtained with a Bruker IFS-66v model. The IR spectra of different solids were recorded as KBr pellets in the range of 4000–400 $cm^{-1}$.

### *A.2.2.6. Elemental analysis*

The elemental analysis was performed in a Thermo Finningan Flash model 1112 equipment that allows the quantification of carbon, hydrogen, nitrogen and sulphur content.

### *A.2.2.7. Deacetylation percentage*

A titration method has been employed to develop this kind of analysis. An accurate excess of hydrogen chloride is added to a known amount of polymers and the remaining amount of hydrogen chloride is back titrated with a sodium hydroxide solution. The resultant titration

curve shows two equivalence points, the first one corresponds to the excess hydrogen chloride, while the second corresponds to the protonated chitosans. Thus, the difference would correspond to the free deacetylated amino groups[382,383]. The two equivalence points (inflection points) of the titration curve allows determine the volume of sodium hydroxide aqueous solution employed to reach these point and on the basis of this values, the deacetylation of polymers is calculated using equation A.3.

$$\%_{NH_2} = \frac{16 \cdot (V_1 - V_2)}{w} \cdot C_{NaOH} \qquad \text{(A.3)}$$

where $V_1$ is the highest inflection point, $V_2$ is the lowest inflection point, $C_{NaOH}$ is the sodium hydroxide solution concentration, $w$ is the mass of the sample. This kind of analysis was performed by triplicate. A Crison 2000 pH meter was used to detect both inflection points.

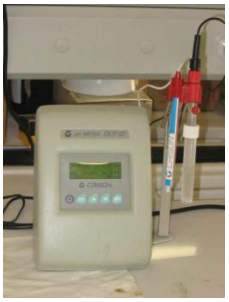

Figure A.8. Crison 2000 pH meter.

[382] Balazs N., Sipos P. Limitations of pH potentiometric titration for the determination of the degree of deacetylation of chitosan. *Carbohydrate Research* 2007, 342, 124-130.
[383] Sweidan K., Jaber A.-M., Al-jbour N., Obaidat R., Al- Remawi M., Badwan A. Further investigation on the degree of deacetylation of chitosan determined by potentiometric titration. *Journal of Excipients and Food Chemicals* 2011, 2(1), 16-25.

### *A.2.2.8. Intrinsic viscosity and average molecular weight*

The average molecular weight determination was achieved via intrinsic viscosity calculation by means of Huggins and Kramer equations[384]. The experimental set up to carry out the intrinsic viscosity determination was a capillary viscometer (Schott Gerate AVS 350) that was immersed in a thermostated bath. The solutions were prepared in sodium chloride aqueous solution, since Mark-Houwink constants have been obtained from literature[385,386,387] and these constants have been determined using this solvent to prevent the polyelectrolyte expansion in solution when the size exclusion chromatography was used to determine these constants. The kinematic viscosity ($\nu$) was determined from the transit time of the liquid meniscus through a capillary viscosimeter. The density and sound speed of polymers aqueous solutions were measured with an Anton Paar DSA 5000 vibrating tube densimeter and a sound analyser.

### *A.2.2.9. NMR spectroscopy*

$^{1}H$ and $^{13}C$ spectroscopy was applied to investigate qualitatively the solutions of pyrrolidine and glucosamine (concentration of solution between 0.1-0.5 M) loaded with $CO_2$ at room temperature in a process of $CO_2$ capture. The MestrReC 4.7 software developed by MestreLab Research was used for spectra processing. Spectra were acquired on 300 MHz Varian Mercury spectroscope. The samples of amine solution were taken from the middle zone of reactor system. Tetradeuterated Methanol ($CD_3OD$) (TMS) was used as internal reference for the processing of $^{13}C$ NMR spectra.

[384] Rao M. A. *Rheology of fluids and semisolid foods: principles and applications*. Aspen Publishers. Gaithersburg 1999.
[385] El-Sherbiny I. M., Smyth H. D. C. Poly(ethylene glycol)–carboxymethyl chitosan-based pH-responsive hydrogels: photo-induced synthesis, characterization, swelling, and in vitro evaluationas potential drug carriers. *Carbohydrate Research* 2010, 345, 2004–2012.
[386] Vongchan P., Sajomsang W., Subyen D., Kongtawelert P. Anticoagulant activity of a sulfated chitosan. *Carbohydrate Research* 2002, 337(13), 1239-1242.
[387] Parada L. G., Crespín G. D., Miranda R., Katime I. Caracterización de quitosano por viscosimetría capilar y valoración potenciométrica. *Revista Iberoamericana de Polímeros* 2004, 5(1), 1-16.

## A.2.3. Kinetics studies

The gas-liquid kinetic experiments were conducted in an experimental set-up employed previously[388](see figure A.9 and A.10), consisting on a stirred cell having a planar interfacial area, working in batches with regard to both phases.

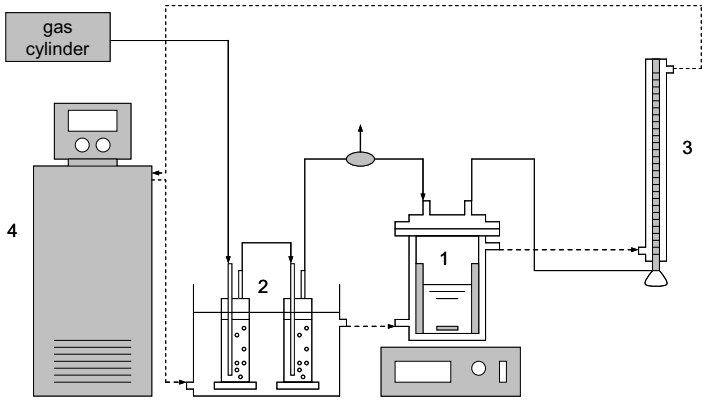


Figure A.9. Experimental set-up for kinetic studies of gas-liquid systems. (1) stirred cell, (2) humidifiers, (3) soap flowmeter, (4) cryostat-thermostat.

The gas phase, pure carbon dioxide, was passed through two humidifiers to prepare the gas phase. This procedure allows the evaluation of the liquid phase resistance to the gas transfer without other influences upon mass transfer. Water was placed into the "humidifiers".

A soap flow-meter was used to determine the carbon dioxide absorption rate accompanied by chemical reaction, produced by the amine present in the liquid phase. The absorption rate was measured by analyzing the movement of the soap film (produced by the consumption of carbon dioxide) along the calibrated glass tube[389]. This soap film was produced in the gas flowmeter for each experiment and then, the liquid phase was introduced in the stirred cell.

[388] Gómez-Díaz D., Navaza J. M. Kinetics of carbon dioxide absorption into aqueous glucosamine solutions. *AIChE Journal*. 2008, 54, 321-326.
[389] Camacho F., Sanchez S., Pacheco R., Sanchez A., La Rubia M. D. Thermal effects of $CO_2$ absorption in aqueous solutions of 2-amino-2-methyl-1-propanol. *AIChE Journal* 2005, 51, 2769-2777.

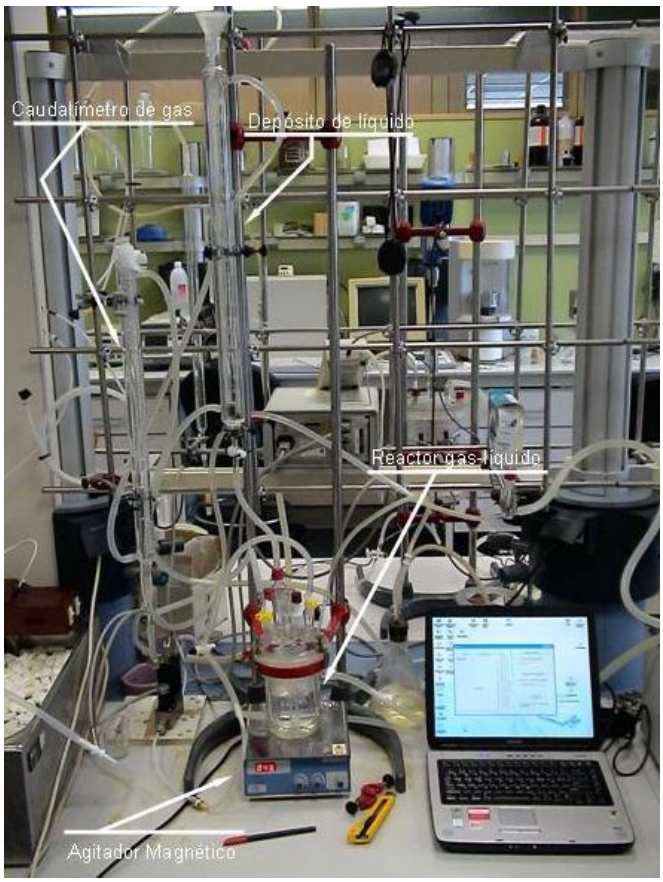


Figure A.10. Photograph of experimental set-up for kinetics studies.

The magnetic stirring began when liquid addition was concluded. At this moment the experimental data recording was developed by means of software (see figure A.11) that allows obtain the rate of the soap film in the flowmeter removing errors in the experiments with a high absorption rate. This procedure was repeated 3 times for each experimental condition, using the mean value for the calculus developed in present work. Absorption processes have been carried out at different temperatures (7 to 55 ºC) by means of the connection of the experimental set-up to a thermostat-cryostat.

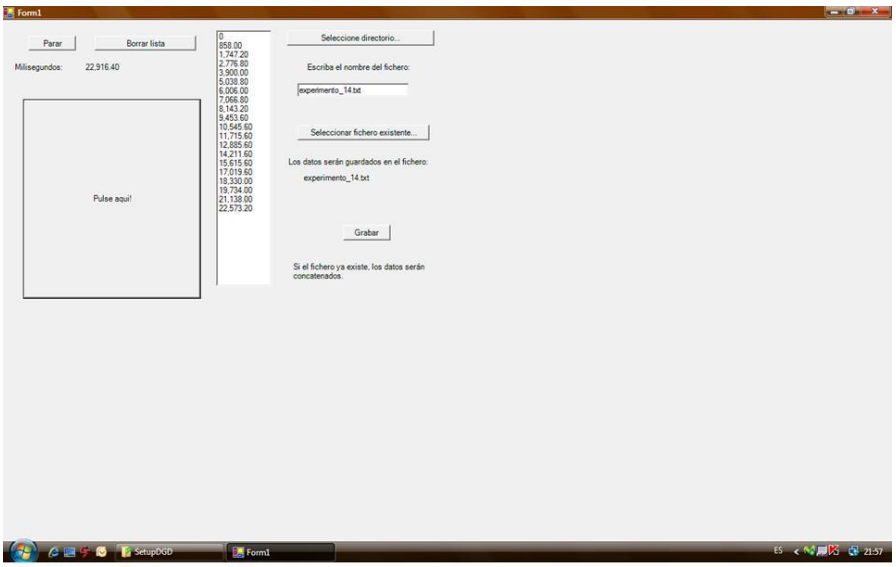


Figure A.11. Screenshot of the software employed to obtain the carbon dioxide absorption rate.

## A.2.4. Hydrodynamics studies

The bubble diameter was measured using a photographic method based on images of the bubbles taken along the height of the column, from bottom to top. A Sony (DCR-PC330E) video camera was used to obtain the images. A minimum number of 100 well-defined bubbles along the bubble column were used to evaluate the size distribution of the bubbles in the liquid phase employed, and for each gas flow-rate that has been used.

The Image Tool v3.0 software was used to carry out the necessary measurements of the bubbles geometric characteristics (see figure A.12).

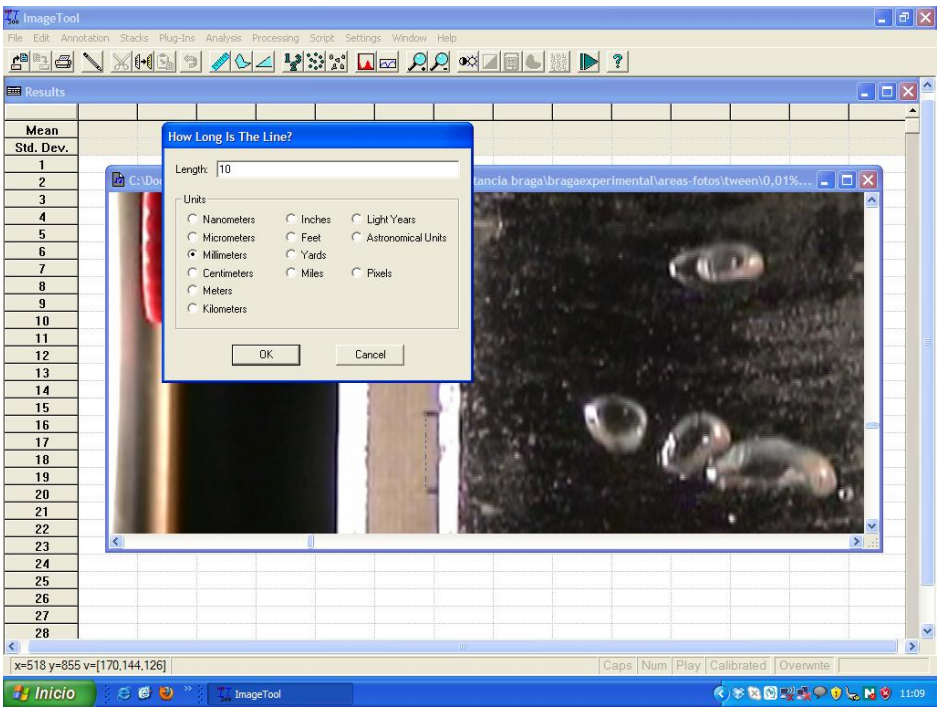


Figure A.12. Screenshot of the software employed to measure the bubbles' diameter.

The overall gas hold-up ($\varepsilon_G$) is an important parameter to determine the gas-liquid interfacial area and it was measured using the volume expansion method. The calculation of the volume change in the bubble column was based on the change observed on the liquid level and on the increase of this value after gassing using the cylindrical bubble column. The overall gas hold-up was measured using the volume expansion method[390]:

$$\varepsilon_G = \frac{\Delta V}{\Delta V + V_L} \tag{A.4}$$

[390] Vasconcelos J. M. T., Rodrigues J. M. I., Orvalho S. C. P., Alves S. S., Mendes R. L., Reis A. Effect of contaminants on mass transfer coefficients in bubble column and airlift contactors. *Chemical Engineering Science* 2003, 58, 1431–1440.

where $V_L$ is the ungassed liquid volume and $\Delta V$ is the volume expansion after gas dispersion, calculated from the liquid level change and the cross sectional area. The change in the gas-liquid dispersion volume was calculated based on the change observed on the liquid level and on the increase of this value after gassing.

The images of the bubbles obtained for the liquid phases that were employed show an ellipsoid shape. For this reason, major ($E$) and minor ($e$) axes of the projected ellipsoid (in two dimensions) were determined. The diameter of the equivalent sphere (equation A.5) was taken as the representative bubble dimension.

$$d = \sqrt[3]{E^2 \cdot e} \tag{A.5}$$

Different authors recommend using the Sauter mean diameter ($d_{32}$), which can be determined[391] using the data calculated for the equivalent diameter.

$$d_{32} = \frac{\sum_i \left(n_i \cdot d_i^3\right)}{\sum_i \left(n_i \cdot d_i^2\right)} \tag{A.6}$$

where ni is the number of bubbles that have an equivalent diameter ($d_i$).

The Sauter mean diameter and the gas hold-up values allow us the calculation of the specific interfacial area using equation A.7[392].

$$a = \frac{6 \cdot \varepsilon_G}{d_{32} \cdot \left(1 - \varepsilon_G\right)} \tag{A.7}$$

[391] Shah Y. T., Kelkar B. G., Godbole S. P., Deckwer W. D. Design parameters estimation for bubble column reactor. *AIChE Journal* 1982, 28, 353–379.
[392] van't Riet V., Tramper J. *Basic Bioreactor Design*. Marcel Dekker, New York, USA 1991.

## A.2.5. Absorption studies

Studies about the carbon dioxide mass transfer to liquid phases have been carried out using a bubble column contactor similar to other employed in previous studies developed and related to the absorption processes[393]. The gas-liquid contactors used in these studies have been described previously.

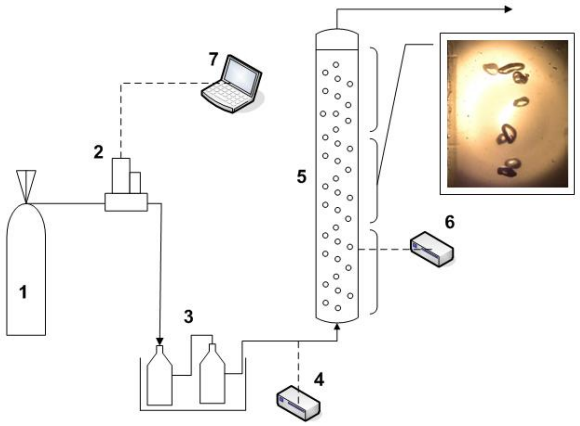


Figure A.13. Gas-liquid experimental set-up. (1) Gas cylinder; (2) Mass flowmeter/controller; (3) Humidifier and thermostatic bath; (4) Pressure gauge; (5) Bubble column contactor; (6) Temperature gauge; (7) Flowmeter controller software.

The carbon dioxide stream was put in contact with water at 25ºC to saturate the gas phase, and then to remove the water transfer from the liquid phase to the gas one. The inlet and outlet gas flow-rate were controlled and measured with two mass flow controllers (5850 Brooks Instruments). The mass flow controllers employed in the present study for the gas flow-rate and pressures were calibrated by the supplier. The pressure drop was measured between the column's inlet and outlet, using a Testo 512 digital manometer. The working regime was continuous in relation to the gas phase and batch regarding the absorbent liquid one. See experimental set-up in figure A.13.

[393] Gómez Díaz D., Navaza J. M., Sanjurjo B. Interfacial area evaluation in a bubble column in the presence of a surface-active substance. comparison of methods. *Chemical Engineering Journal* 2008, 144, 379-385.

### *A.2.5.1. Volumetric mass transfer coefficient calculation in a physical absorption process*

The procedure to determine the volumetric mass transfer coefficient ($k_L \cdot a$) is based on the measurement of the amount of gas absorbed per unit time and volume according to equation A.8[394].

$$\frac{dC}{dt} = k_L \cdot a \cdot (C^* - C) \qquad \text{(A.8)}$$

where $C^*$ is the interfacial concentration of gas compound in the liquid phase at equilibrium (i.e. the solubility of the gas in the liquid phase) and C is the concentration of carbon dioxide in the bulk liquid, that is calculated from the experimental absorption rate data.

$$\ln\left(\frac{C^*}{C^* - C}\right) = k_L \cdot a \cdot t \qquad \text{(A.9)}$$

Integrating equation A.8, equation A.9 is obtained. Then, plot of ln [C*/(C*-C)] against time show a straight line passing the origin and the slop of this line is the value of $k_L \cdot a$.

Using the experimental values of volumetric mass transfer coefficient and the determined specific interfacial area, the mass transfer coefficient values for each experimental condition can be calculated by means of equation A.10.

$$k_L = \frac{k_L \cdot a}{a} \qquad \text{(A.10)}$$

[394] Vázquez G., Cancela M. A., Varela R., Alvarez E., Navaza J. M. Influence of surfactants on absorption of $CO_2$ in a stirred tank with and without bubbling. *Chemical Engineering Journal* 1997, 67, 131-137.

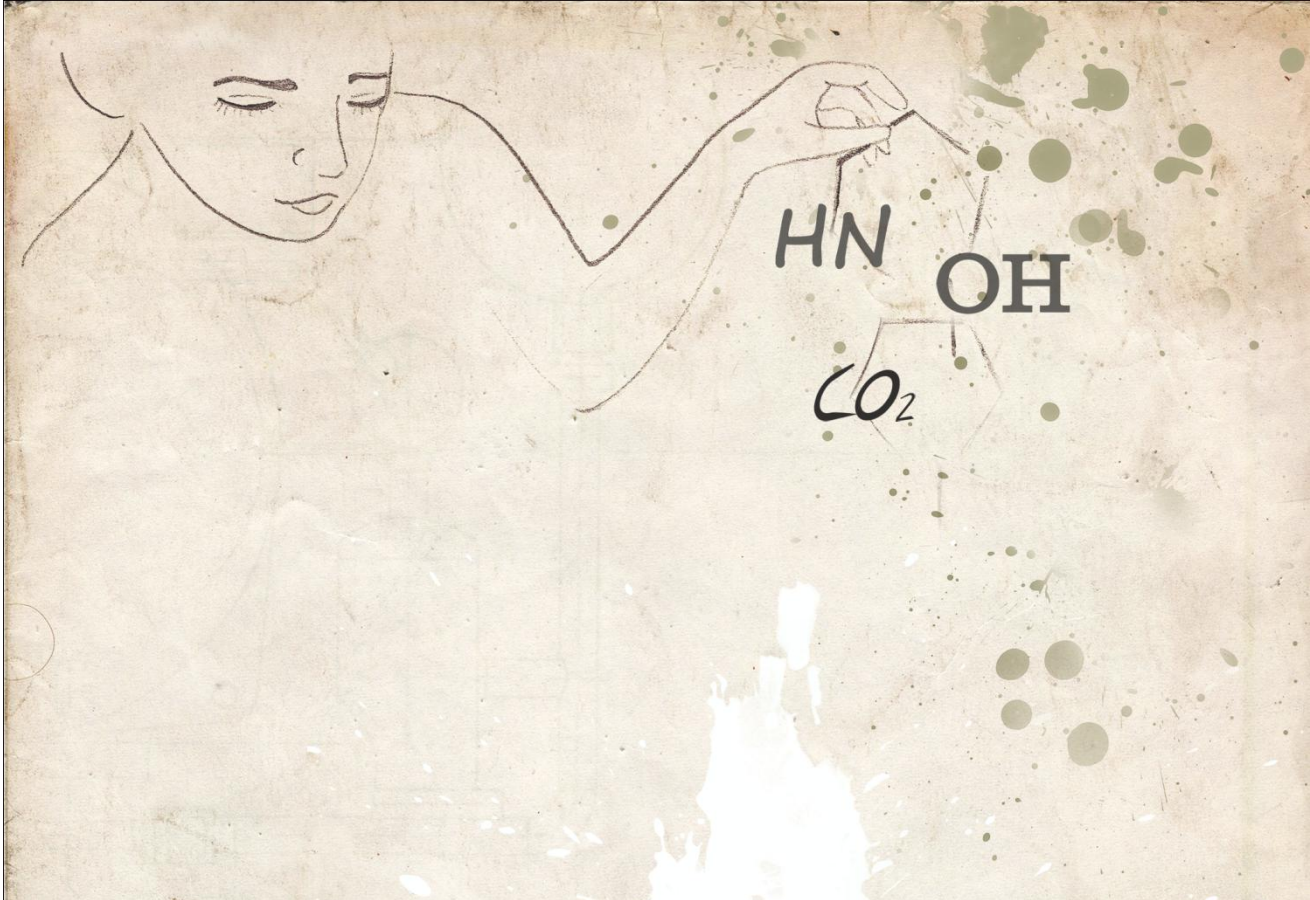


# Appendix B:

## *Published/accepted papers*

**PAPERS CHAPTER 2:**

AIChE

# Kinetics of Carbon Dioxide Chemical Absorption into Cyclic Amines Solutions

**Alicia García-Abuín, Diego Gómez-Díaz, José M. Navaza, and Isabel Vidal-Tato**
PF&PT and Ecoeficiencia Research Teams, Dept. of Chemical Engineering, ETSE, University of Santiago de Compostela, Santiago de Compostela, Galicia E-15782, Spain

*DOI 10.1002/aic.12442*
*Published online December 28, 2010 in Wiley Online Library (wileyonlinelibrary.com).*

*Chemical reaction kinetics between carbon dioxide with two cyclic amines (pyrrolidine and piperidine) have been studied using a stirred tank reactor with a planar interfacial area. The operational variables considered in this work have been the amine concentration in the liquid phase and the reaction temperature. Specific absorption rates have been determined under different experimental conditions. Results indicate that the absorption process occurs in a pseudo first reaction regime exhibited first-order kinetic with respect carbon dioxide and a second order for both cyclic amines. The reaction-rate constant was determined under the different experimental conditions, and it was correlated depending on the temperature by means of an Arrhenius type equation.* © 2010 American Institute of Chemical Engineers *AIChE J*, 57: 2244–2250, 2011
*Keywords: absorption, gas purification, mass transfer, reaction kinetics*

## Introduction

Globally speaking, about one-third of all the anthropogenic $CO_2$ emissions come from fossil fuels, such as coal and oil, used to generate energy. A variety of industrial processes also emit large amounts of $CO_2$ from each plant, for example oil refineries, cement works, and iron production.[1] There is a growing political and public concern, supported by consensus among the scientific community, about the global emissions growth, that will soon drive atmospheric $CO_2$ concentrations to levels never seen before, bringing a growing risk of a fast climate change.

The development of more effective processes for acid gases capture (such as carbon dioxide and sulfur dioxide) have produced an important increase in the research studies based on the development of new systems using chemical absorption between the acid gases and selective liquid phases. Absorption processes represent the most important physicochemical operation to remove $CO_2$ from gaseous streams. The absorption can be done either by using physical solvents such as water, methanol (Rectisol process), or *N*-methyl-2-pyrrolidone (Lurgi's Purisol process), or by using chemical solvents (reactive absorption), for instance, $K_2CO_3$ (Benfield process), monoethanolamine (MEA; Girbotol process), Sulfolan + diisopropanolamine + water (Shell's Sulfinol process)[2] or amines blends.[3–5] Reactive absorption is the most preferred option used in the gas-processing industry for $CO_2$ removal, and the aqueous solutions of alkanolamines remain an industrial important class of compounds, used in the natural gas, petroleum chemical plants, and ammonia industries for the removal of $CO_2$ and $H_2S$ from gas streams. A wide variety of alkanolamines, such as MEA, diethanolamine, di-isopropanolamine, and *N*-methyldiethanolamine have been used industrially for a number of years.[2]

This study pursues two aims: (1) the development of new alternative amine-based solvents, which are attractive for the enhancement of $CO_2$ capture, based on the use of cyclic amines and (2) the kinetic characterization of the reaction between carbon dioxide and cyclic primary amines [piperidine (PIP) and pyrrolidine (PYR)].

## Experimental Section

Commercial grade $CO_2$ gas of 99.998% purity, supplied by Carburos Metálicos, (Spain) was used in this work. PIP and PYR of $\geq$99% purity was obtained from Fluka (USA). MEA has been

Correspondence concerning this article should be addressed to J. M. Navaza at josemanuel.navaza@usc.es.

Chemical Engineering Journal 162 (2010) 37–42

Contents lists available at ScienceDirect

Chemical Engineering Journal

journal homepage: www.elsevier.com/locate/cej

# $CO_2$ capture by aqueous solutions of glucosamine in a bubble column reactor

Alicia García-Abuín, Diego Gómez-Díaz, José M. Navaza*, Isabel Vidal-Tato

*PFEAPT and Ecoeficiencia Research Teams, Department of Chemical Engineering, ETSE, University of Santiago de Compostela, c/Lope Gómez de Marzoa s/n, Campus Vida, E-15782, Santiago de Compostela, Galicia, España, Spain*

ARTICLE INFO

*Article history:*
Received 8 February 2010
Received in revised form 26 April 2010
Accepted 27 April 2010

*Keywords:*
Absorption
Carbon dioxide
Bubble column
Reaction

ABSTRACT

The present work analyses the carbon dioxide ($CO_2$) capture process by means of absorption with chemical reaction with glucosamine aqueous solutions, using a bubble column reactor (BCR). Experimental results indicate that this reagent has a similar behaviour to other common amines (i.e. monoethanolamine, widely used in $CO_2$ capture), as regarding the capture rate of this acidic gas. The value of the mass transfer coefficient corresponding to the liquid phase has been determined, and the effect of different operation conditions upon the value of that coefficient has also been analysed (amine concentration, pH and gas flow-rate).



## 1. Introduction

The fossil fuel combustion from power plants or refineries is one of the most important sources of carbon dioxide emission [1]. Several technologies are available to reduce the carbon dioxide emission from industrial gas streams, but the chemical absorption with alkanolamines (i.e. monoethanolamine: MEA, diethanolamine: DEA, di-2-propanolamine: DIPA, triethanolamine: TEA, and methyldiethanolamine: MDEA) is the most widely used method for low partial pressures of carbon dioxide [2,3]. This method is efficient and it usually permits the removal of a high percentage of the carbon dioxide emitted. Previous studies concluded that primary and secondary alkanolamines react, directly and reversibly, to the carbon dioxide by forming a zwitterion intermediate, which is deprotonated by the bases present in the solution to form a stable carbamate [4,5], even though the formation of the carbamate increases the reaction rate but usually limits the loading to 0.5 mol of $CO_2$/(mol of amine) [6]. By contrast, tertiary amines do not react directly to the carbon dioxide in order to form carbamate. Generally, tertiary amines react more slowly to $CO_2$ than primary and secondary amines [7].

Recently, our research team have performed interesting studies using 2-amino-2-deoxy-D-glucose, called glucosamine (GA), in order to analyse the absorption of carbon dioxide in a gas–liquid contactor. The absorption of $CO_2$ in this system is accompanied by a chemical reaction between the glucosamine and the $CO_2$ previously absorbed in the liquid phase. This is a first-order reaction regarding both compounds ($CO_2$ and GA), as it was concluded by our research group in previous studies [8]. The mechanism suggested for this reaction is a zwiteronic type, where the global process of absorption with a chemical reaction has a moderately fast regime, since the Hatta number (Ha) takes values between $0.3 < Ha < 3$ for the experimental conditions used in the present work [8]. The Hatta number is a dimensionless parameter that compares the absorption rate of a solute in a reactive system to the absorption rate of the same solute, in the case of physical absorption [8].

This new method of $CO_2$ capture has great advantages if we compare it to more conventional systems, based on the use of the amines abovementioned. These advantages are fundamentally a minor need of safety measures and a minor chemical risk when aqueous solutions of glucosamine are manipulated. Moreover, this system shows a kinetic capture of $CO_2$ with a similar rate to other systems based in amines industrially used, such as MEA or DEA [8,9]. These previous studies have analysed the kinetics of the chemical reaction but not the mass transfer process, necessary to evaluate the global absorption process, that is the aim of present study.

Then, in the present work, the behaviour of glucosamine aqueous solutions is analysed in order to capture $CO_2$ by means of an absorption process with a chemical reaction in a bubble column reactor (BCR), and this process permits us the analysis of the mass transfer process and the interfacial area generated between two phases (gas and liquid). Therefore, in addition to the capacity of $CO_2$ absorption, we have also analysed the influence of the $CO_2$ loading, the amine concentration in the liquid phase, as well as the gas flow-rate fed to the contactor upon the global process of $CO_2$ absorption and the interfacial area gas–liquid.

* Corresponding author.
*E-mail address:* josemanuel.navaza@usc.es (J.M. Navaza).

1385-8947/$ – see front matter © 2010 Elsevier B.V. All rights reserved.
doi:10.1016/j.cej.2010.04.050

**PAPERS CHAPTER 3:**

*J. Chem. Eng. Data* **2008,** *53,* 2671–2674 

# Surface Tension of Aqueous Solutions of Short *N*-Alkyl-2-pyrrolidinones

**Alicia García-Abuín, Diego Gómez-Díaz, José M. Navaza,* and Isabel Vidal-Tato***

Department of Chemical Engineering, ETSE, University of Santiago de Compostela, Rúa Lope Gómez de Marzoa s/n, E-15706 Santiago de Compostela, Galicia, Spain

The surface tension of aqueous solutions of 2-pyrrolidinone, 1-methyl-2-pyrrolidinone, and 1-ethyl-2-pyrrolidinone has been measured at temperatures from (20 to 50) °C over the whole range of concentrations. The surface tensions of these aqueous binary mixtures show more concentration dependence on the water-rich side. The addition of a small amount of *N*-alkyl-2-pyrrolidinone drastically reduces the surface tension of water. This effect is related to not only the presence of hydrophobic groups that tend to remain at the air−water interface but also the influence of the complex interactions between *N*-alkyl-2-pyrrolidinones molecules on the surface tension.

## Introduction

Short-chain *N*-alkyl-2-pyrrolidinones are completely miscible over the entire composition range with water. They have been used as cosolvents in the petroleum industry to increase the selectivity and solvent power for extracting aromatic hydrocarbons. These pyrrolidinones are also used in pharmaceutical formulations and in the painless administration of therapeutic agents to the bloodstream in a controlled manner because they enhance the transdermal transport of drugs.

These cyclic amides have excellent thermal and chemical stability and are used as absorbents of sour gases from crude natural gas.[1] The mixed use of amides with certain amounts of water is preferred so that the mixture functions effectively. The knowledge of the physical properties of systems water + cyclic amides over the entire composition range and at different temperatures is very useful for different processes such as mass transfer operations. Surface tension has great importance[2] regarding the behavior and hydrodynamics in mass transfer operations, and the value of this property could play an important role in this kind of operations.

Previous studies have analyzed other cyclic amides with regards to surface tension, such as *N*-cyclohexyl-2-pyrrolidinone,[3] *N*-butyl-2-pyrrolidinone,[4] or *N*-hexyl-2-pyrrolidinone,[5] and certain kind of preaggregation was found before the presence of micelles in aqueous solution.

The present work has obtained the surface tension of different *N*-alkyl-2-pyrrolidinones + water at different temperatures and over the entire composition range to discover the influence of composition, temperature, and the role of substituents on the surface tension and the interactions and aggregation in this kind of system.

## Experimental Section

***Materials.*** 2-Pyrrolidinone (CAS no. 616-45-5), 1-methyl-2-pyrrolidinone (CAS no. 872-50-4), and 1-ethyl-2-pyrrolidinone (CAS no. 2687-91-4) were supplied by Fluka with a purity of ≥ 99 % for 2-pyrrolidinone and ≥ 98 % for the other compounds. All liquid mixtures were prepared by mass using an analytical balance (Kern 770) with a precision of ± $10^{-4}$ g.

* To whom correspondence should be addressed. Fax: +3481595012. E-mail: josemanuel.navaza@usc.es; isabel.vidal.tato@usc.es.

**Table 1. Surface Tension $\sigma$ for Water (1) + 2-Pyrrolidinone (2) from (20 to 50) °C**

| | $T$/°C | | | | |
|---|---|---|---|---|---|
| | 20 | 25 | 30 | 40 | 50 |
| $x_2$ | $\sigma$/mN·m$^{-1}$ | | | | |
| 0.0000 | 72.65 | 72.05 | 71.21 | 69.52 | 67.92 |
| 0.0002 | 60.40 | 58.90 | 57.30 | 55.40 | 53.20 |
| 0.0006 | 55.69 | 54.60 | 53.93 | 52.20 | 51.05 |
| 0.0100 | 52.90 | 51.68 | 50.80 | 49.80 | 49.10 |
| 0.0150 | 52.40 | 51.19 | 50.23 | 49.30 | 48.70 |
| 0.0500 | 50.72 | 49.58 | 48.68 | 47.77 | 46.34 |
| 0.0700 | 50.26 | 49.28 | 48.45 | 47.00 | 45.89 |
| 0.1000 | 49.96 | 48.91 | 48.00 | 46.49 | 45.58 |
| 0.2000 | 48.91 | 48.08 | 47.09 | 45.89 | 45.13 |
| 0.3000 | 47.93 | 47.17 | 46.42 | 45.43 | 44.60 |
| 0.4000 | 47.54 | 46.87 | 46.19 | 45.28 | 44.53 |
| 0.5000 | 47.17 | 46.72 | 46.02 | 45.21 | 44.45 |
| 0.6000 | 47.10 | 46.64 | 45.81 | 44.91 | 44.15 |
| 0.7000 | 47.10 | 46.42 | 45.66 | 45.00 | 44.23 |
| 0.8000 | 46.94 | 46.42 | 45.66 | 44.68 | 43.85 |
| 0.9000 | 46.64 | 46.11 | 45.51 | 44.53 | 43.77 |
| 1.0000 | 46.31 | 45.81 | 45.22 | 44.12 | 43.19 |

The maximum uncertainty of the sample preparations in mole fraction was ± 0.0006.

***Methods.*** Surface tension was determined using a Krüss K-11 tensiometer and the Wilhelmy plate method. A commercial platinum plate supplied by Krüss was employed. The platinum plate was cleaned with water and acetone and was flame dried before each measurement. The uncertainty of the measurement was ± 0.07 mN·m$^{-1}$. In general, each surface tension value reported was an average of ten measurements. Before the surface tension was measure, the samples were stirred in a thermostatted vessel that was closed to prevent evaporation. Surface tension measurements were carried out in the range of (20 to 50) °C. The measurement vessel was connected to a thermostat−cryostat bath (Selecta Frigiterm) controlled to ± 0.1 °C.

## Results and Discussion

The present work analyzes the influence of mixture composition and temperature on the surface tension of systems formed by water and different short *N*-alkyl-2-pyrrolidinones. Tables 1, 2, and 3 show the value of surface tension determined for each system and for all of the compositions and temperatures

10.1021/je800589e CCC: $40.75 
Published on Web 10/21/2008

962 *J. Chem. Eng. Data* **2010,** *55,* 962–965

# Influence of Temperature and Composition upon Density, Viscosity, Speed of Sound, and Refractive Index of Aqueous Solutions of 1-Ethyl-2-pyrrolidinone

**Antonio Blanco, Alicia García-Abuín, Diego Gómez-Díaz, José M. Navaza,* and Isabel Vidal-Tato***

PF&PT and Ecoeficiencia Research Teams, Department of Chemical Engineering, ETSE, University of Santiago de Compostela, Rúa Lope Gómez de Marzoa s/n, E-15782, Santiago de Compostela, Galicia, Spain

Experimental density, viscosity, speed of sound, and refractive index for aqueous solutions of 1-ethyl-2-pyrrolidinone were measured over the entire composition range and at different temperatures (293 to 323) K. Excess properties and deviations have been calculated, and their dependence on composition was mathematically represented by a Redlich−Kister-type equation. The hydration of pyrrolidinone molecules plays an important role in the thermophysical behavior of this mixture.

## Introduction

Short chain *N*-alkyl-2-pyrrolidinones are completely miscible over the entire composition range with water. They have been used as cosolvents in the petroleum industry to increase the selectivity and solvent power for extracting aromatic hydrocarbons. These pyrrolidinones are also used in pharmaceutical formulations and in the administration of therapeutic agents to the bloodstream painlessly in a controlled manner because they enhance the transdermal transport of drugs. These cyclic amides have excellent thermal and chemical stability, and they are used as absorbents of sour gases from crude natural gas or entrainer to alter the separation factor in distillation process.[1]

The knowledge of physical properties of the systems water + cyclic amides over the entire composition range and at different temperatures is highly useful to understand some interfacial phenomena. For example, viscosity plays an important role regarding the behavior and hydrodynamics in mass transfer operations.[2,3]

Previous studies have analyzed other cyclic amides, such as 2-pyrrolidinone, 1-methyl-2-pyrrolidinone, or 1-vinyl-2-pyrrolidinone,[4−7] with regard to different physicochemical properties, and the influence of the substituent upon the behavior obtained for different properties and excess parameters has been analyzed.

The present work shows the behavior of different physicochemical properties (density, viscosity, speed of sound, and refractive index) for 1-ethyl-2-pyrrolidinone + water at different temperatures and over the entire composition range to study the influence of composition and temperature and the role of substituent.

## Experiments

***Materials.*** 1-Ethyl-2-pyrrolidinone (CAS number: 2687-91-4) was supplied by Fluka with a mass fraction purity ≥ 0.98. All liquid mixtures were prepared by mass using an analytical balance (Kern 770). The uncertainty of the sample's preparation in mole fraction was ± 0.0006. Water contents were measured using a Karl Fischer titration method in a Metrohm 737 KF coulometer with a mass fraction of 0.001.

* Corresponding authors. E-mail: josemanuel.navaza@usc.es (J. M. Navaza) and isabel.vidal.tato@usc.es (I. Vidal-Tato).

***Methods. Density and Speed of Sound.*** The densities of pure components and the mixture of different solutes were measured with an Anton Paar DSA 5000 vibrating tube densimeter and sound analyzer. The uncertainty in the density and speed of sound measurements was ± $1.6 \cdot 10^{-4}$ g·cm$^{-3}$ and ± 0.29 m·s$^{-1}$, respectively.

Also, the adiabatic compressibility, $\kappa_s$, was calculated from speed of sound values and density values using the Laplace equation

$$\kappa_s = \frac{1}{u^2 \cdot \rho} \tag{1}$$

where $u$ is the speed of sound and $\rho$ is the density of the solution.

***Viscosity.*** The kinematic viscosity ($\nu$) was determined from the transit time of the liquid meniscus through a capillary viscosimeter supplied by Schott, capillary N° 0c, (0.46 ± 0.01) mm internal diameter, and $K = 0.003201$ mm$^2$·s$^{-1}$, using eq 2.

$$\nu = K \cdot (t - \theta) \tag{2}$$

where $t$ is the efflux time; $K$ is the characteristic constant of the capillary viscometer; and $\theta$ is a correction value to correct end effects. Both parameters were obtained from the capillaries supplier (Schott). An electronic stopwatch with an accuracy of ± 0.01 s was used to measure efflux times. In the measurements, a Schott-Geräte AVS 350 Ubbelohde viscometer was used. Each measurement was repeated at least 5 times, and the uncertainty of this measurement is ± 0.0054 mm$^2$·s$^{-1}$. The dynamic viscosity ($\eta$) was obtained from the product of the kinematic viscosity ($\nu$) and the corresponding density ($\rho$) of the mixture, in terms of eq 3 for each mixture composition.

$$\eta = \nu \cdot \rho \tag{3}$$

***Refractive Index.*** Refractive index was determined using an Atago RX-5000 refractometer. Before measurements, the refractometer was calibrated using distilled−deionized water in accordance with the instrument instructions. The mixtures were directly injected from the stock solution stored at work temperature to avoid evaporation. The refractive index measurements were done after the liquid mixtures attained the constant temperature of the refractometer. This procedure was repeated at least three times, and the uncertainty of the measurement

10.1021/je9003959 CCC: $40.75 
Published on Web 07/09/2009

JOURNAL OF CHEMICAL & ENGINEERING DATA

SHORT ARTICLE

pubs.acs.org/jced

# Density, Speed of Sound, Viscosity, Refractive Index, and Excess Volume of *N*-Methyl-2-pyrrolidone + Ethanol (or Water or Ethanolamine) from $T$ = (293.15 to 323.15) K

A. García-Abuín,[†] D. Gómez-Díaz,*[,†] M. D. La Rubia,[‡] and J. M. Navaza[†]

[†]PF&PT Research Team, Department of Chemical Engineering, ETSE, University of Santiago de Compostela, Galicia, Spain

[‡]Bioprocesos Research Team, Department of Chemical, Environmental and Materials Engineering, EPS, University of Jaén, Andalucía, Spain

**ABSTRACT:** Experimental density, viscosity, speed of sound, and refractive index for binary mixtures of *N*-methyl-2-pyrrolidone with water, ethanol, and ethanolamine were measured over the entire composition range at different temperatures of (293.15 to 323.15) K. The effect of composition and temperature upon different physical properties has been analyzed. Excess volumes have been calculated, and their dependence on composition was mathematically represented by a Redlich−Kister-type equation.

## INTRODUCTION

Cyclic amides have shown important characteristics such as high density, high boiling point, and high polarity solvents, which allow the usability at an industrial level. Also the high solubility in water allows the use of this kind of substance in a wide range of industrial and laboratory operations. More specifically, *N*-methyl-2-pyrrolidone (NMP) has shown selectivity with regard to unsaturated and aromatic hydrocarbons and sulfur gases. The low reactivity and high solubility are important characteristics that allow use of the NMP as an extraction agent in lubricant oil processing and the scrubbing treatment of natural gas.[1] On the other hand, the excellent thermal and chemical stability is another interesting characteristic for the use of NMP as solvent in different reaction systems. Also, the NMP could be used as cosolvent with water, hydrocarbons, alcohols, glycol ether, and ketones.[2] NMP in aqueous solution is used in the carbon dioxide capture process by means of physical absorption.[3] The knowledge of different physical properties of systems that involve NMP is an important starting point to optimize different mass transfer operations.

The present work analyzes different physical properties in NMP-based binary liquid systems. More specifically, the liquid systems employed in this study include NMP + water (or ethanol or ethanolamine). Previous studies have analyzed certain physical properties for the NMP + water system at other temperatures.[4] This kind of system has been chosen due to the important characteristics and uses as a solvent, in the separation process, and in acid gas capture.[4]

## EXPERIMENTAL SECTION

*N*-Methyl-2-pyrrolidone (CAS number 872-50-4) with a mass purity of ≥ 0.99 was supplied by Fluka. Ethanolamine (CAS number 141-43-5) and ethanol (CAS number 64-17-5) were supplied by Sigma-Aldrich with a mass purity of ≥ 0.99 and ≥ 0.995, respectively. Bidistilled water was used to prepare aqueous systems. All solutions were prepared by mass using an analytical balance (Kern 770) with a precision of $10^{-4}$ g. The uncertainty in the mole fraction for prepared sample solutions was found to be ± 0.0005.

**Density and Speed of Sound.** The density and speed of sound of water and aqueous solutions of different solutes were measured with an Anton Paar DSA 5000 vibrating tube densimeter and sound analyzer. The uncertainty in the density and speed of sound measurements was $\pm\ 1.7 \cdot 10^{-4}$ g·cm$^{-3}$ and ± 0.22 m·s$^{-1}$, respectively. In general, each value came from an average of three measurements.

Also, the adiabatic compressibility, $\kappa_s$, was calculated from speed of sound values and density values using the Laplace equation

$$\kappa_s = \frac{1}{u^2 \cdot \rho} \tag{1}$$

where $u$ is the speed of sound and $\rho$ is the density of the solution.

**Viscosity.** The kinematic viscosity ($\nu$) was determined from the transit time of the liquid meniscus through different capillary viscosimeters supplied by Schott, capillary nos. 0c, I, Ic, and Ia, using eq 2.

$$\nu = K \cdot (t - \theta) \tag{2}$$

where $t$ is the efflux time; $K$ is the characteristic constant of the capillary viscometer; and $\theta$ is a correction value to correct end effects. Both parameters were obtained from the capillaries supplier (Schott). An electronic stopwatch with an accuracy of ± 0.01 s was used to measure efflux times. In the measurements, a Schott-Geräte AVS 350 Ubbelohde viscometer was used. Each measurement was repeated at least 5 times, and the uncertainty of this measurement is ± 0.0017 mm$^2$·s$^{-1}$. The dynamic viscosity ($\eta$) was obtained from the product of the kinematic viscosity ($\nu$)

**Received:** September 27, 2010
**Accepted:** January 4, 2011
**Published:** January 24, 2011

**PAPERS CHAPTER 4:**



**Isabel Belo**[1]
**Alicia García-Abuín**[2]
**Diego Gómez-Díaz**[2]
**José M. Navaza**[2]
**Isabel Vidal-Tato**[2]

[1] University of Minho, Department of Biological Engineering – CEB, Chemical and Biochemical Engineering Group, Braga, Portugal.

[2] University of Santiago de Compostela, Department of Chemical Engineering – ETSE, PF&PT and Ecoefficiency Research Teams, Santiago de Compostela, Spain.

Research Article

# Effect of Tween 80 on Bubble Size and Mass Transfer in a Bubble Contactor

Gas absorption in aqueous solutions with Tween 80 and absorption processes based on hydrodynamics and mass transfer is determined. The impact of surfactant concentration on gas holdup and gas-liquid interfacial area is analyzed, observing an increase of these parameters with surfactant concentration. The influence of liquid-phase contamination on the absorption process is investigated on the basis of the liquid-film mass transfer coefficient, removing the effect caused by the presence of a surfactant and the gas flow rate on the interfacial area and, thereby, on the volumetric mass transfer coefficient. The opposite effect on the mass transfer coefficient can be observed which decreases in the presence of the surfactant.

**Keywords:** Absorption, Interfacial area, Mass transfer coefficient, Surfactant

*Received:* March 11, 2011; *revised:* July 14, 2011; *accepted:* August 17, 2011

**DOI:** 10.1002/ceat.201100140

## 1 Introduction

Several industrial processes are based on gas-liquid equipments and for this reason a suitable gas absorption rate is an important point in different chemical and biochemical processes which involve this kind of operation. The gas phase is commonly placed in the contactor by means of small bubbles in order to supply a high interfacial area and consequently an increase in mass transfer between the phases. The liquid phases commonly found in the chemical industry are very complex due to the operating conditions and presence of several compounds. Therefore, important research studies were performed to understand the influence of the liquid phase properties on the bubble formation phenomenon. Nevertheless, whilst the impact of the liquid density and viscosity was extensively studied, the liquid surface tension and its effects must be analyzed in gas-liquid contactors. Taking into account the results and conclusions concerning the effect of the liquid surface tension, its influence is not clearly separated from the effect caused by density and viscosity [1, 2].

In the last few years, several studies enhanced the knowledge about the absorption processes in systems involving the presence of surface-active substances. Several studies concluded that low concentrations of surface-active additives can affect gas-liquid mass transfer parameters such as the volumetric mass transfer coefficient ($k_La$) and/or mass transfer coefficient ($k_L$) [3, 4]. These studies concentrated on the influence of different operation variables on the global mass transfer and, more specifically, on gas holdup [5], bubble diameters and gas-liquid interfacial area [6], interfacial turbulence [7], and mass transfer coefficient [8]. Other researchers were interested in analyzing the influence of the surfactants' nature, taking into account the molecule sizes [9] as well as their ionic character [8].

Nowadays, surface agents in gas-liquid systems have reached great importance, mainly due to the presence of this kind of substances in bioreactors: (i) as product of the bioreaction (production of biosurfactants) [10], and (ii) as stabilizer substance in the two-phase partition bioreactors to maintain the emulsion formed in the liquid phase [11].

Here, the absorption process behavior in complex systems involving the use of a surfactant (Tween 80) commonly applied in numerous processes that imply gas-liquid mass transfer processes [12] such as fermentation operations in gas-liquid bioreactors, is investigated. The system employed in this study is analyzed taking into account hydrodynamic parameters (such as gas holdup, bubble diameter, and interfacial area) and mass transfer based on the determination of the mass transfer coefficient.

## 2 Materials and Methods

Tween 80 (nonionic surfactant) was supplied by Sigma-Aldrich (CAS No. 9005-65-6) with an average molecular weight of 1310 g mol$^{-1}$. Carbon dioxide of 99.998% purity was from

**Correspondence:** Dr. D. Gómez-Díaz (diego.gomez@usc.es), University of Santiago de Compostela, Department of Chemical Engineering – ETSE, Rúa Lope Gómez de Marzoa s/n, E-15786 A Coruña, Spain.

  

Chemical Engineering Journal 171 (2011) 1108–1113

Contents lists available at ScienceDirect

Chemical Engineering Journal

journal homepage: www.elsevier.com/locate/cej

# Hydrodynamics of a carbon dioxide/water/silicone oil bubble column

A. García-Abuín, D. Gómez-Díaz*, J.M. Navaza, I. Vidal-Tato

*Department of Chemical Engineering, ETSE, University of Santiago de Compostela, Galicia, E-15782, Spain*

ARTICLE INFO

*Article history:*
Received 21 February 2011
Received in revised form 29 April 2011
Accepted 4 May 2011

*Keywords:*
Absorption
Emulsion
Surfactant
Silicon oil
Bubble diameter
Interfacial area

ABSTRACT

The present work analyses the hydrodynamic behaviour of a gas phase in a bubble column using different emulsions as liquid phase. The hydrodynamic behaviour was analysed on the basis of gas hold-up, bubble diameter and gas–liquid interfacial area; the different variables employed in this study [gas flow-rate (between 18 and 40 L $h^{-1}$), as well as the organic phase nature, the organic phase concentration (between 0 and 1% (vol)) and the surfactant presence (between 0 and 0.1% (vol))] have been taken into account. The results obtained have been explained on the basis of the liquid phase physical properties and the special characteristics of the gas–liquid–liquid systems.



## 1. Introduction

Reactors or bioreactors that involve two liquid phases (organic and aqueous phases) are used nowadays as an alternative system to other ones, since these kind of reactors may improve the overall process absorption efficiency [1] by means of an increase in the mass transfer rate. Two main application fields have been considered for these reactors: (i) reactors to clean gaseous streams by means of treating pollutant gases (for instance, the presence of an organic liquid phase could enhance the absorption of hydrophobic volatile organic compounds) [2,3]; (ii) bioreactors where the addition of organic liquid phases could enhance the oxygen mass transfer rate [4]. This enhancement is very important when the gas absorption is the limiting step in the global process. In these cases, an increase in the oxygen transfer rate could produce an important increase in the process productivity. Several studies [5,6] have analysed the effect of different organic liquids (i.e. toluene, dodecane, heptane, etc.) on the oxygen absorption process; however, different experimental results have been obtained showing contradictory conclusions.

On the one hand, several studies have found positive effects upon the global absorption process [7,8] but, on the other hand, the opposite behaviour has also been obtained [9]. This variety of results could be due to the lack of experimental data in these studies: those about the analysis of the interfacial area produced between gas–liquid–liquid systems, as well as the influence of the organic substances upon the gas hold-up, the bubbles size and the interfacial area. Some of these studies have found a behaviour that implies a decrease in the value of the interfacial area with an organic phase presence [8,10,11]; however, other studies show the opposite behaviour [12–14]. Being more precise, certain studies have analysed more deeply in the last few years the influence of alkanes upon the bubble size and the interfacial area [15,16] using a stirred tank contactor, observing a decrease in the bubble diameter when the alkanes concentration increases. The same behaviour has been found for the interfacial area due to the reduction in the value of the gas hold-up (caused by the increase in viscosity).

## 2. Experimental

Two different silicone oils (Silicone oil DC 200 or polydimethylsiloxane, CAS number: 63148-62-9), supplied by Aldrich, have been used in the present work with a different polymerisation degree, producing a different viscosity value (10 mPa s and 100 mPa s for S1 and S2, respectively). Tween80, a non-ionic surfactant derived from polyethoxylated sorbitan and oleic acid, was supplied by Sigma-Aldrich (CAS number: 9005-65-6). The silicone oil concentration was varied from 0 to 1% in volume and the surfactant concentration remains constant at 0.1% in volume, when this compound was used. Systems with S1 silicone oil have been studied in the presence and absence of surfactant, but S2 systems can only be used in the presence of a surfactant because, without Tween80, the liquid phases separation is produced in the bubble column.

The photographic method, used in this study to determine the gas–liquid interfacial area, has been developed using a square bub-

* Corresponding author at: Department of Chemical Engineering, ETSE, University of Santiago de Compostela, Rúa Lope Gómez de Marzoa, Santiago de Compostela, E-15782, Spain.
*E-mail address:* diego.gomez@usc.es (D. Gómez-Díaz).

1385-8947/$ – see front matter © 2011 Elsevier B.V. All rights reserved.
doi:10.1016/j.cej.2011.05.007

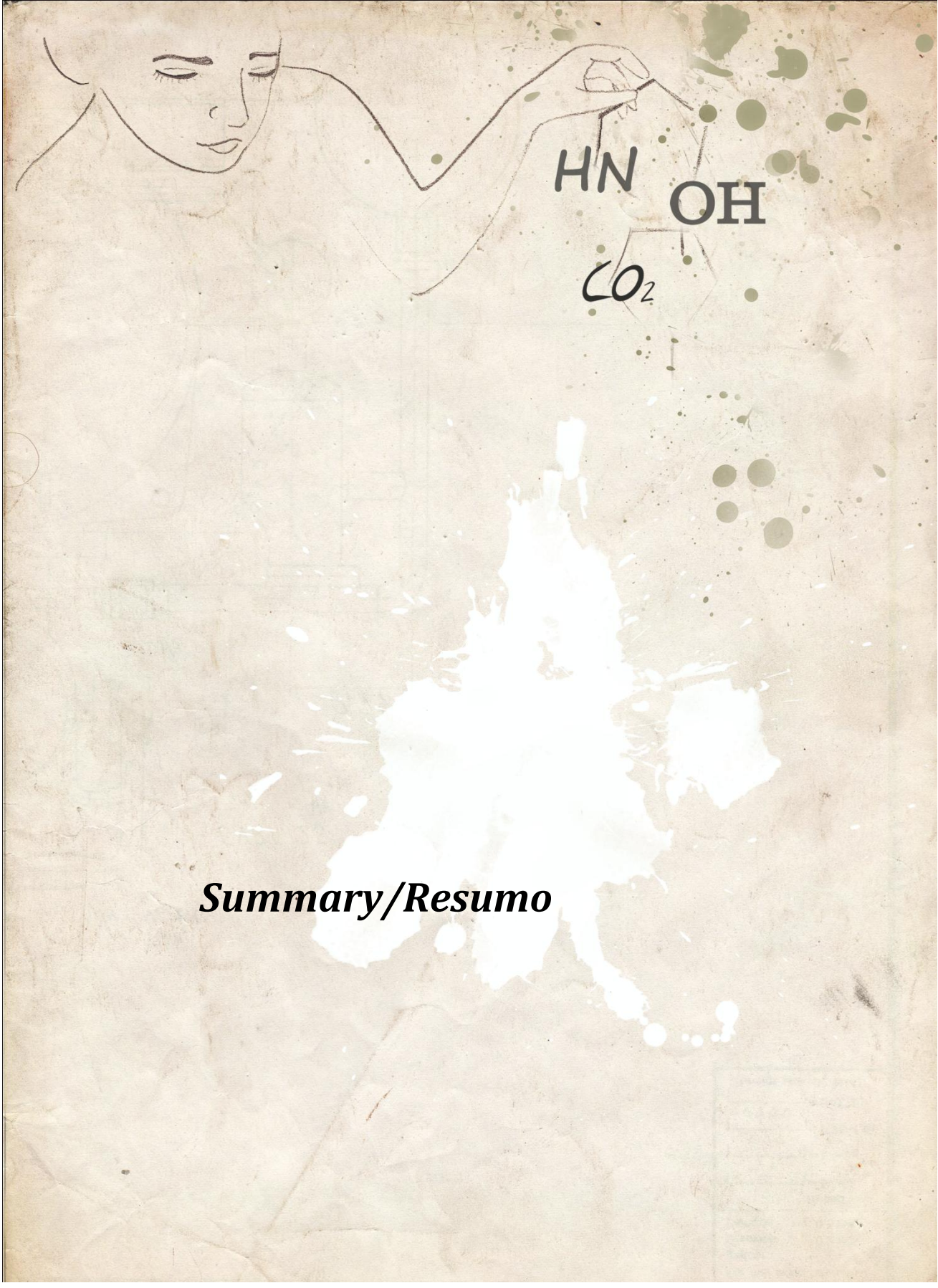


## *Summary/Resumo*

## Summary

The research work included in present PhD Thesis involves the research studies to capture carbon dioxide using different cyclic nitrogen organic compounds (glucosamine (GA), chitosan (C), alkyl-pyrrolidones, pyrrolidine (PYR) and piperidine (PIP).

This investigation is based on the study of three experimental systems. Each of them has characteristics potentially suitable to achieve the aim of this work, that is to say, to improve the carbon dioxide capture process, which is present in gas streams, by means of gas-liquid and gas-liquid-liquid absorption operations. The systems are as follows:

1. Aqueous solutions of cyclic amines

Reactive absorption is the most preferred option used in the gas-processing industry for carbon dioxide removal, and the aqueous solutions of alkanolamines remain an industrial important class of compounds, used in the natural gas purification, petroleum chemical plants and ammonia industries for the removal of carbon dioxide and hydrogen sulfide from gas streams. A wide variety of alkanolamines, such as monoethanolamine (MEA), diethanolamine (DEA), di-isopropanolamine (DIPA), N-methyldiethanolamine (MDEA) have been used industrially for an important number of years. In this study new solvents based on cyclic amines (PYR and PIP) are proposed, and they can introduce improvements in the carbon dioxide capture, both reaction rate and capture capacity.

The chitin-based polymers used in present work (glucosamine and chitosan) were also in contact with carbon dioxide, and this entail a gas-liquid mass transfer process by means of absorption. Due to the complexity of absorption process with chemical reaction, the study of chemical reaction kinetics and the use of suitable gas-liquid reactors are very important studies in order to obtain suitable carbon dioxide absorption, taking into account that this pollutant gas can be present in industrial gas streams with low concentration.

The use of chitin-based polymers, as glucosamine and chitosan, nowadays has no application with regard to carbon dioxide capture; however they are widely used in organic synthesis, since amine group present in these compounds has a great interest.

These substances are widely used in different fields related to chemistry, environmental technology or food processes. For instance, glucosamine is used for animal food and it has loads of possibilities to become an active principle against arthritis in the near future. On the other hand, chitosan has a range of uses both food industries (as food coating, texture additives), as well as flocculants to wastewater treatment, or as polymer to make matrixes in enzyme immobilization.

2. Aqueous solutions of cyclic amides

As has been mentioned above, the separation of certain acidic gases is preferable performed by means of absorption process with chemical reaction. Anyway, another possibility often used for the separation of different substances from gas streams is the physical absorption with solvents as water, methanol (Rectisol process) or N-methyl-2-pyrrolidone (Lurgi's Purisol process). With regard to reactive absorption, the solvents most used are, potassium carbonate (Benfield process), monoethanolamine (MEA; Girbotol process), Sulfolan + diisopropanolamine + water (Shell's Sulfinol process) or amines blends.

The Purisol process, that employs N-methyl-2-pyrrolidone, was first applied to natural gas sweetening; however, this procedure has shown higher importance in other processes such as in the hydrogen purification and carbon dioxide capture, with a subsequent regeneration process of the solvent by means of pressure changes to desorb the pollutant gases. Besides, this substance has the advantage of having a low reactivity, high solubility with regard to gases and high thermal stability.

Due to the interest of the carbon dioxide absorption process using aqueous solutions of N-methyl-2-pyrrolidone (MP), in this work the absorption process of this gas in this kind of aqueous solutions has been analysed. Besides, other cyclic amides, such as 2-pyrrolidone (P) and N-ethyl-2-pyrrolidone (EP) have been used, to evaluate the differences between these solvents and N-methyl-2-pyrrolidone, upon the absorption process in bubbling equipment, what implies the analysis of the hydrodynamic and the mass transfer processes. An important fact is that N-ethyl-2-pyrrolidone and 2-pyrrolidone presents less health hazards than N-methyl-2-pyrrolidone and for this reason these substances could be a more suitable absorbent for carbon dioxide than N-methyl-2-pyrrolidone, if hydrodynamic and absorption studies show comparable results.

3. Gas-liquid-liquid systems

The influence of organic compound presence upon gas-liquid mass transfer coefficient has been studied in different research works during last years, but achieved conclusions do not allow to obtain a single behavior. On the one hand, certain studies have found that the presence of a second liquid phase produces positive effects upon the global process; however, other studies have obtained the opposite behavior. In this work, the effect produced by the presence of an organic substance upon the gas-liquid mass transfer has been determined, both in relation with hydrodynamics as with the absorption process.

Also, using an immiscible organic substance may require the use of an additional compound to stabilize the emulsion. In this case a surfactant (Tween80) has been used, which must be taken into account since this kind of substances can affect to the hydrodynamics or mass transfer considerably and also, upon the chemical reaction in the bulk of the liquid phase.

The research performed in present thesis has been carried out following the thematic distribution shown below:

1. Kinetics studies

Considering that one of the main parts of this work involves chemical reaction between carbon dioxide (previously absorbed in aqueous solution) and different compounds used as liquid phase, the knowledge of chemical reaction characteristics, and therefore of the kinetic of this reaction is completely necessary. The kinetics determination in this kind of systems was more complicated than for homogeneous ones with a single phase, because the mass transfer process associated to reactive absorption had to be taken into account. Therefore, the conditions for performing the experiments had to be specific for each of the systems.

2. Hydrodynamics studies

These studies have included the absorption process characterization according to its hydrodynamics, and therefore the effect of used operation variables (gas flow-rate and liquid phase composition) upon hydrodynamics parameters, such as bubble size distribution or gas hold-up, has been analyzed.

In order to determine the main diameter of bubbles a photograph method was used, which is based on taking photographs to the column. These photographs were subsequently analyzed on the basis of bubble geometric shape, in this case ellipsoidal type.

3. Mass transfer studies

This work includes gas-liquid mass transfer studies for the carbon dioxide absorption, with and without chemical reaction, in different liquid phases, such as pyrrolidine, glucosamine, piperidine, 2-pyrrolidone, N-methyl-2-2-pyrrolidone, N-ethyl2-2pyrrolidone, chitosan, chitosan sulfate, carboxymethyl chitosan aqueous solutions. Mass transfer volumetric coefficient ($k_L \cdot a$) has been obtained from the amount of carbon dioxide transferred to liquid phase and subsequently the mass transfer coefficient was calculated ($k_L$) using the previously determined gas-liquid specific interfacial area, so the influence of different process variables (liquid phase composition and gas flow-rate) upon each parameter was analyzed.

4. Synthesis of polymers from chitosan

The aim of this study was the introduction of functional groups into the chitosan structure, in order to improve the solubility of this molecule in a non-acidic aqueous medium, and to promote the possibility of chemical absorption, since the reaction in acidic medium would be inhibited. After analyzing the literature, the synthesis of chitosan sulfate and carboxymethyl chitosan were chosen.

Once the different studies have concluded these were compiled as shown below:

Chapter 1 includes the objective of this research work, which is to evaluate different systems to capture carbon dioxide, taking into account that some of them are expected to have a carbon dioxide capture capacity higher than the systems used nowadays and other ones present less risk to health or safety. Besides, in order to design industrial absorption equipment, the knowledge of parameters such as mass transfer coefficient, gas-liquid interfacial area and absorption kinetics when chemical reaction takes place, will be required. In addition, certain physical properties as density, viscosity and surface tension of the liquid phase must be known because they are important for the carbon dioxide removal process. This chapter also includes an introduction where the present concern about carbon dioxide emissions worldwide is reflected,

and a compilation of current technologies used to capture this gas in the industry. Besides, it contains the "state of art", that is, a summary of more recent research works performed about this field.

The chapter 2 of this thesis is devoted to the carbon dioxide absorption in aqueous solutions of cyclic amines. This one includes the determination of reaction kinetics between carbon dioxide and pyrrolidine, as well as between carbon dioxide and piperidine. A stirred tank reactor with a known planar interfacial area was used to perform this study. The results indicated that absorption process occurs in a pseudofirst reaction regime exhibiting first-order kinetic with respect carbon dioxide and a second order for both cyclic amines; however the usual behavior for this kind of substances (amines) is a one order kinetic. The hydrodynamics and absorption studies were carried out using a non-mechanically stirrer contactor (bubble column reactor). Then to analyze carefully the reaction mechanism between carbon dioxide and both amines (pyrrolidine and glucosamine) NMR analysis (Nuclear Magnetic Resonance) was used. The obtained results indicated that reaction mechanism is different for both amines (PYR and GA). Besides, this study provides information about the global process stoichiometry and this data is used to determine the mass transfer coefficient when reactive absorption takes place. This chapter also includes the analysis of influence of different operation variables (gas flow-rate and composition of liquid phase) upon some hydrodynamics parameters, such as bubble size distribution, gas hold-up or interfacial area.

At present, the carbon dioxide absorption process using aqueous solutions of N-methyl-2-pyrrolidone is patented and is used at industrial level, as has been mentioned above. For this reason, chapter 3 analyses other amides from the same family (2-pyrrolidone and N-ethyl-2-pyrrolidone), which have a lower risk. Besides, different physico-chemical properties for the pyrrolidones aqueous solutions were obtained, and the results showed characteristic behaviors for the surface tension and viscosity, and both physical properties exert a big influence upon mass transfer processes. Also, hydrodynamics and absorption process for cyclic amide-carbon dioxide systems were studied and the behaviour observed for MP and EP is very similar. For this reason, EP could be a suitable substitute for the MP in the process of carbon dioxide absorption, since EP presents less risk to the health than MP, which is included in the list of substances of very high concern (SVHC) made by ECHA (European Chemicals Agency) and therefore, the use of this substance must be authorized by this institution. Besides, one of the main aims of the REACH European Community Regulation is the progressive change of very hazardous substances

applying the substitution principle. On the other hand, 2-pyrrolidone showed worse conditions to capture carbon dioxide than N-methyl-2-pyrrolidone, since the interfacial area was significantly lower.

Chapter 4 is focused on the study of hydrodynamics and mass transfer process of carbon dioxide from gas phase to liquid-liquid system, which is composed by an organic phase and aqueous phase, immiscible each other. Two kind of silicone oil were used as organic phase (low viscosity silicone oil (S1) and high viscosity silicone oil (S2)). Besides, since the presence of surfactant (Tween80) may affect to the carbon dioxide absorption, this was analyzed. The surfactant was used to stabilize the liquid-liquid system. Finally, this chapter also includes the evaluation of influence of an insoluble organic phase upon the global process of gas-liquid mass transfer in a system with chemical reaction. With regard to glucosamine, the experimental results indicates that the highest absorption rate corresponds to the system in presence of both silicone oil S1 and surfactant and after several studies, including NMR, the impurities present in the surfactant are thought to affect the chemical reaction and produce some type of catalytic effect upon the reaction mechanism. For the systems with pyrrolidine, because it is an absorption regime very fast, the presence of surface active substance does not produce changes upon the results obtained for the absorption process with chemical reaction. The presence of silicone oil produces a decrease in the absorption rate and this reduction is higher if the surfactant is present, since the surfactant is present in all phases and interphases, hindering in the whole cases the gas mass transfer through the liquid phase.

Chapter 5 focuses on carbon dioxide absorption by means of chitosan (C) and modified chitosan (CS and CC) aqueous solutions. The methodology used to synthesize these modified polymers is included in Appendix A (Materials and methods). The first section of chapter 5 includes the physico-chemical characterization of these substances: Fourier transform infrared spectroscopy, elemental analysis, deacetylation degree, intrinsic viscosity and average molecular weight, rheological behaviour and surface behaviour. This characterization was necessary to know if the structural modification in chitosan molecule had taken place and with regard to physical properties, these can show a high influence upon mass transfer process. Subsequently, the behaviour of these polymers aqueous solutions with regard to gas-liquid interfacial area produced in the absorber (bubble column) was analysed. Besides, the analysis about the influence of operation conditions upon gas hold-up and Sauter mean diameter, determined on the basis of the bubble size distribution obtained from photographs taken in the bubble column during

absorption process, was performed. From the obtained results in this chapter it was possible to conclude that chemical reaction between carbon dioxide and chitosan does not exist, and a physical absorption is produced in the contactor. A similar behaviour has been found for chitosan sulphate (CS) and carboxymehtyl chitosan (CC) aqueous solutions. In all cases (for C, CS and CC), polymer concentration produces a decrease in the value of volumetric mass transfer coefficient caused by the increase of liquid phase viscosity.

The currently used substances in industry for cleaning gas streams, in order to separate carbon dioxide and other acidic gases (different kind of alkanolamines) show a lot of problems because they are toxic and cause irritations to the workers. On the other hand, these are corrosive substances and therefore the industrial equipment maintenance should be important. However, polymers from chitosan, 2-pyrrolidone and N-ethyl-2-pyrrolidone have not these negative characteristics previously mentioned. Therefore they can be used and manipulated with lower chemical risk. Besides, they are not corrosive substances and for this reason equipments would need less frequent maintenance. For the systems with pyrrolidine and piperidine, despite they present the negative characteristics previously mentioned for the commonly used amines in industrial processes, improvements in carbon dioxide absorption process, mainly in absorption rate, are produced. For this reason, they will be able to be used with lower concentration, treat a higher flow-rate with the same quantity of amine or decrease the equipment size. All these characteristics are included in the Principles of Green Chemistry and this work is part of the projects dedicated to reducing the carbon dioxide emissions to atmosphere (related with Kyoto Protocol). Also, it is linked with REACH European Community Regulation, since one of the main aims of this normative is the progressive change of very hazardous substances applying the substitution principle, and therefore the research is necessary to make this possible. One of the substances with very high concern is N-methyl-2-pyrrolidone.

With regard to results transfer, due to the high applicability of obtained data in this research work, an important number of industries could be interested in using some of these new proposed technologies, in order to renew or change the gas-cleaning processes or to introduce this technology and this way to reduce carbon dioxide emissions.

## Resumo

A investigación incluída na presente tese de doutoramento engloba o proceso necesario para a captura de dióxido de carbono mediante diferentes aminas cíclicas, dentro das cales están englobadas as derivadas da quitina (mais especificamente a glucosamina (GA) e o quitosano), as alquil-pirrolidonas e a pirrolidina (PYR) e piperidina (PIP).

Dita investigación baseouse no estudo de tres sistemas, cada un dos cales presenta características potencialmente axeitadas para acadar o obxectivo final deste traballo, é dicir, obter melloras no proceso de captura de dióxido de carbono, mediante operacións de absorción gas-líquido e gas-líquido-líquido, presente en correntes gasosas. Estes sistemas son os seguintes:

1. Disolucións acuosas de aminas cíclicas

A absorción química é a opción empregada preferentemente na industria para a captura de dióxido de carbono. Na actualidade, as disolucións acuosas de alcanolaminas seguen a ser empregadas nas plantas de tratamento de petróleo, gas natural e produción de amoníaco para a eliminación do dióxido de carbono e sulfuro de hidróxeno presentes en correntes gaseosas. Entre as alcanolaminas mais empregadas atópanse a monoetanolamina (MEA), dietanolamina (DEA), di-isopropanolamina (DIPA) e N-metildietanolamina (MDEA). Neste estudo propóñense novos disolventes baseados en aminas cíclicas (pirrolidina e piperidina), as cales presentaron melloras na captura de dióxido de carbono, tanto na velocidade da reacción química como na capacidade de captura.

Os derivados da quitina empregados no presente traballo (glucosamina e quitosano) tamén se puxeron en contacto co dióxido de carbono, o cal implica un proceso de transferencia de materia gas-líquido mediante absorción. Debido á complexidade do proceso de absorción acompañada de reacción química, o estudo da cinética da reacción química, así como o uso de reactores gas-líquido adecuados son estudos de vital importancia para conseguir unha captura do dióxido de carbono axeitada, tendo en conta que este gas contaminante pode non ter unha concentración elevada nas correntes gasosas industriais.

O uso de derivados da quitina, como a glucosamina e o quitosano, non ten na actualidade aplicación respecto á captura de dióxido de carbono, mentres que si, son empregados amplamente en síntese orgánica xa que o grupo amino que conteñen é de grande interese.

Estes compostos teñen grande utilidade en distintos eidos relacionados coa química, a tecnoloxía ambiental ou os procesos alimentarios. Por exemplo, a glucosamina emprégase en alimentación animal e ten moitas posibilidades de ser un principio activo para medicamentos contra a artrite nun futuro próximo. Noutra banda, o quitosano ten un amplo abanico de usos tanto na industria alimentaria (recubrimentos para alimentos, aditivo para texturas), así como no tratamento de augas residuais como floculante, ou como polímero para formar matrices na inmobilización de enzimas.

2. Disolucións acuosas de amidas cíclicas

Como foi comentado previamente, a separación de certos gases ácidos lévase a cabo, preferentemente, mediante procesos de absorción con reacción química. De tódolos xeitos, outra posibilidade que se emprega, tamén con certa frecuencia, para a separación de correntes gasosas é a absorción de tipo física con disolventes, tales como auga, metanol (Proceso *Rectisol*) ou N-metil-2-pirrolidona (Proceso *Lurgi's Purisol*). En canto á absorción química, os disolventes empregados son, por exemplo, o carbonato de potasio (Proceso *Benfield*), monoetanolamina (MEA; Proceso *Girbotol*), ou mesturas de aminas.

O Proceso *Purisol* foi, en primeiro lugar, empregado para a desulfuración do gas natural, pero co paso dos anos amosouse como un procedemento de grande interese e eficacia para a purificación do hidróxeno e para a captura de dióxido de carbono, cunha posterior rexeneración do absorbente mediante a desorción dos gases previamente absorbidos. Ademais, este composto presenta a vantaxe de ter unha baixa reactividade, alta solubilidade en relación ós gases e alta estabilidade térmica.

Debido ó interese que xerou a absorción de gases ácidos empregando N-metil-2-pirrolidona (MP), neste traballo analizouse o proceso de absorción de dióxido de carbono empregando este mesmo composto e tamén outros da mesma familia en disolución acuosa, concretamente a 2-pirrolidona (P) e a N-etil-2-pirrolidona (EP), co fin de avaliar as diferenzas entre os distintos disolventes sobre o proceso de absorción, tanto dende o punto de vista da

hidrodinámica como da transferencia de materia, xa que ambos compostos, a P e a EP, presentan menor risco químico que a MP, e polo tanto poderían ser un absorbente máis axeitado para captura de dióxido de carbono, se os estudos hidrodinámicos e de absorción amosan resultados comparables.

3. Sistemas gas-líquido-líquido

A influencia da presenza dun composto orgánico sobre o coeficiente de transferencia de materia gas-líquido foi estudada en diferentes traballos de investigación durante os últimos anos, pero as conclusións acadadas non permiten extraer un comportamento único. Por unha banda, certos estudos atopan que a presenza dunha segunda fase líquida produce efectos positivos sobre o proceso global, nembargantes, outros estudios obtiveron como resultado o comportamento contrario. Neste traballo determinouse o efecto causado pola presenza dun composto orgánico sobre a transferencia de materia gas-líquido, tanto en relación coa hidrodinámica como sobre o proceso de transferencia previamente dito, analizando os distintos efectos producidos sobre o proceso de absorción.

Así mesmo, o feito de empregar un composto orgánico inmiscible pode facer necesario o uso dun composto adicional para a estabilización da emulsión, que neste caso foi un surfactante (Tween80), o cal hai que ter en conta xa que este tipo de compostos poden afectar dun modo importante tanto sobre a hidrodinámica como sobre a transferencia de materia.

A investigación desenvolvida na presente tese de doutoramento realizouse segundo a seguinte distribución en función da temática a analizar:

1. Estudos cinéticos

Considerando que unha das partes principais deste traballo implica a reacción química entre o dióxido de carbono, previamente absorbido en disolución acuosa, cos distintos compostos empregados como fases líquidas, o coñecemento da reacción química e, polo tanto, da cinética de dita reacción química faise completamente necesario. A determinación da cinética de neste tipo de sistemas foi máis complicado que as tradicionais en sistemas homoxéneos dunha única fase, xa que se deberon ter en conta as características do proceso de transferencia de materia asociados ó proceso de absorción acompañada de reacción química. Polo tanto, as condicións para o

desenvolvemento dos experimentos realizados tiveron que ser específicas para cada un dos diferentes sistemas.

2. Estudos hidrodinámicos

Estes estudos incluíron a caracterización dos procesos de absorción segundo a súa hidrodinámica, polo tanto, analizouse o efecto que as variables de operación empregadas (caudal de gas e composición da fase líquida) causan sobre os parámetros hidrodinámicos, tales como a distribución de tamaño de burbulla, a retención de gas e o efecto que estes producen ó mesmo tempo sobre a área de intercambio de materia entre as fases gas e líquido.

Para a determinación do diámetro medio das burbullas de gas formadas empregouse un método fotográfico baseado na toma de imaxes das burbullas ó longo de toda a columna. Ditas fotografías foron posteriormente analizadas en base á forma xeométrica das burbullas, que neste caso eran de tipo elipsoidal.

3. Transferencia de materia

Este traballo inclúe os estudos de transferencia de materia gas-líquido correspondentes á absorción de dióxido de carbono nas fases líquidas empregadas no actual traballo de investigación, como son as disolucións acuosas de pirrolidina, glucosamina, piperidina, 2-pirrolidona, N-metil-2-pirrolidona, N-etil-2-pirrolidona, quitosano, sulfato de quitosano e carboximetil quitosano, así como nos sistemas gas-líquido-líquido. Determinouse o coeficiente volumétrico de transferencia de materia ($k_L \cdot a$) a partir do seguimento da cantidade de dióxido de carbono transferido á fase líquida e posteriormente, o coeficiente de transferencia de materia ($k_L$) empregando o valor do área interfacial específico gas-líquido obtido con anterioridade, analizando así, a influencia das diferentes variables de proceso (composición da fase líquida e caudal de gas) sobre cada un dos parámetros de xeito individual.

4. Síntese dos derivados do quitosano

O obxectivo deste estudo foi a introdución de grupos funcionais na estrutura do quitosano, de xeito que esta molécula poida ser soluble en medio acuoso non ácido, para favorecer a posibilidade de absorción química, xa que en medio ácido a reacción de absorción

atoparíase inhibida. Unha vez analizada a bibliografía existente sobre a materia, optouse, en principio, pola síntese do sulfato de quitosano e tamén do carboximetil quitosano.

Unha vez rematados os diferentes estudos que se levaron a cabo, estes foron plasmados neste traballo de investigación do xeito que se indica a continuación:

No capítulo 1 da tese recóllese o obxectivo deste traballo que, como se indicou anteriormente, é facer unha avaliación de diferentes sistemas para capturar dióxido de carbono, dos cales se espera que presenten unha maior capacidade de captura ou menos riscos para a saúde que os sistemas que se empregan na actualidade nos procesos industriais de captura de dióxido de carbono. Dita avaliación inclúe o coñecemento de parámetros tales como o coeficiente de transferencia de materia correspondente ós procesos de absorción física ou química, a área interfacial gas-líquido e a cinética dos procesos de absorción no caso de que teña lugar reacción química. Ademais, certas propiedades físicas como a viscosidade, a densidade ou a tensión superficial da fase líquida deben ser coñecidas xa que xogan un papel moi importante neste tipo de procesos, e axudan a interpretar os resultados experimentais obtidos. Ademais do obxectivo, o capítulo 1 contén unha introdución na que se reflexa a situación actual do problema das emisións de dióxido de carbono a nivel mundial, e tamén se inclúe un resumo das tecnoloxías que actualmente se están a empregar na industria para levar a cabo a captura deste gas, así como un apartado correspondente ó "estado da arte", é dicir, unha recompilación de diferentes traballos de investigación que diversos investigadores estiveron a realizar neste eido durante os últimos anos.

O capítulo 2 da tese está adicado á absorción de dióxido de carbono en disolucións acuosas de aminas cíclicas. Este, inclúe a determinación da cinética de reacción entre o dióxido de carbono e a pirrolidina, e tamén entre o dióxido de carbono e a piperidina. Para estes estudos empregouse un reactor de tanque axitado cunha área interfacial plana e coñecida. Os resultados experimentais indicaron que o proceso de absorción ten lugar cun réxime de reacción rápido de pseudoprimera orde, presentando unha cinética de primeira orde con respecto ó dióxido de carbono e segunda orde para ambas aminas cíclicas, cando o comportamento mais habitual para este tipo de compostos é a orde un con respecto á amina. Os estudos para a determinación da velocidade de captura, ó igual que os estudos hidrodinámicos tamén se inclúen neste capítulo e foron realizados nunha columna de burbulleo. Para a determinación dos mecanismos de reacción entre a pirrolidina e o dióxido de carbono, así como entre a glucosamina e o dióxido de carbono empregouse a tecnoloxía de Resonancia Margnética Nuclear (RMN). Os resultados obtidos a partir

desta técnica indicaron que os mecanismos de reacción presentes son diferentes en cada caso, é dicir, dependen do tipo de reactivo. Estes estudos son precisos non soamente para coñecer os camiños de reacción neste proceso, senón para poder coñecer a estequiometría global do proceso e empregar este dato para a determinación do coeficiente de transferencia de materia en presenza de reacción química. Ademais, analizouse a influencia de diferentes variables de operación (caudal de gas ou composición da fase líquida) sobre algúns parámetros hidrodinámicos, tales como a distribución do tamaño de burbulla, a retención de gas na fase líquida ou a área interfacial.

Tal como se comentou previamente, na actualidade existe un proceso patentado sobre absorción de dióxido de carbono con disolucións acuosas de N-metil-2-pirrolidona, o cal se está empregar a nivel industrial. Por este motivo, o capítulo 3 analiza outras amidas da mesma familia (concretamente a 2-pirrolidona e a N-etil-2-pirrolidona), pero que presentan menos problemas en canto a risco químico. Ademais foron obtidas diferentes propiedades fisico-químicas para as disolucións acuosas destas pirrolidonas, e os resultados amosaron que presentan comportamentos característicos con respecto ás propiedades físicas con gran influencia sobre os procesos de transferencia de materia, como son a tensión superficial e a viscosidade. Tamén se estudou a hidrodinámica e a absorción dos sistemas dióxido de carbono–amida cíclica. Os resultados experimentais obtidos indican un comportamento moi semellante para as disolucións acuosas de N-metil-2-pirrolidona e N-etil-2-pirrolidona en relación tanto á hidrodinámica como á transferencia de materia, co cal este último composto podería ser un substituto axeitado para a N-metil-2-pirrolidona no proceso de captura de dióxido de carbono, sobre todo tendo en conta que a MP aparece recollida na lista das sustancias de moi alta preocupación (SVHC) elaborada pola ECHA (Axencia Europea de Substancias Químicas) e que polo tanto para o seu emprego é preciso obter un permiso de autorización por parte desta institución da Unión Europea, que recomenda a súa substitución por outro reactivo menos perigoso. Por outra banda, a 2-pirrolidona amosou peores condicións para a captura de dióxido de carbono que a N-metil-2-pirrolidona, observando un área de intercambio de materia sensiblemente menor.

O capítulo 4 céntrase no estudo da hidrodinámica e o proceso de transferencia do dióxido de carbono dende a fase gas ata un sistema líquido – líquido formado por unha fase orgánica e outra acuosa, non miscibles. Como fase orgánica empregáronse dous tipos de aceite de silicona, un de baixa viscosidade (S1) e outro de alta viscosidade (S2). Tamén se analizou cómo a presenza dun axente de superficie (Tween80) pode afectar á absorción do dióxido de carbono.

Este composto emprégase para facilitar a estabilización do sistema líquido – líquido. Por último, neste capítulo tamén se estudou a influencia da presenza de dous compostos químicos que reaccionan co dióxido de carbono, a glucosamina e pirrolidina previamente analizados en capítulos anteriores, sobre a velocidade de absorción nun sistema gas – líquido - líquido. Con respecto á glucosamina os resultados experimentais indican que a maior velocidade de absorción do dióxido de carbono acadase para o sistema en presenza de Tween80 e co aceite de silicona de baixa viscosidade. Tras diferentes estudios realizados coa axuda da RMN (Resonancia Magnética Nuclear) para a determinación da difusión das distintas especies, chegouse á conclusión de que as impurezas presentes no surfactante poderían actuar como catalizadores desta reacción. Nembargantes, o sistema en presenza de pirrolidina presenta un réxime de absorción moito máis rápido que no caso da glucosamina, polo tanto a presenza do Tween80 non produce cambios observables sobre a velocidade de absorción, mentres que e a presenza do aceite de silicona si produce un descenso da mesma, e esta redución vese incrementada cando o surfactante tamén está presente na fase líquida.

O capítulo 5 céntrase na absorción de dióxido de carbono mediante disolucións acuosas de quitosano (C) e quitosano modificado (sulfato de quitosano (CS) e carboximetil quitosano (CC)). Os procedementos para a síntese destes polímeros modificados recóllense no Apéndice A desta tese (Materiais e métodos). O primeiro apartado do capítulo 5 contén a caracterización físico–química destas sustancias e inclúe as seguintes análises: espectroscopía infravermella por transformada de Fourier, análise elemental, grao de desacetilación, viscosidade intrínseca, peso molecular medio, comportamento reolóxico e tensión superficial. Toda esta caracterización foi necesaria xa que era preciso saber se a modificación estrutural na molécula de quitosano tivo lugar e en canto ás propiedades físicas, como se indicou anteriormente, o seu coñecemento é moi importante xa que estas poden ter unha grande influencia sobre o proceso global de transferencia de materia. A continuación, como para os sistemas anteriores, procedeuse a analizar o comportamento das disolucións acuosas destes polímeros en canto á área interfacial gas-líquido producida no absorbedor (columna de burbullo). Analizouse a influencia das condicións de operación sobre o gas retido e o diámetro medio Sauter, parámetro determinado en base á distribución do tamaño de burbulla, obtido a partir de diferentes fotografías tomadas ó longo da columna durante o proceso de absorción. Os resultados obtidos neste capítulo permitiron concluír que non existe reacción química entre o dióxido de carbono e o quitosano, de xeito que no equipo de contacto ten lugar un proceso de absorción física. O mesmo

comportamento atopouse para as disolucións acuosas de sulfato de quitosano e carboximetil quitosano. Ademais, nos tres casos a presenza do polímero produce unha diminución no coeficiente de transferencia de materia debido ó aumento da viscosidade que se produce cando se incrementa a concentración de cada un dos diferentes polímeros.

En canto á seguridade industrial, os compostos empregados actualmente na industria para a limpeza de correntes gasosas co obxectivo de separar o dióxido de carbono e outros gases ácidos (diferentes tipos de alcanolaminas), presentan moitos inconvenientes xa que son tóxicos e causan irritacións. Por outra banda, estes compostos son corrosivos polo que o mantemento dos equipos industriais debe ser importante. Nembargantes, os derivados do quitosano, así como o uso da 2-pirrolidona ou N-etil-2-pirrolidona non presentan as características negativas anteriormente comentadas, así que permiten ser empregados e manipulados con menor risco químico, e ademais non teñen carácter corrosivo, necesitando un mantemento menor dos equipos. No caso dos sistemas que empregan pirrolidina e piperidina, a pesar de que manteñen as características negativas anteriormente mencionadas para as aminas comunmente empregadas nos procesos industriais, estes aportan melloras na captura do dióxido de carbono principalmente na velocidade de absorción, co cal poderán ser empregados en menores concentracións, tratar un maior caudal de corrente gaseosa coa mesma cantidade de amina ou diminuír o tamaño dos equipos de contacto. Estas características sitúanse dentro dos principios da Química Verde xa que estase a tratar de empregar compostos químicos cun menor impacto ou en menor concentración, e ademais o proxecto encádrase dentro dos proxectos adicados a redución en control das emisións á atmosfera (relacionado co cumprimento do Protocolo de Kyoto). Tamén se relaciona co Regulamento REACH da Unión Europea xa que esta normativa ten como un dos seus obxectivos principais a eliminación progresiva das sustancias de alta preocupación, entre as que se atopa a N-metil-2-pirrolidona como foi mencionado anteriormente. Estas sustancias deben ser substituídas por outras que presenten menos riscos para a saúde dos traballadores aplicando o principio de substitución, e para que isto sexa posible é preciso levar a cabo unha serie de traballos de investigación co fin de atopar alternativas viables, tal como acontece neste caso.

Con respecto á transferencia de resultados, debido á alta aplicabilidade dos resultados obtidos neste traballo de investigación, pénsase que un importante número de industrias poderían estar interesadas en implantar algunha destas novas tecnoloxías propostas, ben para

renovar ou para modificar o seu proceso de limpeza de correntes gasosas ou ben para introducilo e deste xeito reducir as súas emisións de dióxido de carbono.

## Acknowledgments

After several years working in this PhD thesis, it's just the moment to thank all the people who have contributed, either in a direct or indirect way, to this work be published.

First of all, I wanted to thank Dr. Isabel Vidal for initiating me into the research world and introducing me to Dr. José M. Navaza, who has given me the chance to carry out this work. Thanks for opening me the doors of "your" laboratory and for the trust you have in me! Thanks to Xunta de Galicia, since part of this work has been financed with the proyect: 07MDS005265PR. The PI researcher has been Dr. José M. Navaza.

I'm especially grateful to Dr. Diego Gómez, thanks so much for all your help, suggestions and advises. To work with you have been an honor.

I thank to Dr. Isabel Belo for allowing me to stay during four months working at the Department of Biological Engineering of the Universidade do Minho, and thanks to the IB girls and company for being so kind to me. I acknowledge Ministerio de Ciencia e Innovación (MICINN) for the funding granted through the project HP2007-0059 (Acción Integrada project among Universidade de Santiago de Compostela and Universidade do Minho).

Thanks to Nuria Martínez for offering me help during her collaboration scholarship.

To Dr. Antonio Rumbo, I thank you for the help interpreting the NMR spectrums. And, to Dr. Pedro R. Dafonte for the DOSY NMR studies.

For this marvelous cover I want to thank Iria García. You are an artist!

Loads of thanks to my ETSE's friends and close friends (I don't write their names because it would be a long list) for your affection and for cheering me up when I needed it.

And finally, to my family thanks for your ongoing support, your patience in my difficult time, for convincing me that it was worth this effort and for loving me so much. I couldn't have better parents. I hope you are proud of me!

Maybe, I'm forgetting some people, thank you very much to all!

Alicia García Abuín, 2012

E-mail: alicia.garcia@rai.usc.es

Thesis University of Santiago de Compostela, Spain

Cover illustrated by Iria García Becerra

Printed by Lápices 4, Santiago de Compostela, Spain